A Comparison of the Environment, Health, And Safety Characteristics of Advanced Thorium-Uranium and Uranium-Plutonium Fuel Cycles

By

Timothy M. Ault

Dissertation

Submitted to the Faculty of the

Graduate School of Vanderbilt University

in partial fulfillment of the requirements

for the degree of

DOCTOR OF PHILOSOPHY

in

Environmental Engineering

May, 2017

Nashville, Tennessee

Approved:

Steven L. Krahn, D.P.A.

James H. Clarke, Ph.D.

David S. Kosson, Ph.D.

Mark D. Abkowitiz, Ph.D.

Allen G. Croff, Eng., M.S., M.B.A.

Andrew G. Sowder, Ph.D.

DEDICATION

To Dr. Jerald Ault

And

To Mrs. Cheryl Gabler

For Inspiring Me to Pursue a Career of Scientific and Engineering Inquiry

ACKNOWLEDGEMENTS

While this dissertation has my name on the front of it, there are many people and entities that have played a pivotal role in enabling me to reach this point.

Thank you, Dr. Steven Krahn, for having guided and advised me through a challenging doctoral degree program while simultaneously providing me with the latitude to plant the seeds of creativity and subsequently reap the benefits. You have always championed for me as both a student and a researcher in the nuclear industry.

Thank you, Dr. Bethany Burkhardt, for having been a close collaborator, mentor, and friend through many projects. You have shown me how to balance a zillion projects that are seemingly at odds with one another, all while maintaining an unbelievably awesome personality.

Thank you to those colleagues and mentors who have guided me at Vanderbilt. To my committee members, your feedback and encouragement has been instrumental in making this dissertation a success. To Allen and Ray, your collaboration and mentorship enabled me to hit the "fast-forward" switch with regards to many aspects of my professional development. Brandon, Andrea, Colin, and Steven...you have all been integral components of my research efforts. Janelle, Thushara, Leah, Yonathan, Harshini, Kate, John, Erin…it was great to have you around as sounding boards over the past few years, and you definitely fostered the learning environment.

Thank you to the US national laboratories which have been so supportive of me during my graduate career. To Andy, Jeff, Josh, and Eva at Oak Ridge, to Brent, Brett, and Ross at Idaho,

and to TK and Temi at Argonne…thank you for providing me with the intellectual resources to succeed in the nuclear research arena, as well as your constant encouragement and support.

Thank you to the US Department of Energy and the Nuclear Energy University Programs. Your fellowship support has permitted me to dream big and tackle some important problems that would have otherwise been difficult to address. In a similar vein, thanks to the Electric Power Research Institute and Andrew for having lent support to my work as well.

A particularly important "shout-out" goes to my family for laying down the groundwork to make me the person that I am today. Thank you, Mom and Dad, for having invested so much of yourselves into your son. Thanks to my sister, Jennifer, for giving me an outlet to stay sane. And lastly, thank you, Sandya, for being there for me day after day.

PREFACE

The environment, health, and safety properties of thorium-uranium-based ("thorium") fuel cycles are estimated and compared to those of analogous uranium-plutonium-based ("uranium") fuel cycle options. A structured assessment methodology for assessing and comparing fuel cycle is refined and applied to several reference fuel cycle options.

Resource recovery as a measure of environmental sustainability for thorium is explored in depth in terms of resource availability, chemical processing requirements, and radiological impacts. A review of available experience and recent practices indicates that near-term thorium recovery will occur as a by-product of mining for other commodities, particularly titanium. The characterization of actively-mined global titanium, uranium, rare earth element, and iron deposits reveals that by-product thorium recovery would be sufficient to satisfy even the most intensive nuclear demand for thorium at least six times over. Chemical flowsheet analysis indicates that the consumption of strong acids and bases associated with thorium resource recovery is 3-4 times larger than for uranium recovery, with the comparison of other chemical types being less distinct. Radiologically, thorium recovery imparts about one order of magnitude larger of a collective occupational dose than uranium recovery.

Moving to the entire fuel cycle, four fuel cycle options are compared: a limited-recycle ("modified-open") uranium fuel cycle, a modified-open thorium fuel cycle, a full-recycle ("closed") uranium fuel cycle, and a closed thorium fuel cycle. A combination of existing data and calculations using SCALE are used to develop material balances for the four fuel cycle options. The fuel cycle options are compared on the bases of resource sustainability, waste

management (both low- and high-level waste, including used nuclear fuel), and occupational radiological impacts. At steady-state, occupational doses somewhat favor the closed thorium option while low-level waste volumes slightly favor the closed uranium option, although uncertainties are significant in both cases. The high-level waste properties (radioactivity, decay heat, and ingestion radiotoxicity) all significantly favor the closed fuel cycle options (especially the closed thorium option), but an alternative measure of key fission product inventories that drive risk in a repository slightly favors the uranium fuel cycles due to lower production of iodine-129. Resource requirements are much lower for the closed fuel cycle options and are relatively similar between thorium and uranium.

In additional to the steady-state results, a variety of potential transition pathways are considered for both uranium and thorium fuel cycle end-states. For dose, low-level waste, and fission products contributing to repository risk, the differences among transition impacts largely reflected the steady-state differences. However, the HLW properties arrived at a distinctly opposite result in transition (strongly favoring uranium, whereas thorium was strongly favored at steady-state), because used present-day fuel is disposed without being recycled given that uranium-233, rather than plutonium, is the primarily fissile nuclide at the closed thorium fuel cycle's steady-state. Resource consumption was the only metric was strongly influenced by the specific transition pathway selected, favoring those pathways that more quickly arrived at steady-state through higher breeding ratio assumptions regardless of whether thorium or uranium was used.

TABLE OF CONTENTS

LIST OF FIGURES

LIST OF TABLES

NOMENCLATURE

Abbreviation/Symbol	Description
Am	Americium
ANL	Argonne National Laboratory
BNL	Brookhaven National Laboratory
BR	Breeding Ratio
BWR	Boiling Water Reactor
CEA	Commissariat a L'Energie Atomique et Aux Energies Alternatives
CETR	Consolidated Edison Thorium Reactor
Cs	Cesium
CThU	Closed Thorium-Uranium (Fuel Cycle)
CUPu	Closed Uranium-Plutonium (Fuel Cycle)
DOE	United States Department of Energy
EH&S	Environment, Health, and Safety
EHPA	Di-2-Ethylhexyl Phosphoric Acid
EPRI	Electric Power Research Institute
FCO-ESS	Fuel Cycle Option Evaluation & Screening Study
FP(s)	Fission Product(s)
FP1	Fission Products Removed During Salt Treatment
FP2	Fission Products Removed During Salt Processing
GIF	Generation IV International Forum
GTCC	Greater-Than-Class-C Low Level Waste
GWe	Gigawatts electric
GWe-yr	Gigawatt-electric year
H_2SO_4	Sulfuric Acid
HCl	Hydrochloric Acid
HLW	High-Level Waste
hr	Hour
I	Iodine
IAEA	International Atomic Energy Agency
IFR	Integral Fast Reactor
ISL	In-Situ Leaching
LLW	Low-Level Waste
KAERI	Korea Atomic Energy Research Institute
LEU	Low-Enriched Uranium
LWBR	Light Water Breeder Reactor
LWR	Light Water Reactor
MA(s)	Minor Actinide(s)
MeV	Mega-electron volts
MOX	Mixed Oxide
MSBR	Molten Salt Breeder Reactor
MSR	Molten Salt Reactor
MSRE	Molten Salt Reactor Experiment
mSv	Millisievert

MT	Metric Tons
MTHM	Metric Tons of Heavy Metal
MThU	Modified-Open Thorium-Uranium (Fuel Cycle)
MTIHM	Metrics Tons of Initial Heavy Metal
MTNU	Metric Tons of Natural Uranium
MUPu	Modified-Open Uranium-Plutonium (Fuel Cycle)
NaOH	Sodium Hydroxide
NEA	See OECD-NEA
Np	Neptunium
NRC	United States Nuclear Regulatory Commission
NTh	Natural Thorium
NU	Natural Uranium
NWTRB	Nuclear Waste Technical Review Board
OECD-NEA	Organisation for Economic Co-Operation and Development's Nuclear Energy Agency
ORNL	Oak Ridge National Laboratory
Pa	Protactinium
ppm	Parts per million
ppb	Parts per billion
ppt	Parts per trillion
Pu	Plutonium
PWR	Pressurized Water Reactor
R&D	Research and Development
Ra	Radium
REE(s)	Rare Earth Element(s)
REO(s)	Rare Earth Oxide(s)
Rn	Radon
SBB	Seed-Blanket Breeder
Se	Selenium
SFR	Sodium-Cooled Fast Reactor
Sn	Tin
SNF	Spent Nuclear Fuel
TBP	Tributyl Phosphate
Tc	Technetium
Th	Thorium
Ti	Titanium
TRL	Technology Readiness Level
TSP	Trisodium Phosphate
U	Uranium
U_3O_8	Triuranium Octoxide
UNF	Used Nuclear Fuel
US	United States
USGS	United States Geological Survey
WNA	World Nuclear Association
Xe	Xenon
yr	Year

CHAPTER 1, INTRODUCTION

The deployment of nuclear fuel cycles and their corresponding facilities and technologies is associated with long timeframes; this means that for sizeable progress to be observed even on the timescale of decades, key decisions on research and development (R&D) allocations must be made promptly. This is particularly challenging for the multitude of nuclear fuel cycle options for which data is scattered, outdated, and/or nonexistent. The family of fuel cycles which relies on thorium and thorium-based radioisotopes (namely uranium-233, thorium's fissile counterpart[1]) is a prime example of this phenomenon. Studies have suggested a number of qualitatively-perceived benefits and disadvantages of thorium, but without a consistent approach to evaluation, it is nearly impossible to accurately gauge the role thorium should play in nuclear energy futures. There are a variety of perspectives to consider when assessing the performance of nuclear fuel cycle options. Proponents of the thorium fuel cycle claim several key benefits, including:

- Preferable (with regards to decay heat, activity, and/or waste form integrity) or greatly reduced waste output
- Increased resource availability due to higher crustal abundance
- Favorable material properties in a reactor, particularly with regards to thermal performance
- Extreme difficulty of producing a nuclear weapon from resultant material

[1] This proposal will frequently refer to "thorium fuel cycles", which is the common terminology to describe fuel cycle options which rely on thorium -232 as a fertile isotope and uranium-233 as a fissile isotope.

On the other hand, proponents of the uranium-plutonium fuel cycle also claim certain benefits, such as:

- The established infrastructure of uranium fuel cycle facilities
- The broad experience base with uranium and uranium-plutonium fuels
- Favorable nuclear properties in the fast neutron spectrum
- The natural occurrence of fissile U-235

Some of these claims are often described with minimal technical elaboration, or the benefits are more accurately attributed to a particular nuclear technology rather than to thorium or uranium themselves. Therefore, it is essential to construct focused assessments, at the fuel cycle level, to distinguish the inherent properties of thorium from its perceived traits and to enable meaningful comparisons against uranium-plutonium fuel cycles. This dissertation seeks to comprehensively examine thorium fuel cycles from an environment, health, and safety (EH&S) perspective[2].

1.1. Background

There is a sizeable pool of thorium-related experience from which to draw, albeit less so than for uranium-plutonium systems. Thorium fuel cycles have an extensive background that reaches back to about the same time period as present commercial uranium fuel cycles. Nearly every possible fuel cycle technology which can incorporate uranium can also incorporate thorium and/or uranium-233. Indeed, thorium-based fuel has been deployed[3] in light water reactors [Connors 1979], heavy water reactors [Kumar 2000], aqueous solution reactors

[2] Other metrics, such as safeguards/security or economics, are not addressed in this study.
[3] Admittedly, the majority of these experiences took place in test- or demonstration-scale reactors.

[Chandramoleshwar 1990], molten salt reactors [MacPherson 1985], high-temperature gas-cooled reactors [Brodda 1977], and liquid-metal fast reactors [Chidambaram 1996]. Various fuel types have been developed, including oxide [Winget 1960], carbide/graphitic [Cook 1965], nitride [Peterson 1973], aqueous nitrate [Chandramoleshwar 1990], and fluoride [Chandler 1970]. Reprocessing schema have been developed for both aqueous [Blanco 1962] and electrochemical [Coops 1982] approaches. In spite of this diversity of experience, thorium-based multi-reactor fleets have not yet materialized, and their outlook remains unclear.

In order to assess the viability of thorium-based fuel cycle options relative to other advanced nuclear fuel cycle alternatives, it is important to establish a well-formed, consistent approach in conjunction with a well-defined problem statement and boundaries. To this end, there are a variety of previous general evaluations of multiple nuclear technologies [GIF 2002] that have developed criteria, attributes, and/or metrics to structure this type of evaluation. Furthermore, studies have been conducted that attempt to comprehensively examine a set of traits for many fuel cycle options [Wigeland 2014] along with others that have delved into deeper detail for specific metrics with regards to small subset of fuel cycle options [EPRI 2009, EPRI 2014]. While these studies are not strictly focused on thorium, they still provide valuable insights regarding how to structure an assessment of advanced nuclear fuel cycles with limited or unstructured data availability.

1.2. Key Questions and Dissertation Structure

After reviewing relevant literature in Chapter 2, Chapters 3 through 5 present the key analysis that constitutes the foundation of this dissertation. In light of the challenges discussed above, this

dissertation identifies and answers a series of interlinked questions which pertain to the viability of thorium as a competitive nuclear fuel cycle option from an EH&S perspective. These questions are:

- How does the sustainability of thorium recovery compare to that of natural uranium recovery, with regards to total and effective resource availability, chemical processing requirements, and occupational radiological impacts?
- What types of metrics are suitable to compare different thorium and uranium/plutonium fuel cycles on an environmental basis? Do these metrics differ from those developed in previous studies (e.g., the methodology described in [EPRI 2014a][4])?
- Is there an overall EH&S benefit, over the life cycle of a nuclear fuel cycle, to the implementation of thorium-based fuel cycles relative to the implementation of conventional uranium- or uranium/plutonium-based fuel cycles when considering…
    - Modified-open recycle?
    - Full (closed) recycle?
- How does a dynamic introduction of closed fuel cycles compare between thorium-based and uranium/plutonium based fuel cycle options? Which transition pathways are most promising to reach desirable end-states quickly and effectively?

Chapter 3 focuses on the first bulleted question. If the thorium fuel cycle is to be deployed on a commercial scale, natural thorium resources will be required. Thorium is known to be a crustally abundant element which exists in a number of large deposits. However, because current thorium

[4] Note: [EPRI 2014a] is the publically available report which serves as a counterpart to Bethany Burkhardt's Vanderbilt University dissertation. All references of [EPRI 2014a] inherently credit the accomplishments of that dissertation as well.

demand is so low, there is little economic incentive to pursue such deposits. In spite of this, the economic and environmental impacts from opening a new mine for thorium may be irrelevant due to the availability of thorium resources via mines currently operating for non-thorium minerals. Thorium can be recovered as a by-product of other elements, including titanium, tin, and uranium. While the additional impacts of recovering thorium as a by-product are not negligible, they are likely to be considerably lower than those associated with opening a new thorium mine. Chapter 3 calculates the total availability of thorium from by-product sources and assesses the environmental impact associated with by-product thorium recovery through the metrics of chemical processing requirements and associated occupational radiological impacts. These insights are compared to the better-known impacts of the major pathways for uranium recovery.

Chapter 4 resolves the second and third bulleted sets of questions, related to steady-state fuel cycle performance. The foundation for most assessments of nuclear fuel cycles is dependent on understanding how different types of material move between stages of nuclear fuel cycles and how this material is converted from one form to another through nuclear, chemical, or physical reactions. In turn, this material flow analysis depends on the impact of power production in a reactor, which provides a normative basis for the remainder of the material balance. Tools are available which can simulate the irradiation of advanced fuels, including those with thorium. To put the material flow results into context, metrics are developed to compare the performance of these fuel cycle options from an EH&S perspective. While not always considered under this category, natural resource usage is included among these metrics, since it is a relevant topic to

the notion of environmental stewardship and fuel cycle sustainability. These metrics also include more conventional EH&S concepts such as routine occupational safety and waste management.

Chapter 5 addresses the final bulleted set of questions, related to transition analysis. While steady-state characteristics are often used to determine which end-state technologies and fuel cycles are most desirable, further assessment is required to understand the difficulty associated with reaching such an end-state and the impacts associated with such a transition. An appealing end state might take much longer to implement than another less-appealing option, resulting in unfavorable performance or unacceptable delays in the interim period. Software tools are available to simulate analyses of nuclear fuel cycle deployment. Chapter 5 specifically focuses on closed fuel cycles; several potential transition pathways are examined as part of this analysis.

1.3. Dissertation Scope

This dissertation emphasizes EH&S factors. There are several parameters that are not addressed within this scope; these are discussed briefly in this section.

While this dissertation emphasizes the safety associated with routine operations, accident safety is another important component of safety for nuclear reactors. However, there are a number of reasons why accident safety is not included among the assessments of this dissertation. One reason is that detailed assessments of nuclear facility safety require specific technology and design details that go far beyond the assumptions governing a generalized fuel cycle. For previously deployed reactor technologies, safety estimates are in part governed by data describing the frequencies of previous component failures, including pumps, valves, pipes,

motors, switches, and other instrumentation [NRC 1975]. Comprehensive reactor safety assessments also incorporate site-specific factors such as hydrology, geology, and the proximity to human populations, and require the development of criteria and analytical methods for assessing radiological, thermal-hydraulic, and other performance types [Westinghouse 2009]. This leads to the next reason for accident safety's omission, which is that a completely different set of approaches is required to analyze accident safety compared to routine operational safety. Even preliminary assessments of more commonly studied scenarios, such as the loss of coolant accident (LOCA), require a fairly detailed reference design description and computationally intensive radiation transport and thermal hydraulic simulations [Stosic 2008]. As such, describing "accident safety" as a single parameter is not something that can be easily calculated or communicated, even for well-understood designs. Perhaps the most important reason for omitting reactor safety, however, is that it is already the subject of many studies in the literature, even for advanced designs. Sodium-cooled reactors alone are the dedicated subject of a variety of technology-specific codes (e.g., [Tobita 2006, Schmidt 2011, Dunn 1974, Shire 1977]); the same is true for molten salt reactors (e.g., [Zhang 2009, Suzuki 2008, Guo 2013]). For these reasons, accident safety is not addressed in this study.

EH&S metrics have the potential to intersect with other considerations, in particular the economics of a fuel cycle. The scope of this dissertation is defined to exclude economics; however, the aspects of economic analysis for nuclear fuel cycles is briefly addressed here. As with accident safety, detailed (and even preliminary) economic assessments require fairly detailed design specifications. Because of this, detailed assessments are generally conducted only for specific processes or nuclear fuel cycle scenarios, such as for the recovery of uranium from

seawater [Lindner 2014]. However, detailed analyses such as these rely on cost data (ideally from industry, sometimes from extrapolated from laboratory experience); for advanced fuel cycle options, even if rough data can be collected or extrapolated for certain steps, there will undoubtedly be gaps. As such, there are also reports that conjecture about fuel cycle costs from a more generalized, fuel cycle standpoint. More general reviews of fuel cycle economics have been the subject of studies by the Korea Atomic Energy Research Institute [Ko 2012], Europe's Nuclear Energy Agency [NEA 1994], Idaho National Laboratory [Shropshire 2009], and a component of the US Department of Energy's Fuel Cycle Option Evaluation and Screening Study (FCO-ESS) [Wigeland 2014]. Such studies, in themselves, run to hundreds or even thousands of pages. These reports are recommended as economic complements to the EH&S conclusions in this dissertation.

CHAPTER 2, BACKGROUND AND LITERATURE REVIEW ON THE ANALYSIS OF THORIUM FUEL CYCLES

This literature review presents the background of some key topics and concepts pertinent to this research. Additional literature will be presented in the subsequent chapters, but there are three overarching concepts that are helpful to introduce more generally prior to subsequent technically-oriented chapters. This chapter will discuss three overarching topics, each closely tied to one particular chapter in this dissertation: thorium resources and availability (closely tied to Chapter 3), fuel cycle assessment and performance metrics (closely tied to Chapter 4, but also connected to Chapters 3 and 5), and fuel cycle transition analysis (closely tied to Chapter 5).

2.1. Thorium Resources and Availability

Resource availability is not always considered as a conventional EH&S measure; nevertheless, the effective preservation and use of natural resources is a key topic related to the stewardship of the environment and to the tenets of environmental engineering. Namely, continued resource availability is a measure of sustainability, which is an important consideration of the environmental performance of a system. Excessive use of a limited resource may have unfavorable economic or other less predictable consequences, such as regional conflict or the need to reconfigure existing infrastructure [Ayres 1992] In addition to the notion of rare or overly-used resources becoming depleted, natural resource consumption imparts its own EH&S footprint through mining excavation, energy requirements for separations, and chemical processing for separations and purification. Previous assessments of "resource sustainability" have been conducted for a variety of naturally occurring commodities, such as gold [Mudd 2007], copper [Northey 2013], and aluminum [Liu 2012]. Chapter 3 will entail an EH&S

assessment of thorium recovery, but it is first helpful to understand the nature of global thorium resources.

Thorium is frequently cited as being an abundant element in the Earth's crust, with estimates ranging from 4.5-7 ppm [Lambert 1968], with the possibility that abundance is even higher (~10 ppm) in the uppermost layer of the crust [Mernagh 2008]. This is somewhat higher than estimates for uranium (1.1-1.7 ppm [Lambert 1968]), and the seemingly elevated abundance of thorium is often cited as a perceived advantage of the thorium fuel cycle. The significance of this difference requires further review, though, because it does not reflect considerations such as the concentration, distribution, and size of major deposits from which minerals are generally recovered.

In terms of thorium's total abundance worldwide, there are at least two major sources for global estimates, from the US Geological Survey (USGS) [USGS 2013] and the Organisation for Economic Co-operation and Development's (European) Nuclear Energy Agency [OECD-NEA 2011]. As Table 1 notes below, the two estimates are inconsistent with one another. An obvious source of the discrepancy is the NEA's incorporation of a greater amount of "inferred" deposits in certain countries that provided estimates. However, both sets of estimates are highly uncertain, and in any case these figures don't provide information about the effective availability of thorium, since deposits must be both concentrated and accessible to be economically viable [Watson 2014].

Table 1, Comparison of Different Estimates of Global Thorium Reserves

Country	Reserve Estimate (MT), [USGS 2013]	Reserve Estimate (MT), [OECD-NEA 2011]
India	290,000	846,000
USA	440,000	434,000
Australia	410,000	521,000
Canada	100,000	172,000
South Africa	35,000	148,000
Brazil	16,000	606,000
Turkey	--	744,000
Egypt	--	380,000
Norway	--	320,000
Venezuela	--	300,000
Russia	--	155,000
China	--	100,000
Others		2,004,000
TOTAL	1,400,000	6,730,000

Thorium occurs in a diverse array of geological deposits and mineral types. The major geological categories of thorium deposits are igneous intrusive, igneous diffusive, epigenetic, metamorphic, and sedimentary (including placer deposits) [Barthel 1992]. In the 1950s, the US Geological Survey (USGS) reviewed about 100 mineral types that could contain thorium and/or uranium [Frondel 1958]. However, many of the documented minerals are rare, and more importantly, most of the minerals were (and remain) irrelevant from a commercial standpoint. Only a handful of thorium minerals have been seriously considered from the perspective of thorium recovery, namely: monazite [Keni 1990], bastnasite [Wang 2013]; and to a much lesser extent, xenotime [Vijayalakshmi 2001] and thorite/uranothorite [Borrowman 1962]. Most of these minerals contain significant amounts of rare earth elements (REEs), especially those with atomic numbers equal to or smaller than gadolinium's (the "light" REEs). The common coexistence of thorium and the "light" REEs can be attributed to their affinity for valence electron states larger than two,

which in turn gives them similar long-term chemical behavior during geological sedimentary processes [McLennan 1980].

In the US, a number of thorium deposits have been studied in some detail. The most studied site, referenced in several national laboratory reports, is the Lemhi Pass site on the Idaho/Montana border. Lemhi Pass contains most of its thorium content in the mineral thorite, and the thorium concentration in the ore ranges from 0.2% to 3.9% [Meyer 1978]. Oak Ridge National Laboratory (ORNL) described a hypothetical mining and processing facility at the site in order to estimate the radiological impacts associated with facility's airborne releases. The maximally exposed individual was estimated to receive 2.4 millirems (0.024 mSv) [Tennery 1978]. The Wet Mountains deposit in Colorado has a similar grade to that of Lemhi Pass [Tennery 1978]. The Bald Mountain site in Wyoming was found to contain 4.3 pounds of monazite per ton of ore, with the monazite containing 8.8% thorium oxide [Borrowman 1962]. Alaska's Bokan Mountain contains significant quantities of thorium, uranium, and REEs [Thompson 1980] and may be of interest if commercial activity to recover REEs occurs at the site. Alaska has another thorium-bearing deposit at Salmon Bay [Warner 1989]. There are also a handful of REE mineral deposits around the country which have been documented, including Mountain Pass in California, Pea Ridge in Missouri, the Bear Lodge Mountains in Wyoming, and various placer deposits along the mid-Atlantic seaboard [Long 2010, Van Gosen 2014]. Figure 1 visualizes the distribution and variety of these deposits. The size and accessibility of these deposits led many studies to conclude that thorium availability would not pose a problem for future deployment (e.g., [Bell 1971]).

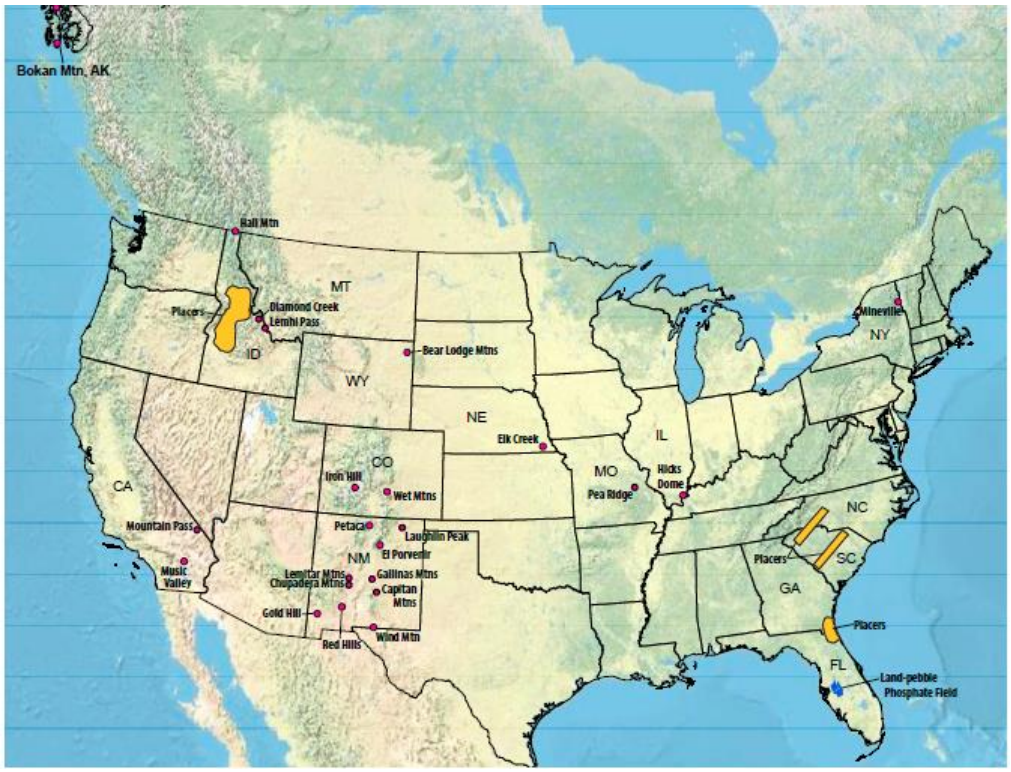

Figure 1, Major Known REE Deposits in the US [Long 2010]

Outside the US, the locations of individual deposits are generally not as well-characterized, even though some of these countries are thought to have very large thorium reserves. Given its interest in thorium fuel cycles, India has surveyed its coastal placer deposits, identifying significant deposits in the states of Andhra Pradesh, Orissa, Tamil Nadu, and Kerala (along the eastern and southern coasts) [Bhola 1964, Mohanty 2004]. Australia, another country with significant thorium resources, has had its thorium resources characterized at a preliminary level. Like in India, most of Australia's known thorium reserves are held in coastal placer deposits, particularly in Western Australia near Perth and in southeastern Queensland [Mernagh 2008]. There are also several vein-type and igneous-intrusive deposits in various parts of Australia's interior [Mernagh 2008]. Brazil also hosts many thorium-bearing coastal placer deposits, along with at least one major igneous-intrusive deposit in the state of Minas Gerais [Waber 1992]. Other specific

deposits have been described in South Africa, Norway, Greenland, China, Nigeria, Namibia, Kyrgyzstan, Italy, Canada, Sierra Leone, Madagascar, Guyana, and Pakistan [Barthel 1992].

As Chapter 3 will discuss at length, the opportunity exists for thorium to be recovered as a by-product of other commodities, particularly titanium. The subject of thorium recovery will also be addressed in that chapter.

2.2. Fuel Cycle Performance Metrics

Meaningful comparisons of nuclear fuel cycle options need to incorporate well-developed and consistently-applied performance metrics. This concept is not limited to assessments of nuclear energy; the notion of metrics development can be applied to many fields and is essentially the selection of quantitative measurements to inform decision-makers with regards to the following types of questions (adapted from [Tatikonda 2007]):

- How well is the system doing (or how well would it do if it were implemented)?
- What have we learned from previous operations or efforts, and how relevant are they to the proposed efforts?
- What should we do in the future?

Performance metrics can be used to evaluate all of the facets of a design, system, or approach, or it can focus on specific areas such as sustainability [Schwarz 2002], economics [Morales 2009], societal impact [Szekely 2005], and energy security [Sovacool 2011]. Of particular interest to this study is the development of metrics related to EH&S. Environmental metrics are routinely developed and applied in the energy industry to advanced concepts. An assessment of the

installation of large-scale solar plants conducted by Brookhaven National Laboratory is indicative of this type of approach; BNL used the metrics of land use, human health, resource usage, and energy use to compare alternatives [Turney 2011]. Similar analyses can be identified for geothermal plants [Axtmann 1975], fossil fuels [Jenner 2013], and wind [Kunz 2007].

The assessment of nuclear fuel cycles is in some ways similar to that of other energy options, but with a few distinct considerations (e.g., radiation, fissile material management, and institutional challenges like licensing). Fortunately, the selection of performance metrics, as specifically applied to nuclear fuel cycle assessment, can be informed by prior efforts. Among the most comprehensive recent efforts for nuclear fuel cycles has been the US Department of Energy's Fuel Cycle Option Evaluation and Screening Study (FCO-ESS) [Wigeland 2014]. The FCO-ESS sought to identify preferable fuel cycles for focused R&D efforts. As a basis for quantitatively distinguishing the most preferable fuel cycles (while avoiding specific technology assumptions to the maximum extent possible), a number of criteria were defined which could impact a fuel cycle's favorability. In the final version of the FCO-ESS, nine criteria were selected [Wigeland 2014]:

- Nuclear Waste Management
- Proliferation Risk
- Nuclear Material Security Risk
- Safety
- Environmental Impact
- Resource Utilization
- Development and Deployment Risk

- Institutional Issues
- Financial Risk and Economics

Of these, the Nuclear Waste Management, Safety, Environmental Impact, and Resource Utilization metrics are most relevant to the work discussed in this proposal. Relevant metrics included the activity- and mass-related metrics under Waste Management, "Challenges of Addressing Safety Hazards" under Safety, "Radiological Exposure" under Environmental Impact, and the "Natural Uranium" and "Natural Thorium" requirement metrics under Resource Utilization [Wigeland 2014].

In a similar vein, the Generation IV International Forum (GIF) has identified four goals that Gen-IV reactor designs would strive to meet: sustainability, safety and reliability, economics, and proliferation resistance. Under GIF definitions, sustainability incorporates both resource utilization and waste management, while the safety goal only addresses the likelihood and extent of accident scenarios (i.e., no routine hazards were considered) [GIF 2002].

The Electric Power Research Institute (EPRI) has developed a comparative risk assessment tool, which could be viewed as the predecessor for the work described in this proposal. EPRI used the comparative risk assessment approach to compare the performance of the current once-through nuclear fuel cycle with uranium in light water reactors and a modified-open nuclear fuel cycle with a single recycle of plutonium in mixed-oxide-fueled light water reactors [EPRI 2014a]. The comparison focused on environmental attributes and considered occupational radiological impacts, low-level waste volumes, and repository waste volumes.

Other relevant EPRI work includes the Decision Framework, which enables nuclear decision-makers to inform the decision-making process. In the past, the Framework has emphasized making distinctions between different fuel cycle options and design attributes, and it is flexible so that it could be re-worked to compare specific nuclear technologies or development pathways as well. In early iterations, five criteria (which would later be re-named "attributes") were considered: Sustainability of Fuel Supply, Proliferation Resistance & Physical Security, Waste Management, Fuel Cycle Safety, and Economic Competitiveness [EPRI 2011]. These criteria were considered only semi-quantitatively and did not identify specific metrics within these areas. The next iteration demonstrated how more detailed approaches might be taken beneath these high-level attributes by examining driving factors in Waste Management and Fuel Cost, but detailed examinations were not conducted for each criterion [EPRI 2013b]. Vanderbilt became involved in the process and identified a number of sub-attributes (re-named from criteria at this point) for each of the top-level attributes [EPRI 2014b]. The most implementations have identified the additional top-level attributes of "Infrastructure and Development" and "Flexibility" [Gardiner 2015a, Gardiner 2015b].

The Nuclear Waste Technical Review Board (NWTRB) has evaluated several facets of the environmental impact of nuclear fuel cycles, with an emphasis on the back-end of the fuel cycle. The NWTRB's review of the disposal and storage of spent nuclear fuel examines several technical aspects of SNF management, but EH&S concerns are the first (and presumably important) group of parameters discussed. These parameters included [NWTRB 1996]:

- Radiation exposures to workers

- Radiation exposures to the public
- Air and water quality
- Land use
- Transportation risks

It is also possible to conduct "deeper dives" into major categories of environmental impact; for instance, the NWTRB has done follow-up studies on transportation risk that its constituent factors, such as radiological impact, accident tolerance, and the impact of potential damage to waste package constituents on long-term stability [NWTRB 2010].

There are a handful of other studies from academia which have examined some particular EH&S aspect of the nuclear fuel cycle. A collaborative Swedish-Australian university team has attempted to quantify the environmental impact associated with premature phasing out of nuclear reactors, using the Swedish fleet as a representative case. The primary EH&S metrics applied include carbon emissions and human mortality associated with fuel cycle operation [Qvist 2015]. A study in Brazil simply attempts to list categories of possible environmental metrics, rather than focusing on their quantification; this paper discusses environmental disturbance from construction, transportation impacts, thermal emission impacts on flora and fauna, aesthetic impacts, radioactive and other hazardous effluent release, transportation risks from moving spent nuclear fuel or other radiological wastes, and long-term repository risk [Paschoa 2003]. The University of Michigan identified and quantified the inventories of major categories of material resulting from nuclear fuel cycles including: spent nuclear fuel (both commercial and weapons-related), reprocessing-based high-level waste, low-level waste, highly-enriched uranium,

separated plutonium, depleted uranium, Cs-137 and Sr-90 capsules, uranium mine and mill tailings, contaminated soil, and contaminated water [Ewing 2008].

2.3. Fuel Cycle Transition Analysis

Section 2.2 emphasized the assessment of attributes of fuel cycles at steady-state operation, i.e., their characteristics after they have already been fully implemented. Additional challenges presented when analyzing transitions from one fuel cycle to another, which includes a range of intermediate fuel cycle phases. There are several examples of parameters associated with fuel cycle transitions that may be of interest which are not elucidated by steady-state analysis alone (adapted from [OECD-NEA 2012a]):

- Time lag to reach equilibrium
- Impact of varying transmutation or breeding performance
- Accumulation of material stockpiles during transition or growth periods
- Investments required to reach equilibrium
- Waste disposition pathways

Chapter 5 will conduct a comparative dynamic assessment for a pair of representative thorium- and uranium-based fuel cycle options, but it is important to keep in mind that a variety of previous transition studies have already been conducted. While the subject of these studies has varied, the most common group of scenarios to examine has been the transition from the present once-through uranium fuel cycle in light water reactors to a recycle-based strategy using uranium and plutonium in sodium-cooled fast reactors (SFRs). The following review of previous

transition studies while highlight the similarities and differences among the assumptions of these studies, which turn helps to pinpoint reasonable approaches for subsequent work.

The NEA has conducted several transition studies, including one that considered regional scenarios for a set of countries in Europe currently totaling 120 GWe of nuclear energy installation; this study emphasized transitions from LWRs to SFRs. Some of the major assumptions are listed below [Bianchi 2011]:

- Scenario goes from 2000 to 2150 (codes start at 1980 to establish initial conditions).
- No plutonium is recycled within LWRs (i.e., no MOX LWRs).
- SFR fuel is fabricated from reprocessed plutonium and depleted U.
- Minor actinides (MAs) are NOT recycled; they are disposed of along with FPs.
- Current generation LWRs are deployed up until 2040.
- Advanced LWRs and SFRs are deployed from 2040-2100.

In addition to these assumptions, the following parameters shown in Table 2 were adopted. The LWR values account for the ratio of PWRs to BWRs. Two sets of SFR characteristics are considered: “SFR-R” represents the approximate extent of SFR technology today, while “SFR-A” represents the hypothetical capabilities of advanced SFRs that may require extensive R&D.

Table 2, Basic Reactor Parameters Used in [Bianchi 2011]

Parameter	LWR	ALWR	SFR-R	SFR-A
Reactor unit capacity (GWe)	1	1.5	0.9	1.8
Heavy nuclei load (t)	80	135	64	120
U^{235} enrichment (%)	4	4.9	0.2	0.2
Burn-up (GWd/t)	45	60	65	140
Unat consumption (tU/GWe yr)	180	150	–	–
Excess fissile Pu production[a] (kg/GWe yr)	–	–	40	295
SNF cooling time (yr)	5	3	3	3
Plant lifetime (yr)	50	60	60	60

[a] Difference between the production and consumption of plutonium for a year of operation at 1 GWe power level.

A subsequent NEA study considered two different types of SFRs in its scenarios. The first is a low-breeding ratio variant of the SFR which is linked with PWRs in a two-stage system. The following Table 3 describes the parameters of both the PWRs and the SFRs (the specific SFR design considered in this study was called "ISOGENERATOR").

Table 3, Reactor Parameters Used in [OECD-NEA 2012b]

	PWR	ISOGENERATOR
Burn-up (GWd/tHM)	50	136
Cooling time (y)	5	2
U-235 enrichment, Pu content (%)	4.5	21.19
Electrical nominal power (GWe)	1	1.45
Efficiency (%)	34	40
Load factor (%)	85	85
Breeding ratio	-	1.022
Cycle length (efpd)	410	340
Total irradiation time (efpd)	1 640	1 700

The study also examined a "high-breeding ratio" alternative with a breeding ratio of 1.5, a doubling time of either 11.7 or 17.8 years (two different ex-core time possibilities), a power of 1400 MWe, and an average burnup of 85.6 GWd/MTHM. For all scenarios incorporating SFRs, assumptions were also required regarding the availability of reprocessing capacity as a function

of time. The addition of new fuel reprocessing facilities over time was represented by a step curve, as shown below in Figure 2.

Figure 2, Assumed Changes in Reprocessing Capacity in Europe over Time [OECD-NEA 2012b]

A study in Japan assumed a deployment of timeline of 2025 for technology demonstration and 2050 for commercial deployment. The Japanese "Basic Energy Plan" consists of adding 14 new plants (contributing 20 GWe of electricity) by 2030. Two breeding-ratio cores are considered [Shiotani 2011]:

- Low-breeding core: breeding ratio of 1.03
- High-breeding core: breeding ratio of 1.2

A breeding ratio of 1.1 was assumed for the analysis. Furthermore, the following transition conditions are assumed [Shiotani 2011]:

- Pu will be recycled in LWRs in years prior to SFR deployment.
- LWRs will be replaced one-by-one by SFRs as their lifetime expires after 2050. This will result in the last LWRs being replaced around 2130.
- Steady-state nuclear capacity will be stable at 68 GWe.

A KAERI study considers the Korean design KALIMER, which is an SFR rated at 600 GWe. The timeline of the scenario assumes that total reactor capacity will rise from 13.8 GWe in 2000 to 27.3 GWe in 2030. By 2050, nuclear will generate 41.3 GWe (59% of total energy use). Annual electricity demand is assumed to rise 0.95%/year. Nuclear fuel cycle timeframe assumptions include the following:

- 8 months for fuel reprocessing
- 8 months for fuel fabrication
- 2-month post-fabrication storage

It is assumed that reprocessing results in 0.1% losses. It is assumed that the first FR begins construction in 2025 and begins operation in 2030. The fraction of new builds that are FRs depends on the assumed conversion ratio [Jeong 2006, Jeong 2010, Jeong 2013].

The Electric Power Research Institute (EPRI) has conducted SFR transition analyses from a cost perspective, both for SFRs operating with modified-open recycle [EPRI 2010a] and full recycle [EPRI 2010b]. Assumptions regarding the flows through reprocessing facilities were important for both of these studies; it was assumed that the fast reactors:

- Operated at 1450 MWe

- Had a conversion ratio of 1
- Had a plutonium content in the fuel of approximately 16%, a minor actinide content of 1%, and a discharge burnup of 140 GWd/MTIHM
- Were subject to reprocessing losses of 0.1% for Pu and the minor actinides
- Had their fuel cooled for five years between discharge and reprocessing
- Had their resulting high-level waste stored for 50 years prior to disposal

ANL has conducted several studies on the topic of transitions to a fleet of SFRs. Two transition pathways were compared as part of the analyses: one proceeding through the intermediate use of a modified-open cycle with MOX fuel in LWRs, and the other proceeding directly from the once-through cycle in LWRs to full-recycle in SFRs. Among the key assumptions of this work [Kim 2011]:

- The first deployment of MOX-fueled LWRs occurs in 2025.
- The first deployment of full-recycle fast reactors occurs in 2050.
- All reactors have a lifetime of 60 years.
- The nuclear energy annual growth rate is 1%, starting in 2015.
- For the pathway involving MOX in LWRs, reprocessing capabilities for used LWR fuel begin in 2023 at 2000 MTHM per year, with an additional 500 MTHM/yr facility coming online to reprocess fuel from the MOX-fueled LWRs to supply to the SFRs.
- For the pathway proceeding directly from the once-through cycle to the SFRs, a 2000 MTHM/yr reprocessing plant starts in 2048.

ANL has also monitored the development of India's Three-Stage Nuclear Power Programme and its implications for realistic deployment scenarios involving fast reactors. This three stage program consists of (1) uranium-fueled pressurized heavy water reactors, supplying plutonium to (2) SFRs capable of operating on U/Pu or Th/Pu fuels, the latter option supporting (3) Th/U-233-fueled advanced heavy water reactors. Stage 1 has been commercialized in India for some time, while the fast breeder reactors are in the advanced demonstration phase (nearly at commercial deployment). However, the timescales over which large numbers of fast reactors will be deployed is uncertain [Bucher 2009].

France's CEA has examined scenarios for fast reactor deployment with plutonium recycle. The study considered two scenarios; an aggressive scenario in which one third of the capacity added beginning in 2040 consists of SFRs, and a more conservative scenario in which no SFRs are constructed until 2080. The conservative scenario places a greater strain on reprocessing capabilities when SFRs are rapidly constructed in 2080, among other trends [Coquelet-Pascal 2013].

Transitions to Th/U-233 MSRs have not been studied to the same extent as those for U/Pu-fueled SFRs; however, there are still some documented efforts in the literature. One of the most well-documented MSR concepts is the Thorium Molten-Salt Nuclear Energy Synergetic System (THORIMS-NES), developed in Japan. This system incorporated essentially the same fuel salt mixture as the MSBR but re-tailored component design to further support safety objectives [Furukawa 1990a]. THORIMS-NES actually represented a category of designs, which included the small FUJI-II 350MWt power reactor. This smaller design was seen as an ideal approach to bring power to less densely populated regions on a global scale without relying on fossil fuels

[Furukawa 1990b, Furukawa 1992]. Additional physics calculations were performed for this smaller design beyond what was available from the MSBR project [Hirakawa 1990, Kanda 1990a, Kanda 1990b]. In the 2000s, a roadmap was envisioned for the deployment of increasing large FUJI-style reactors to gain experience with the technology and ultimately implement many MSR systems to solve global energy needs [Furukawa 2007, Furukawa 2008, Mitachi 2007, Furukawa 2012]. This study was eventually expanded to consider transition scenarios from the world's current LWR-dominated fleet to one primarily consisting of THORIMS-NES reactors on the Th/U-233 fuel cycle [Kamei 2010]. In this analysis, the present LWR fleet would have its fuel processed for all fissile content to start up a fleet of thorium-uranium MSRs. This was viewed as an intermediate step to a fleet of accelerator molten-salt breeders which would rely exclusively on Th/U-233. The deployment of the accelerator-based reactors would begin about 20 years after the initial fleet of MSRs [Kamei 2010].

This review of transition studies for both SFR and MSR-based scenarios suggests a few things. First, while there are some common assumptions that appear in many studies (e.g., a lack of transuranic recycle, annual energy demand growth of 1%), many other assumptions vary slightly from study to study (e.g., precise deployment dates for advanced technology, breeding ratios). Thus, there is always user discretion regarding the values of certain scenario input parameters, although there are guides for ranges of sensible choices. Also, the majority of these studies used "off-the-shelf" software-enabled fuel cycle simulation tools (see Appendix D for more on this subject), suggesting that a similar approach is feasible for work in this study.

CHAPTER 3, A COMPARATIVE REVIEW OF THE OUTLOOK AND IMPACTS OF NATURAL THORIUM AND URANIUM RECOVERY

At the basis of any nuclear fuel cycle is a dependency on some naturally-existing nuclear material, namely thorium and/or uranium. Even fuel cycles which use uranium-233 or plutonium-239 as their primary fissile content must first produce these isotopes from their naturally-occurring counterparts. While the quantity can vary over several orders of magnitude, every fuel cycle will require some amount of natural thorium and/or uranium per unit of electrical energy produced. This mass carries with it the impacts of its recovery, including chemical requirements and radiological impacts. Furthermore, it is important to consider these amounts in the context of the total reserves of the resource that are available. If a fuel cycle requires "x" amount of a resource per year, and only five times "x" of that resource are known to exist in the world, then it would be difficult to argue for the selection of that fuel cycle as a sustainable option even if its other attributes were extremely appealing.

This chapter presents a sequence of research that has been conducted on the front-end of the thorium fuel cycle over the past three years. The environmental impact of the front-end of the fuel cycle is represented herein as the combination of resource availability (and by extension, sustainability), chemical requirements, and radiological impacts. Cumulatively, this work has supported four conference papers, three journal articles (two directly and one indirectly), and several short sections within papers primarily related to other topics.

3.1. Context for Evaluating Natural Thorium Recovery

In 2012, as DOE-NE was conducting its Fuel Cycle Option Evaluation & Screening effort [Wigeland 2014], it became apparent that thorium resource recovery was not being addressed in a realistic fashion; instead, it relied on outdated assumptions and tenuous analogies to uranium recovery. As discussed in Section 2.1, a series of analyses by US national laboratories examined the potential of large thorium deposits (especially Lemhi Pass on the Idaho/Montana border and the Wet Mountains of Colorado) to supply thorium for nuclear fuel cycle applications by opening new thorium mines at those sites. Since that time, these deposits have not been developed further, and global thorium recovery (such as it is) has been dominated by thorium recovered in India as a by-product of titanium mining. At a summit held in December 2012 at the Colorado School of Mines, the reality of by-product recovery was presented by a Vanderbilt team, suggesting that the impacts associated with the front end of the thorium fuel cycle would be more accurately represented as a by-product recovery scenario [Wymer 2012].

Exploration into the concept of "by-product" thorium has yielded further insights about the prospective recovery of thorium from actively operational mine sites. Mines for titanium, uranium, tin, iron, and REEs can surface significant quantities of thorium-bearing minerals such as monazite, bastnasite, and xenotime. Generally, these minerals are discarded, or less frequently they are processed for REEs. However, mining operations in India have recovered thorium and REEs in monazite as a by-product of titanium in ilmenite. The incremental impacts associated with thorium recovery at titanium mining sites are small [Ault 2013], and the by-product recovery option could be environmentally and economically preferable by avoiding the significant environmental "cost" of opening a separate thorium mine. Furthermore, by-product

recovery of thorium may be appealing to the mining organization by removing some of the radioactivity from the waste stream [Ault 2014a]. Even using conservative assumptions, it is possible to recover enough by-product demand for natural thorium [Ault 2014b, Ault 2015] to sustain the present worldwide nuclear fleet, on a once-through thorium fuel cycle, several times over. A preliminary economic analysis of the by-product thorium concept suggests that most of this thorium would be available at a low cost, although trends of mine operators to prefer sites with less radioactive minerals could have the potential to complicate this scenario [Jordan 2014].

Because by-product recovery of thorium is already implemented on a demonstration-scale in India, and because future recovery of thorium is likely to also follow a by-product recovery pathway, this analysis assumes a particular by-product recovery strategy -- after considering several specific options (described in the following sections).

3.2. Cumulative By-Product Thorium Availability

Before determining the environmental impacts of by-product thorium recovery, it is first essential to determine whether by-product thorium recovery is adequate to satisfy any nuclear fuel cycle demand scenario and whether such a recovery process could operate indefinitely (i.e., is sustainable). Several prospective by-product recovery pathways were identified and evaluated: titanium mining, uranium mining, tin mining, iron mining, and rare earth element (REE) mining.

3.2.1. By-Product Thorium Recovery from Titanium Mining

Titanium is a major global commodity that is recovered in quantities greater than 7 million MT/year [USGS 2013a]. It is principally recovered from two minerals: ilmenite and rutile. Both

of these are heavy minerals which are found collocated with the thorium-bearing mineral monazite on a regular basis. Global sources of titanium are abundant, large, and widespread, as is shown by Table 4:

Table 4, Major World Producers of Titanium in 2012 (>50,000 MT/yr) [USGS 2013a]

Country	Annual Ti Production via Ilmenite (MT/yr)	Annual Ti Production via Rutile (MT/yr)	**Total Annual Th Production (MT/yr)**
Australia	940,000	480,000	**1,420,000**
South Africa	1,030,000	131,000	**1,161,000**
Canada	700,000	--	**700,000**
China	700,000	--	**700,000**
India	550,000	25,000	**575,000**
Vietnam	500,000	--	**500,000**
Mozambique	380,000	8,000	**388,000**
Ukraine	300,000	60,000	**360,000**
Norway	350,000	--	**350,000**
USA	300,000	--	**300,000**
Madagascar	280,000	--	**280,000**
Sierra Leone	--	100,000	**100,000**
Sri Lanka	60,000	--	**60,000**
Brazil	45,000	5,000	**50,000**

Thorium is actively recovered as a by-product of titanium in India. There are a number of other countries, distributed across all continents except Antarctica, with titanium mining operations in similar geologies to those of India's titanium mines. The availability of information on the thorium content of these titanium deposits is varied. Virtually all of the titanium mining in the US takes place in one large region, the Piedmont formation (this describes an area between the Appalachian Mountains and the Atlantic Ocean in Virginia, North Carolina, South Carolina, Georgia, and Florida); the only current mines are in Virginia, though Florida and Georgia have operated heavy mineral mines in the past [Long 2010]. In Australia a number of mined deposits

exist. These deposits are highly variable in their composition; however, an average mineral composition of the nation's combined deposits has been estimated: 11.7% rutile, 31.7% ilmenite, 5.9% leucoxene, 21.6% zircon, 2.3% monazite and 0.4% xenotime [Miezitis 2013]. Zircon may also be recovered, as it is the major source of metallic zirconium; leucoxene is a lower-grade titanium mineral which is not typically recovered in the Piedmont region or elsewhere.

It should be noted that both ilmenite and monazite are widely occurring minerals with variable mineral composition. For instance, Indian heavy mineral sand operations have observed Th concentrations in monazite ranging from 5-10%, although Indian monazite tends to have slightly higher thorium content than at other locations [Keni 1990]. Across a string of placer deposits in the coastal eastern United States, monazite was observed to have thorium content ranging from 2.5 to 7.8%, with a mean of 5.7% Th [Long 2010]. In general, while the range of Th contents is variable, most locations' averages seem to hover around 5% Th, which was deemed to be an acceptable average figure for this study. This analysis makes the following assumptions: ilmenite has an average concentration of 31.6% Ti, rutile is 60.0% Ti, and monazite is 5% Th. The titanium composition estimates for ilmenite and rutile are based on typical mineral composition estimates as catalogued in mineral databases [MINDAT 2016]. Recovery of thorium during monazite processing is estimated to be 94%, based on experience in India [Keni 1990]. Thus, potential annual thorium production is computed as:

$$[MT\ Th] = .94 * \left([MT\ Ti]_{ilmenite} \frac{.05x_{monazite}}{.316x_{ilmenite}} + [MT\ Ti]_{rutile} \frac{.05x_{monazite}}{.600x_{rutile}}\right) \quad (1)$$

Here, x represents the mass fraction of the ore body which consists of the mineral designated in the subscript. Mass fraction data was not identified for all nations considered in this analysis. Correspondingly, the mass fractions given by the Australian data are used to extrapolate thorium availability from titanium production for countries other than India, Brazil, and the US in Table 5 below, since these figures represent the averages of many mines located in geographically disparate regions across an entire continent.

Table 5, Summary of Potential Thorium Recovery from Titanium Mining [Ault 2015a]

Mine Country	Annual Ti Production, all sources (MT/yr)	Potential Annual Th Production (MT/yr)	Mineral Type/Notes
India	575,000 (2700 MT/yr REEs)	5,900 (230 possible, 100 actual)	Mostly ilmenite, some rutile; value in parentheses represents potential based on current REE production rates, not Ti production rates. Values in parentheticals show possible Th production based solely on amount of REEs presently recovered in this country.
Brazil	50,000 (550 MT/yr REEs)	540 (47)	Mostly ilmenite, some rutile; values in parentheses represents potential based on current REE production rates, not Ti production rates. Values in parentheticals show possible Th production based solely on amount of REEs presently recovered in this country.
Australia	1,420,000	16,800	Mix of ilmenite and rutile; Based on average composition of many heavy mineral mines
South Africa	1,161,000	12,600	Mostly ilmenite, some rutile; based on Australian mineral ratios
USA	300,000	7,600	Ilmenite only; based on Piedmont region concentrations
Canada	700,000	7,300	Ilmenite only; based on Australian mineral ratios
China	700,000	7,300	Ilmenite only; based on Australian mineral ratios
Vietnam	500,000	5,200	Ilmenite only; based on Australian mineral ratios

Ukraine	360,000	4,000	Mostly ilmenite, some rutile; based on Australian mineral ratios
Mozambique	388,000	3,900	Ilmenite only; based on Australian mineral ratios
Norway	350,000	3,600	Ilmenite only; based on Australian mineral ratios
Madagascar	280,000	2,900	Ilmenite only; based on Australian mineral ratios
Sierra Leone	100,000	1,500	Rutile only; based on Australian mineral ratios
Sri Lanka	60,000	620	Ilmenite only; based on Australian mineral ratios
TOTAL	**6,944,000**	**79,800**	

As alluded to previously, potential sources of error in these estimates could arise from the application of Australian data to non-Australian sites (which, however, accounts for 61% of the total) and unanticipated deviations in the titanium and thorium content in ilmenite and monazite, respectively. However, even with a particularly wide confidence interval, titanium mining represents (by total potential MT of thorium recovered) the largest opportunity for recovery of thorium as a by-product.

3.2.2. By-Product Thorium Recovery from Uranium Mines

Rare earth mining, and mining operations that surface coincidental REE minerals, are probably the most well-understood pathways to thorium recovery (e.g., [Keni 1990], [Mukherjee 2003], etc.). However, a number of other abundant minerals with thorium, such as thorite, exist that are not necessarily associated with REEs. Without the potential for products that are presently commercially viable to drive production, these minerals are frequently disregarded. The Lemhi Pass deposit, an extensive thorite vein on the Idaho/Montana border in the US, is an example; it contains a significant thorium concentration of 0.4% and is located relatively close to the surface

[Van Gosen 2009]. In the US thorium fuel cycle analyses of the 1970s, Lemhi Pass was often considered the most likely thorium resource should a demand emerge [Tennery 1978]. However, this demand never materialized, and it appears unlikely that thorite vein mining will emerge as a profitable source of thorium in near-term decades.

It seems logical to evaluate the potential for co-producing Th with U, as practices for handling radioactive materials are already in place at these sites. Furthermore, there is a precedent for by-product recovery at uranium mine sites, since in the past vanadium has been recovered as a by-product of some uranium mines in the western US [Crouse 1959b]. At some locations, thorite and other thorium-bearing minerals can be found in conjunction with uranium minerals. In fact, as in the case of uranothorite, some minerals contain *both* uranium and thorium. The thorium content of the world's major uranium mines varies due to the array of geologies that are currently exploited. However, mines which currently employ the in-situ leaching (ISL) technique to recover uranium will likely not be able to recover significant thorium content -- even where present. ISL works by using a mildly basic or acidic solution to oxidize uranium to the hexavalent state, where it is soluble and becomes part of the solution "liquor". However, thorium will not oxidize to the hexavalent state and remains insoluble and, thus, locked up in the geological formation [OECD-NEA 2014]. One consequence of this insolubility is that thorium's abundance in seawater is much lower than that of uranium (0.4 ppt for Th vs. 3.3 ppb for U [Bardi 2010]), and any future deployment of uranium seawater extraction would not be expected to recover thorium [Herring 2012].

Table 6 summarizes the world's largest uranium mines which do *not* use the ISL method and their thorium-producing potential. Data for the two Nigerien mines is taken from the ratio of activity

from Rn-220 (for Th) and Rn-222 (for U). Assuming secular equilibrium, it can be inferred that the Th/U ratio at Arlit is 1.21 (Akouta is assumed to be similar to Arlit) [Abdou 2005]. The Canadian mines of northern Saskatchewan are promising options for large-scale thorium recovery due to the presence of considerable monazite concentrations in conjunction with primary uranium mineral, uraninite [Hecht 2000]. A survey of the uraninite in the vicinity of these mines indicated a UO_2 content of 56.29-64.29% and a ThO_2 content of 6.46%-8.65%, yielding an average Th/U ratio of 0.125 [Annesley 2010]. This is likely an underestimate of the total Th content of the Canadian ores, since this area is known to contain small amounts of monazite amidst the uraninite. However, reliable quantitative data for the amount of monazite in the ores was unavailable, so the thorium contribution from monazite in the northern Saskatchewan area is neglected in this study. The Th/U ratio at Russia's Krasnokamensk mine is taken to be 0.42 based on a combination of mineral samples at the site [Wittenberg 2006]. At Kayelekera in Malawi, a Th/U ratio (0.43) can be inferred from soil and mineral samples from around the mine site [Paladin 2006]. In Namibia, a number of uranium deposits exist in both the central and southern parts of the country, and the Th/U ratio is variable. In the highest-grade regions, though, the ratio is more consistent, ranging from about 0.05-0.3 [Roesener 1997]. The median of this range (0.175) is used for both Namibian mines in this analysis.

Table 6, Summary of Potential Thorium Recovery at Largest Non-ISL Uranium Mines (>1,000 MT/yr)

Mine Name	Mine Country	Annual U Production (MT/yr)	Potential Annual Th Production (MT/yr)	Source(s)	Mineral Type/Notes
Arlit	Niger	3,065	3,700	[Annesley 2010, WNA 2013]	Sandstone
Akouta	Niger	1,506	1,800	[Annesley 2010, WNA 2013]	Sandstone
McArthur River	Canada	7,520	940	[Hecht 2000, WNA 2013]	Marine sedimentary
Krasnokamensk	Russia	2,011	850	[Wittenberg 2006, WNA 2013]	Mixed granite-volcanic
Kayelekera	Malawi	1,268	550	[Paladin 2006, WNA 2013]	Sandstone (Tabular)
Rossing	Namibia	2,289	400	[Roesener 1997, WNA 2013]	Magmatic-Hydrothermal
Langer Heinrich	Namibia	1,955	340	[Roesener 1997, WNA 2013]	Magmatic-Hydrothermal
McClean Lake	Canada	2,100	260	[Hecht 2000, WNA 2013]	Marine sedimentary
Rabbit Lake	Canada	1,479	180	[Hecht 2000, WNA 2013]	Marine sedimentary
Olympic Dam	Australia	3,390	<1	[Keegan 2008, WNA 2010]	Mixed granite-volcanic
Ranger	Australia	3,146	<1	[Keegan 2008, WNA 2010]	Sandstone
TOTAL			**9,000**		

Give the scale of uranium mining in northwestern Canada, a favorable change to the assumed Th/U ratio in this area could have a dramatic effect on the cumulative estimated Th available from U mining. However, at 9000 MT/year, uranium is still a significant contributor to total Th availability even with the conservative estimates used herein. It is possible that in the future, mines which currently employ ISL may switch to alternative recovery methods (e.g., open pit) due to interest in the otherwise unavailable thorium content, or other reasons. However, ISL mines are not considered in this analysis.

3.2.3. By-Product Thorium Recovery from Rare Earth Element Mines

In addition to the many mines that surface REE minerals in the pursuit of other commodities, some mines in Australia, China, Russia, and the US have been established specifically for REE recovery. With the exception of Russia, these countries recover the mineral bastnasite to obtain REEs. The ore from Australia's Mount Weld mine contains 9.8% rare earth oxides and 626 ppm Th [Miezitis 2013]. Calculations for the Chinese mines is based on Bayan Obo's bastnasite, which has ore containing 5% rare earth oxide and 0.032% thorium oxide [Wu 2010]. At Mountain Pass in the US, the bastnasite contains 2-12% rare earth oxides and about 0.02% thorium [IAEA 2011b]. Russia's Lovozero mine surfaces a unique local ore known as loparite. Loparite is of the perovskite family of minerals, meaning that it contains considerable amounts of titanium and calcium, but its lanthanum, cerium, and niobium content are what drive production [Mitchell 1996]. The thorium content of loparite from Lovozero is about 1.3% [MINDAT 2016].

While most of the entries in Table 1 are individual mines, certain regions of China are a summation of multiple individual mining sites.

Table 7, Summary of Potential Thorium Recovery at "Direct" REE Mines

Mine Name	Mine Country	Annual REE Production (MT/yr)	Potential Annual Th Production (MT/yr)	Source(s)	Mineral Type/Notes
South China	China	38,400	260	[Long 2010, Wu 2010, IAEA 2011b]	Bastnasite; includes multiple mines
Mountain Pass	USA	34,100	230	[Long 2010, Wu 2010, IAEA 2011b]	Bastnasite
Mount Weld	Australia	18,800	130	[Long 2010, Miezitis 2013]	Bastnasite; represents high-grade portion of site
Lovozero	Russia	2,130	100	[Long 2010, Mindat 2013]	Loparite
Sichuan	China	8,500	57	[Long 2010, Wu 2010, IAEA 2011b]	Bastnasite; includes multiple mines
TOTAL		**101,930**	**780**		

The most significant sources of uncertainty in these estimates are expected to originate from the application of Bayan Obo data to the other Chinese mining regions, although Th content seems to be more widely reported for REE mines than for other types of mines examined in this study.

3.2.4. By-Product Thorium Recovery from Tin Mining

One of the primary ores of tin, cassiterite, is a heavy mineral which is frequently associated with the rare earth mineral xenotime. The worldwide market for tin is considerably less than that for titanium, but it remains a major global commodity. A few countries dominate global tin production, as can be seen in Table 8:

Table 8, Major World Producers of Tin in 2012 (>10,000 MT/yr) [USGS 2013b]

Country	Annual Sn Production (MT/yr)
China	100,000
Indonesia	41,000
Peru	29,000
Bolivia	20,000
Brazil	11,500
Other Countries	26,500
TOTAL	230,000

None of the first five countries, which collectively account for over 85% of global tin production, recover any REEs in conjunction with tin mining. However, one minor tin producer, Malaysia, recovers 325 MT REE/yr (in the form of xenotime) in conjunction with mining and processing cassiterite [Long 2010]. This is a significant amount relative to the 3300 MT/yr of tin recovered in Malaysia [USGS 2013b]. While xenotime is thought to be a common mineral, its availability is not presently as widely reported as those of monazite and bastnasite. However, it is known to be present in considerable amounts in the tin deposits of China, Indonesia, and Brazil [Jiang 2004, Bodenhausen 1954, Linharo 2003]. Furthermore, samples of xenotime from Malaysia and China indicate remarkably consistent elemental compositions between locations [Krishnamurthy 2004]. Thus, in this paper, xenotime is assumed to have an average composition of 65% REEs and 3.2% Th [Mindat 2003] at all locations.

Little data is available concerning the thorium or rare earth content at most individual tin mining sites. No records of monazite and xenotime could be identified for Peruvian tin mining, which generally occurs in conjunction with considerably more lucrative copper mining in deposits which are significantly different than the heavy mineral deposits observed in China and Malaysia. Bolivia appears to have some monazite and xenotime at its tin deposits, but the monazite tends to

be an unusual variety with virtually no thorium [Kempe 2008]. Thus, Peru and Bolivia were not evaluated as potential tin-based thorium sources. China, Indonesia, and Brazil all have clear documentation of high monazite and/or xenotime content with their tin ores [Jiang 2004, Bodenhausen 1954, Linharo 2003]. The ratio of REE/Sn production is based on what is currently achieved in Malaysia, and the potential production of Th is based on the composition of xenotime (which, in any case, has a REE and Th content which is similar to that of monazite). Table V summarizes potential thorium recovery from tin mining. Since the nature of monazite-xenotime collocation is not reported for most minor tin producers, other countries are not included in this analysis. However, it is likely that total thorium availability is slightly higher than the figure given in Table 9 due to potential contributions from these minor producers.

Table 9, Summary of Potential Thorium Recovery from Tin Mines

Mine Country	Annual Sn Production (MT/yr)	Potential Annual Th Production (MT/yr)	Source(s)	Mineral Type/Notes
Malaysia (#)	3,300	16	[USGS 2013b, Long 2010]	
China	100,000	480	[USGS 2013b, Long 2010]	Derived from REE/Sn ratio observed in Malaysia
Indonesia	41,000	200	[USGS 2013b, Long 2010]	Derived from REE/Sn ratio observed in Malaysia
Brazil	11,500	60	[USGS 2013b, Long 2010]	Derived from REE/Sn ratio observed in Malaysia
TOTAL	**156,000**	**760**		
(#) - designates country as actively recovering by-product REEs in conjunction with Sn				

Uncertainty in these estimates is expected from the application of Malaysian data to non-Malaysian sites; however, as mentioned previously, China, Indonesia, and Brazil have all been observed to feature significant monazite-xenotime collocation.

3.2.5. By-Product Thorium Recovery from Iron Mining

This entry is restricted to discussing one mine in particular, Bayan Obo in China, because of its unique properties compared to other iron mines. Bayan Obo is a massive mining complex in Baotou, Inner Mongolia, about 600 km northwest of Beijing. The mine principally recovers iron from the minerals magnetite and hematite. In 2006, Bayan Obo produced about 9 million metric tons of iron and steel products [Wu 2010]. Bayan Obo also contains what is sometimes referred to as the world's largest REE deposit in the form of both bastnasite and monazite [Long 2010]. While the size and location of the largest REE reserves can be debated [Long 2010, Els 2013], Bayan Obo *is* undeniably the single mine with the greatest current REE production, at 47,000 MT/yr [Long 2010].

A Chinese study reports that the REE-producing portion of Bayan Obo contains 34% iron, 5% rare earth oxides (REO), and 0.032% Th oxide [Wu 2010]. Renormalizing to ignore the oxygen content, this equates to about 4.3% REEs and 0.028% Th. An IAEA report contains similar values, 5-6% REEs and 0.04% Th oxide (or 4.7% REEs and 0.035% Th) [IAEA 2011b]. Taking the average of these two sources, the ore is estimated to be 4.5% REEs and 0.032% Th. Thus, on average for the production of 1 MT of REEs, 7.1 kg of Th are contained in the ore. There may be additional REE content in other portions of the Bayan Obo complex, but data could not be located.

Table 10, Summary of Potential Thorium Recovery from REE Operations at Bayan Obo Iron Mine

Mine Name	Mine Country	Annual REE Production (MT/yr)	Potential Annual Th Production (MT/yr)	Source(s)	Mineral Type/Notes
Bayan Obo	China	47,000	**330**	[Long 2010, Wu 2010, IAEA 2011b]	Carbonatite with mostly bastnasite, some monazite

There are other iron deposits of the world where monazite, xenotime, or bastnasite may be present in small amounts. At Sweden's Kiruna iron mine, monazite appears irregularly at various areas of the ore body, although never in particularly high concentrations [Harlov 2002]. Small amounts of monazite have also been observed in the regions near the large iron mines of Western Australia [Muller 2005]. Even at the largest iron mines (other than Bayan Obo), thorium recovery does not appear to be a significant option and thus is not included in this paper.

3.2.6. Summation and Final Perspectives on By-Product Thorium Availability

Cumulatively, the potential for by-product recovery from all sources is presented in Table 11, below.

Table 11, Summary of Cumulative By-Product Thorium Availability from Multiple Sources [Ault 2015a]

Primary Commodity	Potential Associated Thorium Yield (MT Th/yr)
Titanium	79,800
Uranium	9,000
Rare Earth Elements ("Direct")	780
Tin	760
Iron	330
TOTAL	**90,700**

To put this figure in perspective, a maximum possible annual demand for thorium from nuclear fuel cycle applications has been estimated. As of 2011, 434 nuclear reactors generate 370.4 GWe of electricity worldwide [WNA 2013]. These reactors do not currently use thorium, but this analysis considers the case where the entirety of this 370.4 GWe production is replaced by a postulated fuel cycle that relies on thorium. As part of DOE's Fuel Cycle Option Evaluation and Screening effort [Wigeland 2014], a number of nuclear fuel cycle options have catalogued material flows available online [Sandia 2016]; some of these fuel cycle options use thorium. As a bounding case, the option analyzed by DOE which uses the most natural thorium on an energy-normalized basis is considered: that is, a molten-salt thorium blanket, driven by an external accelerator-driven neutron source and used in a once-through configuration. This option requires about 37 metric tons of thorium per gigawatt-year of electricity [Sandia 2016]. Even if the entire world switched over to this highly-thorium-intensive fuel cycle, the annual by-product yield of thorium would be sufficient to satisfy this demand more than six times over. Other fuel cycle options, especially those involving thorium recycle, would require less thorium per year.

3.3. Chemical Requirements for By-Product Thorium Recovery

Among the most important environmental considerations of front-end processing is the quantity of reagents that is required to isolate a pure thorium stream. Chemical requirements imply both an economic cost as well as an environmental cost in terms of an energy requirement associated with each reagent's production [Schneider 2014]. Furthermore, chemical inventories are related to safety concepts, since substance hazard and environmental hazard indices are functions of chemical inventory [Greenberg 1991, Cave 1997]. This section thus emphasizes the determination of chemical requirements normalized to the mass of thorium produced, since they can be used to derive subsequent chemical performance measures and are also useful parameters in their own right.

Section 3.2 demonstrated that by-product recovery from titanium is likely to be the dominant recovery pathway for thorium. With this in mind, an analysis was conducted to determine the chemical requirements for recovering thorium from the mineral monazite as a by-product of titanium mining -- based on the site with the most detailed deposit characterization and process experience, India's Kerala state. In this by-product scenario, thorium exists within minerals which primary consist of REE oxides and contain thorium is a minority constituent; monazite, for instance, is generally 3-10% thorium oxide. Following the physical isolation of these REE minerals at a high purity, processing generally consists of an extraction step (using a strong acid or base to pull the constituent components into solution from the refractory mineral form) and a refining step (use of one or more chemical separations processes, often solvent extraction, to obtain a nuclear-grade thorium product stream). Variants of these separations processes have been developed; however, it is necessary to assume certain approaches to quantitatively analyze

the impacts and requirements of thorium by-product recovery. For the Kerala monazite, sodium hydroxide was assumed to be the primary extractant, permitting by-product recovery of monazite's phosphate content as trisodium phosphate (an attractive commercial chemical), while also enabling the straightforward precipitation of thorium as a hydroxide. A second selective precipitation step is used to remove most of the REEs from the thorium product stream, and then a multi-stage solvent extraction system is employed based on TBP-nitrate chemistry to purify the thorium. This recovery approach is consistent with documented thorium recovery practices in India [Keni 1990, Mukherjee 2003].

Using published information from the Indian experience ([Keni 1990], [Mukherjee 2003], [Krishnamurthy 2004], [Haridasan 2008], [Haridasan 2010], etc.), it is possible to estimate the chemical demands of thorium processing normalized to a basis of one ton of thorium product. Flowsheets were developed by breaking down the process into key steps and estimating requirements of these steps.

Monazite processing schemes begin with the use of aggressive chemicals to disrupt the tightly bound phosphate mineral structure. This can be accomplished with either a highly concentrated strong acid or a strong base. Early experience was mostly with the acid process; however, the caustic process is currently preferred since monazite's phosphate content can be separated at a much earlier stage [Hughes 1980]. Large-scale recovery in India has consistently relied on the caustic process. At a sufficiently high pH, virtually all of the rare earth, uranium, and thorium content precipitates as hydroxides, leaving the phosphate content in the aqueous phase as sodium or potassium phosphate. Employing a phase separation process (generally filtration) enables this

aqueous solution to be recovered, and further processed, to yield a marketable trisodium phosphate (TSP) by-product. The solids, which still include a fair amount of undigested monazite, are acidified to return the desired elements to the aqueous phase [Keni 1990]. Any remaining solids are then removed and managed as waste. The pH can then be adjusted to shift thorium and uranium to solid hydroxides while keeping most of the rare earth content in the aqueous phase. A final filtration/drying step produces two distinct product streams, a rare-earth bearing filtrate and a thorium/uranium-bearing hydroxide slurry [Keni 1990]. Figure 3 illustrates the resulting flowsheet for the thorium by-product extraction process, based on parameters from Indian experience.

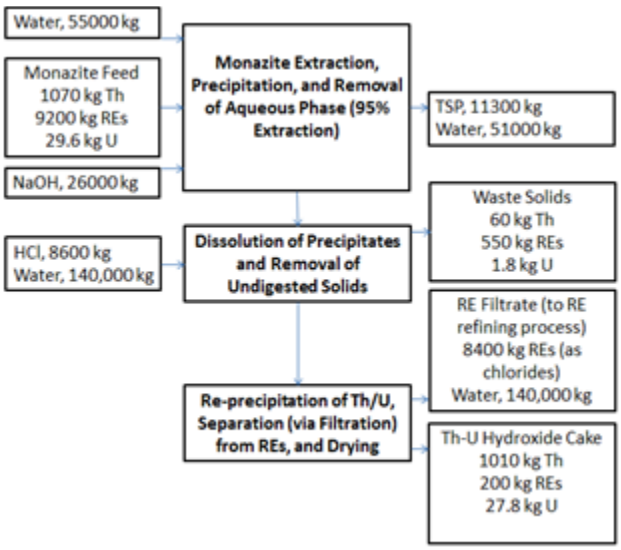

Figure 3, Kerala Monazite Extraction through Divergence of Rare Earth and Thorium Streams [Ault 2013]

In cases where monazite is already being processed for its rare earth content, all steps listed thus far are already being performed for non-nuclear purposes. Only the incremental requirements needed to generate a refined thorium product would be attributed to thorium production. The thorium/uranium-bearing hydroxide cake/slurry, which is frequently managed as a monazite

waste stream (e.g., as described in several process variants within [Krishnamurthy 2004], is the starting point for thorium refining.

There are essentially two steps in the thorium refining process: a step to convert the slurry into an aqueous solution that can be fed to a solvent extraction system, and the actual solvent extraction system to isolate thorium and uranium from any residual rare earth content [Kaya 2003]. A concentrated strong acid is generally used to dissolve the hydroxides (which by this time have been dried to form a cake). Most REEs are in a trivalent state whereas thorium and uranium are in tetravalent and higher[5] oxidation states, so REEs can be readily separated from thorium and uranium in solvent extraction. However, about half of the rare earth content is cerium, which under acidic conditions is generally in the tetravalent state, the same state as thorium, and tends to follow thorium if left in this oxidation state [Hughes 1980]. To counter this, a reducing agent must be added to ensure that cerium remains in the trivalent state along with the other rare earths. A common choice is hydrogen peroxide, which is considered as the representative reducing agent in this analysis. Traditionally, solvent extraction has been carried out with tributyl phosphate (TBP) in kerosene [Keni 1990]. More recently, amines have been used to greater extents to accomplish this separation [Mukherjee 2003]. A number of amine species have been demonstrated to effectively isolate thorium and uranium from residual REEs [Crouse 1959a, Hughes 1980, Mukherjee 2003]; however, there is no clear leading candidate. Therefore, TBP is assumed to be the extracting agent in this analysis. TBP has a higher affinity for uranium than thorium; correspondingly, two solvent extraction loops are usually required,

[5] Uranium has complex valence chemistry; for instance, uranium octoxide (U_3O_8), the primary chemical form of "yellow cake", in which each uranium atom has an average oxidation state of +5.33. Simply calling it "tetravalent" or "hexavalent" is misleading, although uranium also routinely takes those oxidation states as well.

first to remove high-purity uranium and then to remove high-purity thorium from the dissolved REEs. The high-purity uranium can also be recovered as a by-product, although its quantity is much smaller than that of thorium. Figure 4 shows the chemical inputs and outputs from the thorium-byproduct recovery process.

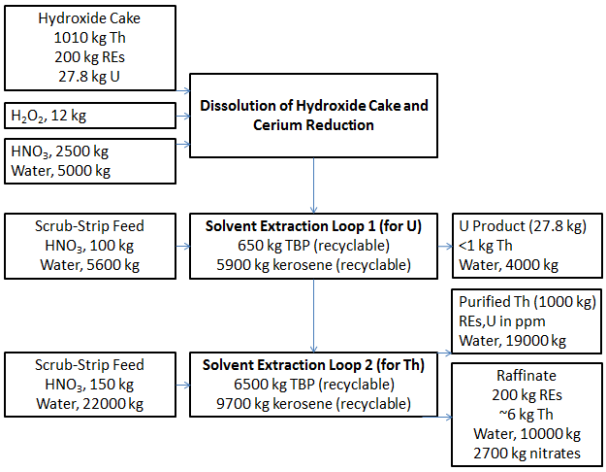

Figure 4, Kerala Thorium Refining from Hydroxide Slurry/Cake [Ault 2013]

The cumulative chemical usages in by-product thorium recovery are then determined by combining the usages from extraction and refining. The following

Table 12 gives the requirements corresponding to 1 MT of thorium product for the Kerala site.

Table 12, Chemical Requirements for Basis of 1.0 MT Th Product for Kerala Site [Ault 2013]

Reagent	Quantity Used (in kg/MT Th produced)
Water	220,000
NaOH	26,000
HCl	8,600
H_2O_2	12
HNO_3	2,800
TBP*	71
Kerosene*	160
*Assuming a 1% degradation of recycled TBP-kerosene per 1 MT Th product	

Reagent usage is significant, primarily due to the fact that monazite is chemical-resistant and because thorium is challenging to back-extract into the aqueous phase due to its lack of a hexavalent state. It should be noted that the chemical requirements attributed to recovering thorium may be reduced somewhat by the yield of other products. This process could also yield 8.6 MT REEs and 11 MT trisodium phosphate for every MT of Th. Of course, each of these products would also require additional purification themselves. The figures above do not account for the recycle of process water since no data is available to support an estimate, although such recovery could be implemented.

3.4. Radiological Impacts of Thorium By-Product Recovery

Radiological impacts are another important component of the cumulative environmental impact of any nuclear fuel cycle process. The presence of thorium in mineral sites often presents challenges due to its radiological hazard. The gaseous radon species that results from Th-232's decay chain, Rn-220 (often-called "thoron"), is considerably shorter lived than the equivalent of

the U-238 decay chain, Rn-222, with half-lives of 55.6 sec and 3.82 days, respectively. As a consequence, Th-232 generally poses less of a long-distance radiological hazard to the public than U-238, but it can still be a significant on-site inhalation hazard during mining and processing. Thorium-based radiological hazards have impacted cassiterite operations in Malaysia [Ismail 2001] and ilmenite operations in India [Haridasan 2008], among others. The Malaysian facility, in particular, garnered international attention when it became the subject of an International Atomic Energy Agency review of its radiological hazards to the public [IAEA 2011a].

It should be noted that most of these hazards are already present -- whether or not by-product thorium is recovered. During monazite processing in India, individual workers typically receive doses of 3.0 to 7.8 mSv per year. Normalized to thorium oxide content and accounting for the number of workers, the routine processing of REEs results in an occupational dose of 6.2 person-mSv/MT ThO_2, or 8.0 person-mSv/MT Th [Haridasan 2010]. These processes result in the formation of a Th-bearing hydroxide slurry which is frequently discarded. The slurry is sometimes processed to create a nuclear-grade thorium oxalate product. This incremental processing leads to an additional occupational dose of 1.6 person-mSv/MT Th [Haridasan 2010]. In other words, when processing for REEs, most of the radiological dose is associated with processing of the primary product, and refining of Th contributes approximately 20% to the overall process dose. In the case of uranium mining and processing, radiological safeguards are already in place, and additional impacts from thorium by-product processing in this industry would not be expected to significantly impact overall process management.

3.5. Comparison of Environmental Impacts between the Recovery of Natural Uranium and Natural Thorium

This dissertation places an emphasis on comparing the environmental performance of thorium- and uranium-based nuclear fuel cycles. Resource recovery and processing is an important component of these fuel cycles that may impact the overall viability of the options. Thus, this section is dedicated to comparing these front-end characteristics. In general, parameters associated with uranium resources and recovery are much more well-established than for thorium, and this section makes use of reported operational data from the sites of actual uranium deposits and mines.

An important consideration to note is that most of these comparisons are made on the basis of mass vs. mass. However, the nuclear utility of one 1 kg of natural thorium is not equivalent to that of 1 kg of natural uranium. There is no clear-cut way to determine which is more "valuable", but some of the more salient points are described here:

- There is a small difference in molar mass between the two elements (232.04 g/mol for Th and 238.03 g/mol for U), so a kilogram of thorium has slightly more total atoms than a kilogram of uranium
- Natural thorium is 100% comprised of a single isotope, Th-232, while natural uranium is comprised of two isotopes (99.28% U-238 and 0.72% U-235)
- Natural thorium contains no fissile material, while U-235 is a naturally-occurring fertile isotope
- Th-232 has a somewhat larger thermal neutron capture cross-section than U-238, meaning that for an equivalent neutron flux Th-232 will be better at producing new fertile

matter than U-238 but it requires somewhat higher fissile material concentrations. This difference is much smaller in the fast neutron spectrum.

- Many uranium-based fuel cycles require natural uranium to undergo conversion/de-conversion and enrichment, processes which carry their own environmental impacts (see [EPRI 2013a])
- Many fuel cycles described as "thorium-based" actually rely more on natural uranium resources than on natural thorium resources

These are some points to keep in mind when describing impacts in terms of "[quantity] per kg natural thorium recovered". Nonetheless, a mass basis is still the most intuitive way to discuss the subject matter and there is not an obvious alternative, so most comparisons in this section will be based on mass.

3.5.1. Differences in Availability vs. Demand, and Implications of Comparing Against "By-Product" Uranium

Compared to thorium, uranium resources are well-studied and many deposits have been characterized in detail. In two-year intervals, the IAEA and Europe's Nuclear Energy Agency collaborate to produce an account of all uranium resources and production, known as the "Red Book". At the time of this writing, the most recent edition was the 2014 Red Book [NEA 2014] which included data from immediately preceding years. Prospective uranium deposits have been identified in 50 countries and are sorted into grades based on their anticipated cost of recovery. Across all grades in all countries, 4.59 million MT of uranium are known, with the figure rising to 7.64 million MT if "inferred" deposits are added to the total [NEA 2014]. To put this figure in perspective, in 2015 global uranium production was approximately 60,000 MT/year and

accounted for 90% of demand (the remainder being supplied by downblended weapons material) [WNA 2015a]. In the bounding case that (1) 100% of uranium was immediately supplied from mines, (2) that only known deposits were considered and no new deposits were considered (also neglecting uranium extraction from seawater, as it presently not economic [Lindner 2015]), that (3) a demand for uranium increased by an aggressive 3% per year, known deposits would satisfy demand for another 143 years. At a more moderate 1% annual increase in demand, the deposits would last 425 years. Of course, more advanced fuel cycles with reprocessing could actually decrease the annual demand for uranium during this period.

In comparison, global thorium deposits, while more poorly understood, are thought to exist in similar total quantities to uranium (6.36 million MT according to [NEA 2014]). Thorium demand by mass would likely be much lower than the present demand even if thorium-based fuel cycles fully replaced uranium-based fuel cycles, since even the most "thorium-intensive" fuel cycle only requires 37 MT of thorium per GWe-yr compared to the 189 MT of natural uranium per GWe-yr required by the present LWR-based fuel cycle [Sandia 2016].

However, these figures do not account for the potential by-product recovery of thorium presented in earlier sections. A more meaningful comparison is the juxtaposition of "near-term" resource recovery potential, meaning those deposits which have current mining infrastructure and may be feasibly used to recover nuclear resources over the next few years.

The first step is to see how by-product uranium recovery stacks up against the by-product thorium recovery scenarios analyzed above. Of the world's fifteen largest uranium mines, the

only one that presently operates using a by-product recovery scheme is Australia's Olympic Dam. Olympic Dam's primary product is copper, and its relatively low uranium concentration would not otherwise warrant a uranium mine at its location. Nonetheless, the importance of uranium recovery at the site is not trivial as it has historically accounted for 20-25% of the mine's revenue [APH 2006]. In 2014, Olympic Dam accounted for 5% of global uranium production [WNA 2015a], which is remarkable for a single mine but still small compared to the total amount of uranium that is recovered as a primary product at other sites.

Other by-product uranium recovery pathways have been implemented in the past. Gold deposits located in the Vaal River region of South Africa have periodically recovered uranium as a by-product when economic conditions are favorable [Lottering 2008]. In the US, uranium has intermittently been recovered from phosphate mines in Florida, and studies suggest that such recovery would be technically feasible at a number of similar phosphate geologies in various countries around the world [De Voto 1979].

In conclusion, there is no meaningful comparison to be made between by-product recovery of uranium and thorium. For thorium, by-product recovery is not only viable, but it is the most sensible short-term (and probably long-term) recovery option among all available choices. However, for uranium, by-product recovery is generally only viable in a small (<10%) subset of instances, and in many cases mines where uranium is the primary product are economically preferable due to their much higher grades. Present low-cost uranium recovery is thus primarily not achieved through by-product pathways, so the by-product uranium recovery concept is not incorporated into subsequent sections.

3.5.2. Differences in Chemical Processing Requirements

Like thorium recovery, uranium recovery can be broken down into major phases. The exact phase breakdown depends on the specific mining approach being used, and each approach imparts its own set of chemical requirements. Global uranium sources supply 17.3% from open-pit mines, 37.5% from underground mines, and 45.2% from in-situ leach approaches [Burkhardt 2013]. While chemical "milling processes" are essentially the same for ores originating from open-pit and underground mines, in-situ leaching presents a distinct processing flowsheet that must be evaluated separately.

3.5.2.1. Chemical Processing Requirements for Milling of Underground or Open-Pit Derived Uranium Ores

"Conventional" uranium milling involves the delivery of uranium ore to a mill site for subsequent processing. The ensuing steps have similarities to the extraction steps for thorium recovery, in that the ore must be sized down to smaller particles before being leached with some kind of acidic or basic solution. Historically, the dominant practice has been the use of sulfuric acid solutions [Seidel 1979], a preference that has carried over to the current day [NRC 2015].

The sequential process that takes uranium ore to yellow cake precipitate that is ready for conversion consists of five major steps [Seidel 1979]:

- Crushing and grinding
- Acid Leaching
- Solid-Liquid Separation and Solids Washing

- Solvent Extraction or Ion-Exchange (this analysis focuses on solvent extraction, which has become the dominant approach for this step)
- Yellow-cake precipitation and drying

Of these five steps, all but the first step requires some chemical reagent inventory to achieve its purpose. There is no "standard" milling process since each site has its own geological considerations which may require additional specialty reagents (such as manganese dioxide for increased oxidation, etc.). Furthermore, estimates of the major quantities of reagents per mass of product depend largely on the concentration of uranium at the site; deposits with highly-concentrated uranium will use "less" reagents per amount of product, at least for the initial leaching step. In the 1970s, the IAEA reported that typical values ranged from 500 to 5000 kg ore required per kilogram of recovered uranium (i.e., 0.02% to 0.2% U in the ore) [Seidel 1979]. In contrast, more recent assessments of commercial uranium deposits indicate that many higher-grade deposits have been identified and that most commercial deposits exist at sites with concentrations well above 0.1% U [IAEA 2009]. Nine uranium mines in Australia and Canada had U concentrations ranging from 0.13% U to 17.8% U. The grade concentration used has a significant impact on chemical estimates. In light of this, three tiers of grades (0.05%, 0.5%, and 5%, or 2000, 200, and 20 kg ore/kg U product) are used as reference values. The sample calculations below are done for the 0.5% grade, but the values for all three grades will be shown in a table at the end of the section.

Acid Leaching: Sulfuric acid consumption typically ranges from 60 to 110 lb. H_2SO_4 per MT of ore [Merritt 1971, Rotty 1975]; taking the median of this range, this is equivalent to 8.5 kg

H_2SO_4 per kg of U product. Standard concentrations for this solution are about 50 g H_2SO_4 per liter of solution, which renormalizes to 170 kg water per kg of U product. While sulfuric acid serves the primary dissolution role, extraction efficiencies are further enhanced by the addition of an oxidant such as manganese (IV) oxide or sodium chlorate. The amount and species used varies by site, but quantities are similar for both MnO_2 and $NaClO_3$ and range from 3 to 10 lb. per ton of ore [Merritt 1971], which using the median of this range, is equivalent to 0.65 kg oxidant per kg of U product.

***Solid-Liquid Separation**:* These separations are primarily achieved through mechanical means based on washing and thickening the extracted uranium solution in stages. While residual bases such as sodium hydroxide may be recycled from latter process steps to improve efficiency, the primary reagent that is added at this step is water. A representative amount of water added at this step is 1 ton of water per 1 ton ore [Merritt 1971], which is equivalent to 200 kg water per kg U product. Flocculating agents (i.e., "sticky" particles that pull suspended colloid material out of solution), most frequently polyacrylamides, are added to improve separations. This typically requires 0.04 to 0.1 lb. per ton of ore; taking the median of this range, this is equivalent to 0.007 kg polyacrylamide per kg of U product.

Solvent Extraction: While the solvent may vary by site, solvent extraction tends to incorporate some species of alkyl phosphate or phosphoric acid, such as Di-(2-ethylhexyl) phosphoric acid (EHPA) or TBP. Some amine species have also been evaluated, but they are not commonly used in industry, and flowsheet data for those methods is scarce [Merritt 1971]. Thus, this analysis will adopt the alkyl phosphate solvent extraction technique as the reference process. Kerosene is

the standard diluent for this process. Extraction typically employs more than one phosphate species; the widely-used Dapex process uses approximately 0.1 M EHPA and 0.1 M TBP per 5.75 g U_3O_8/L [Merritt 1971]. Considering that the molar masses of EHPA and TBP are 322.43 and 266.2 g/mol, respectively, and implementing the same 1% loss per MT of product that was assumed for thorium recovery, this is equivalent to 0.066 kg of EHPA and 0.055 kg of TBP per kg of U product. Since one liter of kerosene carries 5.75 g U_3O_8/L and the density of kerosene is approximately 0.80 g/cm^3, using the same loss rates this process consumes 0.164 kg of kerosene per kg of U product. Additionally, for every 57.5 g of U_3O_8, one liter of 1 M Na_2CO_3 is used for stripping purposes. This renormalizes to 2.2 kg Na_2CO_3 used per kg of U product. There is also the 1 L of water that is added at this stripping step per 57.5 g of U_3O_8, which is equivalent to 20.5 kg water per kg of U product.

Yellow-Cake Precipitation*:* The outgoing solutions from solvent extraction in an acid process, will have a pH in the range of 1.5 to 4 [Merritt 1971]. These must be neutralized by a base, which may take a number of forms: MgO, NaOH, or NH_4OH, especially. Typical consumption of these bases ranges from 0.2 to 0.4 pounds per pound of U_3O_8 [Merritt 1971], which when taking the median of this range, is equivalent to 0.3 kg NaOH per kilogram of U product. Typical concentrations of an NaOH solution are about 10%[6], implying 3 kg of H_2O is used per kilogram of U product at this step.

Combining the reagent use of, the cumulative normalized chemical requirements for uranium milling following underground or open-pit ore recovery is summarized in Table 13:

[6] The publication ([Merritt 1971]) is not clear on the definition of "%", but it is assumed here that it means weight per volume as is conventional for an aqueous solution of a salt.

Table 13, Reagent Use for Uranium Milling Following Open-Pit or Underground Mining

Reagent	Quantity (in kg/MTNU produced)…		
	…at 0.05% Grade	…at 0.5% Grade	…at 5% Grade
Water	3,723,500	393,500	60,500
NaOH	300	300	300
H_2SO_4	85,000	8,500	850
MnO_2 or $NaClO_3$	6,500	650	65
Polyacrylamide	70	7	0.7
Na_2CO_3	2,200	2,200	2,200
EHPA*	66	66	66
TBP*	55	55	55
Kerosene*	164	164	164
*Assuming a 1% degradation of recycled TBP-kerosene per 1 MT U product			

3.5.2.2. Chemical Processing Requirements for ISL-Derived Uranium Ores

In-situ leaching (ISL) is the other major recovery pathway for uranium. Chemically speaking, there are two primary variants to ISL: acid and alkaline leaching. The vast majority of ISL mining worldwide takes place in Kazakhstan (23,800 MT in 2015) and Uzbekistan (2,385 MT in 2015), which both overwhelmingly employ the acid-variation of the process [WNA 2015a]. The next largest ISL uranium recovery site is the Four Mile mine in Australia, which in 2015 recovered 922 MT of uranium [WNA 2015a], and after this there is a further drop to small, intermittently-operating ISL recovery sites in the US. Thus, the acid-leach variant of ISL probably accounts for *at least* 90% of all ISL recovery, and it is thus reasonable to approximate the chemical requirements of ISL altogether as those of the acid-leach variant as it is used in nearly all sites in Kazakhstan.

In Kazakhstan's ISL mines, sulfuric acid is piped into the orebody to serve as both an oxidizing agent and a complexing agent. The oxidation of uranium largely converts it into a soluble

hexavalent sulfuric acid solution which is piped to the surface. Subsequently, the uranium is stripped from the solution using an ion exchange system which requires a resin/polymer. The uranium must then be flushed from the ion exchange column[7] and precipitated using hydrogen peroxide to form the final pre-refining product, U_3O_8.

The WNA has consolidated several estimates of acid consumption at ISL sites in Kazakhstan. A general figure is 40 kg acid per kg U [WNA 2009]. For comparison, acid usage is expected to be closer to 7.7 kg acid per kg U in Australian ISL mines [WNA 2009] Concentrations of U at Kazakhstan's five largest U deposits range from 0.042% to 0.086% U, which, when weighted by their production, average to 0.061% [Taylor 2004]. Furthermore, sulfuric acid is typically consumed in quantities of 5-6 kg per MT of rock [Taylor 2004], which when taking the median of this range in conjunction with Kazakh ore concentrations, is equivalent to 9.0 kg H_2SO_4 per kg of U product. Acid solutions typically contain 2-5 g/L H_2SO_4 [Taylor 2004]; taking the median of this range and assuming that no water is recycled, this implies water consumption of 2576 kg of water are used per kg of U product. Oxidants such as H_2O_2 or $NaClO_3$ are also often (but not always) used in conjunction with ISL. Since no data could be identified regarding the quantity of these oxidants, it is assumed that the same quantity of oxidants is applied as during the first step of open-pit ore milling (0.65 kg oxidant per kg of U product).

Alternative data is available from early American tests with ISL. Typical ISL solutions are comprised of 1.0-1.5 g H_2SO_4 per liter, and is typically injected at about 75 gallons per minute for about 48 hours [Merritt 1971], for a total of 817,650 liters (thereby containing 1020 kg of

[7] The incremental amount of water required to accomplish the flushing process is assumed to be trivial compared to the total amount of water used during ISL.

H_2SO_4). Resulting U concentrations range from 0.20 to 0.35 g/L [Merritt 1971]; using the median of this range and assuming that 95% of the uranium in solution is ultimately recovered as a product, 214 kg of U would be recovered from this single acid injection. Renormalizing, this means that 4.77 kg of H_2SO_4 and 3821 kg of water are used per kg of U product. These parameters are not considered to be as representative of modern processes and are not used in the tables below; however, they are useful for confirming that the previously derived estimates are similar to estimates derived from other sources.

To generate a solid precipitate product, ISL will also require the subsequent separation, solvent extraction, and precipitation steps that were required for open-pit/underground-derived ores. It is assumed here that reagent use is the same as for those cases for 0.05% uranium concentration, which is comparable to the ores in the Kazakh mines. In summary, Table 14 below describes anticipated reagent use for ISL recovery of uranium.

Table 14, Reagent Use for ISL Uranium Recovery and Subsequent Processing for Kazakh Ores

Reagent	Quantity Used (in kg/MTNU produced)…
Water	2,576,000
NaOH	300
H_2SO_4	9,000
MnO_2 or $NaClO_3$	650
Polyacrylamide	70
Na_2CO_3	2,200
EHPA*	66
TBP*	55
Kerosene*	164
*Assuming a 1% degradation of recycled TBP-kerosene per 1 MTNU product	

3.5.2.3. Chemical Processing Requirements for Early Stages of Uranium Conversion

Direct comparisons to thorium's "refining" stage, where the rough solid concentration achieves nuclear-grade purity with only parts-per-million impurities, are difficult to make. The best relationship can be drawn between thorium refining and the first portion of uranium conversion, which begins with yellowcake containing impurities at concentrations of 1-20% and removes most of these impurities prior to hydrofluorination [Carlsen 2013]. In the dominant "wet" conversion process, this is accomplished by dissolving the yellowcake in nitric acid and using a TBP/nitrate-based solvent extraction system which is very similar to the standard approach for thorium refining. Previous analyses have indicated that the initial purification stages of wet refining use 0.41 MT of HNO_3 (approximately 45% of which is fresh and un-recycled) and .000235 MT of TBP[8] per MT of product uranium [Carlsen 2013]. For a consistent comparison of

[8] Actual reported inventories are 0.90 MT of HNO_3 and 0.0235 MT of TBP required per unit of uranium product per cycle, but 55% of nitrate is recycled (reducing actual "fresh" requirements to 0.41 MT), and all of the TBP is recycled aside from 1% losses to radiolytic degradation [Carlsen 2013].

the impacts of thorium and uranium recovery and purification, these estimates should also be included.

3.5.2.4. Cumulative Comparison of Chemical Requirements for Uranium and Thorium Recovery

In summary, the cumulative chemical impacts of uranium recovery are summed from their constituent steps and are compared to those of thorium recovery in Table 15, below. The numbers for the open-pit mining pathway are taken using the values for the 0.5% ore grade.

Table 15, Comparison of Cumulative Chemical Requirements for Thorium and Uranium Recovery and Processing

	Conventional Milling (Open-Pit, Underground)	In-Situ Leach	Early Conversion (Refining)	**Cumulative Requirements for U Recovery**	**Cumulative Requirements for Th Recovery**
Weighting Factor	0.548	0.452	1.00	**n/a**	**n/a**
Water	393,500	2,576,000	0	**1,380,000**	**220,000**
H_2SO_4	8,500	9,000	0	**8,700**	**0**
NaOH	300	300	0	**300**	**26,000**
HCl	0	0	0	**0**	**8,600**
HNO_3	0	0	410	**410**	**2,800**
Na_2CO_3	2,200	2,200	0	**2,200**	**0**
Oxidants (H_2O_2, MnO_2, and/ or $NaClO_3$	650	650	0	**650**	**12**
EHPA*	66	66	0	**66**	**0**
TBP*	55	55	0.235	**55**	**71**
Kerosene*	164	164	0	**164**	**160**
*Assuming a 1% degradation of recycled TBP-kerosene per 1 MT U or Th product					

Again, it is important to recall the context of these chemical requirements when making comparisons between uranium and thorium recovery. These parameters are taken for a globally

typical uranium concentration in ore of 0.5%; some large-scale uranium mines such as those in Western Canada have U concentrations that are over an order of magnitude larger than this, and product-normalized water and sulfuric acid consumption would be anticipated to be far lower at those sites. Unlike for thorium minerals and ores, which have remarkably similar thorium concentrations around the world once monazite has been isolated, uranium mineral characterization is incredibly diverse, and pinpointing a single set of representative values is challenging. A more detailed description of the chemical requirements for each uranium mine site would entail an entire multi-year project in itself; this table is simply intended to serve as a "starting point" for this discussion and comparison.

The greatest uncertainties are associated with the estimates for water consumption, for the following reasons:

- The extent of recycle is generally not identified, and the estimates in this analysis account for almost no recycle, which is likely to be unrealistic
- Additional "small" steps such as washing, rinsing, etc. are likely to consume additional large quantities of water yet are often unquantified or completely ignored in discussions of chemical flowsheets, which sometimes don't regard water as a "chemical"
- Even when quantities of water are provided, they are often given in highly general forms (e.g., a single significant digit or an order of magnitude)

Thus, it is difficult to draw any significant conclusions regarding a comparison of the water consumption for thorium and uranium recovery, other than that ISL likely consumes large amounts of water that cannot be recycled.

For other chemical reagents, some trends can be readily observed. Besides water, the reagent used in the greatest quantities for both uranium and thorium recovery, by far, is the dissolution agent (sulfuric acid for uranium and sodium hydroxide for thorium). A key difference is that monazite requires high-molarity solutions of strong caustics or acids (6-12 M) to achieve dissolution, whereas uranium minerals are effectively dissolved at concentrations as low as 1 M. This is due to not only the mineral structures themselves but also thorium's inability to form highly-soluble hexavalent cations in the manner that uranium does. Regarding secondary reagents, while co-occurrence with REEs does present co-production opportunities, it also requires an intermediate precipitation step that uses additional sodium hydroxide, plus significant amounts of hydrochloric acid to re-dissolve the precipitate. No analogue to this process exists during uranium recovery. Chemical usage of both stripping agents (nitric acid for thorium, sodium carbonate for uranium) and solvent extraction agents (EHPA, TBP, and kerosene) appear to be roughly comparable for thorium and uranium recovery.

3.5.3. Differences in Radiological Impacts

Uranium is recovered primarily through three different recovery pathways: open-pit mining, underground mining, and in-situ leaching. The radiological impacts have been determined in prior work [EPRI 2013a] by grouping data from a variety of mines of each type; these impacts were 0.37 person-mSv per metric ton of natural uranium (MTNU) for open-pit, 0.41 person-mSv/MTNU for underground mining, and 0.63 person-mSv/MTNU for in-situ leaching. However, the open-pit and underground mining approaches require additional processing, which imparts another 0.25 person-mSv/MTNU. Recalling the breakdown of each mining technology

(17.3% from open-pit mines, 37.5% from underground mines, and 45.2% from in-situ leach approaches [Burkhardt 2013]), the combined, weighted impact from uranium mining and milling is **0.64 person-mSv/MTNU**.

Table 16, Occupational Doses of Uranium Recovery Pathways

	Open-pit Mining + Acid Leaching	Underground Mining + Acid Leaching	In-Situ Leaching	**Total**
Normalized Collective Dose (person-mSv/MTNU)	0.62	0.66	0.63	**0.64**
Relative Contribution	17.3%	37.5%	45.2%	**100%**

In comparison, thorium imparts either 1.6 or 9.6 person-mSv/MT Th, depending on the recovery scheme. It is not surprising that radiological doses are larger for thorium recovery than for uranium recovery, given the presence of the hard gamma-emitting Ra-228 in Th-232's decay chain. However, it is important to keep in mind how these values stack up against regulatory limits: peak individual worker doses at thorium recovery facilities were reported to be 7.8 mSv/yr [Haridasan 2010], which is still much lower than the annual occupational dose limit of 50 mSv/yr [NRC 1991].

3.6. Summary of Differences between the Recovery of Natural Uranium and Natural Thorium, and Concluding Thoughts

Differences exist between by-product thorium recovery and conventional uranium recovery from the perspectives of radiological hazards, physical beneficiation requirements, waste management, and others. Table 17 summarizes these differences.

Table 17, Summary of Qualitative Environmental Impacts of Thorium Recovery Relative to Those of Uranium Recovery [Ault 2014a]

Parameter	Th Performance (Relative to U)	Rationale
Mine "Environmental Capital" Cost	↑	Th can rely on pre-existing Ti mines
Occupational and Public Mining Hazard	↑	Nonexistent for by-product Th
Physical Beneficiation Impacts	=	Possibly lower for Th since partly attributable to Ti, but extra steps as well
Chemical Processing Requirements	↓	Monazite/Th require high concentrations of strong acids compared to more readily-dissolved uranium minerals
Occupational Processing Chemical & Radiological Hazards	↓	Rn present in both, but greater quantities of hazardous chemicals for Th
Public Radiological Hazard	↑	Short-lived Rn-220 species limits hazard
Transportation Impacts	=	No evidence to suggest notable distinctions
Waste Management Impacts	↑	No mine waste, less mill tailings, possible TENORM declassification

While thorium by-product recovery is capable of utilizing the pre-existing infrastructure for titanium and heavy mineral recovery, there are incremental requirements for obtaining a nuclear-grade thorium product from what is currently a monazite waste stream, and these would lead to some added impacts. Specifically, additional physical processing and separations would be required to purify the monazite feed supply, and several hazardous chemicals are required to

extract thorium, TSP, and REEs from monazite. In spite of the presence of strong acids and bases, none of these chemicals is particularly exotic (see
Table 12), and operational safety experience is extensive for each of the reagents. Radiological impacts to the public are expected to be minimal, and long-term impacts may actually be reduced because thorium is removed from the "tailings" of other mining activities. Occupational radiological protection may prove to be more challenging than is the case for uranium recovery. The most hazardous steps from a radiological standpoint occur during REE processing due to the presence of Ra-228 and its corresponding production of Rn-220. REE recovery is not necessary to obtain a Th product, but synergistic recovery of both products is more likely to economically incentivize monazite processing.

While the additional impacts of recovering thorium as a by-product are not negligible, they are considerably lower than those associated with opening a new, dedicated thorium mine [Tennery 1978]. While the chemical requirements would not change much, the energy requirements would be dramatically higher due to excavation, on-site transportation, and crushing rock into hundred-micron-scale particles. In addition to the ongoing impacts, a high environmental "capital" would have to be paid to initially prepare the site for operation. In summary, by-product thorium recovery permits both economic and environmental "savings". The environmental impacts expected from thorium by-product recovery should not be viewed as an impediment to thorium fuel cycle implementation.

CHAPTER 4, A COMPARISON OF ENVIRONMENTAL IMPACTS OF FUEL CYCLES WITH MODIFIED-OPEN RECYCLE WITH THORIUM/URANIUM-233 OR URANIUM/PLUTONIUM

The previous chapter considered the sources of natural material that can be used to sustain a nuclear fuel cycle option. This chapter emphasizes the actual implementations of these fuel cycles across a spectrum of possibilities. After carefully defining an appropriate, meaningful, and consistent reference set of fuel cycles for both thorium- and uranium-based options, along with varied extents of recycle, material flow analyses are conducted to determine the mass throughputs in the constituent steps of the fuel cycles. These mass flows are combined with mass-normalized environmental metrics encompassing safety, waste management, and resource sustainability to provide overall perspectives on the EH&S performance of these fuel cycles. This chapter specifically examines the implementations of these fuel cycle options at steady-state; transition analysis will be considered in the following chapter of this dissertation.

Statements of thorium's performance relative to that of uranium are often made generically, without regard to the particular nuclear fuel cycles that are being evaluated. For instance, one might claim that thorium produces "less nuclear waste" than a uranium-based option, but the underlying estimates to support this claim could involve a thorium-based closed cycle in a molten salt reactor compared to the present once-through uranium fuel cycle in pressurized water reactors. If "less waste" is narrowly defined as the volume of spent nuclear fuel or something similar, then it is easy to present an argument that favors the "thorium" option. In reality, the conclusion is primarily driven by the extent of recycle rather than the fuel type, and the choice of waste metric can also be misleading. A similar example could reach the opposite result if a

closed uranium-based fuel cycle and an "open" thorium-based fuel cycle were compared along the same lines.

To arrive at meaningful conclusions, this analysis compares plausible fuel cycle analogues for thorium-based and uranium-based options. There are inherent, unavoidable limitations in how precisely the two fuel types can be compared. Because thorium contains no naturally-occurring fissile material in the way that uranium does, it requires a significant external fissile input from external sources to "jump-start" any thorium fuel cycle implementation. For fuel cycle options that do not employ either a full or nearly-full fissile material recycle approach, fissile content from external sources will continue to be required even at steady-state, potentially adding complexity to fueling strategies. This absence of fissile thorium isotopes also leads to an important difference in supporting fuel cycle facility requirements; natural thorium will not require enrichment or conversion[9], although thorium-based fuel cycles may still require those facilities to the extent that external fissile requirements are supplied by natural U-235. In spite of these fundamental differences, the sections that follow will present some intriguing insights regarding the comparison of thorium- and uranium-based options.

4.1. Fuel Cycle Descriptions

This analysis considers four representative fuel cycle options that are intended to broadly encompass major categories of possible implementations of fuel type and recycle. To this end, fuel cycles that employ uranium/plutonium and thorium/uranium are considered, but also those

[9] However, as noted in the previous chapter, the analog to the refining step of natural thorium recovery is the first component of the wet conversion process of the uranium fuel cycle, i.e. the purification step

that employ varying extents of recycle. It is important to consider both dimensions in this study, since comparisons between uranium and thorium are occasionally confounded by inconsistent assumptions regarding the extent of recycle for the different options.

Table 18, below, lists the specific options that were evaluated in this study. Note that the "no recycle" option is not considered in this study because there is nothing that can accurately be classified as a "once-through thorium" fuel cycle option. While such labels have been applied in previous studies, they do not accurately represent the character of the fuel cycle. For instance, the once-through system studied at Brookhaven National Laboratory (BNL) considers a heterogeneous matrix of uranium-based driver fuel and thorium-based blanket fuel that is configured to be taken to high burnups without subsequent fuel reprocessing. The work supporting the BNL once-through option is extensive, spanning several years and incorporating an optimization component [Galperin 1999, Todosow 2004]. Nonetheless, thorium only comprises about 2% of the total heavy metal loading requirements of the system, while uranium comprises the other 98% [Sandia 2016]. The system is better described as a uranium-based fuel cycle with small amounts of thorium added for specific functional enhancements. As this study will show, modified-open recycle systems will generally also use more uranium than thorium, but at least in this case the balance is not nearly as lopsided, and thorium plays a more central role to supporting the fuel cycle.

Table 18, Fuel Cycle Options Considered in Steady-State Analysis

Extent of Used Fuel Recycle	Representative Fuel Cycle with Uranium or Uranium/Plutonium	Representative Fuel Cycle with Thorium/U-233
No Recycle	Not Considered in This Study; all once-through "thorium-based" options are either overwhelmingly uranium-based or involve external neutron sources	
Modified-Open (Limited) Recycle	Low-Enriched Uranium Fuel in PWRs; Mono-Recycle of U/Pu for MOX-fueled PWRs	Low-Enriched Uranium Driver Fuel and Thorium Blanket Fuel in PWRs; U-233 and Some Thorium Recovered and Added to Th/U-233 MOX PWR
Full Recycle (Closed)[10]	Natural Uranium, Recovered Uranium, and Plutonium in IFRs	Thorium and U-233 Recycle in MSRs

Each of the options shown in Table 18 is described further in the subsequent sub-sections.

4.1.1. Uranium-Based Modified Open Option: Mono-Recycle of U/Pu in MOX-Fueled PWRs

The reference fuel cycle for the uranium-based modified-open option is a two-stage system involving two pressurized water reactors. The term "stage" in this context refers to a specific reactor-fuel combination in addition to its supporting front-end (e.g., resource recovery, conversion/enrichment, fuel fabrication) and back-end (reprocessing, disposal) fuel cycle steps and facilities; the "stage" terminology is adopted from the Office of Nuclear Energy's Fuel Cycle Option Evaluation and Screening Effort (FCO-ESS) [Wigeland 2014]. A stage may receive nuclear materials from another stage and send nuclear materials to another stage. The first stage is a "conventional" PWR fueled by uranium dioxide, where natural uranium is enriched to

[10] The definition of "closed" used in this table does not include the recycle of minor actinides.

relatively low levels (≤ 5% U-235) and fabricated into dioxide fuel. The uranium dioxide fuel is irradiated to a pre-specified burnup and then stored for a fixed period. After this interim storage period, the fuel is sent to reprocessing, where all of the plutonium and some of the uranium are recovered to be fabricated into MOX uranium-plutonium fuel for the second stage. The excess uranium, the minor actinides, the fission products, and any process losses become constituents of high-level waste. The MOX fuel is irradiated to a pre-specified burnup in the Stage 2 PWR, and the spent fuel will be sent to disposal (without reprocessing, following interim storage). The shorthand label of "MUPu" for "modified-open uranium/plutonium fuel cycle" will be used as shorthand for this option throughout this analysis. The material flow and component steps of this fuel cycle are shown below in Figure 5. Only initial-heavy-metal and heavy-metal-derived (i.e., fission products) material flows are shown. Material streams in bold italics are those that must be managed as high-level waste streams, i.e., which will require further storage and eventual geologic disposal.

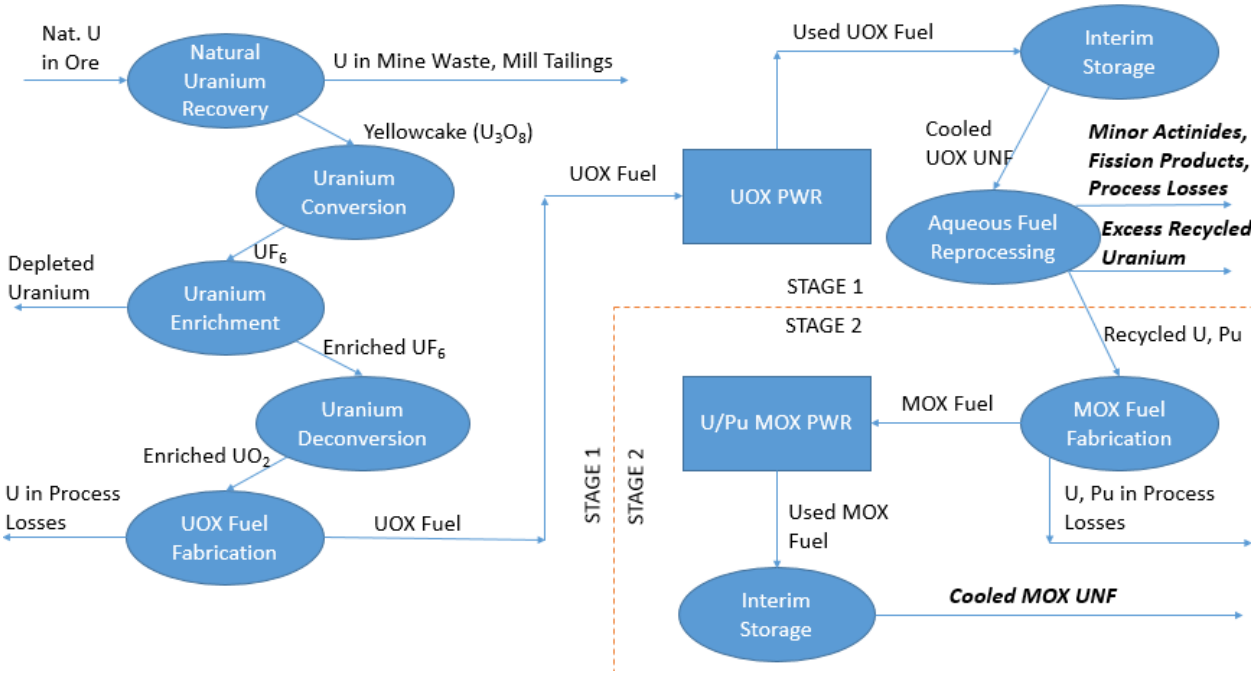

Figure 5, Schematic of Material Flows in the Uranium-Based Modified-Open Fuel Cycle

There are a few features of this fuel cycle that require further elaboration. One is the use of recycled uranium to supply the balance of MOX fuel, where plutonium constitutes the majority of the fissile content. Operational practice with MOX fuel fabrication to-date has tended to incorporate depleted uranium. There are a few reasons to consider the use of recycled uranium as the primary reference case as opposed to the use of depleted uranium. The first is that depleted uranium doesn't have an obvious analogue to the thorium fuel cycle, and the primary purpose of this study is to make consistent comparisons between thorium- and uranium-based options. Another argument is that depleted uranium may not be a resource that is indefinitely available, when considering the strict definition of "indefinite" (although present and foreseeable inventories and accumulation of depleted uranium are so vast [IAEA 2001b] that the availability of depleted uranium as resource could be reasonably argued to be "effectively indefinite"). Lastly, but importantly, high-quality isotopic data is available from previous studies that have examined the use of recycled uranium in MOX fuel [Sandia 2016]. Nonetheless, this study recognizes the importance of considering the depleted uranium case as well, and the implications of adopting this pathway instead will be discussed at several stages of this analysis. Figure 6, below, shows what this variation of the MUPu fuel cycle would resemble.

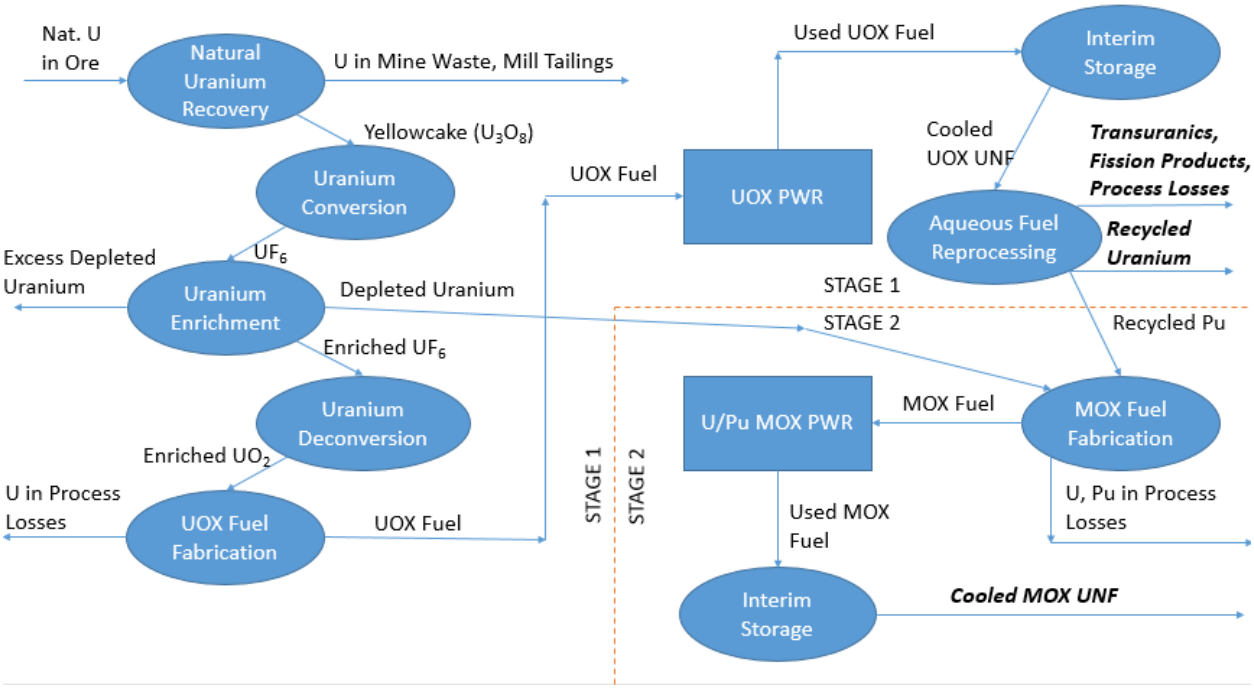

Figure 6, Schematic of Material Flows in the Uranium-Based Modified-Open Fuel Cycle with Depleted Uranium Used as Fertile Matrix in Stage 2, Rather than Recycled Uranium

There are other features of this reference fuel cycle that differ from those featured in previous related studies at Vanderbilt [Smith 2014]. The primary reasons for this difference, which in general leads to a more simplified version of the MOX fuel cycle being considered in this study when compared to previous work, are related to (1) the ability to compare to thorium-based counterparts and (2) the emphasis on steady-state "indefinite" analysis versus the emphasis on present or near-term implementation in [Smith 2014]. As a result, complicating features such as re-enrichment of uranium from used fuel, re-enrichment of enrichment tails ("first-cut" depleted uranium), and downblending of weapons-grade uranium are not considered in this study.

4.1.2. Thorium-Based Modified Open Option: Mono-Recycle of Th/U-233 in MOX-Fueled PWRs

The reference fuel cycle for the thorium-based modified-open option is a two-stage system with a single recycle of U-233 between the stages. The shorthand label of "MThU" for "modified-open thorium/uranium fuel cycle" will be used as shorthand for this option throughout this analysis. Figure 7 shows the major material flows of this fuel cycle. The color blue is used for steps related to uranium/plutonium, the color yellow is used for steps related thorium/U-233, and the color green is used for steps that involve both uranium/plutonium and thorium/U-233.

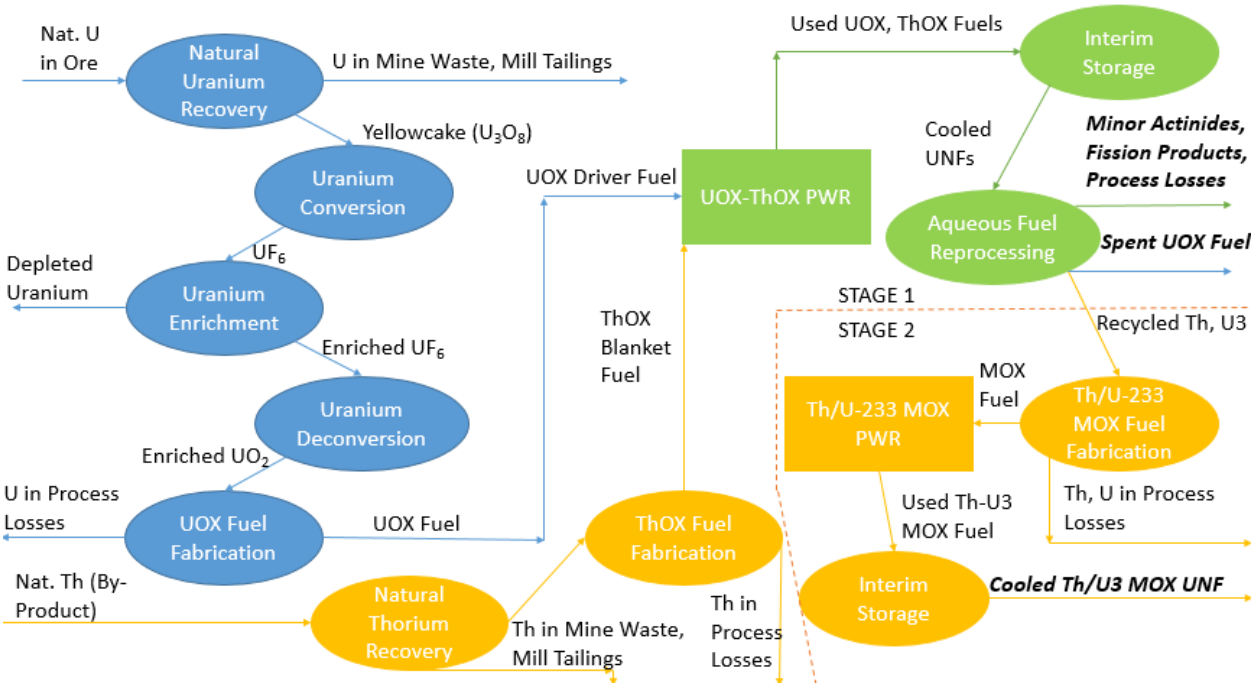

Figure 7, Schematic of Material Flows in the Thorium-Based Modified-Open Fuel Cycle

The MThU fuel cycle is intended to be an analogue to the MUPu fuel cycle to make direct comparisons defensible. That being said, there are some important (and unavoidable) differences between the two fuel cycles. The most important difference is that external fissile material (in this case U-235 from enriched natural uranium) is used to breed the supply of U-233 in Stage 1

to be used later in Stage 2 because thorium does not contain fissile material. Either relatively high enrichments or a significant uranium fuel fraction (or both) is necessary in Stage 1 to sustain criticality and to breed appreciable quantities of U-233 in thorium blanket fuel. The consequences of relying on enriched uranium are that (1) the front-end facilities associated with enriched uranium (U mining, conversion, enrichment, and de-conversion) will also be required for this thorium-based fuel cycle (albeit to a lesser extent than for the MUPu fuel cycle) and (2) the used uranium fuel from Stage 1 is not used in Stage 2, meaning that the MThU fuel cycle will produce two separate streams of used fuel as opposed to the MUPu fuel cycle's single spent nuclear fuel (SNF) stream. Regarding the second point, hypothetically it would be possible to recycle the uranium-based SNF for re-use in Stage 1, but this would hamper direct comparison to MUPu, and in any case, the residual fissile content of the used UOX driver fuel will be quite low. Thus, the version of MThU that is displayed above is the one included in this analysis.

4.1.3. Uranium-Based Closed-Recycle Option: Recycle of U/Pu in SFRs

This fuel cycle involves the continuous recycle of uranium and plutonium metal fuel arranged in a driver-blanket configuration in sodium-cooled fast reactors (SFRs). The fresh driver fuel consists primarily of uranium, plutonium, and zirconium, while the blanket fuel consists of uranium and zirconium[11]. The adoption of this specific fuel cycle option should not be read as an endorsement or a conviction that is necessarily the best or most likely option to be implemented. Rather, it is the fuel cycle option that has the most comprehensive and applicable material flow data sets among those with "typical" closed uranium and plutonium recycle in an SFR. The

[11] Zirconium is used as an alloying agent in metallic nuclear fuel and is not considered in the material balance of the heavy metals of the system. It should be considered most closely analogous to oxygen in the MUPu and MThU fuel cycles and fluorine in the CThU fuel cycle.

shorthand label of "CUPu" for "closed uranium/plutonium fuel cycle" will be used as shorthand for this option throughout this analysis.

Both fuel types are reprocessed and re-fabricated at the end of each fuel residence time in the reactor, with the driver fuel re-fabrication plant receiving both uranium and plutonium recycle streams from reprocessing, and the blanket fuel receiving uranium from reprocessing. Interim storage of spent driver and blanket fuel takes place between discharge and reprocessing. Figure 8, below, shows the major material flows of this fuel cycle.

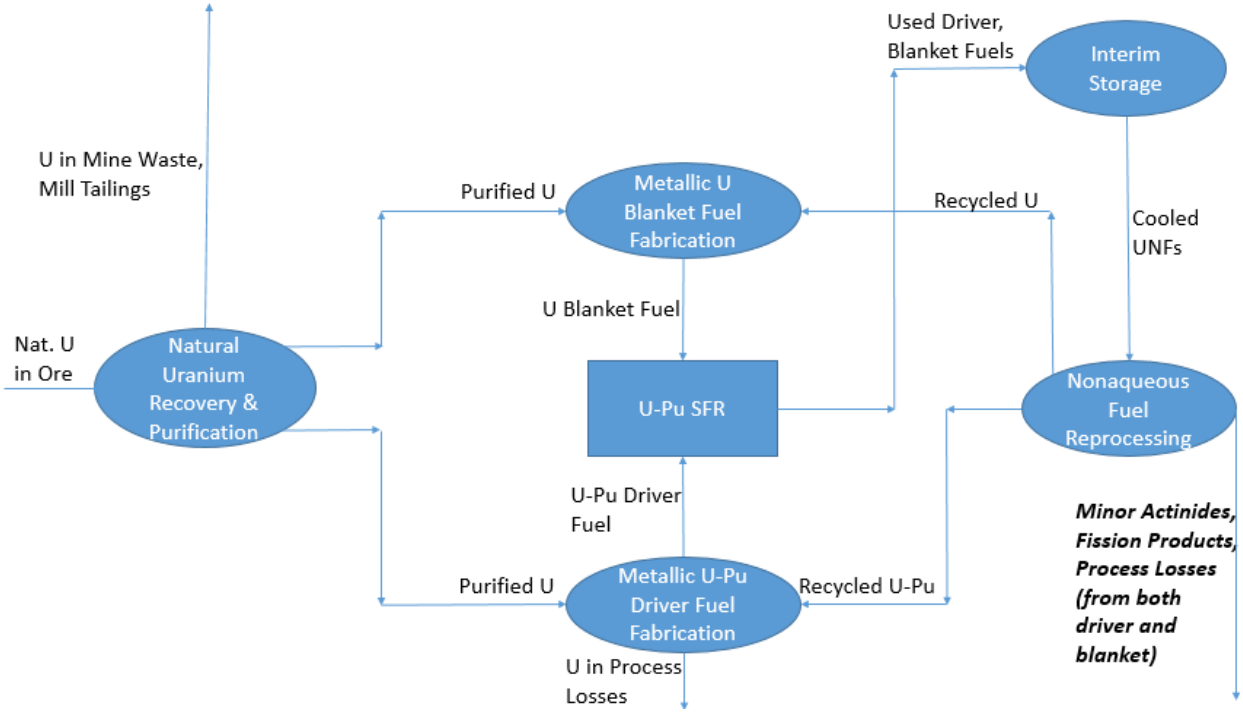

Figure 8, Schematic of Material Flows in the Uranium-Based Closed Fuel Cycle

It is evident from the above figure that a definition of a "closed" fuel cycle has been chosen to only encompass the "primary" actinides of Th, U, and Pu (and to a lesser extent, Pa for the thorium-based fuel cycles). Recycle of transuranic elements is not considered in this analysis; its

inclusion or lack thereof does not impact the performance of most steps of the fuel cycle, and in any case, even for the fuel cycle steps that would be impacted, no systematic studies have been identified that describe the incremental environmental impact posed by transuranic recycle for these steps.

4.1.4. Thorium-Based Closed-Recycle Option: Recycle of Th/U-233 in MSRs

The reference technology for the closed thorium-based fuel cycle is a thermal-spectrum liquid-fueled salt reactor. There are a number of reasons for using a different reference technology and neutron spectrum for the closed uranium- and thorium-based options. Historically, the most popular and well-studied implementation for closed uranium fuel cycles has been the SFR, with demonstration or small-commercial-scale reactors existing in France (Superphenix) [Gourdon 1990], Russia (BN-600) [Oshkanov 2004], and Japan (Monju) [Sato 2007]. In contrast, the results of a thorium literature review [Ault 2016] indicate that MSRs have been the dominant technology associated with closed implementations of thorium-based fuel cycles, especially, Th/U-233 fuel cycles. While lacking the demonstration-scale experience associated with U-based SFRs, U-233 loading was the primary objective of ORNL's Molten Salt Reactor Experiment and a Th/U-233 fuel cycle was the emphasis of the major Molten Salt Breeder Reactor project that took place at ORNL in the 1960s and 1970s. Thorium has been considered for Indian SFRs as part of India's Three Stage Power Programme, but in conjunction with plutonium and not recycled U-233 [Chellapandi 2012]. In addition to the differences in research and operational emphasis, thorium offers improved breeding in the thermal spectrum due to neutron-capture cross-sections, etc., whereas a U/Pu single-stage closed option would not be viable in the thermal spectrum [David 2007]. In the other direction, it would be possible to have a fast-spectrum

thorium-based molten salt reactor, but this option does not have yet readily available material flow data or a standardized, well-recognized modeling approach. Thus, the best balance of technical sensibility and practicality leads to a comparison of a fast-spectrum U-based SFRs and thermal-spectrum Th-based MSRs, with an understanding that future investigations of fast-spectrum Th-based MSRs would also be informative (as information becomes available).

In this fuel cycle, a thorium-based fuel salt is dissolved in a fluoride-lithium-beryllium (FLiBe) salt; the primary fissile agent is U-233. The salt is continuously circulated through the reactor core and then a salt treatment system (continuously removing easily-isolated elements such as noble metals and volatile elements through various physicochemical methods), and then a more sophisticated salt processing system (removing transuranic elements and the more "difficult" fission products such as the rare earth elements) [McNeese 1967, Savage 1977, Powers 2013]. The processed salt will be immediately circulated back to the reactor with the addition of fresh thorium fluoride for recombination and then on to the reactor again. The thorium is added in quantities equivalent to the sum of the losses from salt treatment, salt processing, and salt discard, and conversion to U-233. The shorthand label of "CThU" for "closed thorium/uranium fuel cycle" will be used as shorthand for this option throughout this analysis. Figure 9, below, shows the major material flows for the CThU fuel cycle. Unlike the previous fuel cycles, the four boxes that form a rectangle at the heart of the fuel cycle are actually components of a single facility rather than separate facilities. However, they are still broken out separately in this diagram to clarify how mass streams are being separated.

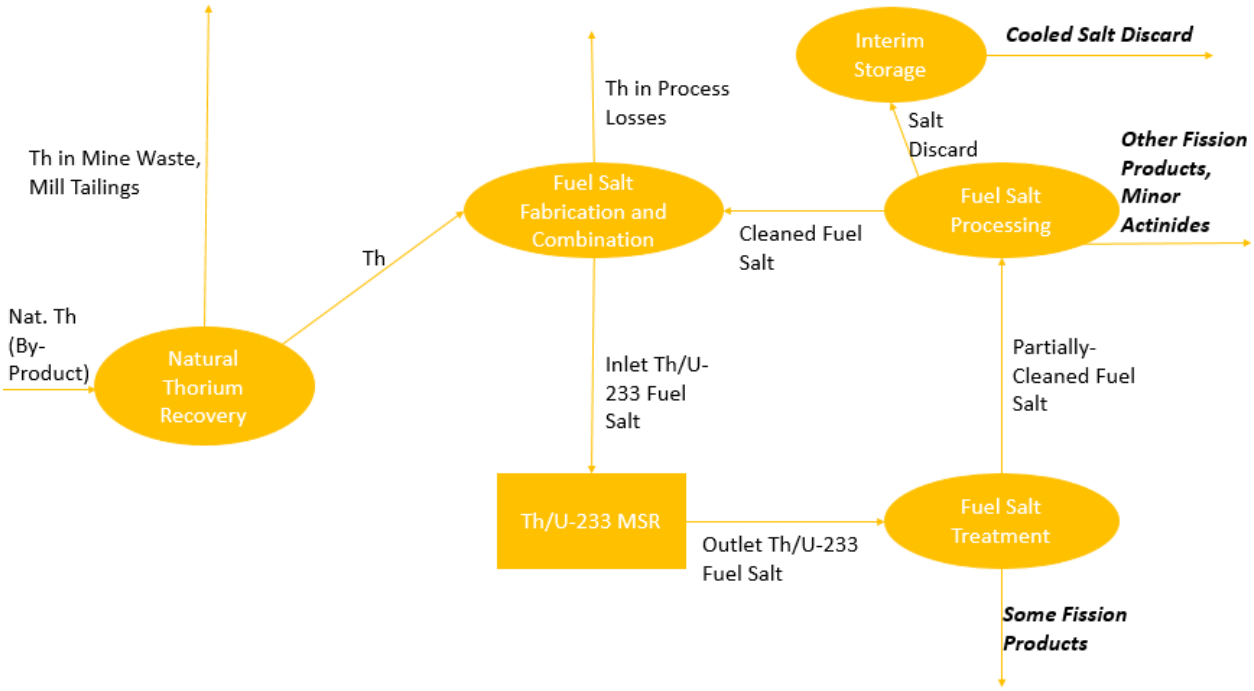

Figure 9, Schematic of Material Flows in the Thorium-Based Closed Fuel Cycle

4.2. Environmental Performance Metrics

Having introduced the fuel cycle options being compared in this analysis, this section turns to the measures by which the fuel cycles are being compared. This is among the most important components of this assessment, since the use of different metrics or assumptions can potentially lead to one fuel cycle option being favored more than the other. This analysis is limited to EH&S metrics, so other common performance metrics such as power density, breeding ratios, and economics are not considered (other than to the extent that they indirectly impact the EH&S results).

The first part of this section will identify the metrics that are used to evaluate a fuel cycle's environmental performance, while noting some caveats with each one. Subsequent sections describe the assumptions or calculations that were used to derive estimates for the values of these

metrics. These metrics are defined on a mass-normalized basis, whereas the final comparisons will be made on an energy-normalized basis. Since electrical energy is the primary product of nuclear energy systems[12], energy is a more meaningful basis by which to draw comparisons between different fuel cycles. Nonetheless, it is almost always necessary to first collect data on a mass-normalized basis and later convert to an energy-based normalization. The implications of the metrics defined in this section are therefore not obvious until they are combined with the material flow analyses described in Section 4.3. This combination of mass-normalized metrics and the material flows is described in Section 4.4.

4.2.1. Identification of Appropriate Environmental Metrics for the Evaluation of Advanced Nuclear Fuel Cycles

Table 19, below, shows the metrics that are used in this analysis to evaluate the environmental performance of the fuel cycles. The seven metrics are grouped into three major categories: the safety of routine operations, waste management, and resource stewardship. As noted previously, this analysis only considers the environmental impacts of routine operations; thus, measures related to accidents and isolated events are not considered. In any case, reactor safety (in terms of accident prevention) is the subject of many other reports and requires highly specialized assessment tools which are not a part of the work described here.

[12] There are other potential products of reactors, such as radioisotopes [Fisher 2009], but secondary product missions are not presently significant contributors to revenue for commercial-scale reactors and fuel cycles (although some research-scale reactors perform product missions other than electricity generation). The direct output of the reactor is thermal energy, which is then converted to electrical energy by an energy conversion system, but the efficiency of these conversion systems is dependent on properties of the reactor technology (especially the coolant outlet temperature). Comparisons of fuel cycles by bases other than electrical energy output were not considered in this analysis.

Table 19, Energy-Normalized EH&S Metrics Used in Analysis

Metric Category	Metric	Unit	Calculation Methodology Summary
Safety of Routine Operations	Collective Occupational Dose Imparted per GWe-yr of electricity production	person-mSv/GWe-yr	Determine best mass-normalized estimate for each fuel cycle step and multiply by mass throughput at each step
Waste Management	Volume of Low-Level Waste (Classes A, B, & C) Produced per GWe-yr of electricity production	m^3 LLW / GWe-yr	Determine best mass-normalized volume estimate for each fuel cycle step and multiply by mass throughput at each step
	Activity of Used Nuclear Fuel and High Level Waste per GWe-yr of electricity production, integrated over a time interval of interest	Bq-yr/GWe-yr	Calculate or identify isotopic inventories for each mass stream and use ORIGEN code to compute activity of those streams. Integrals determined by sampling at various times and taking a Riemann sum. Multiply the result by the mass throughput.
	Decay Heat of Used Nuclear Fuel and High Level Waste per GWe-yr of electricity production, integrated over a time interval of interest	kW-yr/GWe-yr	Calculate or identify isotopic inventories for each mass stream and use ORIGEN code to compute decay heat of those streams. Integrals determined by sampling at various times and taking a Riemann sum. Multiply the result by the mass throughput.
	Ingestion Radiotoxicity of Used Nuclear Fuel and High Level Waste per GWe-yr of electricity production, integrated over a time interval of interest	m^3 water-yr/GWe-yr	Calculate or identify isotopic inventories for each mass stream and use ORIGEN code to compute radiotoxicity of those streams. Integrals determined by sampling at various times and taking a Riemann sum. Multiply the result by the mass throughput.
Resource Stewardship[13]	Metric Tons of Natural Uranium Required per GWe-yr of electricity production	MTNU/GWe-yr	Core simulations combined with consistent front-end assumptions (e.g., enrichment tails, fabrication losses, etc.) Use previous studies if available.

[13] Note that the impacts associated with thorium recovery will be addressed separately and in more detail in the third part of this proposed work, described in Section 4.1

	Metric Tons of Natural Thorium Required per GWe-yr of electricity production	MT NTh/GWe-yr	Core simulations combined with consistent front-end assumptions (e.g., fabrication losses, etc.) Use previous studies if available.

The sections that follow describe the rationale for including each of these metric groups, as well as how they are implemented in this study. Separate treatment is given to the LLW and HLW metrics within waste management.

4.2.1.1, Safety of Routine Operations: Collective Occupational Dose

Occupational dose is a key representative metric of the routine risk presented by nuclear fuel cycle operations to workers. Dose is a measure which incorporates the radiation energy imparted to a person, multiplied by weighting factors according to the health impacts of a particular type of radiation on a mass-normalized basis. Every nuclear facility imparts some radiological impact, although the magnitude of the contribution from facilities varies. Historically, uranium recovery accounted for over half of the total occupational radiological impact of the fuel cycle [UNSCEAR 1993]; today, for the once-through fuel cycle, the cumulative impact is dominated (nearly 90%) by reactors, primarily because fewer workers are required for uranium mining with the advent of modern recovery technologies [Krahn 2014]. In addition, the collective doses from reactors have also steadily declined over time during this period.

Occupational doses impart immediate design requirements due to regulatory limits; for instance, the US Nuclear Regulatory Commission requires that on an annual basis, an individual worker cannot have a dose equivalent greater than 5000 mrem (50 mSv) [NRC 1991]. While such limits

are important from the perspectives of individual safety and compliance, they do not provide an indication of the total number of workers or the distribution of doses among multiple workers. To get a better sense of the radiological impact associated with a particular fuel cycle option, the concept of collective occupational dose can be useful for comparative purposes. Thus, the units of the metric used in this analysis are person-millisieverts, per metric ton (on a mass-normalized basis), or per gigawatt-year (on an energy-normalized basis when multiplied by the mass throughput per unit of energy produced, which is the ultimate objective of this chapter to enable meaningful comparisons of fuel cycles).

Another metric that is sometimes discussed in the context of routine operations is the dose to the public. Inclusion of such a metric may be beneficial for studies for which public approval is significant. While identified public receptors generally refer to local human populations (e.g., [Pennington 2009], [NCRP 1987]), estimates are also occasionally performed for non-human biota such as aquatic wildlife [Blaylock 1975]. The biggest challenge with these approaches is that they are site-specific, involving many assumptions regarding the density of the nearby population, etc. and effluent management. Furthermore, public dose estimates require assumptions about waste form and packaging release rates and subsequent regional transport phenomena. These factors tend to dominate any intrinsic properties of the fuel cycles. For these reasons, public dose is not included in this study.

4.2.1.2, Waste Management (Low-Level): Low-Level Waste Volumes

Low-level waste (LLW) is a category of waste that, in the US, is defined by exclusion: that is, it is radiologically-contaminated waste that does not fall into another formally defined category

such as spent nuclear fuel or high-level waste [NRC 1991]. Within LLW, there are different sub-categories: Class A, Class B, Class C, and Greater-than-Class-C (GTCC), listed in order of increasing disposal hazard. GTCC requires special disposal considerations which are closer to those of used nuclear fuel and high-level waste, while classes A, B, C are appropriate for "near-surface" disposal, as opposed to "geological" disposal which is required for other waste categories. These distinctions would be important when comparing different variations of the once-through fuel cycle with operational data, but for advanced fuel cycles, making meaningful estimates of the different types of LLW challenging; thus, in most cases, the different LLW categories are lumped together in this study. GTCC LLW is not considered due to a lack of data.

There are currently four low-level waste disposal facilities which are available to accommodate wastes from commercial sources. One, EnergySolutions' Clive Operations in Utah, only handles Class A waste. The other three (U.S. Ecology in Washington, EnergySolutions' Barnwell Operations in South Carolina, and Waste Control Specialists in Texas) can receive wastes from Classes A, B, and C, although some regional restrictions apply to the U.S. Ecology and Barnwell sites.

Correspondingly, standard package types have been developed and implemented for each of the near-surface LLW classes [SCDHEC 2007]. These packages have well-documented capacities which, combined with the total volume of LLW produced by nuclear fuel cycles, dictate the capacity requirements of the LLW disposal facilities. Saling's comprehensive book on radioactive waste management discusses the impacts of Class A, B, and C LLW in terms of its volume, noting that costs at Barnwell are defined on a per-cubic-foot basis [Saling 2001].

Subsequently developed fuel cycle analyses which have used waste metrics, such as DOE-NE's Fuel Cycle Option Evaluation & Screening Study (FCO-ESS) [Wigeland 2014], have also followed this convention, and no literature was identified which advocates or uses an alternate metric for LLW impacts.

4.2.1.3, Waste Management (High Level): Activity, Decay Heat, and Radiotoxicity

There are no consistently applied metrics to gauge the risk posed by spent nuclear fuel (SNF) and high-level wastes (HLW), which include both wastes associated with reprocessing as well as used nuclear fuel, following the source-based definitions given in US regulatory schemes [NRC 2015]. The most comprehensive measures of the risk posed by SNF and HLW are repository risk performance assessments (e.g., [Wilson 1994], [Hansen 2011]). However, these assessments require exceptional levels of detail (hundreds to thousands of pages for a full performance assessment report), and furthermore, they require site-specific characterization of the repository environment and the behavior of the wastes in it. The most complete performance assessments will require data from an individual location, but even simplified assessments entail assumptions about a particular type of geology. As a result, the results of a performance assessment are not directly dependent on the intrinsic characteristics of a fuel cycle, but rather of a geology.

However, preliminary efforts have been undertaken to draw out the most significant components of performance assessment results to make inferences at the fuel cycle level. The underlying principle is that the number of radionuclides that contribute significantly to repository risk is limited, regardless of the particular geology being considered [Croff 2015]. Some, such as I-129, dominate risk in any environment, while others (e.g., Np-237) only contribute significantly to

risk in certain oxidizing ground chemistry conditions. In any case, the resulting postulated metric related to this concept is the energy-normalized production of these "key" radionuclides (by mass) [Croff 2015]. However, this concept has only recently been introduced, and has not yet been applied to specific case studies.

Aside from the potential offered by the presently unadopted "simplified repository risk measure" above, there is no straightforward measure of the repository risk posed by a nuclear fuel cycle. Out of necessity, this analysis turns to measures of hazard, rather than risk, as a surrogate for the high-level waste performance of the system. Hazard has the advantage of being an intrinsic property of the fuel, without assumptions of specific implementation strategies. This was a problem that faced previous analyses, e.g. [Burkhardt 2013]. For instance, the use of waste volume metric requires assumptions regarding both waste treatment technologies and waste packaging; both can impact the potential result by several orders of magnitude. Therefore, this analysis considers three intrinsic parameters: activity, decay heat, and ingestion radiotoxicity. Any three of these parameters, individually, is insufficient to characterize SNF/HLW disposal requirements; however, the combination of these parameters may be useful.

Activity is a measure of the total number of nuclear decay reactions that takes place in a sample over a period of time. The SI unit for this parameter, the Becquerel (Bq), is actually defined as a single disintegration (or decay) per second. Total activity has been included in previous comparisons of fuel cycles, such as the FCO-ESS [Wigeland 2014]. An inherent challenge with using activity is determining when to evaluate it; as this study will show and previous studies have also shown (e.g., [Croff 2015]), conclusions regarding the favorability of one fuel cycle

versus another can switch depending on the time at which activity is evaluated (say, 100 vs. 1000 years). To partially alleviate this issue, this analysis will consider integrated (over time) measures of activity, although this does not completely eliminate the challenge; the beginning and final limits of the integration may strongly impact both the value of the metric and its performance compared to other fuel cycles.

Decay heat is a measure of the energy carried by decay particle emissions from a sample over a period of time. Since energy is divided by time, the actual measure of decay heat is power (SI unit: watts). Different decay reactions can pose very different contributions to decay heat. For instance, Te-131 and Te-132 are fission products that each have half-lives between 1 and 4 days and both decay via beta-minus mechanism…yet the decay power from Te-131 is four times larger than that of Te-132. This being said, there is still expected to be some strong correlation between activity and decay heat, and the results in subsequent sections of this analysis confirm this expectation. Decay heat is an important parameter for SNF/HLW management since packaging and repository design is frequently limited by heat densities [Dickey 1982]; thus, lower decay heat could be linked to a better perceived performance for a particular fuel cycle.

Radiotoxicity is probably the least intuitive of the SNF/HLW metrics described here. There are two types of radiotoxicity, inhalation and ingestion; the latter is widely used (e.g., [Shelley 2001], [Bergelson 2005], [Arafat 2011]) and is also adopted in this analysis. Both assume unlikely exposure pathways; ingestion radiotoxicity assumes that radionuclides are directly ingested in water at some point to be determined in the future. The units for ingestion

radiotoxicity are also unusual; it is measured in cubic meters of water[14], which is equivalent to the amount that a radioisotope would need to be diluted in order to satisfy dose maximum thresholds for the general public [Arafat 2011]. Ingestion radiotoxicity does tend to correlate with activity and decay heat somewhat, but it puts a much larger weight on actinides than on fission products at long timescales. Radiotoxicity has been described as potentially useful in situations where large uncertainties limit the ability to conduct a full performance assessment, as is frequently the case when different fuel cycles are being compared [Piet 2013].

It should be emphasized that while three different properties are described here, all three are expected to be closely correlated with one another given their dependence on actinide inventories. Thus, while each of the three properties is reported in this dissertation, they should be viewed as three alternative representations of a single metric of "repository waste hazard", rather than three independent metrics. In other words, repository waste hazard should not be viewed as being three times more important than other metrics discussed in this paper.

4.2.2. Radiological and Low-Level Waste Metric Quantification for Uranium-Plutonium Systems

Many of these metrics were previously developed for Vanderbilt-EPRI work that was applied to a comparison of once-through and modified-open uranium-based fuel cycles [Burkhardt 2013, EPRI 2013a, EPRI 2014a]. An important exception is the impact of the sodium-cooled fast reactor, which was not previously considered. This includes SFR reprocessing and fuel fabrication impacts as well as the impacts from the reactor itself. Most of the data from [EPRI 2014a] and [Wigeland 2014] includes LLW associated with decommissioning, which can

[14] It can also be converted to dose by using the dose rate used to establish the maximum thresholds

represent a significant fraction of LLW production over a facility's life cycle (especially for reactors). In most cases, only combined figures for operational and decommissioning LLW are provided here, with more detailed descriptions available in the referenced literature.

4.2.2.1. Uranium Recovery

Uranium is recovered primarily through three different recovery pathways: open-pit mining, underground mining, and in-situ leaching. The radiological impacts have been determined in prior work [EPRI 2013a] by grouping data from a variety of mines of each type; these impacts were 0.37 person-mSv per metric ton of natural uranium (MTNU) for open-pit, 0.41 person-mSv/MTNU for underground mining, and 0.63 person-mSv/MTNU for in-situ leaching. However, the open-pit and underground mining approaches require additional processing, which imparts another 0.25 person-mSv/MTNU. Global uranium sources supply 17.3% from open-pit mines, 37.5% from underground mines, and 45.2% from in-situ leach approaches [Burkhardt 2013]. So, the combined, weighted impact from uranium mining and milling is **0.64 person-mSv/MTNU**.

With regards to low-level waste, wastes from the open-pit and the underground mining pathways are actually categorized as mining wastes, which are regulated by the US Environmental Protection Agency (EPA) rather than the Nuclear Regulatory Commission. Mining wastes will not be counted among the conventional LLW, primarily because they would otherwise dominate the volume of low-level waste volume and mask the characteristics of "real" LLW. However, mining waste is significant from a volumetric standpoint and presents a non-trivial management challenge; thus, it will still be addressed as a separate waste category.

It is worth noting that open-pit mining produces 6059 m^3 of mine waste and underground mining produces 548 m^3 of mine waste/MTNU [EPRI 2014a]. The US NRC regulates the mill tailings that arise from the acid-leach milling process [NRC 2017], but these are inconsequential contributors to volume compared to the mining overburden. In-situ leaching produces another unique category of waste—leach solutions from which uranium has been stripped—which amounts to 0.19 m^3/MTNU [EPRI 2014a]. After calculating a weighted average based on the prevalence of each method, as was done for dose, the resulting mine waste volume is **1254 m^3/MTNU**.

Table 20, Mass-Normalized Occupational Doses and Mining Waste Impacts of Uranium Recovery Pathways

	Open-pit Mining + Acid Leaching	Underground Mining + Acid Leaching	In-Situ Leaching	**Total**
Normalized Collective Dose (person-mSv/MTNU)	0.62	0.66	0.63	**0.64**
Mining Waste (m^3/MTNU)	6059	548	0.19	**1254**
Relative Contribution	17.3%	37.5%	45.2%	**100%**

4.2.2.2. Uranium Conversion

There are two distinct categories of uranium conversion technologies: wet and dry. Most of the world's uranium conversion capacity uses the wet technology, although the Honeywell conversion facility in the US uses the dry process. With regards to radiological impacts, the differences between the two technologies are notable, with dry conversion imparting 0.118 person-mSv/MTNU and wet conversion imparting only 0.0101 person-mSv/MTNU [EPRI

2013a]. While the exact market share of the two methods is not described, a related report indicates that the dry method accounts for 62.5% of the total dose in the U.S. [Burkhardt 2013], meaning that 12.5% of the mass throughput must come from dry conversion and the remainder from wet conversion. Thus, the overall mass-normalized impact of all conversion technologies is .**024 person-mSv/MTNU**.

Table 21, Occupational Doses of Uranium Conversion Options

	Dry Conversion	Wet Conversion	**Total**
Normalized Collective Dose (person-mSv/MTNU)	0.118	0.0101	**0.024**
Relative Contribution	12.5%	87.5%	**100%**

The dry conversion technology was estimated to produce 0.0371 m^3 of LLW/MTNU, while the wet process produces 0.0103 m^3 of LLW/MTNU (both also produce small amounts of RCRA mixed wastes which are not included here) [EPRI 2014a]. Using the same weighting factors as for dose, the combined radiological impact is **0.0137 m^3 LLW/MTNU**.

4.2.2.3. Uranium Enrichment

Enrichment radiological impacts have been developed for three different technology options: diffusion (0.170 person-mSv/metric ton low-enriched uranium, or MTLEU), centrifuge (0.136 person-mSv/MTLEU), and laser (0.370 person-mSv/MTLEU) [EPRI 2013a]. Of these, laser enrichment is not currently contributing to production on a commercial scale, and the two gaseous diffusion plants (Paducah and Piketon) are closed as of 2015. So, the centrifuge value (**0.136 person-mSv/MTLEU**) is the most useful.

Along the same lines, looking at gas centrifuge enrichment technologies with regards to LLW production, **1.36 m^3 LLW/MTLEU** is produced. A much smaller amount of mixed LLW, which is mixed with hazardous material, is also produced (0.0000776 m^3 MLLW/MTLEU) [EPRI 2014a]. However, there is no comparable data for MLLW from thorium-based fuel cycles, so this value is not considered further. Depleted uranium is not included in either of these values and is tracked separately.

4.2.2.4. Uranium Oxide Fuel Fabrication

The radiological impacts of uranium oxide fuel fabrication are estimated to be **1.75 person-mSv/MTIHM** (metric ton of initial heavy metal) [EPRI 2013a]. This is based on data from hands-on fuel fabrication facilities in the US.

In terms of LLW production, 49.1 m^3 LLW/MTIHM are produced (averaging two different sets of data, with 88.5 m^3 LLW/MTIHM prior to 1995 and 9.66 m^3 LLW/MTIHM after 1995) [EPRI 2014a]. While the original report used the average figure, the more recent figure (**9.66 m^3 LLW/MTIHM**) seems more representative of current practices.

4.2.2.5. Uranium-Plutonium MOX Fuel Fabrication

Previous EPRI estimates considered the radiological impacts experienced during both French and US MOX fuel fabrication efforts. The French data indicates **11.7 person-mSv/MTHM MO**X, while the US data indicates 26 person-mSv/MTHM MOX [EPRI 2014a]. The French data

is more relevant to this study since it involves the recycle of reactor-grade plutonium and does not rely on a limited stockpile of weapons-grade Pu.

As mentioned in Section 4.1.1, the MUPu fuel cycle fabricates MOX fuel from recycled uranium and plutonium. There is limited data from the OREOX process for a small facility that used recovered material in fuel fabrication. It produced **2.42 m^3 LLW/MTHM MOX** [OECD-NEA 2006], which is the figure adopted here. In the event that MOX fuel was instead fabricated using depleted uranium, a different figure is available: 0.621 m^3 LLW/MTHM MOX [EPRI 2014a].

4.2.2.6. Pressurized Water Reactors Fueled with Uranium or Uranium/Plutonium

The U.S. Nuclear Regulatory Commission annually reports occupational radiation exposure data at US nuclear power reactors. As of the time of this report, the latest available data is from 2012 which reports an average collective dose of 0.067 person-rem/MWe-yr [Brock 2014], or **670 person-mSv/GWe-yr**.

With regards to LLW production, previous EPRI work took the average of two methods which summed different categories of LLW, to reach an estimate of **288 m^3 LLW/GWe-yr** [EPRI 2014a]. 205 m^3, or 71%, of this amount comes from decommissioning-related LLW.

4.2.2.7. Integral Sodium-Cooled Fast Reactors Fueled with Uranium/Plutonium

Until 2014, the world's only commercial-scale SFRs were in Russia, previously the BN-350, followed by the BN-600. The third evolution in this sequence, the BN-800, has also been designed and a preliminary unit has been constructed; however, it is not expected to supply

notable amounts of electricity to the grid until about 2020 [Korobeinikov 2013]. However, the BN-600 continues to operate and has documented radiological impacts [Vasilyev 2010]. As part of the FCO-ESS, this data was extended to estimate a normalized collective unit [Wigeland 2014], as shown in Table 22 below:

Table 22, SFR Dose Estimation Based on BN-600 [Wigeland 2014]

Parameter Description (Unit)	Parameter Value
Average Annual Worker Collective Dose (person-mSv/yr)	540
Electricity Generating Capacity (MWe)	600
Capacity Factor (unitless)	0.78
Annual Electrical Energy Production (GWe-yr/yr)	.468
Normalized Worker Collective Dose Metric for SFR system (person-mSv/GWe-yr)	**1200**
Source: 5-year average from 2005-2010 (annual breakdown is not available) was adopted from [Vasilyev 2010] describing the Russian BN-600 fast reactor.	

With regards to LLW production arising from SFRs, data is scarce for the operational and decommissioning contributions to LLW, and unlike for previous fuel cycle steps it is necessary to analyze these components separately. The only thorough estimate for the operational contribution for SFRs is by the OECD-NEA, which identifies a number of likely contributions to LLW, such as wastes arising from cleaning excess sodium from various surfaces along with many of the LLW types associated with PWRs, and then attempts a rough quantification of the sum of these streams [OECD-NEA 2006]. The waste classification system is different than in the US; in addition to being property-driven rather than source-driven, there are separate classifications of short lived intermediate- and low-level waste (LILW-SL) and long-lived

intermediate- and low-level waste (LILW-LL). These two contributions combined, amount to 58.7 m^3 LLW/GWe-yr [OECD-NEA 2006].

For the decommissioning portion, it was assumed in the FCO-ESS that the LLW impact of decommissioning would be identical for all reactor technologies on an energy-normalized basis; evidently, this is nearly true based on data for PWRs, BWRs, and HWRs, on which the estimates for the remaining technologies is based. This value is 205 m^3 LLW/GWe-yr [Wigeland 2014]. The combination of these contributions, then, leads to a sum of **264 m^3 LLW/GWe-yr**.

4.2.2.8. Reprocessing for the SFR-Based Fuel Cycle

This estimate is impacted by the assumption of an integral fast reactor (IFR) design, which is more analogous to the online reprocessing approach used in the MSR design considered in this proposed work. More of a novel fuel cycle facility configuration than a unique reactor type, the IFR considers a scenario in which the reprocessing of spent SFR fuel occurs on-site through an electrochemical process [Brock 2014]. While no studies have been identified which specifically concern the radiological impact of an IFR, a preliminary assessment likens the IFR's impact to the sum of the individual impacts of an SFR, a separate small electrochemical fuel reprocessing facility, and a separate small metallic fuel fabrication facility. For the reprocessing facility, a "placeholder" approach, as used in the FCO-ESS [Wigeland 2014], is to assume the same impacts as aqueous processing (see next section), which is **0.52 person-mSv/MTHM SNF**.

Regarding low-level waste production, there is limited data from which to draw estimates from electrochemical recycling. Estimates have been generated as part of a DOE study on used fuel

disposition, but they are centered on a representative facility size of 300 MTHM/year. Section 4.3.2 will show that the CUPu fuel cycle only requires about 12 MT fuel (combined driver and blanket) per GWe-yr, so even a facility with multiple 1 GWe units would not expect to have anywhere near a need for 300 MTHM/year of fuel in an IFR system. The DOE study also emphasizes that the LLW impacts of the reprocessing facility would not be expected to scale linearly with the size of the facility. Nonetheless, this is the best estimate that is available to work with. The estimates are given for broad categories of LLW; no granularity is available beyond the level shown in Table 23 (e.g., there are no individual estimates for the volumes of Class A, Class B, and Class C wastes.

Table 23, Low-Level Waste Production Estimate from Electrochemical Fuel Processing for SFRs (300 MTHM/yr Capacity) [Jones 2011]

Parameter Description (Unit)	Parameter Value
Classes A, B, C (m^3/MTHM)	9.1
TRU and GTCC (m^3/MTHM)	3.1
Mixed LLW (m^3/MTHM)	0.1
Mixed GTCC (m^3/MTHM)	0.15
Total for All LLW Types (m^3/MTHM Reprocessed)	**12.45**

4.2.2.9. Aqueous Processing of Uranium Oxide Fuels

EPRI estimates, based on French reprocessing data from La Hague, indicate that the radiological impact of aqueous processing of uranium oxide fuels is about **0.52 person-mSv/MTHM SNF** [EPRI 2014a].

Total LLW volumes from reprocessing are estimated to be **4.95 m^3/ MTHM reprocessed** [EPRI 2014a].

4.2.3. Radiological and Low-Level Waste Metrics for Unique Steps of the Thorium Fuel Cycle

To the extent that the thorium fuel cycle relies on the uranium/plutonium fuel cycle, many fuel cycle facility requirements may be shared between thorium-based and U/Pu-based fuel cycles, and the impacts associated with their use in a thorium fuel cycle facility can be scaled from the above discussion. However, there are a few facility requirements which are unique to thorium fuel cycles. The impacts of these facilities are described and estimated below.

4.2.3.1. Thorium Recovery

See Chapter 3 of this dissertation for details about thorium recovery beyond the limited discussion of these metrics, and for the details of the concept of by-product thorium recovery. This section discusses a more narrowly metrics-focused scope of thorium recovery.

Occupational radiological dose data for thorium recovery from monazite is not available from North American nations since commercial monazite processing has not recently been operated. In India, separate data is available for the process to extract thorium and REEs from monazite and the thorium refining process. The first process poses a greater radiological hazard since the REEs are still present and the primary radon-generating dose contributor, Ra-228, follows the REEs [Haridasan 2010]. Based on Indian experience, the cumulative occupational dose from monazite extraction is 8.0 person-mSv/MT Th [Haridasan 2008] and 1.6 person-mSv/MTTh for thorium refining [Haridasan 2010]. The actual impact depends on whether REEs are already

recovered from the hypothetical ore or not. If REEs are already recovered, the monazite extraction step would be attributed to the REE recovery, and the thorium-related impact would just be 1.6 person-mSv/MTTh. If thorium was the driving factor for monazite extraction[15], then the total impact would be the sum of extraction and refining, or 9.6 person-mSv/MT Th. It is not clear which of these two scenarios would emerge as the dominant mechanism if thorium were to be recovered, so the arithmetic average of these values is used (**5.6 person-mSv/MT Th**).

No mining wastes are expected to be attributable to by-product thorium recovery (they would be attributable instead to the primary product), although subsequent extraction and refining processes would lead to the production of mill tailings. Overall losses of thorium in the recovery flowsheet are about 6% [Keni 1990], with the bulk of this contribution coming from undigested ore, which is between 5-10% Th (the lower end of this figure seems more consistent with sources from other nations, e.g. [Long 2010], [Yiezitis 2012]). If .06 MT Th is lost for every ton of Th, and if all the losses are at the same ore fraction of 5% Th, then there are 1.2 MT mining losses/GWe-yr. Monazite densities of 5.0 g/cm^3 are typical [Harjanto 2013], which implies a mill tailing volume of **0.24 m^3/MT Th**. This is comparable to the estimated mill tailings arising from in-situ leaching or from uranium milling (0.19 m^3/MTNU).

4.2.3.2. "Fresh" Thorium Oxide Fuel Fabrication

The radiological impacts of fuel fabrication are largely dictated by the extent of radiological protection used (i.e., hands-on, glovebox, or remote) and the nuclear material involved rather than the fuel type. Due to some of thorium-232's energetic decay products, thorium oxide fuel is

[15] In the case where REEs provide some of the justification for monazite extraction, the thorium-related impact would lie somewhere between these two figures.

fabricated in a glovebox setting. The level of shielding is likely to be the primary determining factor for occupational dose; thus, the glove-box-based value for U/Pu MOX fuel fabrication is used again (**11.7 person-mSv/MT fuel**). This is consistent with the approach used during the FCO-ESS [Wigeland 2014].

Without grounds for a different approach, LLW impacts are assumed to be comparable to those of MOX fuel fabrication (**2.42 m^3 LLW/MTIHM**) [EPRI 2014a].

4.2.3.3. Recovered Thorium/Uranium Mixed Oxide Fuel Fabrication

Historically, one of the challenging aspects of thorium fuel cycles featuring reprocessing is the necessary management of U-232. U-232 is produced in secondary (n, 2n) nuclear reactions in both U-233 and Pa-233, which are both neutron capture products of Th-232. The challenge with U-232 is that one of the nuclides in its decay chain, Tl-208, has a beta decay with an associated gamma energy of over 2.6 MeV. This species was noted beginning with early thorium fuel cycle research for its complication of both thorium recovery and re-fabrication processes [Arnold 1955], and U-232 minimization was a major consideration in some early thorium fuel fabrication campaigns [Gross 1965, Tew 1968]. In any case, the few designs available for thorium fuel fabrication facilities using reprocessed thorium, such as the design for the uncompleted Thorium Uranium Recycle Facility at ORNL, employed remote fabrication technologies [Fitzgerald 1977]. This is a step of radiological protection beyond that of glovebox handling that will be required for facilities handling reactor-grade U-233 and irradiated thorium.

Japan's Power Reactor and Nuclear Fuel Development Corporation conducted an assessment of the expected reduction in occupational dose if their MOX fabrication facility were to shift from a glovebox-handled facility to a fully remotely-handled facility. While not supported by experimental data, shielding calculations projected a reduction to 4.6 person-mSv/MT MOX fuel [Ryoji 1988]. This is somewhat larger the FCO-ESS's value of 0.38 person-mSv/MT fuel for remotely fabricated fuel [Wigeland 2014], which was determined by likening the fabrication facility to a reprocessing facility, so that mass-normalized values from France's La Hague facility could be used [NRC 2010]. Both of these data points are imperfect; the Japanese data is not experimentally driven and was intended for a facility with only a small annual output (5 tons per year), and the La Hague is based on actual facility operation, but for a completely different facility type. It is not clear that either of these data points is more valid than the other, so both data points are treated equally. Since the two data points span about an order of magnitude, it is advisable to use a geometric average to prevent the domination of the larger data point in the average [Spizman 2008]; the result is **1.32 person-mSv/MT fuel**.

No data was identified for the LLW associated with fabricating thorium/uranium oxide fuel. However, in the FCO-ESS, subject matter expertise was consulted to estimate that LLW arising from thorium/U-233 oxide fuel re-fabrication would be 50% larger than for U/Pu counterparts [Wigeland 2014]. Applying this to the figure previously used for U/Pu fuel in Section 4.2.2.5 (2.42 m^3 LLW/MTHM fuel), a value of **3.63 m^3 LLW /MTHM** fuel is computer for reprocessed Th/U-233 oxide fuels.

4.2.3.4. Thorium and Thorium/Uranium-233 Fluoride Salt Fabrication

At steady-state, a closed fuel cycle with only MSRs will only require a small addition of pure natural thorium fluoride in small batches of molten salt to offset conversion to U-233 and any processing losses. Circulated salt will be cleaned by the system's online reprocessing unit and returned to the reactor without requiring re-fabrication. However, it should be noted that in transition scenarios where U-233 is being supplied from an external source, or in steady-state scenarios where U-233-providing LWRs provide a fraction of the overall fuel cycle electricity source term, the fabrication of new U-233-bearing fuel salt will be required. This parameter will not be used in the steady-state analysis, but it will still be calculated now since the next chapter of the dissertation will employ this parameter.

For fresh thorium fuel, salt preparation operations would employ glovebox techniques; for solid fuel fabrication in gloveboxes, this was previously identified to have an associated collective dose of **11.7 person-mSv/MT fuel**. There is no basis for an alternative figure (although recent work on salt test loops could change this in the near term).

As noted in the previous description for reprocessed solid Th/U fuel, complications with the fabrication of any fuel type containing U-233 arise from the presence of impurities of U-232. This feature means that the fabrication of any fuel with a U-233 component will require remote handling [Sease 1966]. The previous section described a dose of 1.32 person-mSv/MT fuel for remotely-fabricated fuel. However, this estimate was intended for solid fuel fabrication, so its applicability to liquid fuel may be limited.

U-233-bearing fuel salt was prepared for the later phases of operation of the Molten Salt Reactor Experiment. The salt had a relatively high U-232 content (222 ppm of the total U mass), and the work was conducted in a shielded cell [Chandler 1970]. Collective dose data for the process is not available, but it is reported that the collective protective measures reduced dose rates to somewhat less than 0.1 mrem/hour (0.01 mSv/hr) [Chandler 1969]. However, it is not clear how much product was created per unit of time, so it is impossible to reconstruct a dose estimate from this experience.

A handful of reports are available on the topic of the preparation of molten salt fuel mixtures from the Molten Salt Reactor Experiment era [Chandler 1969, Chandler 1970, Shaffer 1971], but these reports do not quantitatively address radiological impacts. Thus, the estimate for remotely-fabricated solid fuel, which is **1.32 person-mSv/MT fuel**, is also assumed here. This figure will not be used in the steady-state analysis, but it will be considered in Chapter 5, when fresh fuel salt is added for new MSRs.

There is no data to indicate the amount of LLW generation associated with any type of salt fuel fabrication. The FCO-ESS neglected possible LLW contributions from salt fabrication entirely [Wigeland 2014]. This seems unlikely, but salt fabrication would also probably not have the same high LLW accumulation associated with enriched UOX fuel fabrication. The lower value that was used for MOX fuel fabrication, **2.42 m^3 LLW/MTHM**, is used instead.

4.2.3.5. Pressurized Water Reactors Fueled by Thorium

A handful of pressurized water reactors (PWRs) have operated with significant core inventories of thorium-based fuels. In addition to the variety of fuel tests in which small amounts of thorium were placed into an otherwise uranium-based core[16], some programs have featured more significant deployment of thorium. The most important examples are probably the Indian Point Reactor, which partly implemented the Consolidated Edison Thorium Reactor (CETR) concept, and Shippingport Reactor, which fully implemented the Light Water Breeder Reactor (LWBR) concept.

At Indian Point, a number of thoria-urania fuel elements with stainless steel cladding and a Zircaloy "fuel can" were irradiated, and a sampling of fuel rods from these elements were selected for analysis via gamma scanning and fission gas release tests [Bishop 1968a]. Chemical separation techniques were developed to separate the uranium, plutonium, neptunium, and select fission products for individual analysis [Bishop 1968b, Bishop 1968c]. The completion of various mechanical fuel performance tests determined that the fuel rods did not show signs of excessive damage and that irradiation behavior had been acceptable[17] [Bishop 1968d, Bishop 1968e].

The thorium/U-233-fueled Shippingport core went critical in 1977 [Connors 1979]. Operation of the Shippingport LWBR confirmed previous calculations that achieving breeding in a thermal-

[16] E.g., Elk River [Brooksbank 1978] and Hanford K-East and K-West [Gross 1964]

[17] One caveat not addressed in these reports but gleaned from personal communication with those involved in the CETR experiment was that while the fuel performed very well, the reactivity prediction was inaccurate and the actual reactivity was lower than expected, resulting in a shorter cycle length.

spectrum reactor was (barely) possible, provided that a neutronically transparent cladding material (e.g., zirconium) is selected and that an optimal core geometry is used to capitalize on high-flux regions in the core and minimize leakage [Ullo 1980, Hecker 1981]. Ultimately, the reactor was shut down in 1982 with relatively successful operations throughout irradiation, with relatively few incidents to report and fairly smooth maintenance periods [Bettis 1986]. An end-of-life fuel analysis was performed and determined that the fuel performance had been "excellent", and no evidence of fuel rod failure was observed in the twelve fuel rod samples that were analyzed [Richardson 1987].

The trouble with using Indian Point and Shippingport as a basis for estimating the radiological impacts for prospective thorium-based-fueled PWRs--in addition their datedness--is that both were essentially large-scale demonstration reactors with research and demonstration missions beyond simple power production. There is no reason to expect notable differences in the radiological impacts of thorium- and uranium-based PWRs since exposure in a regulated nuclear industry is driven by the extent of barriers and shielding between the source term and receptor, not the fuel type. Thus, the much-better-known data for uranium-based PWRs (**670 person-mSv/GWe-yr**) is an appropriate surrogate.

The generation of LLW is anticipated to be driven by the technology rather than the fuel type, so the PWR LLW production assumed previously (**288 m^3 LLW/GWe-yr**) is also applicable here.

4.2.3.6. Fluid-Fueled Molten Salt-Cooled Reactors with Thorium

Thorium-based MSRs have a long design history, although operations have been limited to ORNL's Molten Salt Reactor Experiment (MSRE) which operated from 1965 to 1969[18,19]. For a detailed account of this experience with extensive literature documentation, please refer to Appendix A.

Dose records for the MSRE, or estimates from other systems, are unavailable. The FCO-ESS approach for estimating the radiological impacts from MSRs involved an observation of the similarities between an MSR and a reprocessing plant; most importantly, both systems include a hot-cell-type reprocessing unit with remote maintenance requirements. When renormalizing for the mass throughput of each facility, the MSR was estimated to have a collective dose of **490 person-mSv/GWe-yr** [Wigeland 2014].

While there is no data that provides a value for LLW impacts from MSR impacts, it would be expected to have LLW sources of conventional reactors (e.g., filters, core components, primary and secondary loop structural materials) plus those of a reprocessing plant. Regarding the reactor portion, the PWR and SFR were calculated to have relatively similar LLW contributions per GWe-yr. Since the PWR is supported by more data, this figure is also adopted for the SFR (288 m^3 LLW/GWe-yr). For the chemical processing portion of the MSR, analogies are drawn from generic electrochemical salt processing systems, based on work performed by past DOE-NE

[18] The Aircraft Reactor Experiment was an even earlier operational MSR system, having operated in 1954 [Bettis 1957]; however, it was not based on thorium or U-233.

[19] Strictly speaking, the MSRE did not have thorium but used U-233 from other reprocessed sources, and only part of the four-year operational period used a U-233-driven core.

used fuel disposition campaigns [Jones 2013]. Estimates for LLW from salt processes are given to be 0.176 m^3/MTHM; the "MTHM" denominator in this case is the total throughput in the reprocessing system; this will be determined in the material flow analysis for the CThU fuel cycle.

4.2.3.7. Aqueous Reprocessing of Oxide Fuels with Thorium

Experience with the dissolution and reprocessing of thorium-based fuels also has some pilot- and demonstrate-scale background. In the FCO-ESS [Wigeland 2014], all reprocessing approaches were considered to have similar radiological impacts; thus, the "placeholder" estimate here is to use the value from Section 2.3.2.8, which is **0.52 person-mSv/MITHM**. The FCO-ESS previously developed an estimate for thorium fuel separations where thorium and U-233 were co-extracted. The process was estimated to yield **14.2 m^3 LLW/MTHM** throughput [Wigeland 2014]. This estimate was derived from uranium-plutonium co-extraction process (COEX) data augmented by a scale-up factor to represent additional waste associated with complications with Th/U separations compared to U/Pu separations. The scale-up factor was determined through subject matter expert judgment.

4.2.4. High-Level Waste Metric Quantification

Unlike for the previously described metrics, which have been estimated independently of their particular relevance to any specific fuel cycle option, the "intrinsic" SNF/HLW metrics described and quantified in this section are an inherent property of the particular fuel cycle. Thus, separate calculations will be described for each of the four fuel cycle options identified in Section 4.1, although the methodology used is similar between the four calculations.

All three of the high-level waste metrics calculated in this work are calculated using the combination of the "ORIGEN-S" and "OPUS" tools within SCALE [ORNL 2011][20]. The ORIGEN-S tool is used to computationally process material inventories for many radioisotopes simultaneous and to deplete and/or decay radionuclides in these inventories. OPUS is used to "print" the results in plain text and also has access to libraries to convert the default and confusing unit of "gram-atoms" into more useful units such as grams, becquerels, watts, or radiotoxicity units (m^3 water required to dilute to regulatory limits) [ORNL 2011].

For one of the options considered (MThU), new reactor physics simulations were required to calculate new material inventories for use in subsequent calculations; this reactor analysis method is discussed in Section 4.3. For the other three options (MUPu, CUPu, CThU), data from the FCO-ESS was taken and adapted [Wigeland 2014, Sandia 2016]. In its initial form, the data describes the radionuclide inventory of each entering and exiting reactor fuel stream by mass, normalized to one kilogram. While these accurately represent the radionuclide content of the spent fuel streams exiting the second stages of MUPu and MThU, they do not represent the HLW streams exiting the first stages of MUPu and MThU nor any of the waste streams from CUPu or CThU. Generally, HLW and similarly-managed wastes will contain the entire fission product inventory at the end of the residence time of a solid fuel and perhaps all of the minor actinides, plus some "lost" fraction of thorium, uranium, and plutonium. For liquid fuels, this determination is slightly more complicated, as will be described below. This section will

[20] The SCALE manual ([ORNL 2011]) is a lengthy document (thousands of pages) with different chapters afforded to individual modules of SCALE, including for ORIGEN-S and OPUS.

describe the calculations and results of energy-normalized SNF/HLW metrics for each of the four fuel cycle options being considered in this analysis.

This analysis assumes that during reprocessing, 99% of desired actinides are recovered, and that 1% of these actinides and 100% of unwanted products (e.g., fission products, minor actinides) are sent to disposal. Thus, HLW masses are expressed in terms of radionuclide content and are determined by taking the combination of 100% of the fission products and non-recycled actinides plus 1% of the recovered actinides. In cases where a fuel is not reprocessed, the entirety of the fuel mass is considered SNF. An example of a complete material flow calculation for a different fuel cycle option, with supporting equations and calculated values, is available in Appendix B.

MUPu: There are two high-level waste streams resulting from this fuel cycle:

- The HLW stream exiting Stage 1 resulting from fuel reprocessing raffinate and losses
- The SNF from Stage 2

Not surprisingly, the mass-normalized values for each of the Stage 1 HLW metrics are about an order of magnitude greater than those of the Stage 2 SNF metrics at early times, since the Stage 1 HLW is much more highly concentrated in fission products and transuranic actinides that dominate contributions to these integrated metrics. This is not because there are more total fission products in HLW, but that there is a lower mass of uranium in HLW to "dilute" the fission product concentration in terms of mass fractions. At later times, where uranium and plutonium are more important, the streams converge to very similar mass-normalized values.

Figure 10, Figure 11, and Figure 12 give the activity, decay heat, and radiotoxicity curves, respectively, for the MUPu fuel cycle.

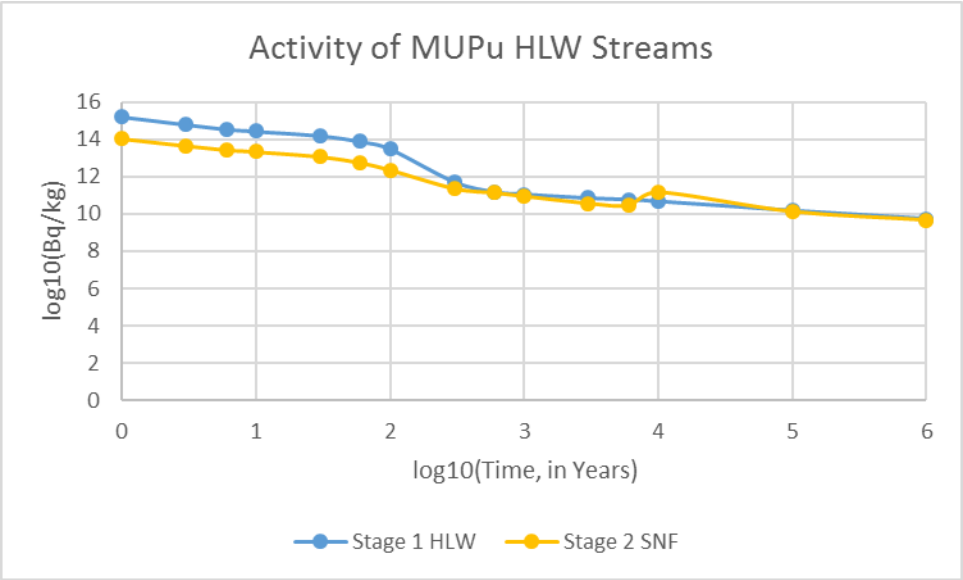

Figure 10, Activity of MUPu SNF/HLW Streams over Time

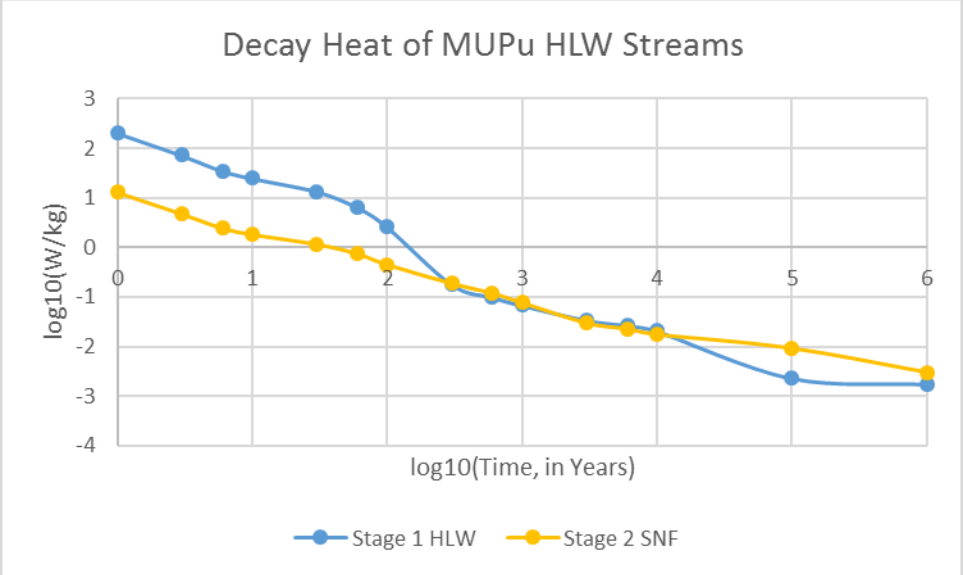

Figure 11, Decay Heat of MUPu SNF/HLW Streams over Time

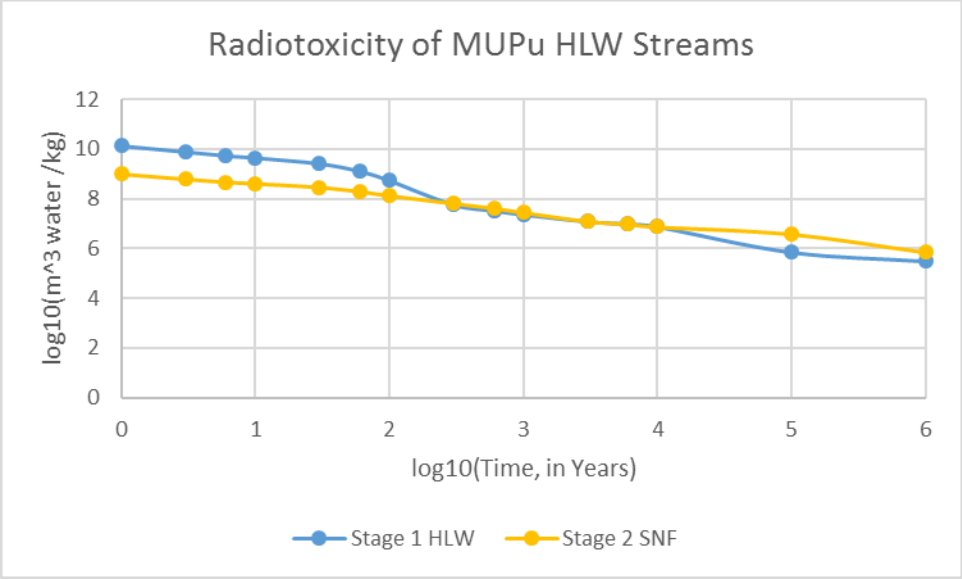

Figure 12, Radiotoxicity of MUPu SNF/HLW Streams over Time

Not included above is the stream consisting of excess recycled uranium, which will be nearly free of fission products and transuranic actinides, the species that (by many orders of magnitude) dominate radiotoxicity, activity, and decay heat over the timeframes considered in this study. It is likely that recycled uranium would be eligible for separate, less stringent disposal classification and requirements compared to those of HLW and SNF; studies have been dedicated to the management of reprocessed uranium in Europe (e.g., [IAEA 2007]).

MThU: There are three high-level waste streams to consider in this analysis:

- The HLW stream exiting Stage 1 resulting from fuel reprocessing raffinate and losses
- The spent driver fuel that is discarded from Stage 1
- The spent fuel from Stage 2

At early times, as was observed for the MUPu fuel cycle, the HLW has about an order of magnitude higher impact (for all three metrics) than either of the SNFs. At intermediate times (in

the vicinity of 300 to 3000 years), the Stage 1 (uranium-based) SNF has about on order of magnitude higher values than the Stage 2 (thorium-based) SNF. This is due to significant contributions from the Am-241, Pu-240, and Am-243/Pu-239 decay chains which are virtually absent in the Stage 2 Th/U-233 fuel. At longer times, as these isotopes decay, the contributions from the U-234 and U-233 decay chains lead to the Stage 2 fuel posing greater hazards at times up to the end of this analysis (1,000,000 years). Figure 13, Figure 14, and Figure 15 give the activity, decay heat, and radiotoxicity curves, respectively, for the MThU fuel cycle.

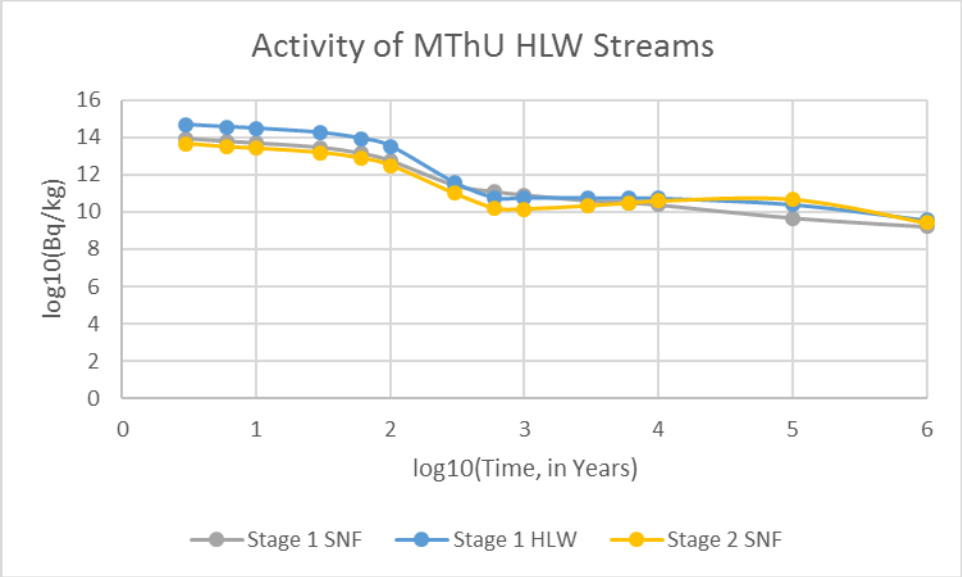

Figure 13, Activity of MThU SNF/HLW Streams over Time

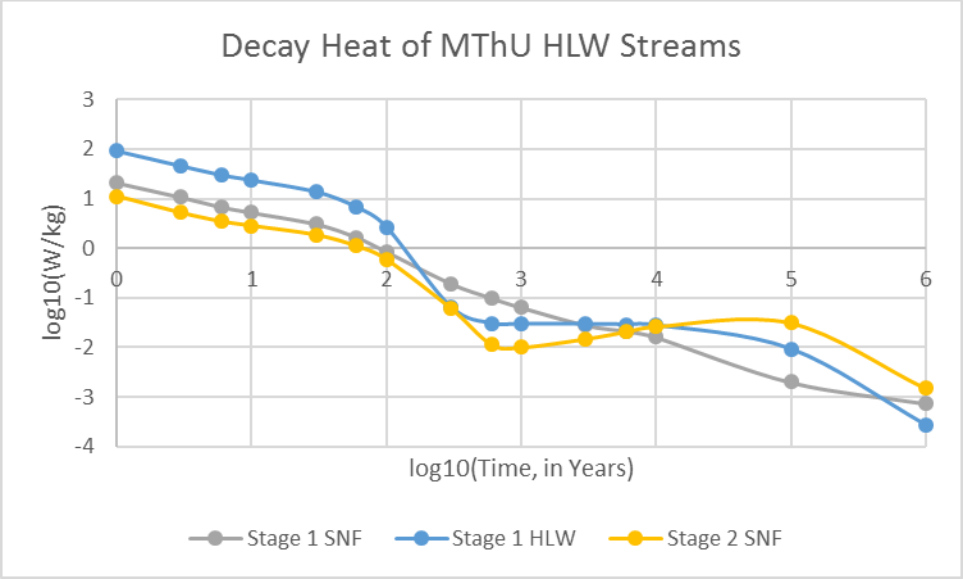

Figure 14, Decay Heat of MThU SNF/HLW Streams over Time

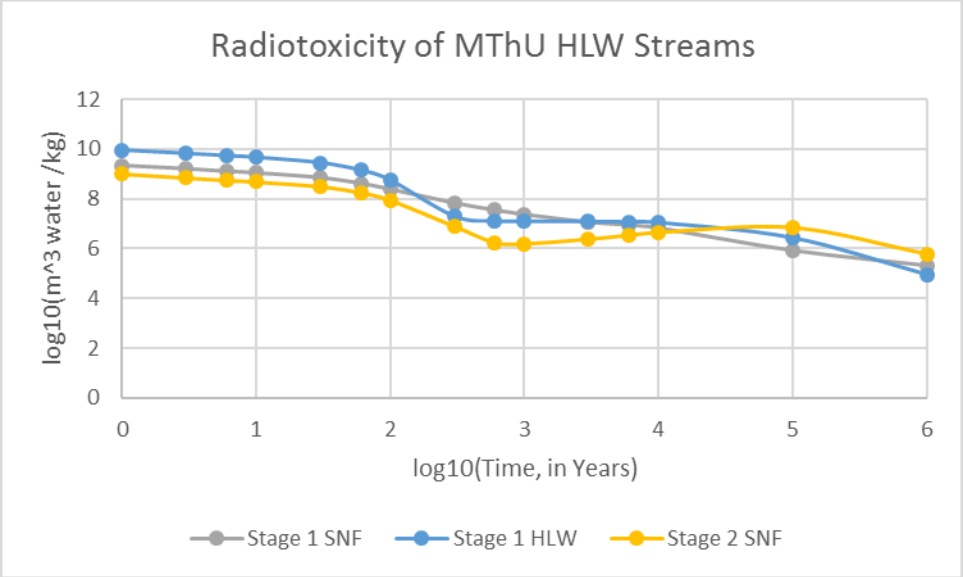

Figure 15, Radiotoxicity of MThU SNF/HLW Streams over Time[21]

CUPu: There are two high-level waste streams to consider in this analysis:

- The HLW stream from reprocessing the driver fuel

[21] The radiotoxicity results are generally consistent with those described in [Croff 2016a].

- The HLW stream from reprocessing the blanket fuel

It is possible that if this technology were implemented, the two fuel types could be separated via the same process or by two different processes at a single facility. Regardless of which of these is actually more likely, this analysis considers the streams separately for the purpose of comprehensiveness and ease of results tracking; in any case, the total HLW impact of the CUPu fuel cycle is described in Section 4.4.3.

Both the streams have significant fission product content and are based on the U/Pu fuel cycle, so the curves are very similar for most times. At intermediate times where contributions from americium and plutonium become most important, the curve for the driver fuel rises somewhat above that from the blanket fuel since it contains a much higher concentration of these elements. Figure 16, Figure 17, and Figure 18 give the activity, decay heat, and radiotoxicity curves, respectively, for the CUPu fuel cycle.

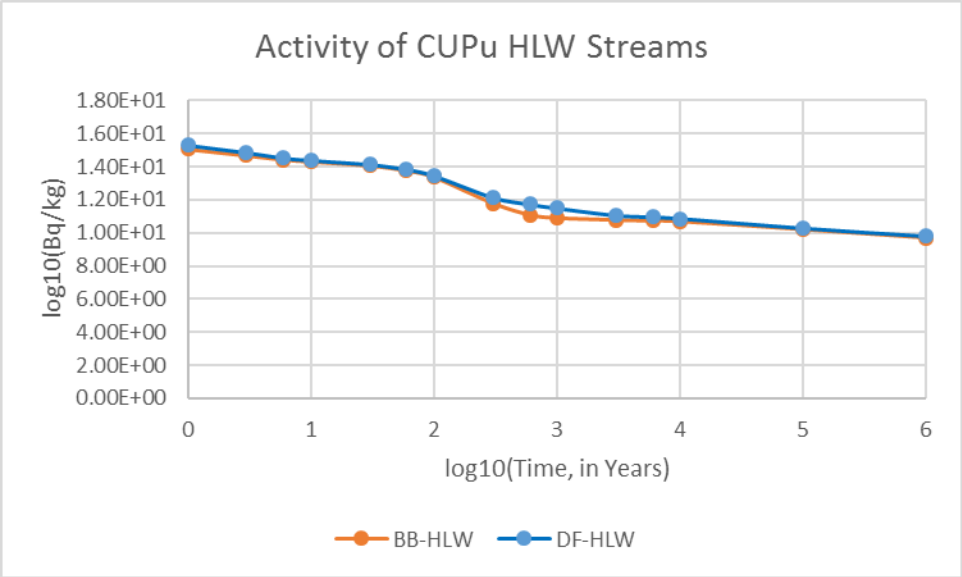

Figure 16, Activity of CUPu HLW Streams over Time

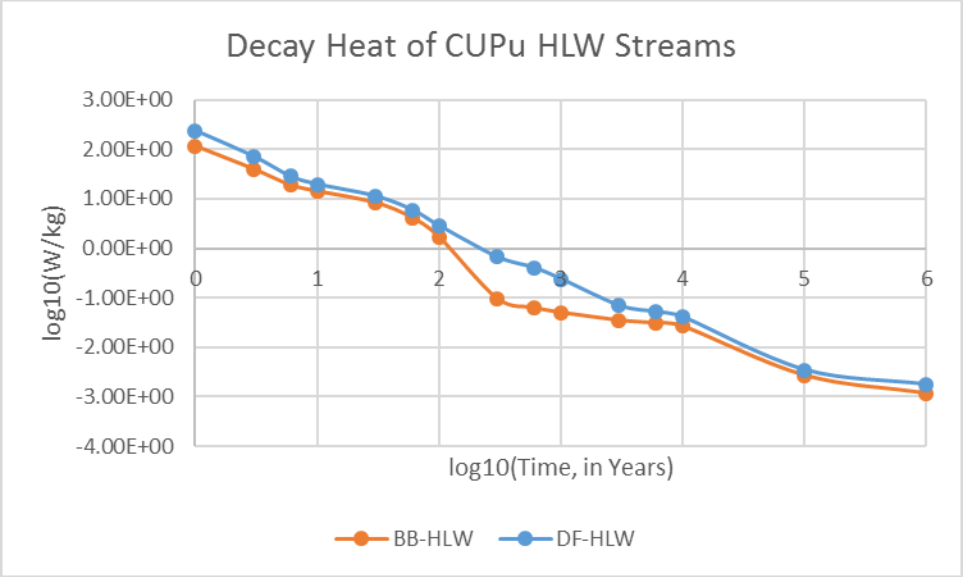

Figure 17, Decay Heat of CUPu HLW Streams over Time

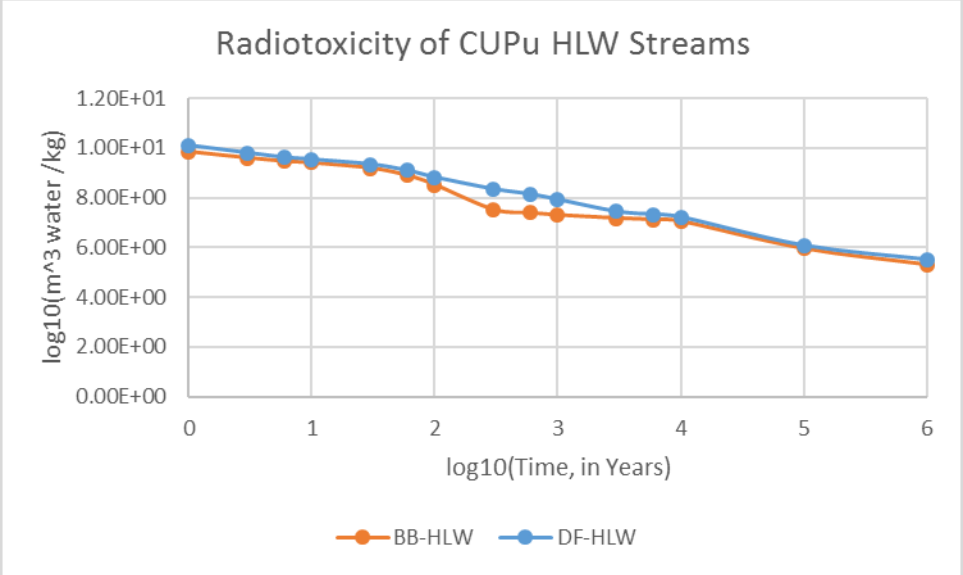

Figure 18, Radiotoxicity of CUPu HLW Streams over Time

CThU: The HLW streams associated with the continuous processing of molten salts are somewhat more complicated than those of the previous three fuel cycle options. The three major streams include:

- Fission products removed during salt treatment (“FP1”)
- Fission products and transuranic elements removed during salt processing (“FP2”)
- Salt Discard

The salt treatment removes groups of fission products that are readily isolated from the salt, such as volatile elements and noble metals, while salt processing is necessary to remove fission products with more actinide-like behavior, particularly the lanthanides. While an MSR-based fuel cycle could be configured to intentionally discard salt, this was not assumed in this study, so the salt discard stream is essentially processing losses. Both the FP1 and FP2 streams are dominated by fission products, the majority of which decay on much shorter timescales than other waste stream types. MSRs are assumed to be capable of more efficient processing than other technologies, and as such the MSR HLW streams contain considerably less actinide losses than the HLW from reprocessed solid reactor fuels. Thus, the rate at which the decay heat and radiotoxicity curves decline is much greater than for the HLW streams of previously described fuel cycles, particularly between 100 and 1000 years; the few fission products that do survive for longer times (e.g., Sb-126m, Tc-99, Zr-93/Nb-93m, Se-79, I-129) are not present in quantities to rival the mass-normalized contributions from waste streams with large actinide contents at times beyond 1000 years or so. The salt discard, on the other hand, behaves very similarly to the Stage 2 Th/U-233 SNF from the MThU fuel cycle. Figure 19, Figure 20, and Figure 21 give the activity, decay heat, and radiotoxicity curves, respectively, for the CThU fuel cycle.

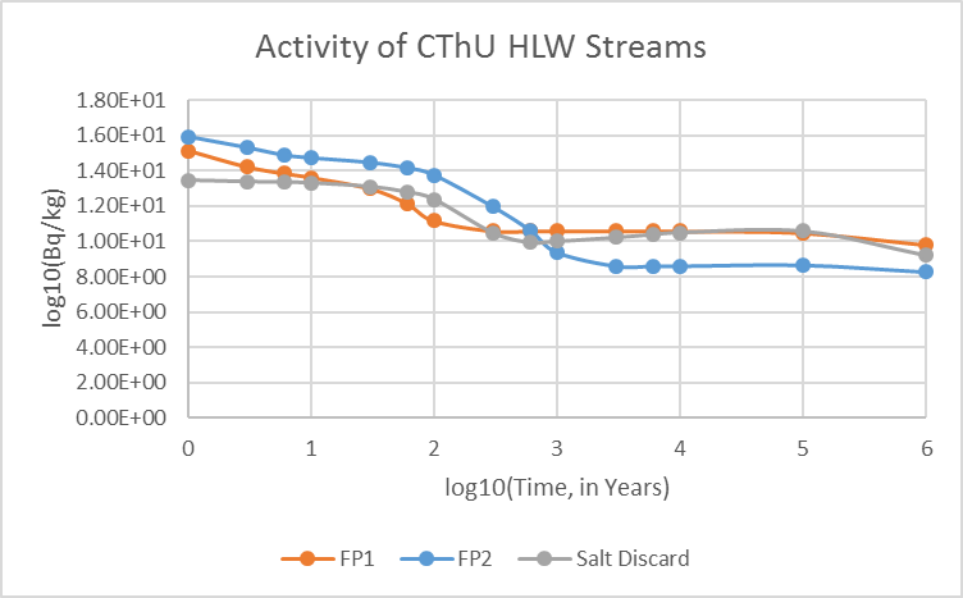

Figure 19, Activity of CThU HLW Streams over Time

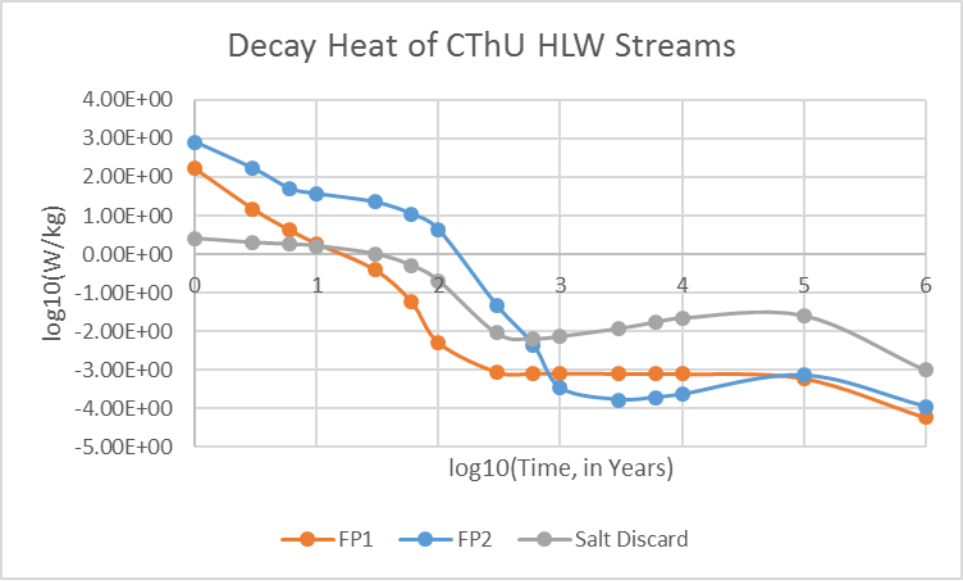

Figure 20, Decay Heat of CThU HLW Streams over Time

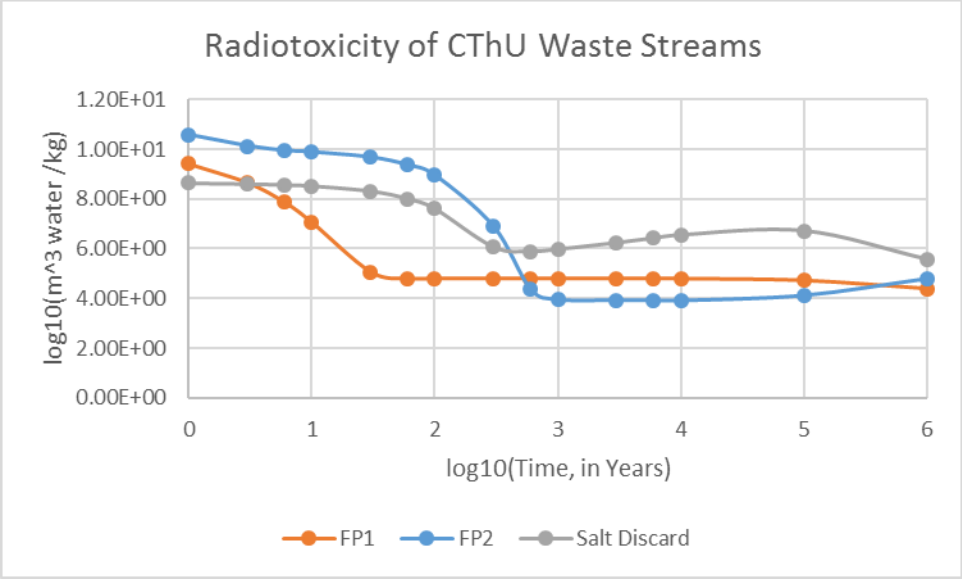

Figure 21, Radiotoxicity of CThU HLW Streams over Time

Sometimes, plots along the lines of those of shown previously (i.e., those that are normalized by mass) are used to make definitive statements regarding comparisons between fuel cycles. In some cases this may be acceptable, but there are examples that are clearly misleading. For instance, the salt discard stream from CThU might look notably hazardous on an mass-normalized basis, but it is produced in very small amounts compared to the mass flows of other waste stream types from other fuel cycles. In general, it is preferable to instead consider the energy-normalized results that will be described in Section 4.4.3.

4.2.5. Resource Stewardship Metrics

The resource usage characteristics of the different fuel cycle options cannot be calculated independently from the material flow analysis that is described in the next section. The energy-normalized results for resource stewardship are described in Section 4.4.4.

4.3. Material Flow Analysis through Advanced Nuclear Fuel Cycles at Steady-State

Most of the metrics described in the previous section were normalized by mass. However, material flows may differ substantially between streams; e.g., one would expect a modified-open fuel cycle to have a significantly higher loss of heavy metal from used fuel compared to those in the reprocessing waste streams. Furthermore, different fuel cycles can have varying total mass flows, so direct comparisons cannot be made between fuel cycles on a mass-normalized basis.

The next step of the process, therefore, is to determine the energy-normalized material flows through each step of the representative fuel cycles in this study. This enables the mass-normalized metrics to be multiplied by the energy-normalized material flows to compute energy-normalized metrics.

The first portion of this section will introduce the reader to the mass flow calculation methodology that was applied for each of the fuel cycles. The latter portion of the section will describe the results of this exercise, which will carry forth into the subsequent section.

4.3.1. Approach and Techniques

The basic tenants of material flow balances stem from the identification of a "basis" from which all other material flows are calculated [Himmelblau 1962]. The basis is a normative unit that can used to standardize the calculations relative to a parameter of interest. For energy systems, including nuclear fuel cycles, a frequently used basis is electrical energy output, in this report described as gigawatt-years of electricity (GWe-yr). This is an appropriate basis since the "final

answers" are readily interpreted and compared when normalized by electrical energy, and there is a direct relationship between electrical energy and the mass throughput of the system.

Electrical energy is provided by just one component of the fuel cycle, the reactor[22]; therefore, this is the logical point at which to begin when analyzing the material flows through the fuel cycle. This is also the step at which significant physical (nuclear) reactions occur, as different elements and isotopes are converted to others primarily through fission, neutron capture, and decay-based nuclear reactions. A fraction of the total initial mass entering a reactor is converted directly to energy, as dictated by the famous relationship: "$E = mc^2$". However, for every kg of U-235 that fissions, only about one gram (0.1%) is converted directly converted to thermal energy (the remainder remains as mass in fission products and neutrons); furthermore, only a small percentage of material added to a reactor actually undergoes fission [Shultis 2007]. Therefore, it is reasonable to approximate that the total mass of fuel entering a reactor is equivalent to the total mass (including the fission products) leaving it, even for a system with multiple reactor core passes such as a molten salt reactor.

The first step of determining the mass throughput of the reactor stage (or in the case of multi-stage systems, each reactor stage) is to determine the composition of the input and output composition vectors of the reactor fuel. The ways in which nuclear reactions transform the fuel material over time is highly dependent on many radiation transport behaviors that are functions of the geometry and evolving composition of the fuels and the other core material. To account for these effects, even at a relatively simplified level, it is necessary to introduce particle

[22] More accurately, electricity is produced by the electricity generation systems that are integrated with the reactor. However, in this analysis, these systems as treated as components of the reactor step of the fuel cycle.

transport and depletion calculation tools into the problem-solving process. Thankfully, the input and output compositions were previously determined for a number of relevant fuel cycles as part of the FCO-ESS [Wigeland 2014]. This material composition data has been made available in an online format [Sandia 2016] and was frequently applied during this study. In particular, data was adopted for both stages of the MUPu cycle, as well as for the CUPu and CThU cycles. For the MUPu cycle, simple reactor input and output compositions were provided. For the CUPu cycle, separate input/output compositions for the blanket and driver fuel were provided, and additional information could be used to determine the relative contributions of each fuel type to the total core mass. For the CThU cycle, mass stream information was provided for a variety of streams: the fresh freed (pure thorium), the salt output before salt treatment, the salt output after salt treatment but before salt processing, the post-processed salt returning to the reactor, the exiting salt treatment stream (entirely fission products), the exiting salt processing stream (mostly fission products, some transuranics), and salt losses. Only heavy metal and "heavy-metal-derived" isotopes (e.g., fission products) were included in these mass compositions; that is, fuel component anions (e.g., oxygen, fluorine), structural materials (e.g., iron, nickel), and coolant or coolant contaminant material (e.g., hydrogen, chlorine) were not included. Each mass stream was normalized to one metric ton of material.

For original depletion calculations, in particular those applied to the MThU fuel cycle, SCALE was used. SCALE is a comprehensive modeling and simulation suite for nuclear safety analysis and design developed and maintained by Oak Ridge National Laboratory (ORNL) under contract with the US Nuclear Regulatory Commission (NRC), the US Department of Energy (DOE), and the US National Nuclear Security Administration (NNSA) to perform reactor physics, criticality

safety, radiation shielding, and spent fuel characterization for nuclear facilities and transportation/storage package designs [Bowman 2011]. Certain modules of SCALE enable the simulation of cores partly or primarily oriented around the use of thorium, and there has been extensive experience with using the tool for thorium fuel cycle applications with a variety of reactor technologies. This study made use of a number of SCALE modules including TRITON for the depletion code and ORIGEN-S for burnup calculations, along the lines described for previous applications of SCALE to both uranium- and thorium-based fuel cycles [Ganda 2012].

The next step is to combine the stream composition data with key assumptions that link material flows to electrical energy output. For conventional-solid fueled systems (applicable to the MUPu, MThU, and CUPu cycles), the key parameters are burnup (a measure of thermal energy output per initial mass of fuel), fuel residence time (the average amount of time a unit of fuel mass spends in a reactor), capacity factor (ratio of actual to potential output), and electrical efficiency (the fraction of thermal energy that is converted to electrical energy). For fluid-fueled systems (namely, the one in CThU), the notion of "burnup" is not applicable. Burnup is traditionally defined in terms of "initial mass", but the fluid fuel is continuously circulated[23] and fresh fertile salt is also added, making it impossible to distinguish between fresh and recycled fuel. Because no alternative fuel utilization metric exists for liquid-fueled systems, power density must be used instead. Power density is defined as the rate of thermal energy output (i.e., power) per unit mass heavy metal. For fluid-fueled systems, there are two potential ways to define the denominator of power density; the mass of heavy metal in the core at any given time, and the

[23] A fluid-fueled system could also employ a "batch" mode of operations, where fuel is circulated for a fixed period without reprocessing, eventually to have it reprocessed all it once. The traditional metric of burnup could be used in this case, but this is not the system that was modeled in this analysis.

total mass of heavy metal in the system. Either can be used to calculate electrical energy output, but the former must be combined with knowledge of the allocation of material within and outside of the core, whereas the latter can be used to directly calculate the electrical energy output.

For single-stage systems (CUPu, CThU), the above steps are sufficient to relate the mass throughput of the core to the electrical energy output of the system; thus, also subsequent material flows can be defined relative to 1 GWe-yr, for instance. For two-stage systems (MUPu, MThU), it is necessary to determine the relative power contributions of the multiple stages. This can be complicated for systems which employ "intra-recycle"; that is, recycle within a stage. Conveniently, neither of the multi-stage fuel cycles in this study employs intra-recycle, and the mass dependency between Stages 1 and 2 is simpler and is based on the behavior of different material types during reprocessing. The material composition of the outgoing Stage 1 fuel is known; each of the material types (e.g., thorium, uranium, plutonium, minor actinides, fission products) is assigned a stream mass fractionation that is based on assumptions. For instance, for both the MUPu and MThU fuel cycles, it is assumed that 100% of fission products and minor actinides are sent directly to disposal. For other materials, such as plutonium in the MUPu cycle, it is assumed that the maximum amount possible (say, 99.9%) is recovered for re-use in Stage 2, but that there are still some process losses (0.1%) that are also sent to disposal. Also accounting for losses from the fabrication of Stage 2 fuel, the material balance assumes that the mass of a key fissile material (for MUPu, plutonium; for MThU, U-233) remaining after process losses from Stage 1 is precisely equal to the amount entering the reactor in Stage 2. One approach is to start with 1 metric ton of fuel in Stage 1, apply burnup and electricity generation parameters, find the amount of the key material that results from Stage 1, comprise fuel for Stage 2 that contains

this amount of key material, apply new burnup and electricity generation parameters, and calculate the total rate of electricity generation for the system. This calculated rate can then be compared to the parameter of interest, and all the material flows of the system can be scaled up based on the ratio of the basis to the calculated rate. Now, the material flows are normalized to the parameter of interest, and the fractional power shares of each stage are also known.

Most of the material flow analysis is characterized after these steps. Remaining efforts involving back-calculating through the front-end of the fuel cycle (i.e., fuel fabrication, then enrichment, then conversion, then resource recovery) to determine the material flows through the remaining steps of the fuel cycle. A few standard fuel cycle assumptions are implemented, keeping with the standards established in by the FCO-ESS [Wigeland 2014]. These assumptions include:

- 99% reprocessing efficiency for recovered actinides.
- 100% reprocessing efficiency for the removal of fission products and non-recycled actinides (e.g., neptunium, americium, curium, protactinium for MThU, and plutonium for CThU)
- 99.8% fuel fabrication efficiency

4.3.2. Material Flow Results

This section describes the quantitative results of the application of the techniques described in the previous section for each of the four fuel cycle options under consideration. The material flows themselves are not the primary objective of this study; rather, they are a means to an end for calculating energy-normalized metrics. Thus, the discussions of these material flows are kept brief (assessments of resource consumption will be deferred until Section 4.4.4, even though the

resource consumption of the fuel cycle options will be immediately evident from the graphics included in this section.

4.3.2.1. MUPu Material Flows

Figure 22, below, shows the material flow moving through the MUPu fuel cycle, normalized as the material flows needed to support 1 GWe-yr of combined system electrical output:

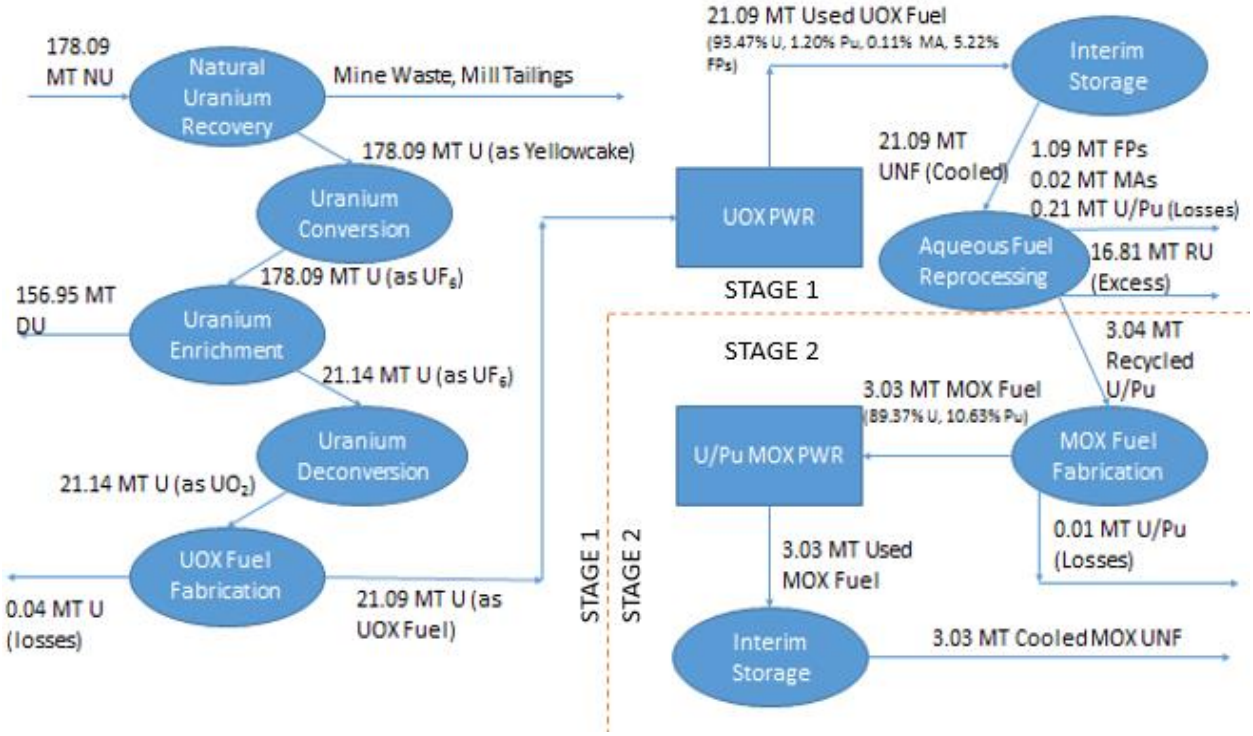

Figure 22, Material Flow Results for the MUPu Fuel Cycle

Stage 1 constitutes 87.4% of the electrical energy output of the MUPu system, while Stage 2 constitutes 12.6% of the electricity energy output of the system. Subsequent analysis shows that these material flows would not change significantly if the governing assumptions of uranium recycle were modified. If, for instance, depleted uranium were used to constitute the fertile

matrix of Stage 2 MOX fuel rather than recycled uranium from the used fuel of Stage 1, then the amount of depleted uranium that would need to be managed as waste would decrease by 2.7 MT – a difference of only 1.7% of the total depleted uranium output. Furthermore, this same quantity would be added to the excess uranium from the Stage 1 spent fuel. Furthermore, if excess recycled uranium were sent for re-use in Stage 1, the fissile content of this uranium is nearly identical to that of natural uranium (0.80% vs. 0.72%). This means that even if all 16.8 MT of excess recycled uranium were supplied for re-enrichment, the natural uranium requirement would decrease by slightly less than 10%, *at most*. In fact, the savings could be even less than this, since re-enrichment of uranium also concentrates U-236, which is a parasitic neutron absorber and often requires slightly higher enrichments to counteract [Del Cul 2009].

4.3.2.2. MThU Material Flows

Figure 23, below, shows the material flow moving through the MThU fuel cycle, normalized as the material flows needed to support 1 GWe-yr of combined system electrical output:

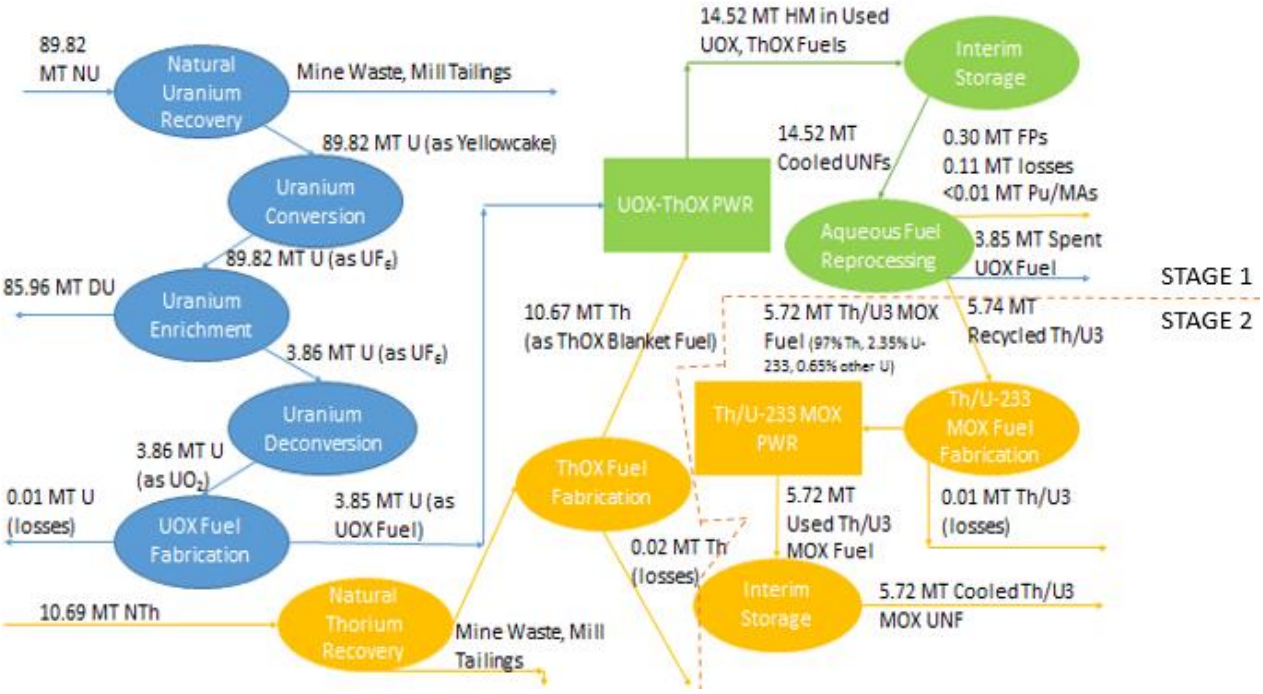

Figure 23, Material Flow Results for the MThU Fuel Cycle

Stage 1 constitutes 73.7% of the electrical energy output of system, while Stage 2 constitutes 26.3% of the electricity energy output of the system.

4.3.2.3. CUPu Material Flows

Figure 24, below, shows the material flow moving through the CUPu fuel cycle, normalized as the material flows needed to support 1 GWe-yr of system electrical output:

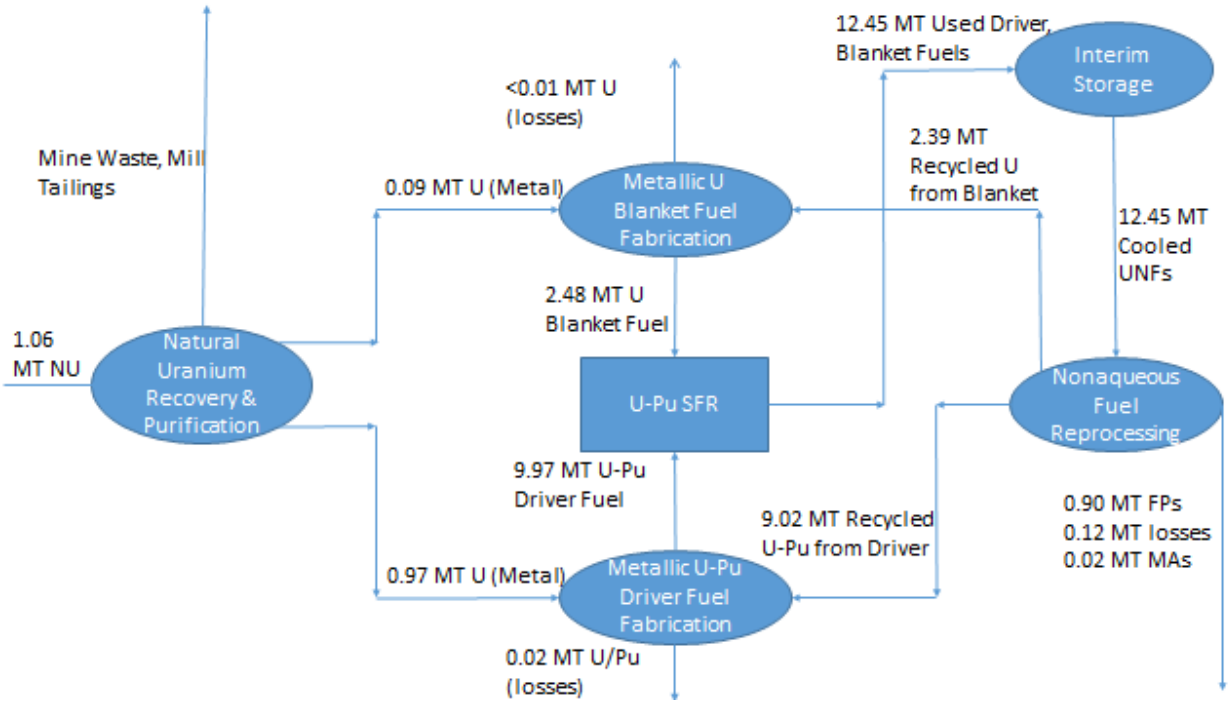

Figure 24, Material Flow Results for the CUPu Fuel Cycle

4.3.2.4. CThU Material Flows

Figure 25, below, shows the material flow moving through the CThU fuel cycle, normalized as the material flows needed to support 1 GWe-yr of system electrical output:

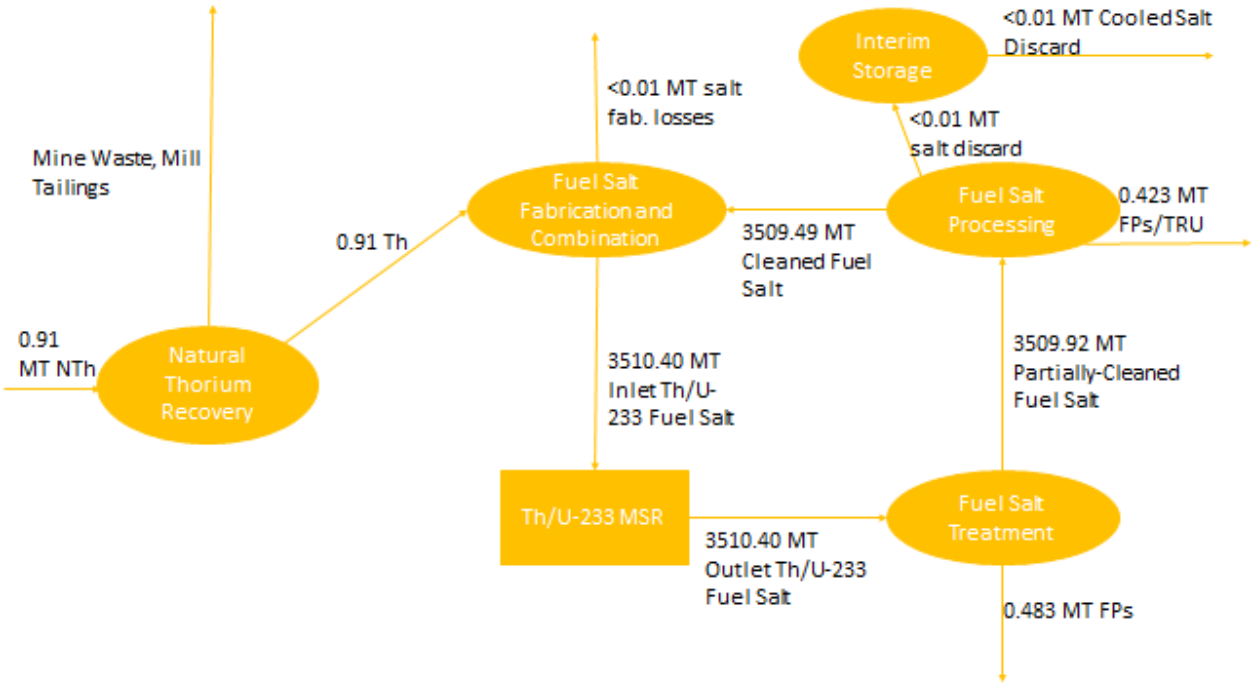

Figure 25, Material Flow Results for the CThU Fuel Cycle

4.4. Amalgamation of Material Flows and Environmental Metrics: Impacts Analysis

With the material flow results calculated in the previous section, this section combines the mass-normalized metrics from Section 4.2 with the mass flows calculated in Section 4.3 to determine the energy-normalized metrics by which to compare the EH&S performance of the four fuel cycle options. Each sub-section within this section focuses on results for a separate metric or group of metrics.

4.4.1. Impacts of Safety of Routine Operations

The mass-normalized doses determined for each component of each fuel cycle in Section 4.2.2 and 4.2.3 were combined with the mass flow calculations described in Section 4.3.2. Figure 26, below, illustrates the comparative routine occupational radiological impacts of each fuel cycle,

broken down by major contributions. “Front-end” includes the combination of resource recovery, conversion, enrichment, de-conversion, and fuel fabrication. Because geological disposal of HLW and SNF is not included in this analysis, the “back-end” is effectively limited to reprocessing.

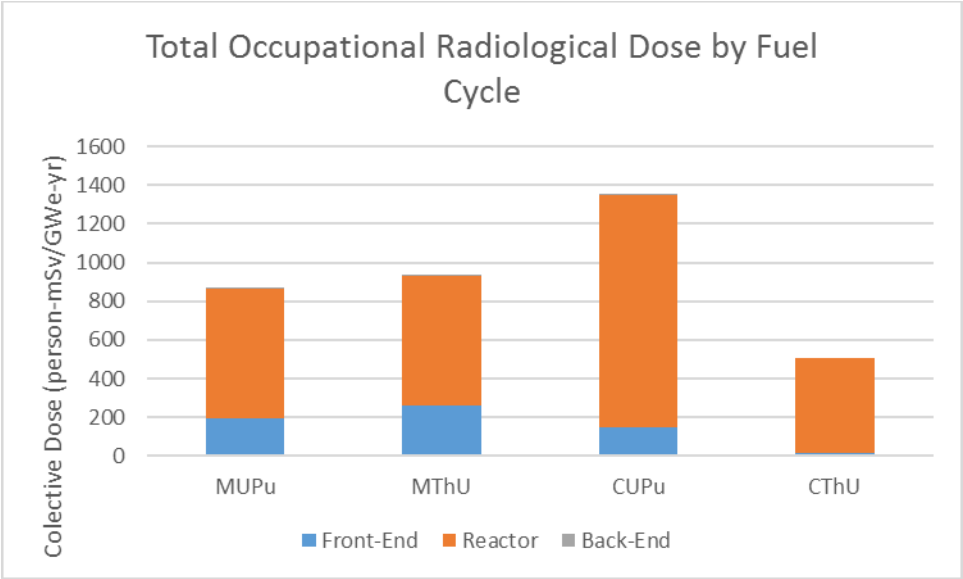

Figure 26, Energy-Normalized Occupational Radiological Dose by Fuel Cycle[24]

The most immediate takeaway is that the two modified-open fuel cycles have comparable total radiological impacts, CUPu has about a 50% higher radiological impact than the modified-open fuel cycles, and CThU has about a 45% lower radiological impact than the modified-open fuel cycles. However, there are more meaningful takeaways from this graphic than simply the total numerical results. Most significantly, for all fuel cycles, reactors dominate total contributions to occupational fuel cycle dose. The extent of domination varies between the options (72% for MThU to 97% for CThU), but it is clear that regardless of the potentially complex variations in

[24] Note that the back-end contributions are so small that they are difficult to visually distinguish at the tops of the bars.

material flow results based on a range of plausible assumptions, comparative radiological impacts will instead be dictated by the assumed dose from the reactor. This is actually independent of the material flow[25], since the reactor(s) are the only source of the fuel cycle's electrical output and the reactor dose is normalized by electrical energy.

For comparison, using the same data sets and assumptions, the once-through fuel cycle (OTC) has a total fuel cycle impact of 851 person-mSv/GWe-yr, with 21.2% of this coming from the front-end and none coming from the back-end since there is no reprocessing. This is within 3% of the occupational dose impact for the MUPu fuel cycle, which generally has similar characteristics since most of its power is contributed by the Stage 1 PWR.

For modern fuel cycle implementation, it has been established that reactors dominate total fuel cycle dose impacts for the once-through fuel cycle [Krahn 2014]. Subsequent work comparing the uranium-based once-through fuel cycle to the modified-open uranium-based fuel cycle showed that dose impacts between the two fuel cycles were quite similar, in large part due to the fact that both used the same reactor technologies, so that differences in the front- and back-ends of the fuel cycle between the two fuel cycles were not important at the cumulative level [Burkhardt 2014]. In the new results presented in this chapter, though, different reactor technologies are used, each with their own assumed radiological impacts using highly variable

[25] The only exception would be for fuel cycles that are comprised of multiple reactors, and at least two different reactors had different energy-normalized doses. In this instance, the total dose would depend on the material flow breakdown (and more specifically, the different power share of each reactor of the total electricity generated). However, for this study, only two of the representative fuel cycles had two reactors, and in each instance the two reactors were of the same technology (PWR) and were assumed to have the same energy-normalized dose contribution. Thus, the conclusion about mass flow independence still applies.

approaches. In this case, the resulting discrepancies give the impression that the fuel cycles have distinctly different radiological performances.

In reality, there is a good chance that the differences between fuel cycles would not be as large as this analysis indicates. The figures for PWR doses are based on many years of experience with multiple commercial units, and are a reasonable indicator of how future PWRs would perform. In contrast, the SFR dose assumption is based on documented experience with a single commercial reactor in Russia that has experienced frequent operational challenges. The combination of the technology's level of maturity with different radiological requirements between countries means that the true dose for an nth-generation SFR may be lower than the value for the BN-600. This is probably a reasonable argument, considering that average individual doses at light water reactors worldwide fell by more than 75% between 1975 and 2000 [Krahn 2014]. However, even if this argument were not accepted, the uncertainty for a single data point is exceptionally large; there is no standard formula that applies for a sample size of 1 and estimations require expert judgment, but regardless of approach the uncertainty would be *at least* half the value of the data point, or 600 person-mSv/GWe-yr [SELA 2016]. If the SFR were assumed to have half of its presently assumed radiological impact, the CUPu fuel cycle would have a 17% *lower* dose than the modified-open fuel cycles.

Meanwhile, the assumption regarding the MSR is even more uncertain, as it relies on a highly tenuous analogy based on the perceived similarities between an MSR and a reprocessing facility due to an absence of relevant data. Modifications in the assumed flowrate through the MSR alone would change the numerical estimate significantly, and an equally plausible argument is

that an MSR would have radiological impacts somewhere in between the extremes of a sole reprocessing plant and the combination of a reactor and a reprocessing plant. At this other extreme, if the MSR's dose was assumed to be equivalent to that of a reprocessing plant AND that of a PWR, the CThU fuel cycle would have a 30% *higher* dose than the modified-open fuel cycles.

The argument might be made that because (1) large uncertainties exist in reactor dose assumptions which dominate any quantitative comparison between fuel cycles and (2) nth-generation advanced reactors at steady-state might be expected to have nearly-identical radiological impacts based on requirements imposed by laws and regulations, then the differences in the reactor contributions to dose should be assumed to be negligible[26]. This article does not necessarily support or reject that notion, but it may be worth at least considering for the sake of argument. If only the front- and back-end contributions to dose are compared, the results come out as shown in Figure 27, below.

[26] There are probably some inherent differences in dose based on variations in the *availabilities* (i.e., the fraction of time a system is operational) of different reactor systems, because higher maintenance frequencies will lead to higher doses. However, availability is difficult to predict for nth generation advanced reactor systems. Nth-of-a-kind SFRs might be predicted to have higher maintenance frequencies than nth-of-a-kind LWRs given the challenges of managing metallic sodium, but this is not known with certainty.

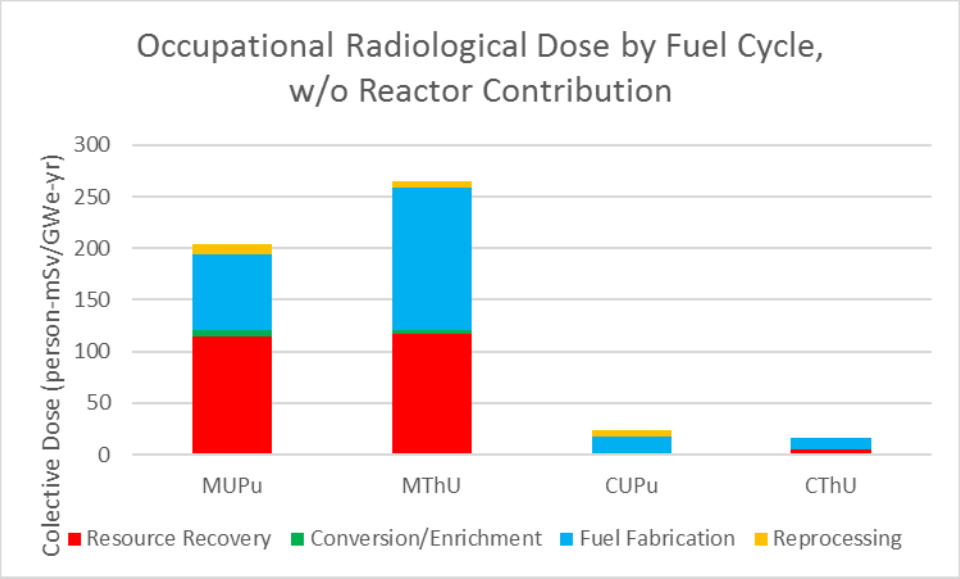

Figure 27, Collective Non-Reactor Occupational Radiological Dose by Fuel Cycle

Uncertainties in parameter assumptions are still important to consider for any nuclear fuel cycle analysis, but with the reactor doses removed the inherent characteristics of the fuel cycles are more readily apparent. Both of the closed fuel cycles have minimal natural resource requirements and, by extension, avoid a significant portion of the non-reactor fuel cycle dose. CThU, in particular, avoids many fuel cycle steps altogether (conversion and enrichment, along with reprocessing being lumped into the reactor dose) and minimizes fuel fabrication due to the reactor's high power density and correspondingly small heavy metal throughput. The other dominant factor that is also apparent here is the difference between "hands-on" and glovebox fuel fabrication. This is required for natural thorium fuel, and is the driving force for the MThU fuel cycle having the highest non-reactor dose among the four options (and the reason for CThU's resource impacts being visible while CUPu's resource impacts are not). Meanwhile, both fuel types in the CUPu fuel cycle require at least glovebox fuel fabrication, and this fuel cycle correspondingly has the largest fuel fabrication dose of all the fuel cycles. Even if the CUPu fuel cycle began to employ remote fabrication instead of glovebox techniques, its fuel

fabrication impact would still be 60% larger than that of the CThU fuel cycle, since CUPu must refabricate fuel at the end of each cycle whereas salt reprocessing returns most of the fuel back to the reactor directly in the correct chemical form. Regardless of these findings, it is important to remember the context of this "sub-investigation"; at most, the non-reactor dose contributions would amount to 28% of the total dose contributions, and usually less than this.

4.4.2. Impacts of Waste Management (Low-Level)

With regards to LLW production, there are some visible differences between some of the fuel cycle options. Figure 28, below, shows the energy-normalized results for this metric. For the time being, mining wastes are not included as they utterly dominate the category by volume (they will be addressed separately).

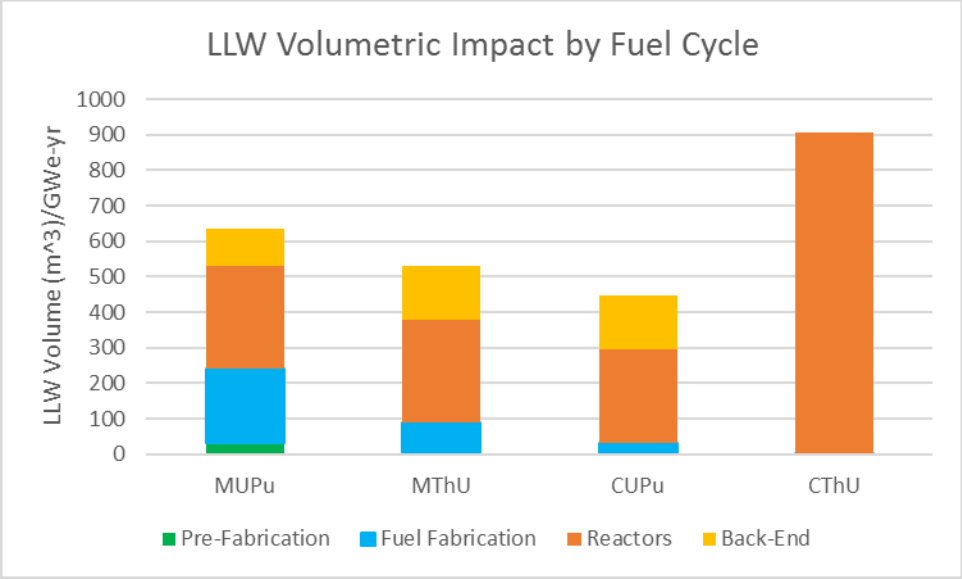

Figure 28, Energy-Normalized Low-Level Waste Volume by Fuel Cycle

As with the previous section, uncertainty with single data points or estimates must be considered with caution. Nonetheless, there are some takeaways from the above that are indicative of the

fundamental properties of the fuel cycle options. In particular, CThU is calculated to produce significant amounts of LLW from reactor operations because of the large throughput of material through the salt treatment and processing systems per unit of energy, compared to that of other fuel cycles. While the impact from an individual pass is small, filters, resins, and other separations agents are eventually going to be depleted and require disposal assuming that LLW accumulation is proportional to the material throughput. Recall that separations are lumped together with the reactor for the MSR, so there is no ability to parse the reactor and separations contributions in the CThU column; however, much of CThU's LLW impact (68%) is attributed to the reprocessing portion of that system.

Among the other fuel cycle options, the differences are not as large, primarily because the LLW contributions from the reactors are roughly equivalent for each fuel cycle. However, there are still some important differences, namely that the CUPu LLW impacts are somewhat lower than those of MUPu and MThU. This is because the CUPu fuel cycle requires less total fuel fabrication on an energy-normalized basis due to higher fuel burnup and also because of the differences in mass-normalized LLW production for fresh and recycled fuel fabrication (9.66 m^3 LLW/GWe-yr vs. 2.42 m^3 LLW/GWe-yr). As a reminder, these results did not separately break out different types of LLW (Classes A, B, and C) since this level of specificity could not be determined for any fuel cycle except MUPu based on a lack of data or defensible assumptions.

For comparison, using the same data sets and assumptions, the once-through fuel cycle (OTC) has a total fuel cycle impact of 557 m^3 LLW/GWe-yr, with 48.3% of this coming from the front-end and none coming from the back-end since there is no reprocessing. This is within 12.3% less

than the occupational dose impact for the MUPu fuel cycle, which generally has similar characteristics since most of its power is contributed by the Stage 1 PWR; however, the additional LLW contributions from reprocessing are avoided.

Mining waste was not included in the preceding graphs in this section, since for certain fuel cycles the volumetric contribution from the rest of the fuel cycle would be completely dwarfed by this waste category (for instance, for CUPu, mine wastes would account for 99.8% of the total combined volume of mine wastes and LLW). Mine wastes do represent a comparatively low-hazard contribution of the overall fuel cycle; however, given their massive volume and their nevertheless significant management challenges [Thomas 1981], they are still addressed briefly. Figure 29, below, shows the mine waste results. Because the differences are so significant, the results are plotted on a logarithmic scale. Note that the true log10 values are actually one smaller than what is plotted below; the mine waste contribution for CThU is so small that the log10 value is actually negative, so one is added to all the log10 values so that all bars appear above the axis line (for ease of graphical viewing only).

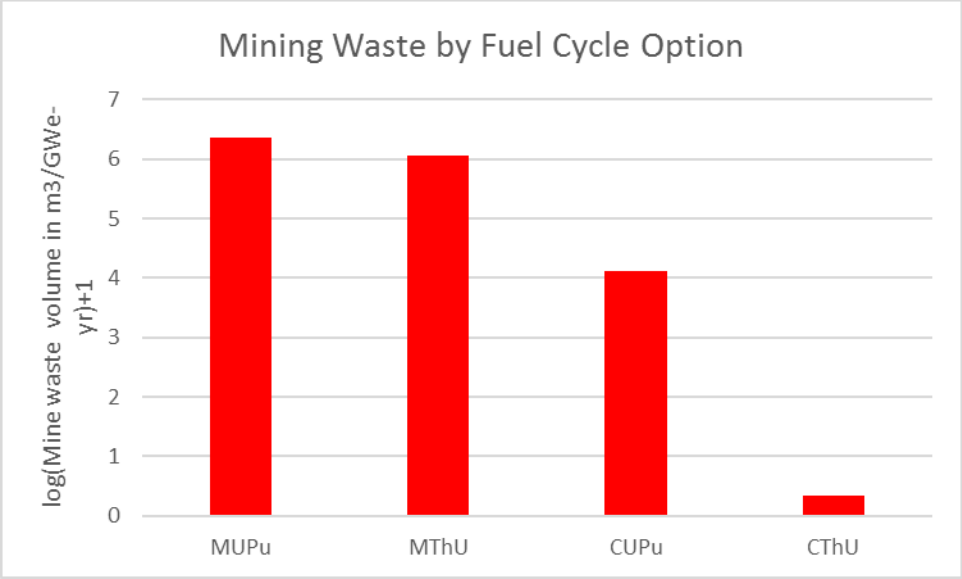

Figure 29, Energy-Normalized Mining Waste Volume by Fuel Cycle

On the logarithmic scale, the difference between MUPu and MThU appear small even though there is actually about a factor of 2 difference. Both of these fuel cycles employ significant quantities of enriched uranium and therefore require substantial inputs of natural uranium, which results in a significant mine waste burden of both fuel cycles. The MThU fuel cycle actually uses only about a quarter of the amount of uranium-based fuel that the MUPu fuel cycle does, but the use of higher enrichments results in the difference in NU consumption only being a factor of 2. For comparison, the OTC produces another 14% more mining waste than MUPu given its even greater demand for natural uranium.

The CUPu fuel cycle also relies on natural uranium and its associated mining waste, but it only requires small amounts of new material and also does not require enrichment, so its consumption of natural uranium is two orders of magnitude less than that of the modified-open fuel cycles. The CThU fuel cycle does not rely on natural uranium at all; since natural thorium recovery is assumed to be achieved from by-product sources for perpetuity, its associated mining waste

volume is very small. This is coupled with the CThU fuel cycle's inherently low requirement for new material to make the mining waste impacts for this fuel cycle more than 5 orders of magnitude lower than the modified-open fuel cycles and more 3 orders of magnitude lower than CUPu. Again, these are steady-state results; transitions to a CThU-like fuel cycle would still require significant initial loadings of external fissile sources, and will therefore directly and indirectly require natural uranium. However, this is the subject of the next chapter, not this one.

There are two additional categories of material that would require disposal or some other form of repurposing: depleted uranium and excess recycled uranium. Of the four fuel cycle options considered in this study, only MUPu and MThU produce depleted uranium (156.95 MT/GWe-yr and 85.96 MT/GWe-yr, respectively), and only MUPu produces excess recycled uranium (16.81 MT/GWe-yr). For reference, the OTC produces 179.50 MT DU/GWe-yr. The prospective disposal of depleted uranium in the US has been the subject of several reviews, and there are several areas of uncertainty including the disposal site, the disposal chemical form, regulatory classification (e.g., whether or not it should be reclassified as LLW), and the economics of disposal [Hertzler 1994, Ranek 2002, Camper 2011]. The management of excess recycled uranium has not been studied in as much detail in the US since reprocessing is not currently practiced and the quantities of depleted uranium are much larger, but it has been the subject of international efforts [IAEA 2007]. While the precise disposal outlook for these material streams is not clear, the management of both depleted and recycled uranium presents a challenge that has not yet been resolved, and there will be at least be some impact associated with their disposal.

4.4.3. Impacts of Waste Management (High-Level)

The results of the SNF/HLW analysis are discussed with two separate metrics: radioactivity and decay heat (further simplified to decay heat, for reasons discussed subsequently) and radiotoxicity.

4.4.3.1. Radioactivity and Decay Heat

The curves for total energy-normalized radiotoxicity and total decay heat for each fuel cycle option are shown in Figure 30 and Figure 31, respectively. It is necessary to plot the results on a logarithmic scale since the values for both metrics vary significantly both over time and between fuel cycles.

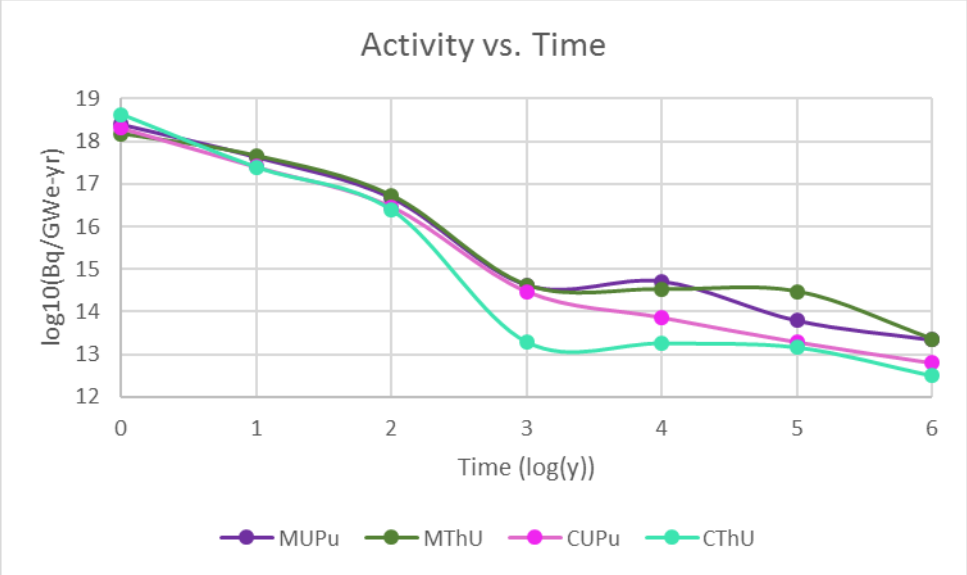

Figure 30, Energy-Normalized Radioactivity as a Function of Time for Four Fuel Cycle Options, with Radioactivity and Time Each Plotted on a log-10 Scale

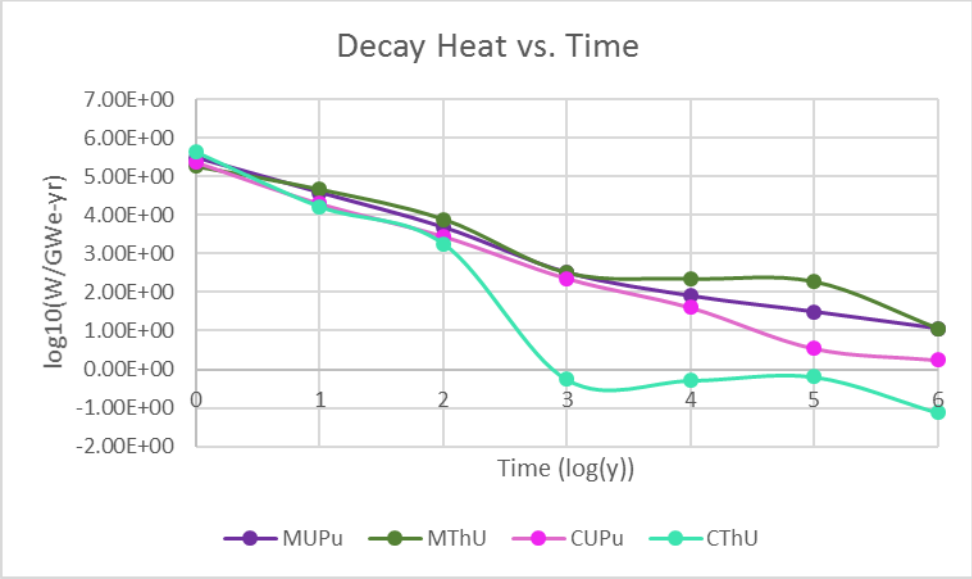

Figure 31, Energy-Normalized Decay Heat as a Function of Time for Four Fuel Cycle Options, with Decay Heat and Time Each Plotted on a log-10 Scale

It was originally planned to consider separate insights from radioactivity and decay heat metrics within the topic of SNF/HLW management. Calculations were performed for both parameters for each SNF/HLW stream from each of the four fuel cycle options across a range of start and end times after stream discharge. However, it was quickly discovered that activity and decay are so closely correlated that including both metrics does not yield much incremental comparative information, regardless of the particular timescale being considered. Consider Figure 32 and Figure 33, below, which select two arbitrary time intervals, one at relatively short times (1 to 100 years) and one at relatively long times (1000 to 100,000 years).

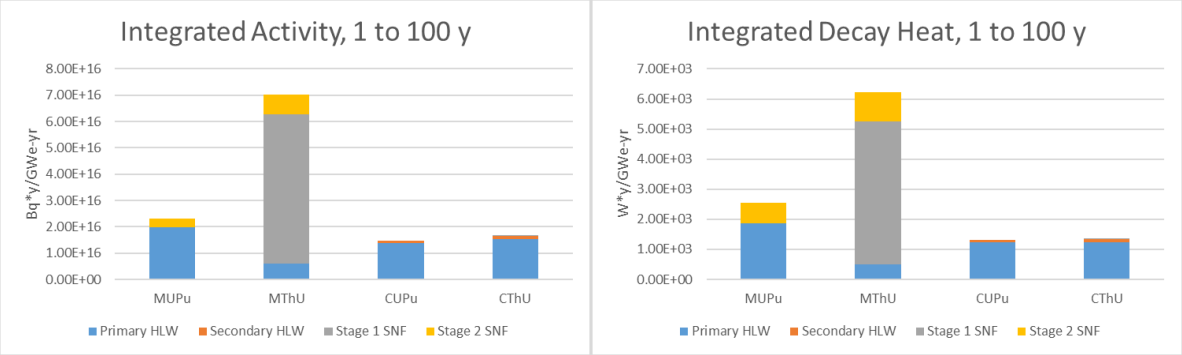

Figure 32, Side-by-Side Comparison of Energy-Normalized Activity and Decay Heat Integrals from 1 to 100 Years

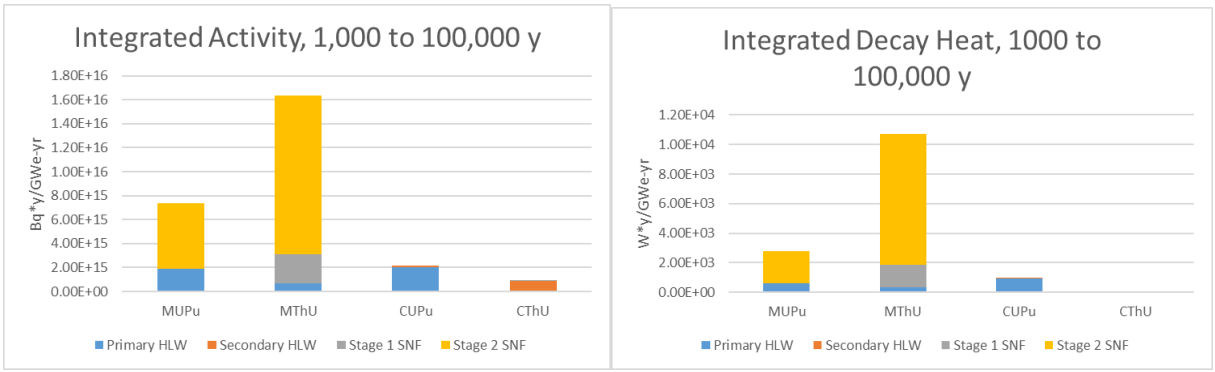

Figure 33, Side-by-Side Comparison of Energy-Normalized Activity and Decay Heat Integrals from 1000 to 100,000 Years

In both cases, there are some subtle differences between the activity and decay heat charts (especially the Stage 2 SNF from the MUPu fuel cycle and the secondary HLW from the CThU fuel cycle), but for the most part the graphs for activity and decay heat appear nearly identical for all time scales. Visualized another way, Figure 34 and Figure 35 show the fuel cycle options with the highest energy-normalized radiotoxicity and decay heat impacts, respectively, for each major starting and ending integral timeframe:

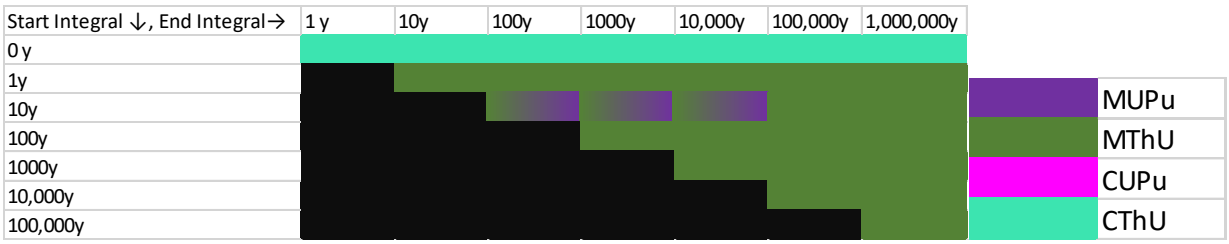

Figure 34, Fuel Cycle Options with Highest Energy-Normalized Integrated Activities at Various Starting and Ending Timescales

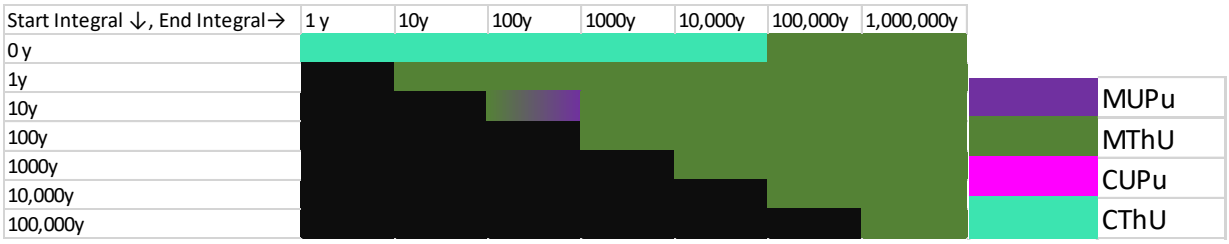

Figure 35, Fuel Cycle Options with Highest-Energy-Normalized Integrated Decay Heats at Various Starting and Ending Timescales

In these figures, black cells denote irrelevant integrals (e.g., any reverse integral, such as from 10,000 to 100 years). The fuel cycle with the highest integrated decay heat for each cell is indicated by the color in the legend. Cells with multiple colors denote cases where the two fuel cycle options having the highest integrated decay heat were within 10% of one another. Switching from between activity and decay heat does not change which fuel cycle option has the largest impact at nearly any timescale except those beginning and ending at very early times that are unimportant to disposal timeframes. The results are similar when considering the fuel cycle options with the lowest integrated activities and decay heats, respectively, as shown in Figure 36 and Figure 37 respectively, below:

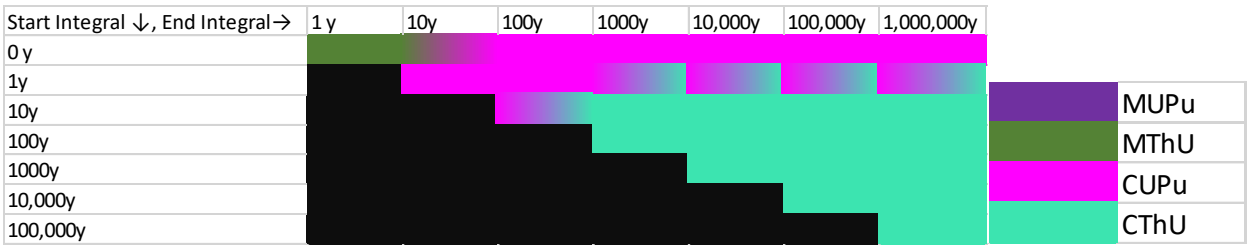

Figure 36, Fuel Cycle Options with Lowest Energy-Normalized Integrated Activities at Various Starting and Ending Timescales

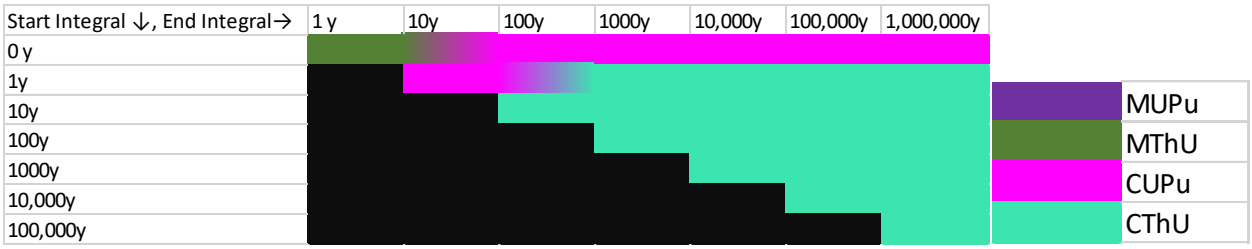

Figure 37, Fuel Cycle Options with Lowest Energy-Normalized Integrated Decay Heats at Various Starting and Ending Timescales

Once again, the two figures are nearly identical. It is therefore concluded that considering both activity and decay heat is unnecessary, and that since decay heat is probably the more important of the two factors with regards to both waste package and repository design [Hill 2010], it is the metric discussed further in this analysis.

Previous figures have indicated that for more nearly all conceivable timeframes, CThU has the most favorable integrated decay heat properties while MThU has the least favorable integrated decay heat properties. Exceptions occur for integrals that begin at very early times, especially those that begin immediately at the time of discharge (t=0). For the closed fuel cycle options, a large fraction of the total decay heat integral between 0 to 1,000,000 years is attributed to the first year: for CUPu, this fraction is 14%, while for CThU, this fraction is 84%. It is believed that the large variations in the dominance of these “short-term effects” between fuel cycles is not

necessarily an intrinsic difference between the fuel cycle options, but rather a consequence of different assumptions in the isotopic inventory data from which these results were generated. These inventories for MUPu, CUPu, and CThU were taken from results from the FCO-ESS [Wigeland 2014] that were later posted to a database [Sandia 2016], while the inventories for MThU were generated independently. While guidelines are not published for the timeframe of the isotopic inventories of these fuel cycle (as they are of little relevance to nearly purpose except this HLW property exercise), it is thought that the values for MUPu and CUPu must account for some short storage period while the values for CThU represent those that are straight out of an MSR, immediately after discharge.

To avoid these misleading "edge effects", this analysis will consider integrals that begin well after 1 year. In any case, SNF/HLW would be unlikely to be disposed any earlier than 10 years after discharge, and in all likelihood this interim period would be even longer than 10 years. Thus, this analysis considers integrals beginning at 100 years. Regulatory timescales have changed over time and have covered periods at least to 10,000 years and occasionally to 1,000,000 years. The results of integrals beginning at 100 years and ending at times 10,000 years, 100,000 years, and 1,000,000 years are shown in Figure 38, Figure 39, and Figure 40 respectively, below:

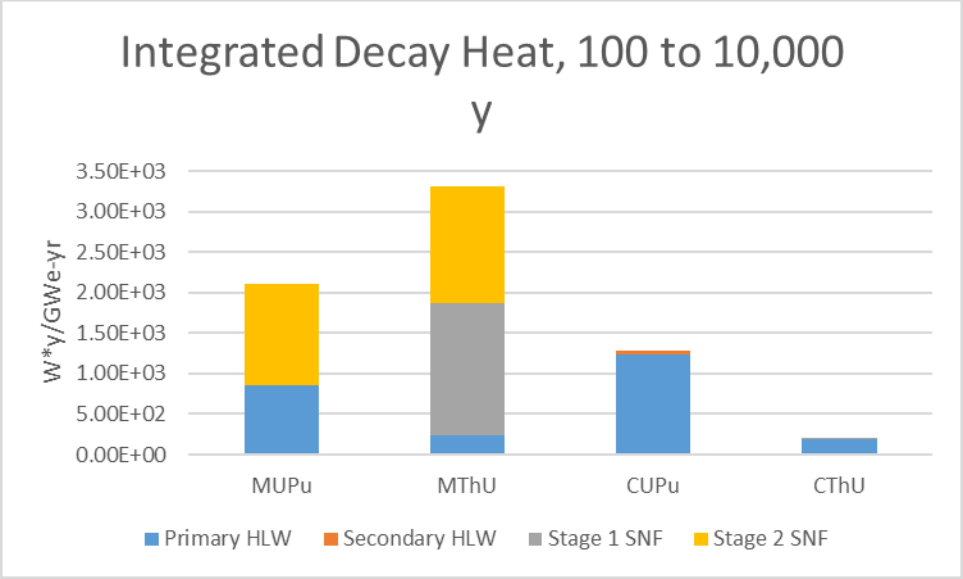

Figure 38, Energy-Normalized Integrated Decay Heat from 100 to 10,000 Years

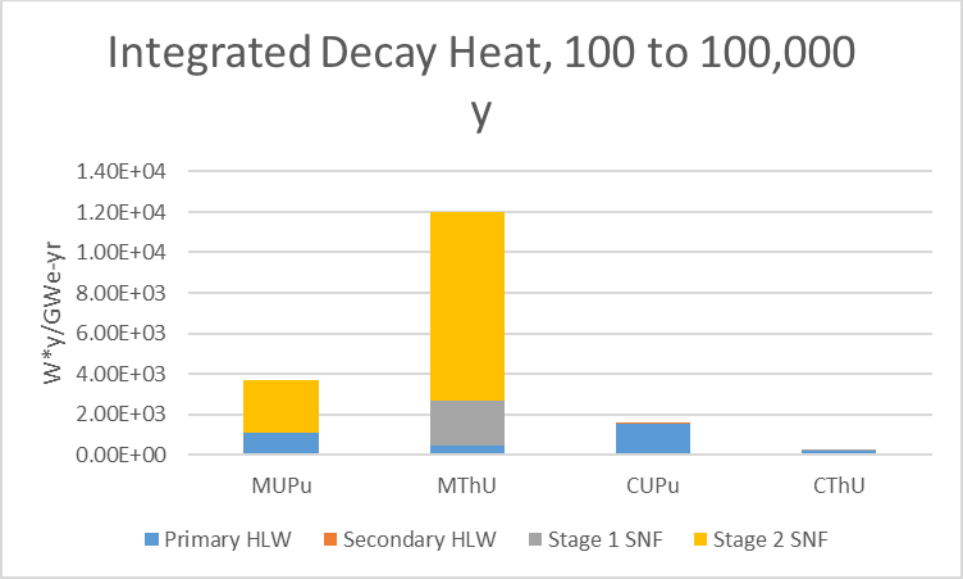

Figure 39, Energy-Normalized Integrated Decay Heat from 100 to 100,000 Years

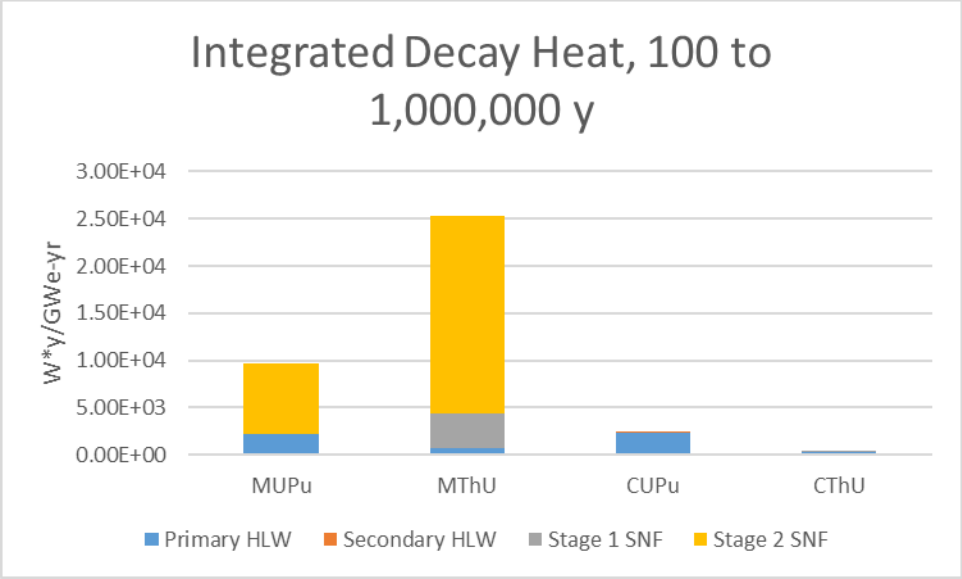

Figure 40, Energy-Normalized Integrated Decay Heat from 100 to 1,000,000 Years

"Secondary HLW" refers to the less-hazardous waste stream for the closed fuel cycles that have two HLW streams: the blanket-processing HLW stream for CUPu and FP2 for CThU. While the magnitude of integrated decay heat changes considerably between these three timescale options, the comparative trends between the four fuel cycle options are relatively consistent for all three time. At each timescale, MThU has the highest SNF/HLW decay heat impact, with the bulk of this contribution coming from the discharged Th/U-233 fuel of Stage 2. Even though Stage 2 only accounts for about a quarter of the power share in MThU, the decay chains of first the U-233 decay chain and later the U-234 decay chain contribute comparatively significant amounts of decay heat for very long periods of time. Even at shorter timescales not shown in the previous three figures, the MThU fuel cycle is compromised by having the "worst of both worlds"; since it discharges both used UOX and Th/U-233 MOX fuels, its decay heat plot shows the peaks of both fuel types.

MUPu has the second least favorable SNF/HLW decay heat impact at all three timescales; its decay heat integral varies between 33% and 64% of the value for MThU depending on the particular timescale that is used. The Stage 2 discharge fuel comprises an increasingly dominant fraction of the total decay heat of the fuel cycle at longer times, primarily due to the Np-237 decay chain (essentially the same as the U-233 decay chain), and to a lesser extent due to the Pu-242/U-238 decay chain.

The most important message to be taken from these results is the difference between modified-open and closed fuel cycles, rather than between U/Pu and Th/U fuel cycles. At long timescales, actinides dominate the contribution to decay heat, and closed fuel cycles send far fewer actinides to disposal on an energy-normalized basis. The significant difference between CUPu and CThU is due more to differences in the reference technology than it is to the properties of thorium versus uranium. The actinide losses are essentially limited by reprocessing efficiency, and even 0.1-0.2% losses from SFR fuel reprocessing are significant compared to the practically perfect reprocessing efficiency that is supposedly permitted by MSR separations (actinide-bearing HLW/GWe-yr: 1.04 MT for CUPu vs. 0.002 MT for CThU). However, even if salt discard losses were much larger than initially assumed, say 100 times larger, the CUPu fuel cycle would still have a higher integrated decay heat impact than CThU, as can be seen below in Figure 41:

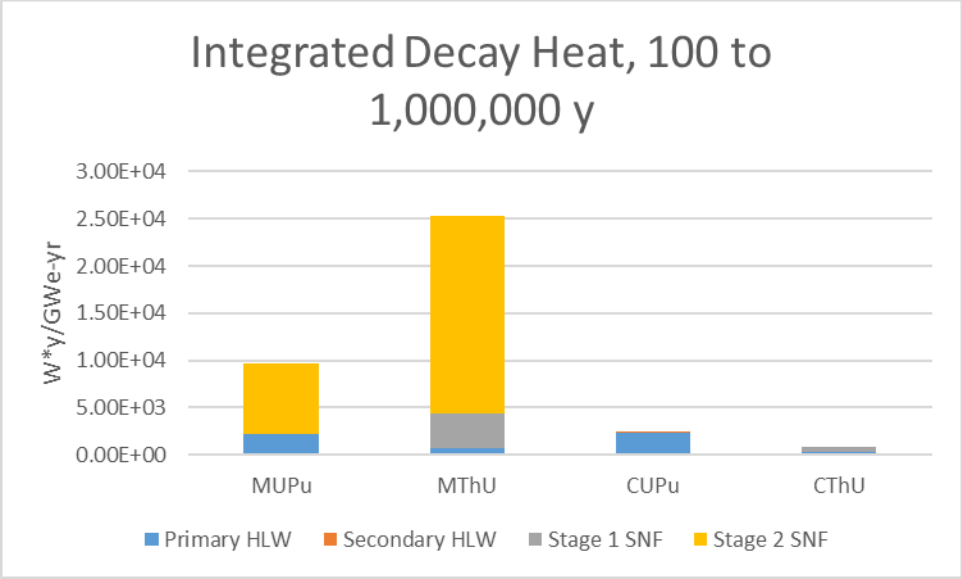

Figure 41, Energy-Normalized Integrated Decay Heat from 100 to 1,000,000 Years if CThU's Salt Discard Losses Are Increased by a Power of 100

Granted, the values for CUPu and CThU are now about a factor of 3 different instead of a factor of 9, but this still a significant difference. The salt discard stream actually has quite a large integrated decay heat on a mass-normalized basis, given the significant presence of both the U-233 and U-234 decay chains, but even the revised mass flow rate, 0.2 MT/GWe-yr, is still much smaller than the 1.04 MT/GWe-yr for the CUPu fuel cycle. It is unlikely that the MSR salt discard rate would be larger than this; even if the MSR disposed of its entire salt inventory every 80 years (which would completely imbalance the steady-state assumption), which is equivalent of an annual loss of 1.25%, the salt discard rate would still only be .09 MT/GWe-yr which is less than the 0.2 MT/GWe-yr for which the previous results are shown. In other words, there is no reasonable variation of the assumptions which would result in the MSR-based CThU not having the lowest decay heat impacts. Again, this conclusion is primarily attributed to the technological differences between SFRs and MSRs and their associated reprocessing techniques: a uranium-based MSR would probably have similar decay heat properties as a thorium-based MSR, and the

same would be true for a comparison of a uranium-based and thorium-based SFR. In other words, the driving force for the energy-normalized integrated decay heat is actinide losses in the HLW and UNF.

4.4.3.2. Radiotoxicity

The results for energy-normalized radiotoxicity for each fuel cycle over time are shown in Figure 42, below:

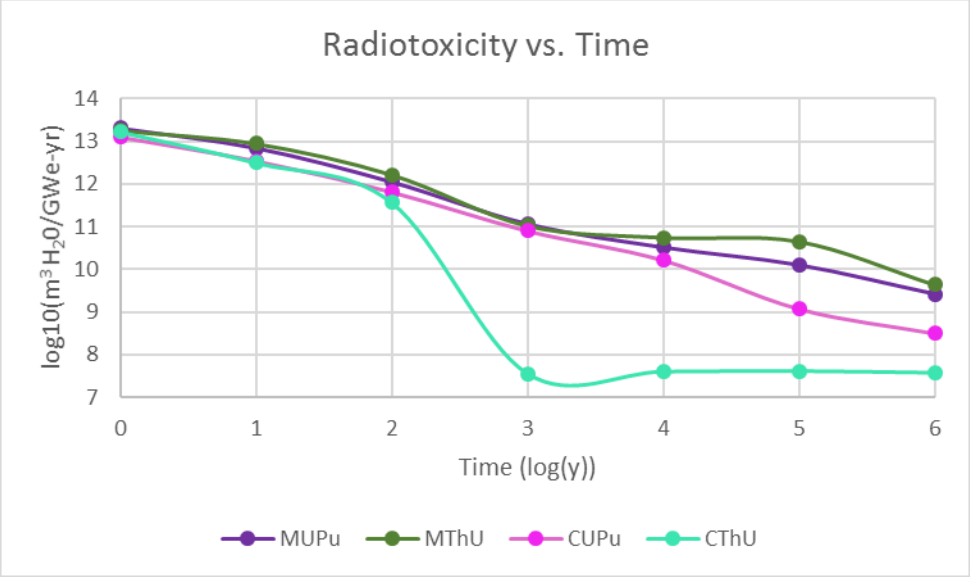

Figure 42, Energy-Normalized Radiotoxicity for Fuel Cycle Options

The Figure above indicates that the curves don't frequently cross each other, which explains why the following Figure 43 and Figure 44 show the same "best" and "worst" fuel cycle options for nearly all possible timescales of integration:

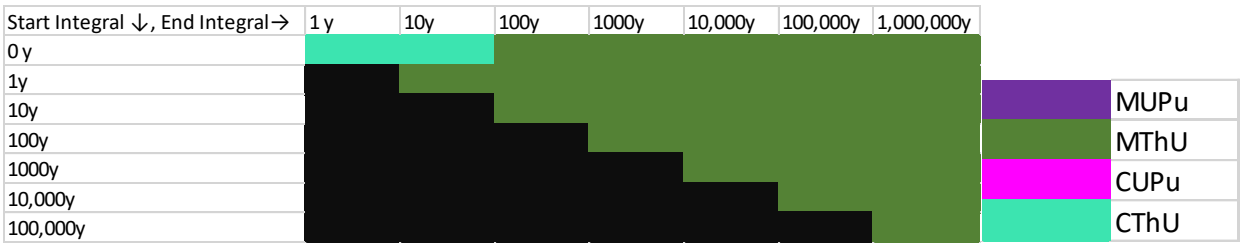

Figure 43, Fuel Cycle Options with Highest Energy-Normalized Integrated Radiotoxicities at Various Starting and Ending Timescales

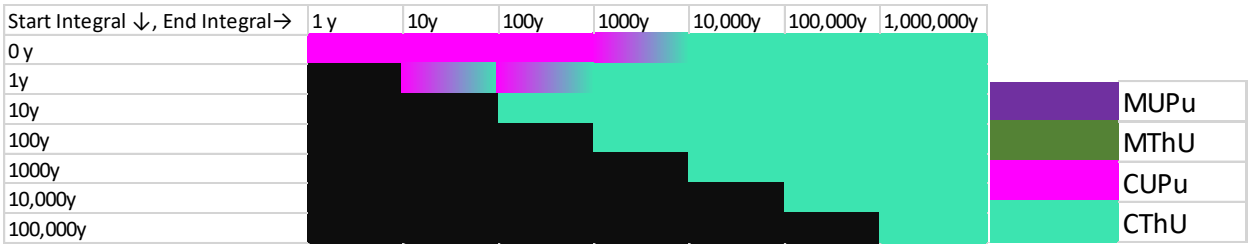

Figure 44, Fuel Cycle Options with Lowest Energy-Normalized Integrated Radiotoxicities at Various Starting and Ending Timescales

While radiotoxicity trends are not identical to decay heat and radioactivity, they both depend on the mass inventories of the same classes of radionuclides, and thus there is still some correlation between radiotoxicity and decay heat (see [Stauff 2015]). Conclusions regarding integrated radiotoxicity regardless of whether short-, medium- or long-term timescales are of interest, as is shown by Figure 45, Figure 46, and Figure 47, below:

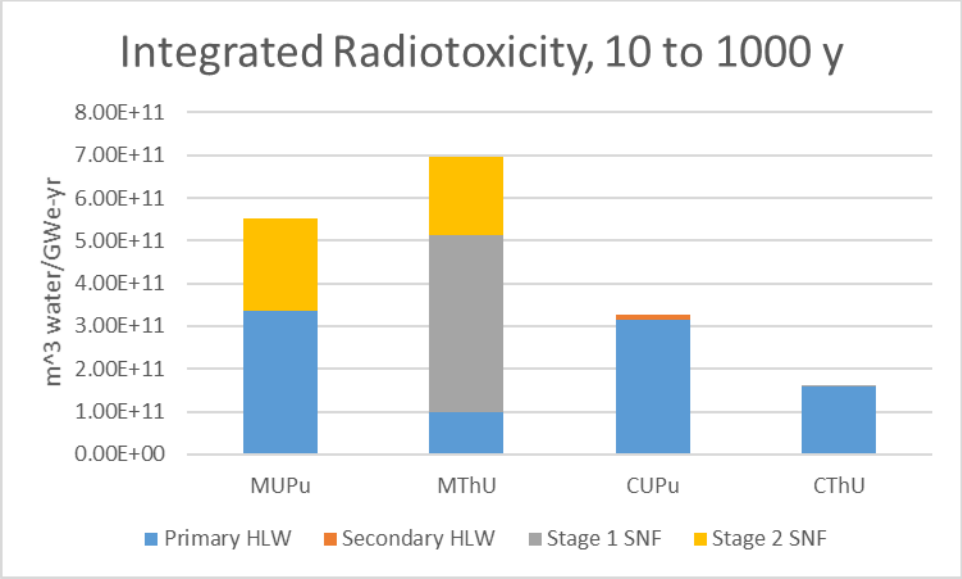

Figure 45, Energy-Normalized "Near-Term" Integrated Radiotoxicity Impacts (10 to 1000 Years)

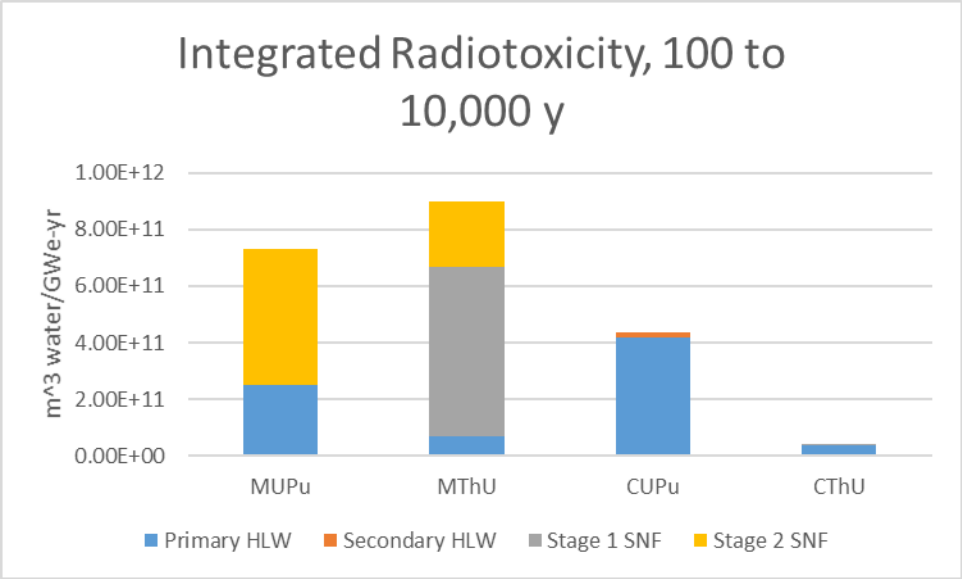

Figure 46, Energy-Normalized "Medium-Term" Integrated Radiotoxicity Impacts (100 to 10,000 Years)

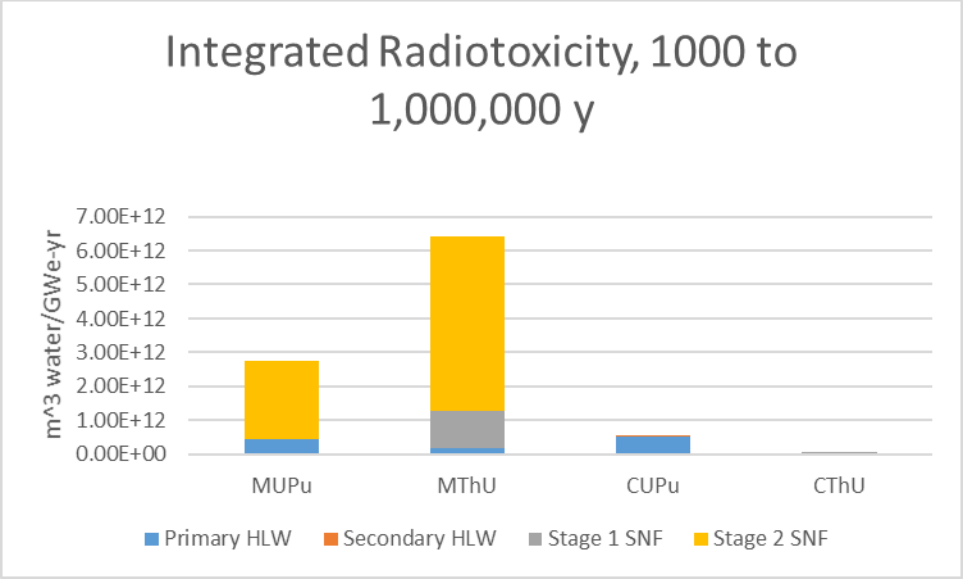

Figure 47, Energy-Normalized "Long-Term" Integrated Radiotoxicity Impacts (1000 to 1,000,000 Years)

While the magnitude of the differences changes over time, the order of most radiotoxic to least radiotoxic is always MThU, MUPu, CUPu, and CThU. Once again, the gap between the modified-open fuel cycles and the closed fuel cycles becomes increasingly large over time as the quantity of actinides, and to a lesser extent the identity of those actinides, dictates radiotoxicity performance. The U-233/Np-237 and U-234 decay chains turn out to be the driving forces for radiotoxicity for MUPu and MThU, just as they were for decay heat.

4.4.3.3. Additional Insights Regarding Repository Risk

The previously calculated parameters of activity, decay heat, and radiotoxicity are actually measures of waste hazard rather than true measures of risk in a repository; in particular, they do not consider the ability of a particular radionuclide to mobilize and be transported through repository barriers and geologies to the accessible environment. This is a very important consideration when determining the threat that is actually posed by a particular fuel cycle –

waste package – repository configuration. To account for these transport phenomena, detailed performance assessments (PAs) can be conducted that make assumptions regarding the probability distribution functions of the escape of radionuclides from waste forms and waste packaging over time, then combine these fractional escape rates with complex transport physics (e.g., [Wilson 1994], [Hansen 2011]). While the information they yield is useful, even the less comprehensive PAs are major undertakings generally requiring multiple software tools and extensive data collection, and they are well beyond the scope of this study. In any case, they require very specific assumptions about waste packaging and repository geology that would confound the emphasis on intrinsic fuel cycle properties.

An alternative approach has been identified based on a review of trends in previously conducted PAs. This review determined that in spite of the range of waste forms and geologies that can be considered, the same list of seven fission products and activation products dominate contributions to risk, albeit at varying magnitudes for different assumptions: C-14, Cl-36, Se-79, Tc-99, Sn-126, I-129, and Cs-135 [Croff 2015]. This is very different than the driving factors behind decay heat or radiotoxicity, which were dominated by actinides and their decay chains at long times.

Two of these, C-14 and Cl-36, are activation products from reactions with naturally occurring material in the reactor. C-14 is produced by impurities from three different sources: N-14, O-17, and C-13. Nitrogen, oxygen, and carbon are among the planet's most common elements and will always form some impurities in fuel, moderator, and other hardware structures [Davis 1977]. Chlorine-35 is an impurity in graphite rods, coolant water, and other hardware structures

[Griffiths 2007]. C-14 and Cl-36 are both frequently major contributors to repository risk (although generally still much less important than I-129); however, the concentrations of C-14 and Cl-36 are not calculated during reactor physics simulations unless the initial concentrations of their precursors is specified, and this is seldom done due to lack of knowledge concerning precursor concentrations. Even for conventional used fuels this data is limited, and for advanced fuels there is no basis for making inferences of the relative concentrations of these impurities. Thus, C-14 and Cl-36 are not considered in this analysis.

The eventual intent of the methods described in [Croff 2015] is to establish weighting factors for the key radionuclides that can be multiplied by the concentrations and/or masses of those nuclides in various spent fuel or waste streams. While some general understanding of the relative risk has been developed (e.g., I-129 is in most cases responsible for 80% or more of the total risk), formal weighting factors have not yet been developed. In the meantime, the total masses of the remaining five fission products that are sent to waste can be compared among the four fuel cycle options, as is shown in Table 24 below:

Table 24, Energy-Normalized Masses of Key Risk-Contributing Radionuclides Destined for Waste by Fuel Cycle (All masses in kg/GWe-yr)

	MUPu**	MThU	CUPu	CThU
Se-79	0.21	0.32	0.14	***0.46***
Tc-99*	***27.33***	21.02	20.75	20.53
Sn-126	1.06	1.02	***1.47***	1.10
I-129	6.77	6.80	6.67	***8.01***
Cs-135	16.40	14.61	***36.21***	4.75
*Also includes mass of parent nuclides Mo-99 and Tc-99m				
** For comparison, the OTC's contributions are similar to MUPu's: 0.21 for Se-79, 27.40 for Tc-99, 1.03 for Sn-126, 6.54 for I-129, and 15.58 for Cs-135				

The most important radionuclide, I-129, is relatively similar for the first three fuel cycles, but CThU produces 19% more I-129 than the average of the other three fuel cycles. This is because I-129 has a somewhat larger fission yield for U-233 than it does for U-235 and Pu-239. MThU is also subject to this characteristic, but a large fraction of the total fissions in the MThU fuel cycle come from U-235, given the high enrichment of the Stage 1 driver fuel. MUPu and CUPu both have larger fission contributions from Pu than MThU does, and Pu-239 has a slightly higher I-129 fission product yield than U-235. When these effects are combined, the resulting I-129 mass is very similar among MUPu, MThU, and CUPu.

For Se-79, production is notably larger for MThU than for either of the uranium-based fuel cycle and larger still for CThU, which has even more U-233 character. As might be expected, U-233's fission yield of Se-79 is significantly larger than for U-235 or Pu-239. Two other radionuclides, Sn-126 and Cs-135, are produced in larger yields by Pu-239 and Pu-241 than is true for U-233 or U-235…as a result, the fuel cycle dominated by plutonium fissions produces considerably larger amounts of those two radionuclides. Tc-99 production is relatively similar for all the fuel cycles.

It should be noted that one point on this data table is primarily a result of technology assumptions rather than nuclear properties; CThU's production of Cs-135 looks particularly low. While it is true that U-233 produces somewhat fewer Cs-135 than other fuel cycles, the primary reason for this exceptionally low value is cesium's chemical similarity to lithium, which comprises a large mass fraction of the circulating fuel salt. Salt cleanup and processing is specifically configured to leave lithium in the reactor so that salt is not wasted. This also means

that most cesium follows the lithium, and only a small amount of cesium is removed during every cycle.

The results of this exercise demonstrate why comparisons of waste hazard must be done cautiously, and why future work in the area of performance assessments of thorium-based fuels is desirable to reach "final" conclusions. The hazard-based metrics do tend to favor the CThU fuel cycle, which has been used to support many pro-thorium arguments over multiple decades. However, when it comes to actual repository risk, which is likely a more practical view of the actual "impact" of the SNF/HLW, the fuel cycles are actually very similar, and if anything, CThU poses a slightly larger risk due to its slightly greater production of I-129.

While the goal of this effort is to focus on fuel cycles rather than technologies, there would potentially be a significant change in the results had another reference technology been considered. If the intent were to revisit this study with a comparison of two fast-spectrum options, a molten-chloride fast reactor would be apt to produce large amounts of Cl-36 given its massive initial concentrations of Cl-35 as the primary anion of the fuel salt. While Cl-36 has trailed I-129 in importance for past performance assessments, no fuel cycle evaluated to-date has produced particularly large quantities of Cl-36, so the order of importance could be impacted for that particular technology implementation.

4.4.4. Impacts of Resource Stewardship

A natural outcome of the fuel cycle material flow analysis is the natural resource requirement of each fuel cycle. These results are shown below in Table 25.

Table 25, Resource Usage by Fuel Cycle

	MT NU/GWe-yr	MT NTh/GWe-yr
MUPu	178.1	n/a
MThU	89.8	10.7
CUPu	1.06	n/a
CThU	n/a	0.91

The MUPu fuel cycle uses about 10% less natural uranium than the once-through fuel cycle, which is consistent with the present understanding of similarly operational fuel cycles in Europe. While the MThU fuel cycle has a relatively high U-235 enrichment due to its significant fissile requirements, with respect to resource usage this fuel cycle benefits from (1) the relatively small fraction of Stage 1 fuel (26.5%) that is comprised of uranium and (2) the larger power contribution from Stage 2 due to the larger accumulation of new fissile material (i.e., U-233) from Stage 1. For equivalent amounts of uranium and thorium fuel, natural uranium requirements will nonetheless be much higher than natural thorium requirements if any appreciable enrichment is performed, due to the significant loss of incoming natural uranium to depleted uranium. Thus, even though most MThU fuel is thorium-based, natural uranium consumption still dominates natural thorium consumption on a mass basis. For comparison, the OTC (under the same assumptions as MUPu's Stage 1) uses 203.7 MT NU/GWe-yr, which is about 14% larger than that of MUPu.

The closed fuel cycles have much smaller energy-normalized resource requirements than those of the modified-open cycles. There is no reason to visualize only the CUPu and CThU requirements, as they are quite similar on a mass basis: 1.06 MT NU/GWe-yr for CUPu and 0.91 MT NTh/GWe-yr for CThU. For comparisons at steady-state, this is not a particularly interesting result, other than to confirm that the resource requirements of CUPu and CThU are similar. As

Chapter 5 will show, the resource comparisons between CUPu and CThU are much more important for transition analyses from the present once-through fuel cycle, as cumulative resource impacts will essentially come down to which fuel cycle is capable of implementing a large fraction of end-state (closed fuel cycle) behavior the quickest.

4.5. Key Insights from Steady-State Comparison of Uranium/Plutonium- and Thorium-Based Options

This chapter has compared four representative fuel cycle options that encompassed a spectrum of recycle options for both thorium- and uranium-based fuels. Metrics were identified and then quantified on a mass-normalized basis for routine occupational dose, LLW volumes, SNF/HLW properties and hazard/risk, and resource stewardship. Mass flow analyses were conducted for each fuel cycle to support the conversion of the quantified mass-normalized metrics to energy-normalized metrics, enabling the fuel cycle options to be compared on a common basis. The results of these energy-normalized metrics were then evaluated, compared, and discussed. Major findings are as follows:

For Occupational Dose:

- The CThU fuel cycle may offer some advantages by effectively consolidating multiple facilities (reactor, reprocessing, and potentially fuel fabrication) into a single facility, limiting the opportunities for separate exposure. In combination with the closed fuel cycles having only a small dependence on front-end services such as resource recovery, this reduction in exposure looks promising.
- However, both the CUPu and CThU fuel cycles are subject to large uncertainties regarding the most important contributor to dose: the reactor. The consequence of

adopting different assumptions for the doses from different advanced reactor technologies is that the effects of all other assumptions are mostly insignificant.

- If the contributions from reactors is assumed to equal for all technologies, CThU still looks promising since it avoids most impacts of the front-end of the fuel cycle, including both recovery and fuel fabrication. CUPu is also preferable to the modified-open fuel cycles given its low resource recovery requirements.

For LLW:

- LLW volumes are also highly uncertain for the advanced fuel cycles in particular, but it appears that CThU will produce larger volumes of LLW than other fuel cycle options given its continuous throughput of material through many processing systems and the tendency to quickly use up small components during chemical purification.
- Among the remaining fuel cycle options, impacts are relatively similar.
- If mining wastes are considered on a volumetric basis, they completely overwhelm all other LLW categories. Because uranium depends on "primary" mining, it has a much larger associated mining waste volume than thorium that is produced as a by-product of titanium.
- Both MUPu and MThU produce depleted uranium, while MUPu also produces excess recycled uranium, these are two additional waste streams that will require management.

For SNF/HLW:

- It is apparent that the CThU can be made to look "good" or "slightly below average" depending on which metrics are considered.

- For most long-term integrals of the hazard-based metrics of decay heat and radiotoxicity, CThU performs favorably when compared to CUPu and even more favorably when compared to the modified-open fuel cycles, primarily due to the relatively small amounts of actinides that are sent to disposal.
- However, repository performance assessments have demonstrated that certain key fission products, rather than actinides, are indicative of the repository risk posed by a fuel cycle. One fission product, I-129, is overwhelmingly the most important radionuclide for nearly all disposal scenarios, and CThU actually produces 19% more I-129 than the other fuel cycles, which perform relatively similarly in this regard.

For Resource Stewardship:

- Conclusions regarding resource stewardship fall much more along the lines of differences in recycle approaches – modified vs. closed – rather than thorium versus uranium. CUPu and CThU have relatively similar resource requirements by mass, which is much lower than the associated requirements for MThU and MUPu.

Overall:

- While closed fuel cycles will face larger implementation challenges than modified-open or once-through options, on the basis of environmental perspectives at steady-state, closed fuel cycles generally perform more favorably than other options.
- Regarding comparisons between closed thorium and closed uranium options, there appear to be tradeoffs depending on the particular metric, with the overall sense that the two will perform similarly with regards to EH&S at steady-state.

- The question then turns to how steady-state will be reached for these two promising options; this is the subject of the next chapter.

CHAPTER 5, THE IMPACTS OF DYNAMIC TRANSITION TO CLOSED THORIUM- AND URANIUM-BASED FUEL CYCLES

The previous chapter considered the relative environmental performance of representative thorium- and uranium-based cycles in their final implementation, at steady-state. In contrast, this chapter considers the near- and medium-term ramifications of transitioning from the present once-through fuel cycle in light water reactors to advanced nuclear fuel cycles. An emphasis is placed on transitions to closed fuel cycles, since these were shown in Chapter 4 to generally offer superior environmental performance than modified-open fuel cycles at steady-state.

While a fuel cycle may look promising at steady-state, it is important to conduct transition analyses to evaluate the likelihood of success of particular options. A relevant analogy is the difference between thermodynamics and kinetics; while a reaction might be thermodynamically favorable, difficult kinetics may make the reaction too slow to occur on relevant timescales, or enable it to be out-competed by faster reactions. Similarly, fuel cycle transitions are dependent on certain intermediate factors. In particular, transition studies can reveal the following types of insights that a steady-state analysis would miss:

- The timeframe over which a transition would need to occur;
- The role of intermediate, potentially unfavorable phases, e.g., a large-scale investment into reprocessing and advanced fuel fabrication facilities without immediately reaping their benefit; and
- The existence of material flow bottlenecks, either temporary or quasi-permanent, that could disrupt otherwise beneficial transitions

This chapter will proceed through a series of logical steps to ultimately compare the dynamic impacts associated with transitions to closed thorium- and uranium-based fuel cycles. First, some general principles of dynamic transitions will be described to provide a computational context for the remainder of the chapter, including some background on the software tool that was used to support the analysis. Next, each of the five scenarios studied in this chapter will be described and defined. The two subsequent sections represent the analytical backbone of the chapter; first, the material flow results of each of the five scenario simulations will be reviewed and discussed. Then, the dynamic material flow results will be combined with mass- and energy-normalized impacts to assess the cumulative environmental impacts associated with the different transition pathways.

5.1. Dynamic Transition Analysis Techniques

This section is broken into two sub-sections. The first will provide some general background for assessing nuclear fuel cycles on a time-dependent basis; the other sub-section will provide background on the implementation of software-enabled fuel cycle simulation tools to support dynamic analysis.

5.1.1. Some Perspectives on Fissile Material Balances for Dynamic Transitions

The underlying principle of a material balance is that the net accumulation or depletion of a substance is equal to the rate of its production and/or entry minus the rate of its consumption and/or loss. However, accounting for these streams becomes increasingly challenging when considering time-dependent problems with evolving terms. Section 2.3 presented some

background on previous applications of dynamic transition analysis, while Appendix C presents a discourse on the computational concepts related to dynamic material balances.

It is necessary to conduct rigorous dynamic simulations using sophisticated modeling approaches to understand scenarios before they reach their self-expanding state. While key growth parameters may eventually become relatively constant at long times, there are likely to be long time periods where fluctuation is significant, and the material balance relationships will be complex. Also, the early transitions are unlikely to occur with *only* contributions from the final closed-recycle stage; thus, there will be a period of time, potentially extended, where co-existence between the SFRs/MSRs and previous-generation LWRs will be necessary. Newer LWRs may need to be built, even after the transition has begun, due to material availability and electricity demand issues. Furthermore, if high breeding ratio requirements present technology development and implementation challenges, it may make more sense to continue to allocation of portion of new builds to LWRs to help carry the weight of fissile material production. These are difficult questions to answer with theory and intuition alone -- presenting the argument for a structured quantitative analysis.

5.1.2. Fuel Cycle Analysis Software Tools

The complexity of the phenomena and the inter-relationships described above makes it necessary to employ sophisticated modeling tools to conduct even simplified dynamic analyses. One computational challenge with dynamic scenario analysis is the variety of objectives and constraints, which can often be mutually exclusive or competitive. A top-level objective is the continuous satisfaction of an imposed energy demand, but possible secondary objectives include

meeting specified reactor portfolio compositions, utilizing all existing reactors to their capacity, and balancing immediate and future energy and fissile materials requirements. Possible constraints include fissile material availability, facility capacity (including deployment dates as well as the scale and efficiency of individual facilities), technological maturity[27], and resource limitations[28]. Given the complex and changeable nature of these objectives and constraints, it is necessary to employ computational and modeling aids to quantitatively evaluate scenarios of interest.

A number of pre-developed, software-enabled tools exist to model the deployment of nuclear technologies. Each of these tools is multi-faceted and capable of accommodating a range of problems; however, each also comes with strengths and weaknesses. Appendix D provides a background on four tools which are known to have diverse capabilities and whose uses in prior work have been well-documented: DANESS, VISION, ORION, and CYCLUS. There are other fuel cycle analysis tools which have developed and used at other times, but these seem to either have been outmoded (e.g., DYMOND effectively being succeeded by VISION) or withdrawn from active recent development (e.g., CAFCA [Boscher 2004]).

This analysis adopts the Verifiable Fuel Cycle Simulation Model (VISION). VISION is a computer software modeling tool, developed at INL, which enables dynamic fuel cycle simulations to determine material flows and potentially other parameters of interest. It was originally developed based on a preceding tool, DYMOND, but has added additional

[27] Economic constraints are another critical real-world constraint, but these were not considered in this analysis.
[28] Environmental metrics were treated as outputs rather than as constraints in this study, but hypothetically they could also be applied as constraints if a tool existed to accommodate such an approach.

functionalities such as economics and isotopic decay. VISION was intended to be general-use tool, without limitations to particular reactor or fuel cycle technologies. It is rooted in the system dynamics software tool, PowerSim [Yacout 2006]. The VISION model consists of three key functionalities: tracing the flow of material through the entire fuel cycle, tracking the life cycle of essential strategic fuel cycle facilities, and calculation of a variety of fuel cycle metrics. The tool tracks 81 isotopes or isotope groups [Jacobson 2006].

No previous work on the application of VISION to thorium fuel cycles was identified (although the tool has been demonstrated to be viable for this purpose, as this study will show). However, insights from the application of VISION to non-thorium systems are available. INL has used the tool internally for a variety of purposes. Among these, VISION was used to simulate the impacts of system uncertainties on partial and total fuel cycle costs. This approach was extended to both light water reactors and fast-spectrum reactors with uranium/plutonium recycle. The simulations showed significant variations in costs in response to changes in burnup, capacity factor, and reactor power [Taylor 2008]. North Carolina State University has used to VISION to support build schedules for constituent facilities of advanced nuclear fuel cycles. The model successfully provided information regarding ideal facility sizes, lead times, and building schedules under a variety of constraints [Schweitzer 2008].

For this study, VISION was selected for its ready availability (VISION is freely available, although its underlying platform PowerSim requires a license), for its ability to model facilities that are commonly found in the US nuclear fuel cycle as well as those anticipated for advanced fuel cycles, and for its demonstration of reliable performance.

5.2. Overviews of Transition Pathways

This section introduces the specific transition pathways that are considered in this study. While an emphasis is placed on transitions that approach two steady-state fuel cycles, CUPu and CThU, there are multiple conceivable pathways to connect the present fleet of uranium-fueled light water reactors[29] to each of those end-state options. Three transitions pathways to CUPu and two transition pathways to CThU are described in this section and are analyzed in subsequent sections. This section emphasizes a qualitative description of the fuel cycles; quantitative assumptions and parameters that are required to perform modeling simulations are described in the relevant subsections of Section 5.3.

5.2.1. CUPu Transition Scenario Descriptions

5.2.1.1. Scenario CUPu-T1 – Expansion by Plutonium-Breeding SFRs

The simplest transition for CUPu (in terms of the complexity of material flow, not in terms of technology maturation requirements) is a rapid switch from the current once-through uranium fuel cycle in PWRs to an initial fleet of SFRs, which then capitalize on their ability to produce excess plutonium via breeding to sustain the growth of new SFRs. Reprocessing plants must come online prior to the deployment of the earliest SFRs to recover plutonium from reprocessed PWR fuel. Figure 48, below shows the evolution of the components of this fuel cycle transition, which is henceforth identified as "CUPU-T1", over time.

[29] To make both computations and interpretation more straightforward, the existing fleet is modeled as entirely PWRs, rather than as approximately two-thirds PWRs and one-third BWRs. The downblending of weapons-grade plutonium is also not incorporated, as its impact is difficult to project for future time intervals.

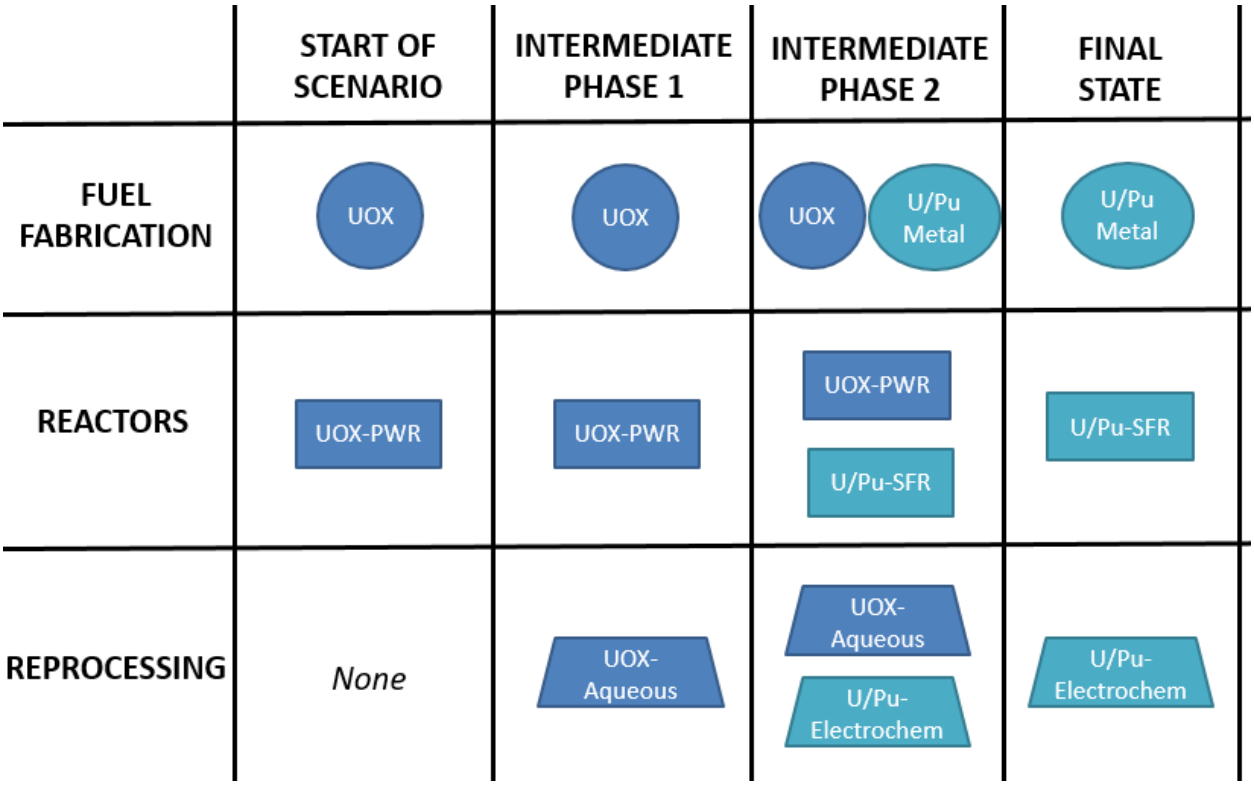

Figure 48, Evolution of Major Fuel Cycle Components over Time for Scenario CUPu-T1

During Intermediate Phase 2, the balance of multiple reactor types shifts to an increasingly larger contribution from SFRs over time. To clarify how material flows evolve as the transition progresses, Figure 49, below, shows the flows of heavy metal-derived material that comprises this transition.

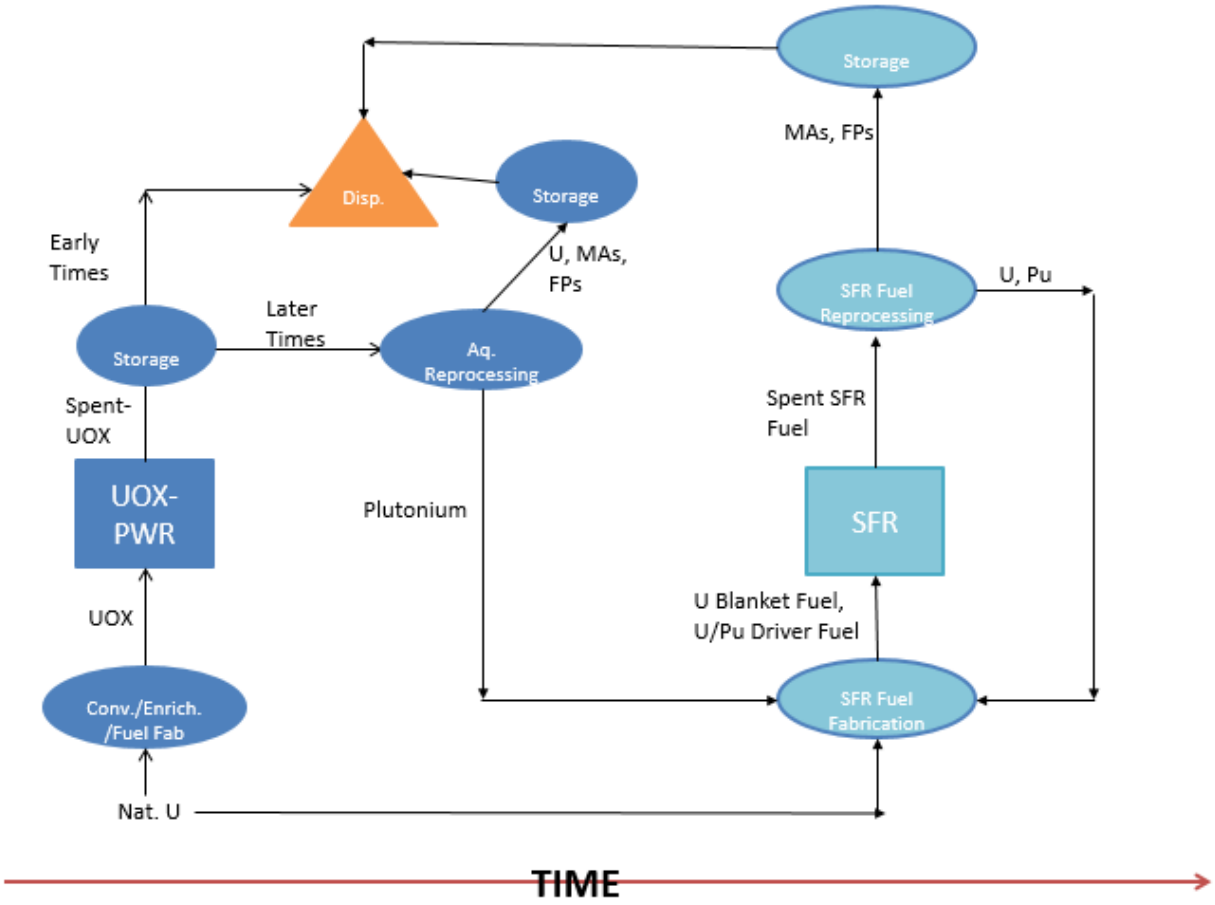

Figure 49, Evolution of Material Flows for Scenario CUPu-T1

To make the diagrams easier to interpret (i.e., less cluttered), this diagram, and the next four similar diagrams, do not show the flow of depleted uranium and/or process losses from reprocessing or fuel fabrication. As discussed in Chapter 4, recovered and natural uranium are used for the fertile matrix of the SFR fuels, so all depleted uranium from the enrichment portion of the UOX-PWR stage will be managed as near-surface disposal waste.

5.2.1.2. Scenario CUPu-T2– Expansion by a Balanced PWR-SFR Fleet

The CUPu-T1 transition requires a sufficiently high breeding ratio to accumulate enough plutonium to sustain the expansion of an ever-growing SFR fleet. While breeding has been

demonstrated in test- and demonstration scale reactors (see Section 5.3.1.1, below), it has not yet been executed at the scale of a multi-reactor commercial fleet. Higher breeding ratios may also be accompanied by economic and materials safeguards challenges [Orlov 1980]. In any case, if decision-makers were to settle on an SFR design with a lower breeding ratio, existing SFRs would be able to sustain their own fuel supply but might not be able to support the expansion of the SFR fleet. However, the plutonium shortage could be overcome by perpetually (even at steady-state) dedicating a fraction of the fleet to new PWR builds; this is the case considered in this scenario. Figure 50, below, shows the evolution of fuel cycle components for this scenario, which is henceforth referred to as "CUPu-T2".

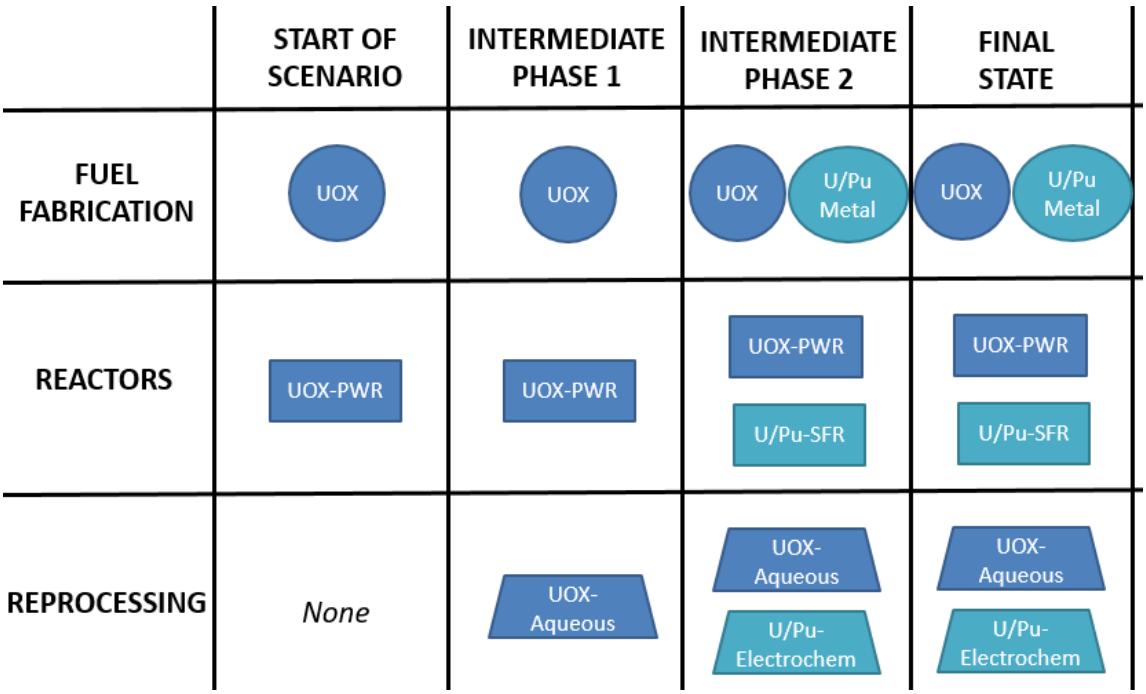

Figure 50, Evolution of Major Fuel Cycle Components over Time for Scenario CUPu-T2

During Intermediate Phase 2, the balance of the reactor types shifts to an increasingly large contribution from SFRs, eventually approaching a constant ratio in the Final State that is mostly

SFRs. The accompanying evolution of material flows for CUPu-T2 is shown in Figure 51, below.

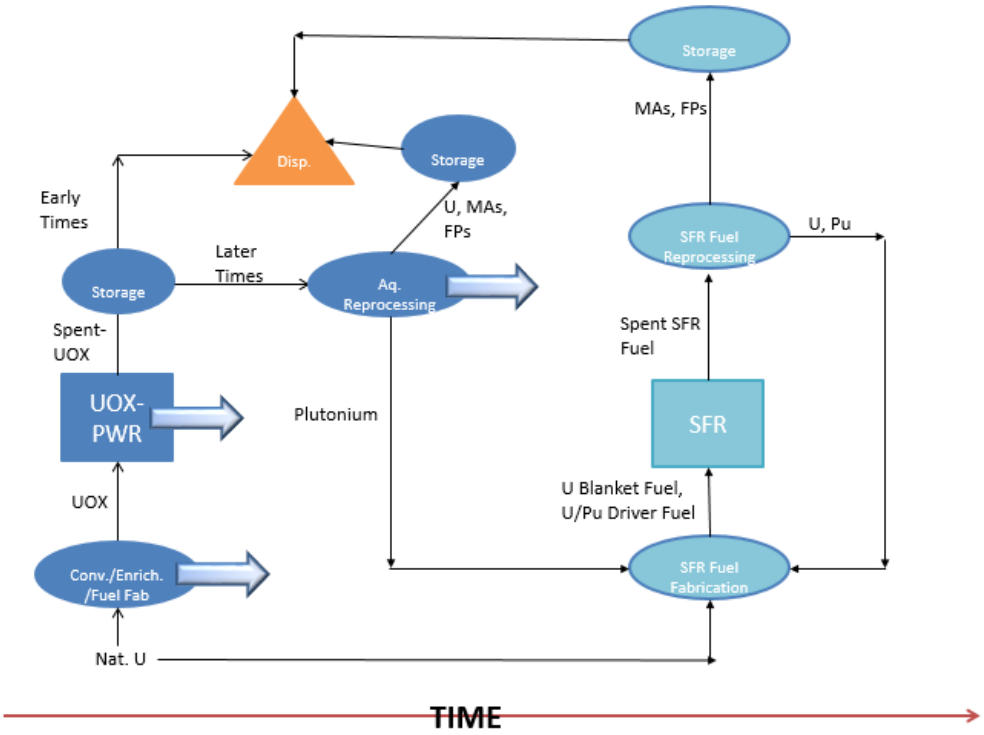

Figure 51, Evolution of Material Flows for Transition CUPu-T2 (with Translucent Arrows Showing Persistence of UOX-PWR Stage)

The diagrams for CUPu-T2 look quite similar to those for CUPu-1, except that UOX-PWRs will persist (intentionally) for the duration of the scenario to offset the lower SFR breeding ratio.

5.2.1.3. Scenario CUPu-T3 – Expansion through an Intermediate MOX-PWR Phase

The third transition returns to a higher-breeding ratio case, but with an important difference: a fuel cycle transition may elect to ease into the implementation of reprocessing and plutonium fuel technologies by adopting the use of uranium-plutonium mixed oxide (MOX) fuel in PWRs

prior to the deployment of SFRs. The earliest reprocessing of plutonium from PWR fuel would allocate its recycled material to MOX-PWRs. After a trial period, the reprocessed plutonium would instead be allocated to SFR fuel. The used fuel from MOX-PWRs, on the other hand, would not be reprocessed, although the MOX-reprocessing case could be considered as an alternative. Figure 52, below, shows the evolution of fuel cycle components for this scenario, which is henceforth referred to as "CUPu-T3".

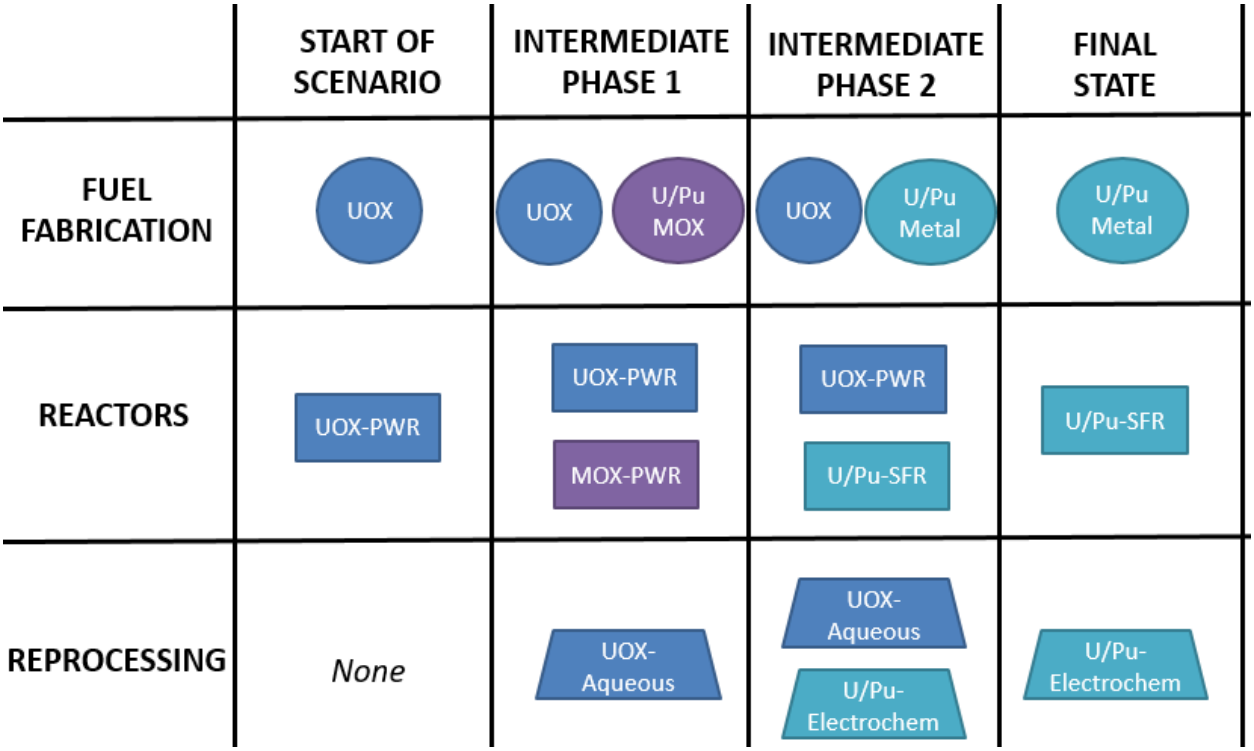

Figure 52, Evolution of Major Fuel Cycle Components over Time for Scenario CUPu-T3

The MOX PWRs in Intermediate Phase 1 do not "disappear", but rather begin to be fueled with UOX at the onset of Intermediate Phase 2 as the plutonium inventory is allocated to SFRs. Over the course of Intermediate Phase 2, the balance of reactors shifts to an increasingly large contribution from SFRs. The accompanying evolution of material flows for CUPu-T3 is shown in Figure 53, below.

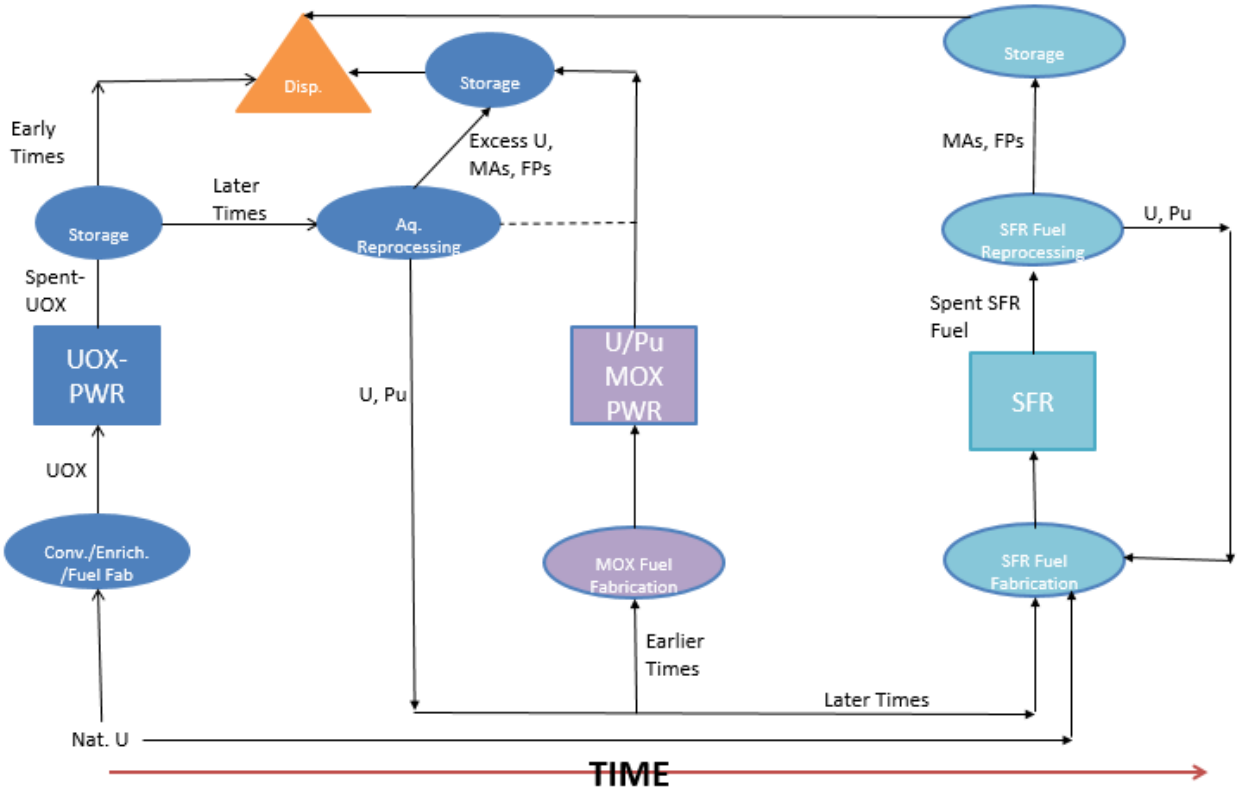

Figure 53, Evolution of Material Flows for Transition CUPu-T3, with Dashed Line Showing Optional Reprocessing of PWR-MOX fuel

As Section 5.3.1.3 will elaborate on below, the "MOX-PWRs" will only use MOX fuel during the trial period described previously. For any remaining period in the reactor's lifetime, these PWRs will be fueled with conventional UOX fuel.

5.2.2. CThU Transition Scenario Descriptions

Each of the next two scenarios involve transitions to thorium-based MSR fuel cycles, which are fundamentally different from the CUPu transitions in that their primary fissile isotope, U-233, is not present in significant quantities in existing UOX-fueled reactors. Thus, an additional step will be necessary to build up an inventory of U-233.

One option is to first accumulate a small inventory of U-233 through the irradiation of thorium blankets in reactors such as PWRs and then use that initial inventory to launch an initial small fleet of U-233-driven MSRs. These MSRs could then generate new U-233, through breeding, to support the fueling of additional MSRs. This sounds promising qualitatively, but a number of papers have noted limitations in the ability of U-233-based thermal-spectrum MSR fleets to beget additional material for new MSRs [Merle-Lucotte 2004, David 2007, Nagy 2008]. A few preliminary calculations suggest that these concerns are warranted. Even before diving into detailed systems analyses, the growth of a hypothetical MSR fleet can be estimated in terms of material doubling times, which is the time required to reproduce an initial fissile material inventory. Consider the case where a U-233 inventory (of any origin) is used to start an initial fleet of 10 thermal-spectrum Th/U-233 MSRs in 2050, with subsequent breeding occurring only in those MSRs. The resulting fleet expansion would resemble Figure 54:

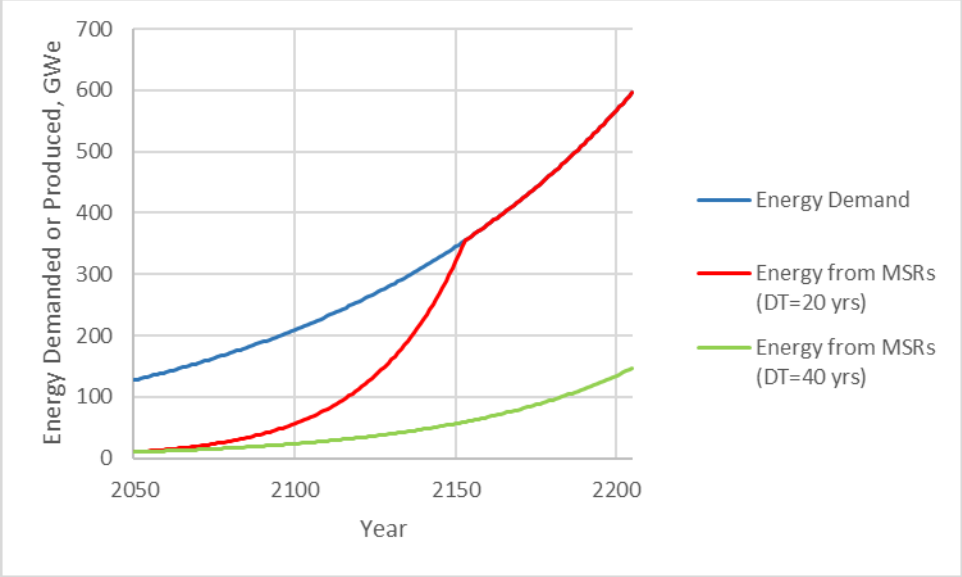

Figure 54, Rate of MSR Expansion in Self-Breeding Case for Two Possible Doubling Times

The 20-year and 40-year doubling time assumptions represent optimistic and conservative perspectives on potential doubling rates in thermal-spectrum MSRs; see Section 5.3.2 for more background on this topic. Even in the 20-year doubling time case, the scenario spends many years lagging far behind the electricity demand curve; as late as 2100, MSRs satisfy less than 30% of the scenario's electricity demand, meaning that the remainder would need to be satisfied by other sources. In the 40-year doubling time case, the fleet never even gets close to approaching the demand curve over the entire 200-year interval. While MSRs are probably the best option for thermal-spectrum breeding, accumulating fissile material at a rapid rate is nonetheless a challenge.

Thus, the scenarios that follow instead consider the case where the use of thorium blankets in PWRs is used for longer periods to continue to support the expansion of a new MSR fleet. This PWR fuel configuration is called a Seed-Blanket Breeder (SBB), in which the seed, or driver, fuel consists of enriched uranium and the blanket fuel consists of thorium. As the fissile content of the driver fuel is depleted, the blanket fuel is steadily converted into U-233. Subsequent reprocessing is applied to recover the desired fissile material from the blanket fuel while discarding the used driver fuel. By maintaining an ample SBB-PWR fleet, existing MSRs constructed are thereby less pressed to supply additional U-233 material for new MSRs.

5.2.2.1. Scenario CThU-T4– Expansion by U-233-Breeding MSRs

The first variant of this scenario entails a case where MSRs exhibit breeding behavior, so the goal is to eventually transition away from the interim SBB-PWR fleet to one that consists

entirely of MSRs. Figure 55, below, shows the evolution of fuel cycle components for this scenario, which is henceforth referred to as “CThU-T4”.

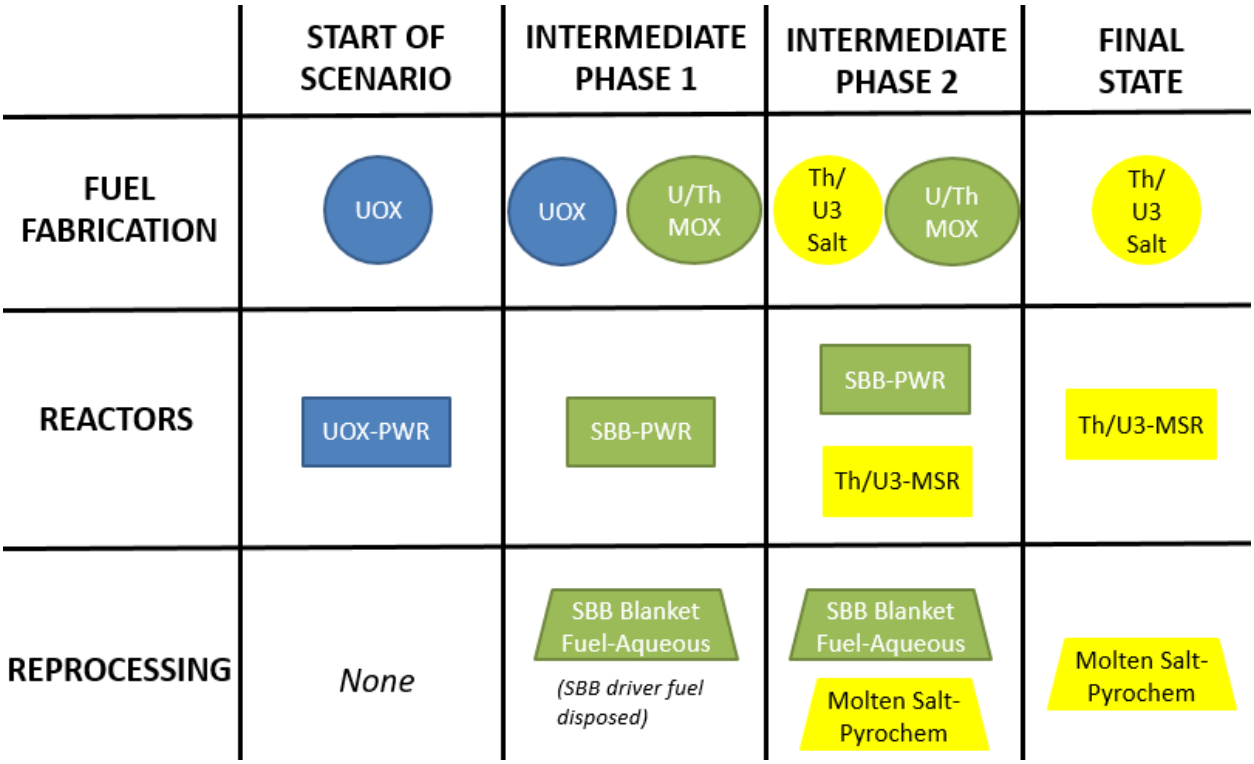

Figure 55, Evolution of Major Fuel Cycle Components over Time for Scenario CThU-T4

During Intermediate Phase 2, the balance of reactors shifts towards increasingly contributions from MSRs over time. The accompanying evolution of material flows for CThU-T4 is shown in Figure 56, below.

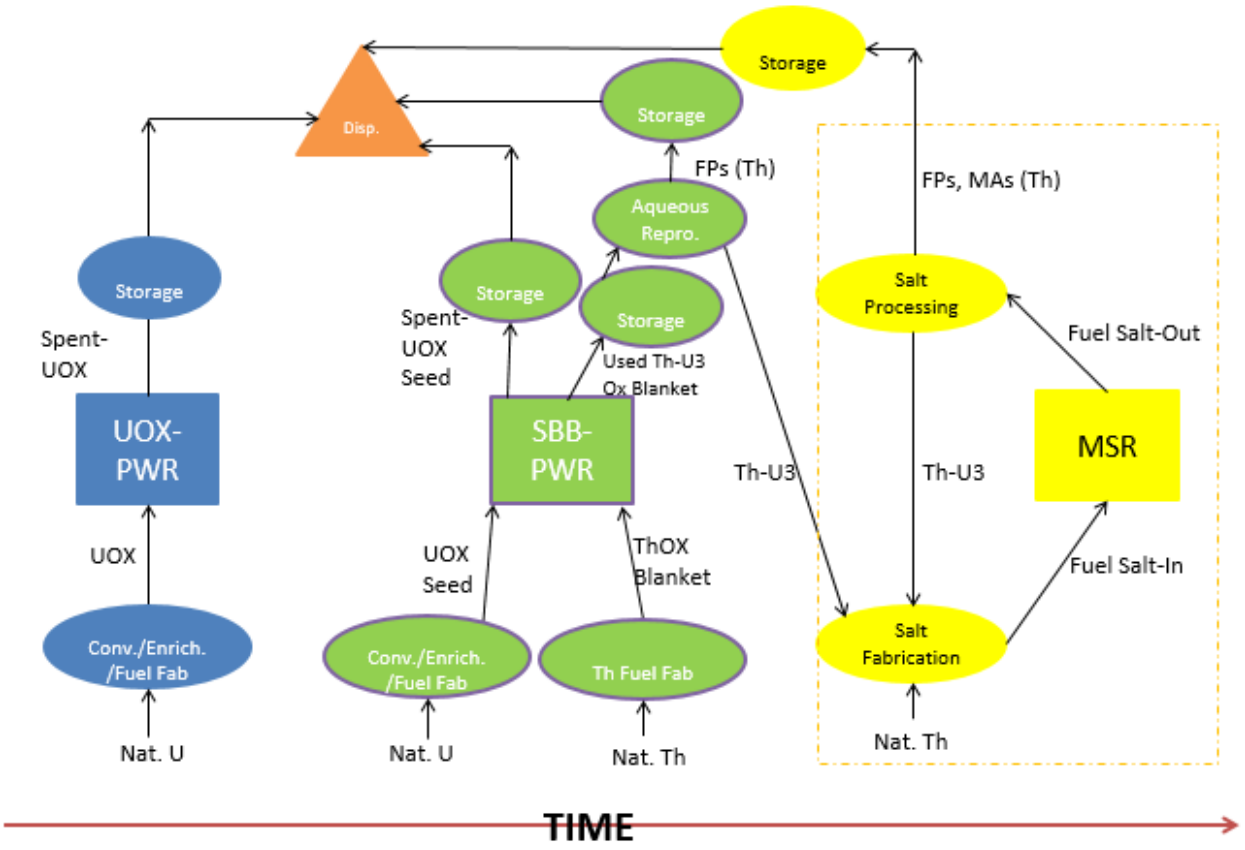

Figure 56, Evolution of Material Flows for Transition CThU-T4[30]

5.2.2.2. Scenario CThU-T5 – Expansion by a Balanced PWR-MSR Fleet

The next transition is similar to the previous one, except that it adopts a less optimistic breeding performance for the MSR, requiring a larger fraction of SBB-PWRs at later times to support continued growth. The relationship between these scenarios is similar to the relationship between CUPu-T2 and CUPu-T1, described in Section 5.2.1.2 and 5.2.1.1, respectively. Figure 57, below,

[30] Note that the dashed yellow line around the MSR facilities designates that the salt processing and salt fabrication "facilities" are in fact integral components of combined molten salt reactor-processing facility. The parentheses around thorium exiting the SBB-PWR blanket processing facility and the MSR processing facility indicate the option to discard some thorium at these stages and replace it with new natural thorium, if thorium recovery is deemed to be challenging. However, the reference assumption in this study incorporates an optimistic recycle of thorium at these junctures.

shows the evolution of fuel cycle components for this scenario, which is henceforth referred to as "CThU-T5".

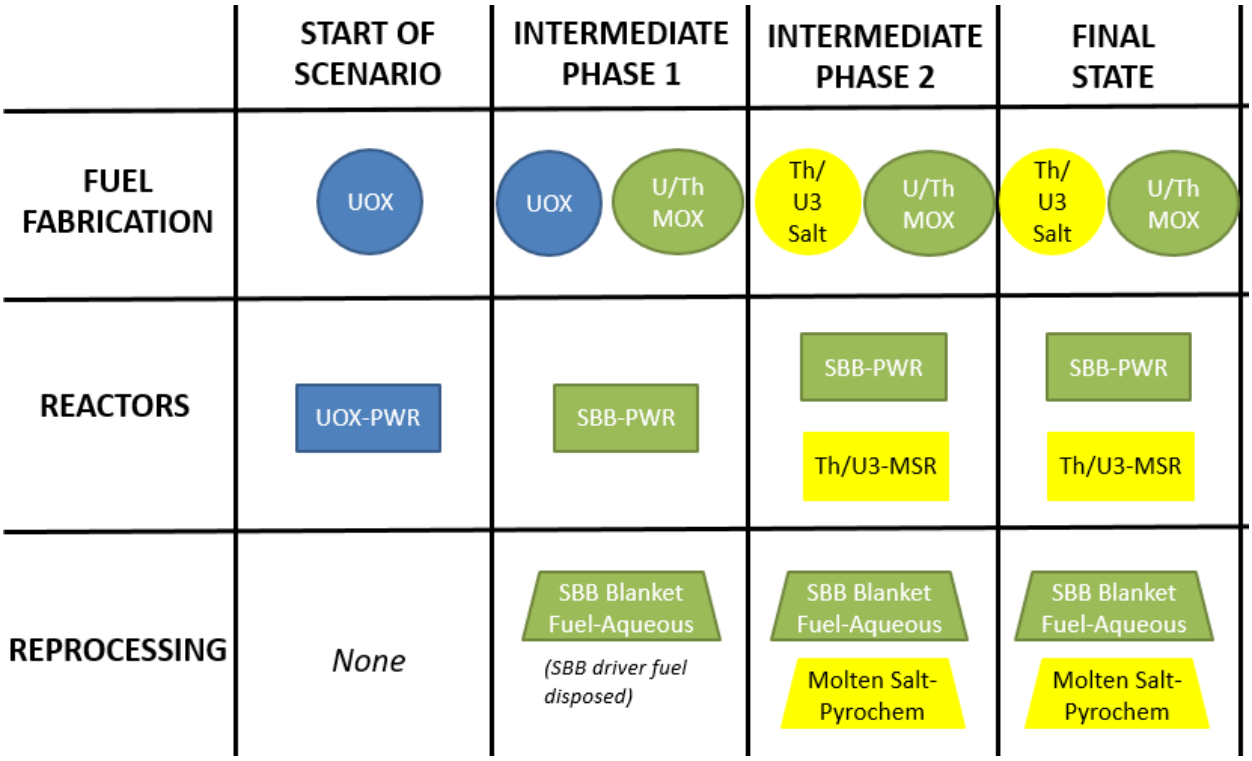

Figure 57, Evolution of Major Fuel Cycle Components over Time for Scenario CThU-T5

During Intermediate Phase 2, the balance of reactors shifts towards an increasingly large contribution from MSRs over time, eventually approaching a constant ratio that is maintained in the final state. The accompanying evolution of material flows for CThU-T5 is shown in Figure 58, below.

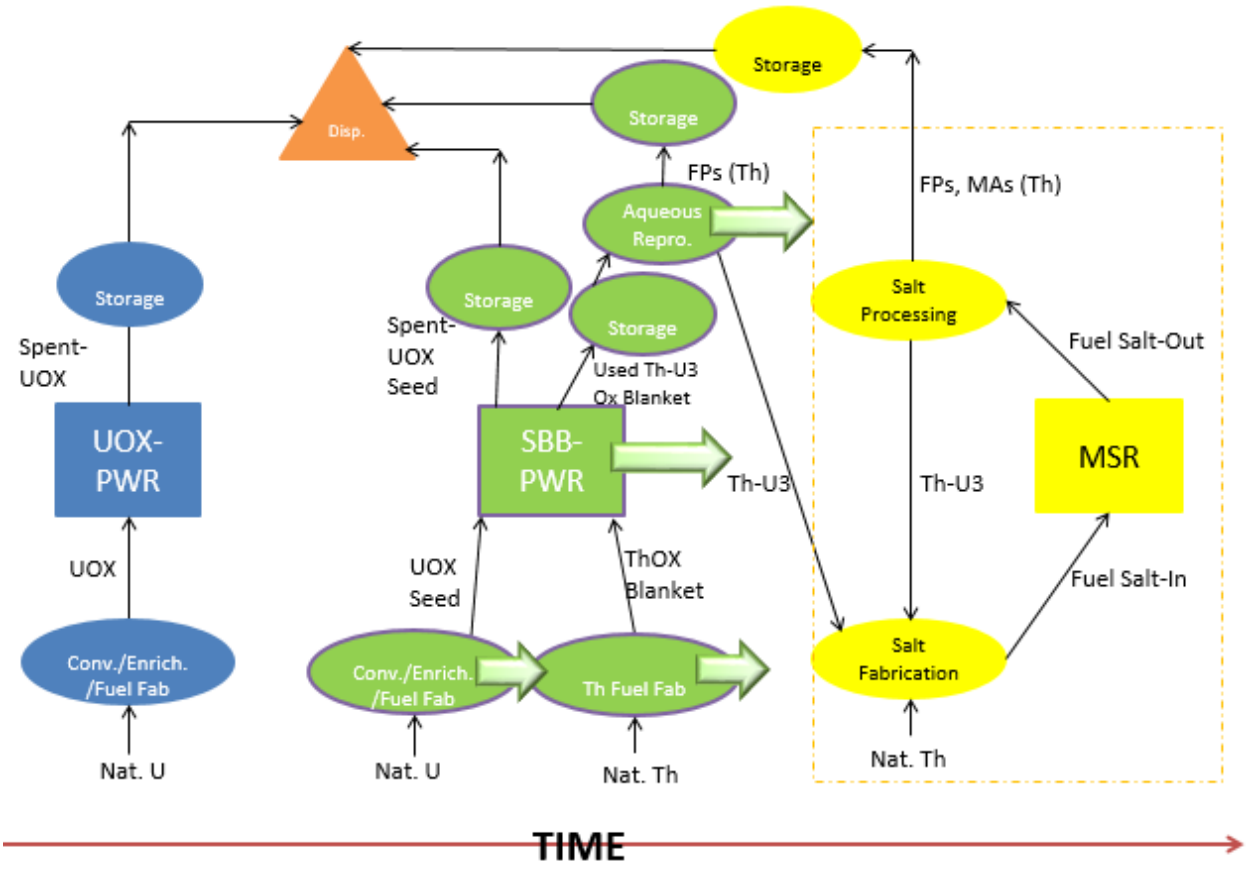

Figure 58, Evolution of Material Flows for Transition CThU-T5 (with Translucent Arrows Showing Persistence of SBB-PWR Stage)

5.3. Material Flow Requirements for Fuel Cycle Transition

The reference scenarios have now been defined qualitatively; this section will present the specific quantitative input parameters that were used to conduct the analyses, and will also describe the characteristics and behaviors that result when the scenarios are modeled in VISION. Also included are results for a variety of perturbations to the "default" assumptions for certain scenarios; however, the environment, health, and safety results described in Section 5.4 will emphasize a single set of consistent assumptions among the five transition scenarios. The "reference" assumptions are listed below:

Scenario Details and Assumptions:

- Scenario begins in 2005[31] to provide approximately a decade for calibration to the present date; proceeds through the maximum number of 200 full time steps (i.e., to 2205)
- The electricity demand is at 90 GWe-yr/yr for the initial 10-year calibration period; beginning in 2015, there is a 1% annual increase in electricity demand
- Initial fleet is approximated as entirely PWRs
- Initial fleet of PWRs is decommissioned at a rate of two units every year, beginning in 2020[32]
- 2030 deployment date for PWR reprocessing facilities; effectively unlimited capacity from this point on, although the impacts of capacity restrictions are also considered in this section (adapted from [EPRI 2013] and [EPRI 2014])
- 2030 "permissible" deployment date for intermediate advanced reactor phases (e.g., MOX PWRs, SBB-PWRs)…but MOX PWRs will have a time delay based on the availability of reprocessed plutonium (adapted from [EPRI 2013] and [EPRI 2014])
- 2045 deployment date for fuel fabrication facilities for SFR or MSR fuels

[31] This starting time is selected to provide approximately a decade for calibration to the present date; proceeds through the maximum number of 200 full timesteps (i.e., to 2205). A calibration period is necessary to initialize VISION's forecasting and energy strategy algorithms.

[32] It is difficult to predict when each member of the existing reactor fleet will retire, so a constant rate of retirement is assumed. 2020 was selected as a near-term starting date for retirement, although some existing reactors could retire before that time.

- 2050 deployment date for the first generation of advanced "end-state" reactors (i.e., SFRs or MSRs, depending on the scenario) and their accompanying reprocessing facilities[33]
- There is no available pre-existing stockpile of non-natural fissile material (e.g., U-233 or Pu-239)

Fuel Cycle Facilities:

- 99% reprocessing efficiency for solid fuels (adapted from [Wigeland 2014])
- 99.8% fuel fabrication and re-fabrication efficiency for all fuels (adapted from [Wigeland 2014])
- Once fuel fabrication technologies are available, unlimited fuel fabrication capacity for all fuel types (provided that necessary materials are available)
- No restrictions on natural uranium recovery or any front-end facilities (conversion, enrichment)
- Uranium enrichment tails are 0.25% U-235 at all times (adapted from [Wigeland 2014])

Reactors:

- Thermal efficiencies: 33.33% for PWRs, 40% for SFRs, 44.44% for MSRs (adapted from [Wigeland 2014])
- Every reactor unit has a rated capacity of 1 GWe
- Every reactor unit has an assumed capacity factor of 90%
- New reactor lifetimes are all 80 years

[33] This is a commonly assumed date for advanced reactor deployment in transition studies. Examples include [Shiotani 2011], [Kim 2011], and [NEA 2012]. 2050 is also the deployment date assumed in ongoing DOE-NE research on fuel cycle transitions, though this is work is mostly unpublished as of 2016.

The general assumptions described in the bulleted lists above are necessary for ensuring that as fair-as-possible comparisons are made between potential implementation scenarios; additional scenario-specific assumptions will be introduced as necessary/relevant throughout the subsequent sections.

5.3.1. CUPu Material Flow Results

5.3.1.1. Material Flow Results for Scenario CUPu-T1

In addition to the general assumptions listed above, CUPu-T1 assumes a reference breeding ratio of 1.2 for the SFR. The separate driver and blanket SFR fuels are not distinguished in VISION, and the fissile plutonium (both Pu-239 and Pu-241) is approximated as being entirely Pu-239 to simplify material balance calculations. The SFR core configuration studied in the steady-state analysis had a large fraction of fuel that achieved high burnups with short residence times, since excess breeding was not a priority. However, excess breeding is an important mission in this transition scenario, so expectations of high burnups and short fuel residence times must be tempered. An adjusted burnup of 47.5 GWd thermal/MTIHM (weighted average of core and blanket) and an adjusted residence time of 5.44 years were adopted from fuel cycle transition work conducted at Idaho National Laboratory and the University of Wisconsin [Carlsen 2016]. For the PWR, standard assumptions from the FCO-ESS report (50 GWdth/MTIHM burnup, 4.21% enrichment in U-235, residence time of 4.5 years) were also used here [Wigeland 2014]. The results of the T1 scenario based on the reference set of assumptions are shown below in Figure 59:

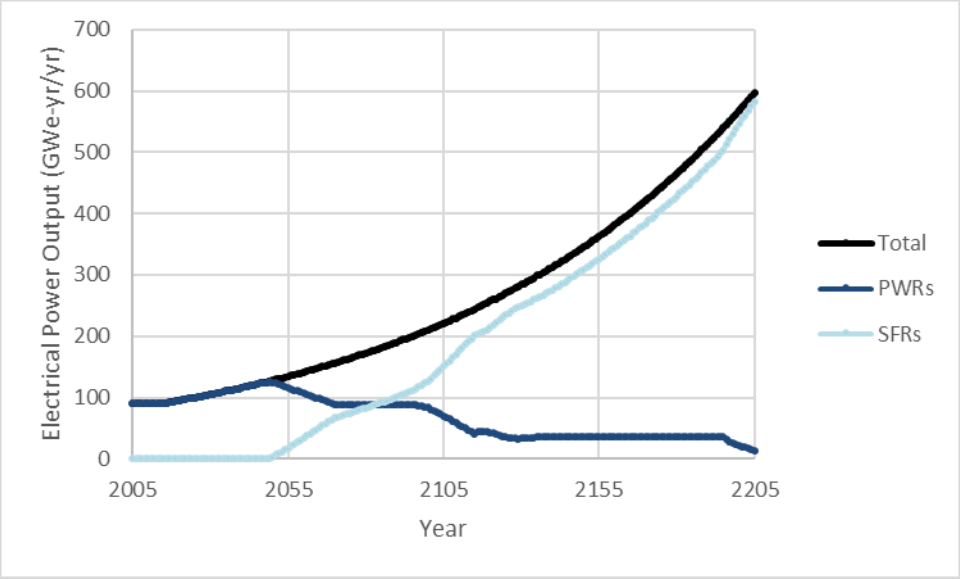

Figure 59, Electrical Output over Time for Scenario CUPu-T1 under Reference Assumptions

As a reminder, the flat line at the start of the plot shows the calibration period between 2005 and 2015, when electrical demand does not grow (because it is already at the 2015 power output during this entire period). Beginning in 2015, electrical demand begins its 1%/year increase and output correspondingly increases through the implementation of new reactor builds. In 2021, the first of the initial "legacy" reactor fleet begin to go offline, at a rate of two reactors per year. However, from 2021 to 2050, 99 new PWRs are constructed, which is equivalent to 3.3 reactors per year, which implies a net increase to the fleet size of 1.3 reactors per year. In 2050, construction priority shifts to SFRs, and PWR construction temporarily ceases during this time. The legacy fleet continues to retire at the same rate, so the number of PWRs decreases by 2 reactors per year until the year 2070, when all legacy reactors have retired. Beginning in 2070 there is a period during which the number of PWRs remains constant, until 2095 when the first of the "non-legacy" PWR builds begin to retire.

To fill the electricity gap caused by the falling and then plateauing number of PWR, SFRs begin construction in large quantities starting a couple years before 2050, with the first set coming online in 2050. The build rate is especially fast from 2050 to 2070, when the number of PWRs is actively falling; the rate slows a bit during the PWR plateau and picks up again once the plateau falls in 2095. By 2100 there are 140 operating SFRs (implying an average build rate of 2.8/yr for the preceding half-century). The trajectory of the scenario appears to be on pace for SFRs to completely replace PWRs within the timespan of the scenario; however, the previous figure does not show the tumultuous trend of plutonium availability which is occurring in the background. Figure 60, below, shows the amount of the available plutonium inventory that is available for SFR fuel fabrication as a function of time:

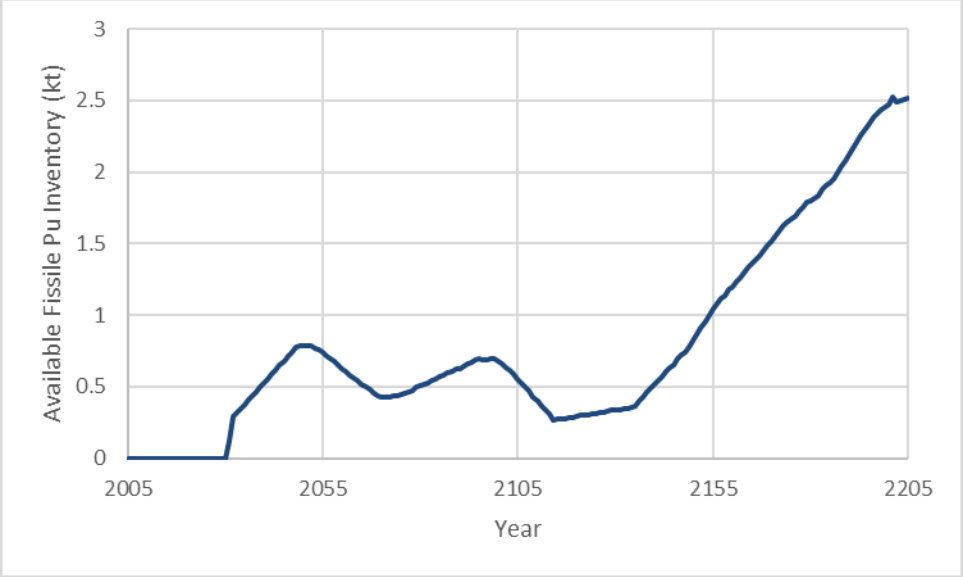

Figure 60, Available Inventory of Fissile Plutonium over Time for CUPu-T1

The sharp jump at the start of separations availability in 2030 is an artifact of the "unlimited separations" condition that is imparted as part of the reference assumptions. However, even with unlimited separations capacity, there are still limits on the total amount of plutonium that is

available from both the PWR and SFR fuel. Before 2050, the available plutonium inventory steadily increases since it is not yet being drawn to produce SFR fuel. In 2050, plutonium consumption begins and the plutonium inventory corresponding decreases. There is a temporary reprieve from plutonium depletion beginning in 2070 due to the stabilization of the PWR fleet, the subsequent slowing of new SFR builds, and the availability of the first batches of plutonium drawn from recycled SFR fuel. For a while the plutonium inventory actually increases again, but as the PWR fleet declines and the SFR build rate begins to accelerate again, the trend shifts toward rapid consumption of plutonium. Around 2110 the remaining Pu inventory and the rate of consumption become sufficiently large that it requires a new "late-stage" fleet of PWRs. This late-stage fleet serves two essential purposes: (1) it helps to meet ever-rising electricity demands without requiring any plutonium to fuel, and (2) the spent fuel from these PWRs can be used to re-populate the plutonium inventory. After a couple decades of building just enough PWRs to resolve the plutonium balance issue (notice the nearly flat line between 2110 and 2130 in Figure 61), the SFR fleet grows large enough to mostly sustain its own growth, and once again only SFRs are constructed. However, the 41 late-stage PWRs are still operated through their full 80-year lifetimes, of which 15 outlast the duration of the scenario.

5.3.1.1.1. Consequences of Varying Breeding Ratio for CUPu-T1

Secondary assessments were also conducted to determine the impact of varying the breeding ratio, with all other parameters remaining constant. The results for transitions spanning a spectrum of breeding ratios, from a low-breeding case (BR=1.05) to an optimistic advanced case (BR=1.50), are shown below.

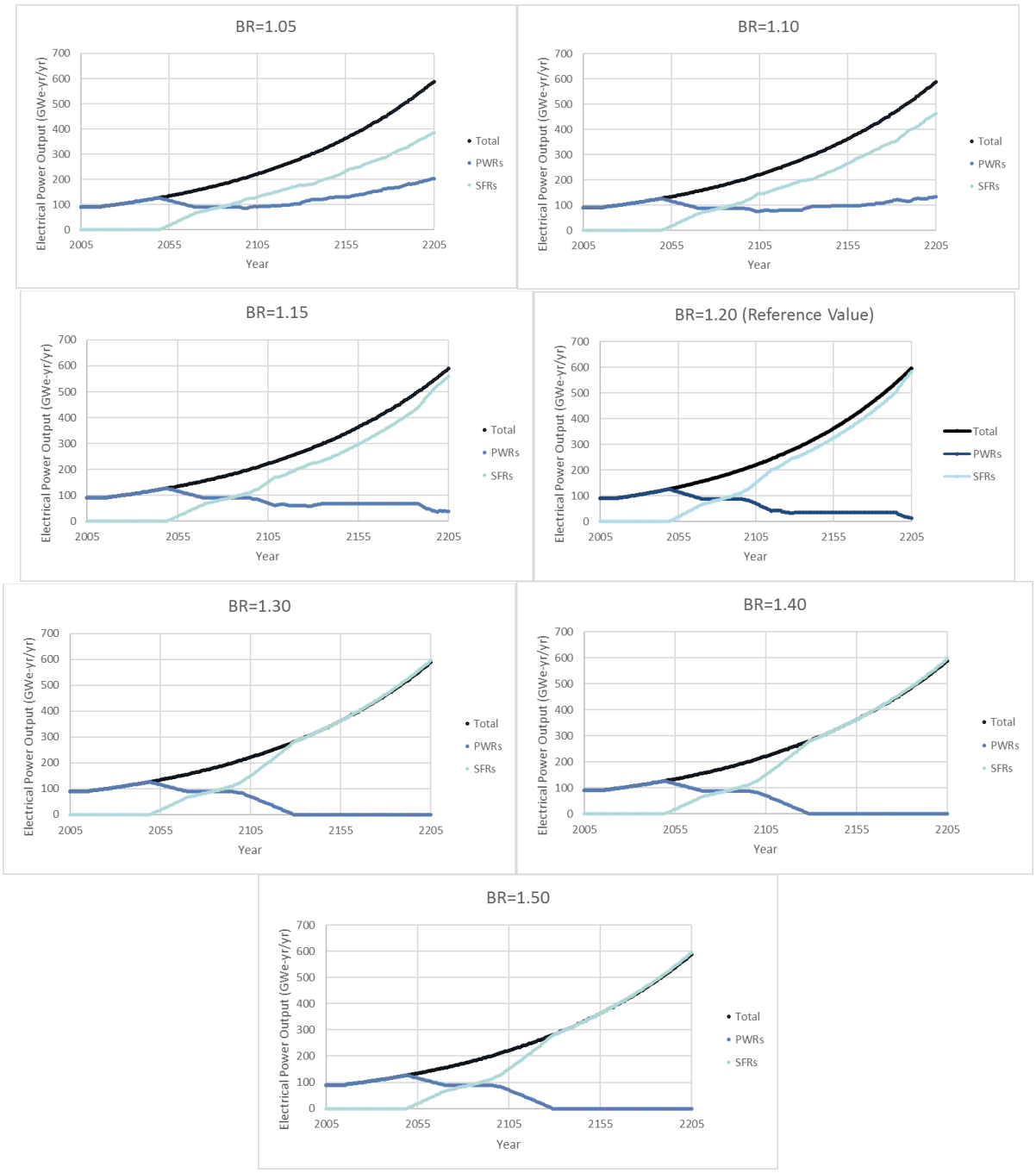

Figure 61, Simulation Results for Breeding Ratio Variations of CUPu-T1

As one might expect, as the breeding ratio increases, the ability to transition quickly to a full SFR fleet with less reliance on PWRs also increases. The results for breeding ratios of 1.30 and larger are virtually identical for the 1% electricity demand growth case. For the BR=1.30 case,

the plutonium inventory also experiences a dip between 2050 and 2075 and a second dip between 2110 and 2130. However, unlike for the reference BR=1.20 case, the second dip is eventually resolved by plutonium production in the SFRs alone, without needing to rely on a "late-stage" PWR fleet. For the BR=1.40 and BR=1.50 cases, the second dip is negligible.

In terms of the ability to enable a fast, smooth transition, SFRs with breeding ratios of 1.30 and larger appear to have the potential to offer benefits. However, systems with this level of performance have not yet been demonstrated and are more poorly understood than systems with breeding ratios of 1.2 or less. The larger-scale SFRs that have operated to-date have had breeding ratios of 1.18 or less, as shown in Table 26 below:

Table 26, Breeding Ratios of Operated Larger-Scale SFRs To-Date

Reactor(s)	Approximate Breeding Ratio	Source
Superphenix (France)	1.18	[Kessler 2013]
Monju (Japan)	1.2 (target) 1.18 (measured)	[Usami 2001]
BN-600 and BN-800 (Russia)	Capable of breeding, but not operated in this configuration	[Kessler 2011]

Recall that both Superphenix and Monju suffered from reliability issues[34], so even breeding near BR=1.18 has yet to be demonstrated consistently at the commercial scale. The world's nearest-term research and development efforts will likely not push the breeding ratio boundary further, although they may help to demonstrate reliability for the SFR technology in general. India's

[34] Superphenix had persistent reliability issues with a lifetime load factor of less than 10%. Major incidents included a leak in the fuel transfer tank in 1987 and an air leakage due to a faulty compressor in 1990 [Schneider 2009]. Monju experienced a major sodium leak and subsequent fire in 1995 in the secondary loop, which had long-lasting political, legal, and economic repercussions [Suzuki 2010].

planned Prototype Fast Breeder Reactor (PFBR) and FBR-600 have target breeding ratios of 1.05 and 1.13, respectively [Vinayagam 2014], while Russia's BN-1200 has scaled back its breeding ratio expectations to 1.2 (if a breeding configuration is used at all) [Vasilyev 2013]. Even if technical barriers are eventually resolved, especially high breeding ratios in fast reactors will present challenges from a materials safeguards perspective [Kutt 2014]. Indeed, this is the primary consideration that has led to the BN-series reactors not having operated in a breeding configuration [Kessler 2011]. With these factors in mind, it is unlikely that SFRs with breeding ratios much larger than 1.2 would be deployed in large numbers by 2050. It is possible that breeding ratios could evolve for later-generation SFRs, although this case was not considered since the BR=1.30 and larger cases already provided bounding results.

5.3.1.1.2. Consequences of Limiting Reprocessing Capacity for CUPu-T1

The default assumption used in this study is that the capacity of reprocessing facilities is unlimited once they first become available in 2030. However, it is possible that a slow deployment of reprocessing facilities could impact the rate at which an SFR fleet can be deployed. The Rokkasho reprocessing facility has a stated annual capacity of 800 tons per year [Heinonen 2010]; this sensitivity study considers the case where one Rokkasho-sized facility is made available per decade to accommodate used PWR fuel. The reprocessing capacity of used SFR is still assumed to be infinite. The results of this modified scenario are shown in Figure 62, below.

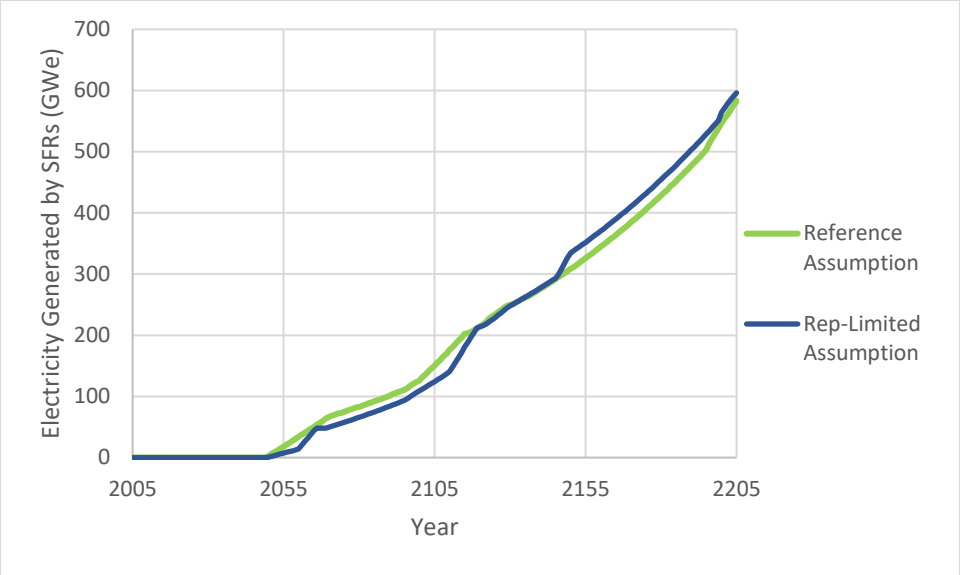

Figure 62, Comparison of SFR Electrical Output over Time for Scenario CUPu-T1 with Limited and Unlimited Reprocessing Capacity

Overall, the rate of additions to the reprocessing capacity combined with the relatively high breeding ratio of the SFR fleet does not impact the transition much from the reference assumptions. The most severe impacts are felt in the earliest years of the transition; by 2055, SFRs are only generating 7.2 GWe of electricity in the reprocessing-limited case, compared to 18 GWe in the same year for reference assumptions. However, by 2065 the gap has closed to 43.9 GWe vs. 50.4 between the two cases. The gap varies from 5 to 30 GWe between 2065 and 2120, when the reprocessing-limited scenario catches up for good. Interestingly, because additional PWRs are constructed at earlier times in the reprocessing-limited case, the reprocessing-limited case actually surpasses the reference case for about the last third of the scenario. This is because by this time in both cases, plutonium availability and processing capacity are no longer issues, but the reference case has additional late-stage PWRs that must be operated through the end of their lifetimes. The temporary gap can be seen to close at the end of the scenario in 2205 as the last of the PWRs retire in the reference case. Overall, the results are sufficiently similar that there

is little concern about the impact of reprocessing capacity on the cumulative material flow performance of the scenario.

5.3.1.2. Material Flow Results for Scenario CUPu-T2

In contrast to CUPu-T1, this scenario examined a lower breeding ratio case with the SFRs coupled by a commitment to a partial PWR fleet for perpetuity. From 2050 onward, a rough reactor balance of 90% SFRs and 10% PWRs was "suggested" to VISION, with the understanding that VISION prioritizes satisfying the electrical demand before attempting to resolve the desired relative fractions of different reactor types. In this case, the breeding ratio was reduced to 1.02 (akin to the "breakeven" core described in [Joo 2008], which is sufficient to support "breakeven" plutonium production but likely not enough to sustain reactor growth with material support from the PWR fleet. However, the use of lower breeding ratios does allow higher power levels to be used; the burnup was raised to the level used in the steady-state analysis (combined burnup of 69.9 GWd th/MTIHM for the driver and blanket fuel [Sandia 2016]). The driver and blanket fuels had difference resident times (3.6 years and 5.4 years); the longer of these was taken as the "effective" residence time[35]. The results of the CUPu-T2 simulation are shown in Figure 63, below:

[35] This is because VISION cannot distinguish between multiple, co-existing fuel types within a reactor.

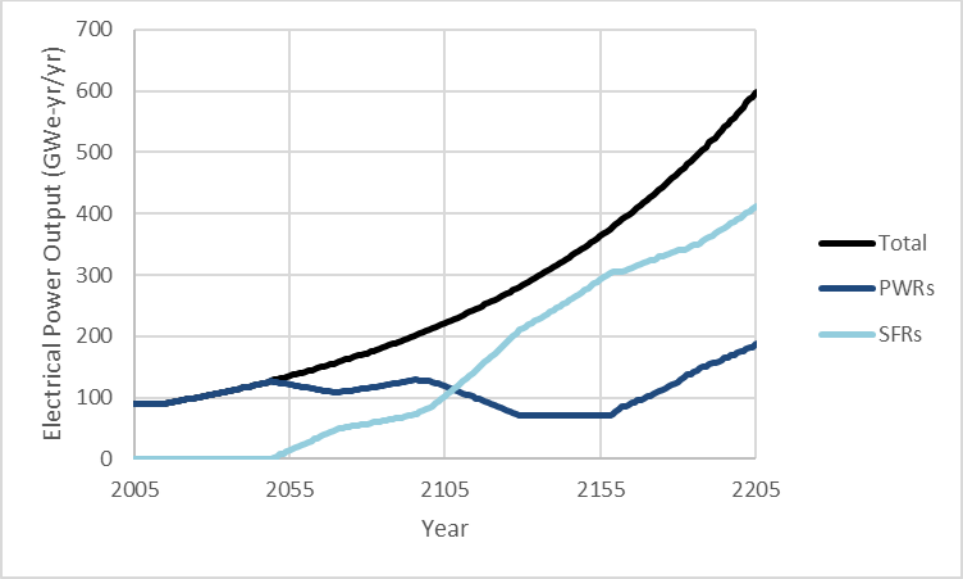

Figure 63, Electrical Output over Time for Scenario CUPu-T2 under Reference Assumptions

For the first 50 years, the scenario is identical to CUPu-T1, where electrical output from the PWR steadily rises to match demand until 2050, after which most new builds are SFRs. However, the fraction of PWRs must remain large in the early years of SFR deployment, since a large fraction of the SFRs are brand new and require their first core load. Between 2050 and 2095, there is a slight dip followed by a slight rise in the size of the PWR fleet, but overall changes in the fleet size are quite small as the rate of new PWR builds roughly matches the legacy fleet retirement rate. Near the end of the 21st century, a significant fraction of the SFRs have existed for some time and the plutonium availability issue is alleviated somewhat, so the scenario attempts to move closer to the 90%-10% that was specified. From 2095 to 2130, the PWR fleet power falls, and the plutonium inventory that was accumulated in the previous century falls with it (see accompanying Figure 64, below). Eventually, in 2130, the number of PWRs going offline decreases sharply because this is 80 years after the first SFRs came online and the PWR build rate was largely replaced by SFR build orders. Between 2130 and 2155,

PWRs are built and retired at equally slow rates, and the PWR fleet remains nearly constant during this interval. However, SFRs continue to come online at a fast pace, and the plutonium inventory continues to drop. Finally, in 2155, the plutonium inventory comes perilously close to bottoming out, so the rate of PWR growth increases significantly to sustain the SFR plutonium supply. From 2185 to the end of the scenario, the ratio of the build rates of SFRs and PWRs remains roughly constant, at about 2.5:1. This build ratio enables the plutonium inventory to stabilize, as seen in Figure 64 below.

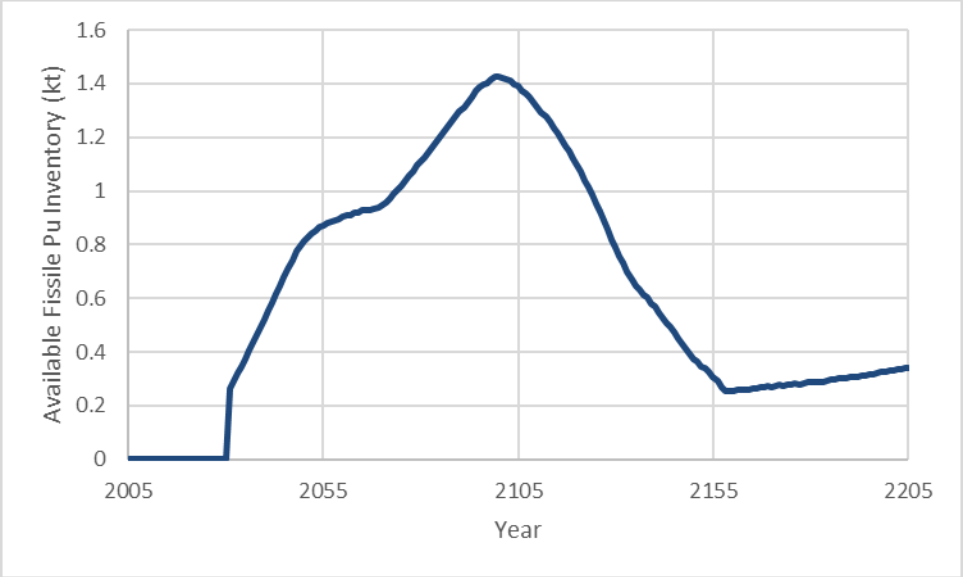

Figure 64, Available Inventory of Fissile Plutonium over Time for CUPu-T2

At the end of the CUPu-T2 scenario in 2205, the fleet consists of 69% SFRs and 31% PWRs, compared to the 97.7%/2.3% balance at the end of the CUPu-T1 scenario. Furthermore, the SFR/PWR ratio appears to be fairly stable at the end of CUPu-T2, whereas CUPu-T1 the scenario ended while moving quickly towards a fleet comprised entirely of SFRs, as the last dozen or so PWRs were within a decade of shutdown in 2205.

5.3.1.3. Material Flow Results for Scenario CUPu-T3

This scenario returns to the first SFR breeding ratio of 1.20 used in CUPu-T1, but this scenario passes through an intermediate step of MOX-fueled PWRs. The MOX-fueled reactors begin to come online in 2030; in the period from 2030 to 2049, a composition of 20% MOX-PWRs and 80% UOX-PWRs is "suggested" to VISION. The composition of the MOX-PWR fuel is about 10.5% plutonium (all isotopes combined). It was assumed that while the MOX-PWRs would still operate to the extent of the operational lifetimes beyond 2050, they would operate with UOX after 2050 in order to make plutonium available for the rapidly emerging SFR fleet. While the MOX-PWR fuel is not reprocessed, UOX fuel added to the originally-MOX-dedicated PWR fleet can be reprocessed after 2050. Figure 65, below, shows the results of the CUPu-T3 scenario:

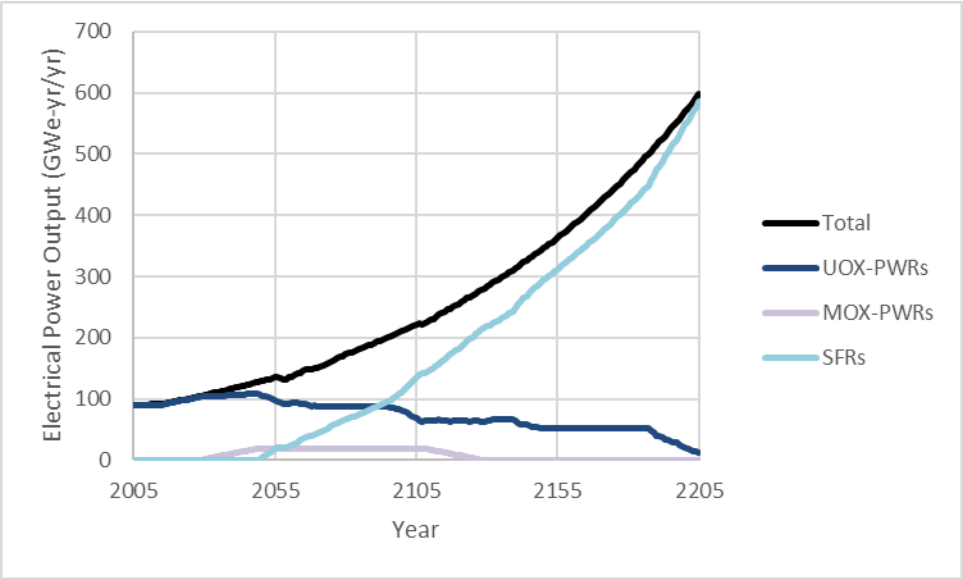

Figure 65, Electrical Output over Time for Scenario CUPu-T3 under Reference Assumptions

Keep in mind that while the “MOX-PWR” fleet persists until 2129 (80 years beyond 2049, the date of the last new MOX-PWR), beyond 2050 the fleet is fueled with UOX fuel rather than MOX fuel. The plot of electrical output features several small changes in slope throughout the transition which are easy to overlook; the transition looks relatively smooth, but as the only CUPu scenario with three different fuel types, there are many challenging materials transactions taking place in the background. Figure 66, below, shows the trend in the plutonium buffer for the SFR fuel supply and better depicts the action behind the scenes in CUPu-T3.

Figure 66, Available Inventory of Fissile Plutonium over Time for CUPu-T3

The three or four major plutonium inventory “events” (~2045, ~2095, and ~2140, with ~2185 being a less dramatic example) are much more easily identified in this representation. In 2045, the first plutonium from the UOX-PWR fleet becomes available, as this resource was previously dedicated to MOX fuel production in the period from 2030 to 2045. This new plutonium inventory doesn’t have long to accumulate before it is quickly depleted by the earliest SFRs.

After the first 22 SFRs are brought online quickly by 2056, the pace slows considerably as only five additional SFRs are added between 2056 and 2061. By this time, the existing SFRs start to become able to re-supply their own fuel, enabling the SFR fleet size to accelerate again. However, plutonium availability continues to be the driving constraint until about 2080, when the breeding capability of the existing SFRs is finally sufficient to outpace the plutonium fuel demand for newly constructed reactors. The plutonium inventory begins to rise again, but in the period between 2095 and 2100, the transition encounters a second challenge as the large portion of PWRs (both "original" UOX and modified "MOX-turned-UOX") constructed before 2050 approach the end of their operational lifetimes. As the production of plutonium in PWRs correspondingly drops, the trend of accumulation plateaus in the period from 2095 and 2100 and then falls rapidly before 2105.

To compensate for the declining rate of plutonium production, a new late-stage fleet of UOX-PWRs ordered with construction beginning in 2104 –the first new PWR builds since 2068. The build rate almost precisely matches the rate of retirement (as can be seen in the near flat trend in Figure 66) to maintain the plutonium inventory at a relatively steady level. The breeding gains eventually once again enable the plutonium inventory to accumulate (about 2135). The transition encounters one last "blip" as the burst of PWRs that was brought on between 2055 and 2065 retires, but the plutonium inventory dips only momentarily before resuming is upward climb through the end of the scenario. The rate of accumulation wanes in about 2185 (80 years after the emergence of the "late-stage fleet"), but it does not appear to pose any lingering effects beyond the end of the scenario in 2205.

At the end of the CUPu-T3 scenario in 2205, the fleet consists of 98.0% SFRs and 2.0% PWRs, which is nearly identical to the balance at the end of the CUPu-T1 scenario. Thus, while the allocation of plutonium to an interim MOX fleet does lead to a more challenging transition in terms of plutonium availability, these effects can be fully overcome within a 200-year span.

5.3.2. CThU Material Flow Results

5.3.2.1. Material Flow Results for Scenario CThU-T4

The CThU transitions represent a significant shift from the CUPu transitions in that they involve a balance of U-233 rather than plutonium. However, in both cases, there is still an underlying dependency on the breeding ratio and the related concept of doubling time. There is not necessarily a consensus regarding what a "reasonable" breeding ratio for a thermal-spectrum, thorium molten salt reactor might be. Unlike for SFRs, there is no operational experience with fissile material breeding in MSRs of any kind (the one operational MSR, the Molten Salt Reactor Experiment, was not used to breed fissile material [Rosenthal 1969]). However, there are a handful of systems studies that describe a range of possible performance, as shown in Table 27 below:

Table 27, Breeding Ratio Estimates from Thermal Thorium-Based MSR Studies

Study/Project	Breeding Ratio for Thermal-Spectrum, Thorium-Based MSR	Fissile Material Doubling Time (if available)
[Mathieu 2002]	1.02	n/a
[Engel 1975], [Rosenthal 1970] (MSBR)	1.06-1.07	20-22 years
[Nagy 2010], [Nagy 2012]	1.05	18 years
[Green 2015]	Up to 1.10	45 years

Somewhat larger breeding ratios have been described for fast-spectrum systems (e.g., 1.12) [Delpech 2009], although these systems have not been studied to the same extent. This study adopts the rounded figures of a breeding ratio of 1.05 and a doubling time of 20 years, which are consistent with what has been described as feasible in the literature.

VISION, along with most other FCSTs, is not specifically designed to accommodate the continuous-processing nature of MSRs. However, it is possible to approximate the behavior of an MSR as a solid-fueled system by considering a total material input vector and a total material output vector over a particular timescale. Fortunately, some previous work performed as part of the FCO-ESS enables a variety of these kinds of these parameters to be determined.

Namely, a "residence time" of 8.8 years is determined in the following manner: from MSR work that was used to populate the FCO-ESS catalog and database, a measure of "effective" burnup for MSR fuel was given to be 101.9 GWd/MTIHM [Sandia 2016]. This was determined by considering the average amount of energy extracted from an entering mass of fresh natural thorium feed before being lost as converted fission products or transuranics, process losses, etc. Recall that in an MSR, fuel salt circulates in both the core and in the chemical processing system. While the power density used in MSR core simulations was 50.8 MW/MTIHM, 37.6% of the salt mass in the MSR is located outside the core in the reference design. When normalizing to all of the heavy metal mass in all regions of the MSR, the adjusted power density is 31.7 MW/MTIHM. The effective residence time (burnup divided by the adjusted power density) is 8.8 years [Sandia 2016].

The input parameters for the SBB-PWR are taken from a reference design in the Sandia Fuel Cycle catalog, which uses driver fuel at 11.37% enrichment and pure thorium oxide blanket fuel in a ratio of about 43:57. To permit ample breeding of U-233, the blanket fuel has a residence time of 9.67 years. The combined burnup of the driver and blanket fuel is 61.7 GWd/MTIHM [Sandia 2016].

Using these parameters to construct a scenario, along with assuming that the reprocessing time is equivalent to the shortest permissible timescale in VISION (0.25 years), it is possible to closely approximate the behavior of an emerging MSR-based fleet. The results of the CThU-T4 simulation are shown in Figure 67, below:

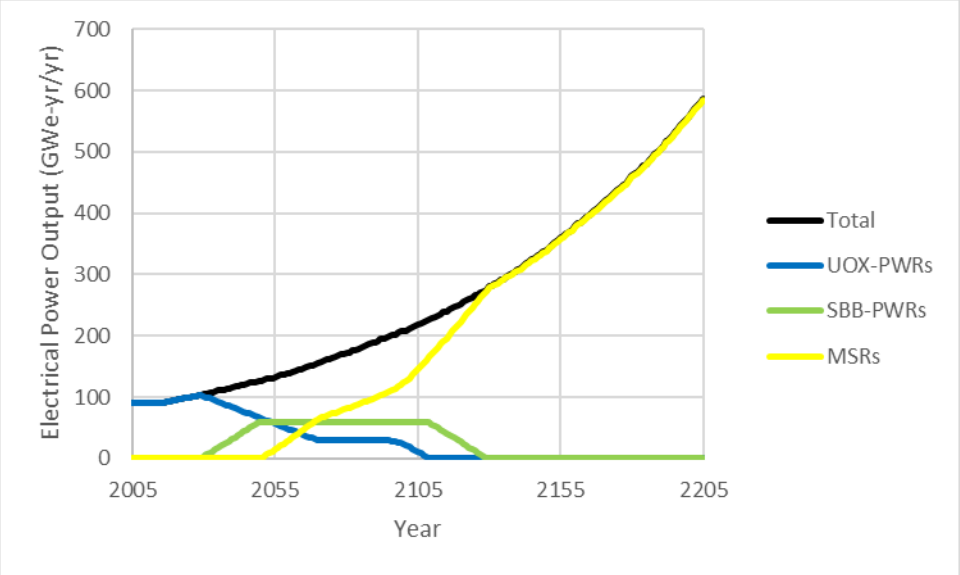

Figure 67, Electrical Output over Time for Scenario CThU-T4 under Reference Assumptions

In contrast to the CUPu transitions, CThU-T4 exhibits very straightforward behavior. The intermediate PWR-SBB fleet comes online somewhat faster than the MOX-PWRs in CUPu-T3,

simply because the PWR-SBBs do not require any reprocessed material for start-up. In 2050, new builds shift over entirely to new MSRs, with the last PWR being constructed immediately before this. The rate of MSR construction accelerates as the last of the PWRs go offline between 2095 and 2130; from 2130 onward, the transition is complete and the fleet consists entirely of MSRs. The rate of material accumulation is sufficient to sustain the growth in electrical demand for perpetuity, since (1.01)^20=1.22, which is considerably less than 2. This means that there is actually a sizeable excess of U-233 produced throughout in this scenario. Using a more conservative doubling time would still not impact the development of this scenario; a doubling time of 50 years yields an identical figure, albeit with a much smaller excess of U-233.

Incidentally, an SFR with a breeding ratio of 1.2 and a fuel residence time of 5.44 years, such as the one studied in CUPu-T1, has a very similar doubling time of 20.7 years. As the results of CUPu-T1 and CThU-T4 have shown, both transitions are eventually capable of sustaining their own growth once a sufficiently-sized initial fleet is available. Most of the complications from transition occur during the early years, when many fresh SFR or MSR cores are required and have not yet begun to recycle their own fuel. In this regard, SFRs require considerably more fissile material to get going than MSRs for a 1 GWe (capacity, not true output) reactor, as shown in the following pair of calculation:

$$SFR\ Pu\ Req. = \frac{1\ GWe * (5.44\ y\ residence\ time)\left(\frac{365.242\ d}{y}\right)(7.64\%\ Pu\ by\ mass)}{(40\%\ thermal\ eff.)\left(47.501\ GWth - \frac{day}{MTIHM}\ burnup\right)}$$

$$= 7.99\ MT\ Pu$$

$$MSR\ U-233\ Req.=\frac{1\ GWe*(8.8\ y\ residence\ time)\left(\frac{365.242\ d}{y}\right)(1.48\%\ U3\ by\ mass)}{(44.4\%\ thermal\ eff.)\left(101.9\ GWth-\frac{day}{MTIHM}burnup\right)}$$

$$=1.05\ MT\ U-233$$

Most of the difference between these two values is attributed to the higher fissile loading in the SFR compared to the MSR (7.64% vs. 1.48%), which is made possible by the MSR's use of homogenous liquid fuels. As a result, even though the Pu content of the UOX-PWR fuel (1.20%) is actually slightly higher than the U-233 content of the SBB-PWR fuel (0.86%), a smaller fissile stockpile is needed to start up the MSR fleet than the SFR fleet; thus, the CThU transition does not encounter the fissile material depletion issues that the CUPU transition encounters in the first hundred years or so.

There are some important caveats to note before leaping to the conclusion that the CThU-T4 transition is "easier" or "faster" than the CUPu-T1 transition. Most importantly, while this analysis assumes equivalent deployment timeframes for initial reprocessing (2030) and advanced reactors (2050) for both scenarios, one could argue that such a timeframe would be much more feasible for CUPu than CThU. The CUPu fuel cycle incorporates technologies (PUREX-like aqueous reprocessing and U/Pu SFRs with breeding ratios near 1.2) that have been commercialized in the former case (e.g., La Hague [NEA 2012]) and demonstrated on a large scale in the latter case (e.g., Superphenix [Latge 2012]). Electrochemical processing is assumed for the SFR fuel separations. A useful concept to illustrate this point is the system of "technology readiness levels" (TRLs), which employ a 1 to 9 scale where TRL 1 refers to a preliminary concept description and TRL 9 refers to a commercially deployed product [Mankins 1995]. As a

commercial technology in Europe, PUREX would likely be at TRL 9 (perhaps with an adjustment to a regional TRL 7-8 in the US given the lack of commercialization there), while THOREX would optimistically be at TRL 6 (demonstration scale) given its use in the 1960s and 1970s (e.g., [Rainey 1962], [Jackson 1977]), although expertise may have declined since its peak use. On the reactor front, the demonstration-scale SFRs warrant a TRL of 5-6 depending on how precisely the deployed design followed previous examples, while a recent Vanderbilt-EPRI review of a representative MSR technology indicated a maximum TRL of 4 for several of its critical components [EPRI 2015]. While the present TRL does not necessarily correspond to the length of time needed to reach commercialization, it is reasonable to expect that the deployment of the required technologies for CUPu could be achieved on faster timescales than the deployment of required technologies for CThU.

5.3.2.2. Material Flow Results for Scenario CThU-T5

The results of this scenario are shown below in Figure 68:

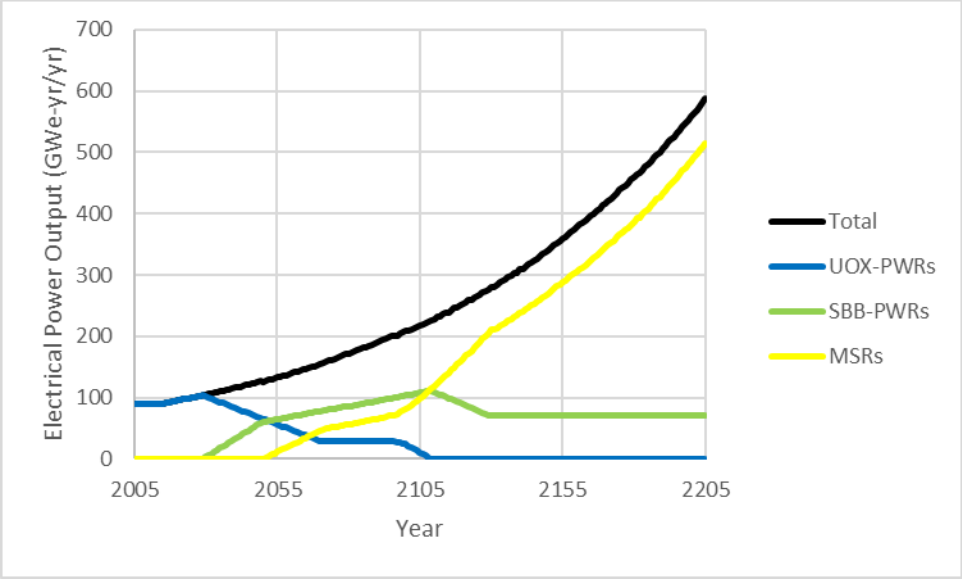

Figure 68, Electrical Output over Time for Scenario CThU-T5 under Reference Assumptions

Not surprisingly, the number of SBB-PWRs required to sustain the growth of the MSR fleet in CThU-T5 is smaller than the required UOX-PWR fleet to support SFR growth in CUPu-T2, because as established previously, the amount of fissile material required to startup new MSRs is relatively small.

5.4. Environmental Impacts of Fuel Cycle Transition

The previous section discussed the results of the dynamic material balance simulations of various transition scenarios to advanced closed fuel cycles. However, the emphasis of this chapter (and this dissertation as a whole) is on the environmental, health, and safety impacts associated with these transitions. This section applies the mass-normalized environmental metrics developed during the previous chapter of this dissertation and applies them to the dynamic mass calculations determined in this chapter. The results were tabulated by multiplying the material flows for each year by the mass-normalized impacts for each type of flow; cumulative results

were tabulated by adding each new year to the previous cumulative sum. The end result is a comparison of both the time-dependent behaviors and cumulative impacts of key environmental parameters.

5.4.1. Dynamic Impacts of Safety of Routine Operations

As in the previous chapter, the safety of routine operations is expressed in terms of collective occupational dose (person-Sieverts). Figure 69, below, shows the results for occupational radiological dose impacts for the fuel cycle transitions.

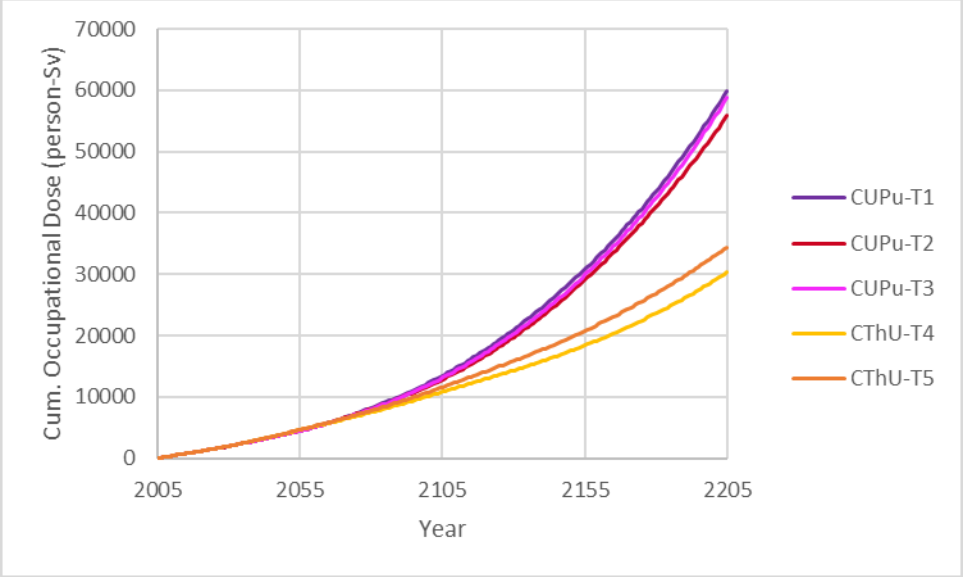

Figure 69, Comparison of Cumulative Occupational Radiological Dose Impact for Different Transition Scenarios

The results for occupational dose during transition largely reflect the results that were determined for the steady-state calculations in the previous chapter: that is, contributions to fuel cycle dose are overwhelmingly dominated by the reactor facilities. As a result, the dose impacts for the five transition scenarios are nearly indistinguishable prior to 2050, since in each scenario

the fleets consist of entirely PWRs up to this point (recall that the dose from all PWRs is assumed to be equal, regardless of whether UOX or MOX fuel is used). As the electricity contributions from SFRs and MSRs increase in the CUPu and CThU scenarios, respectively, the difference in the assumed dose impacts from the two advanced reactor technologies (1200 person-mSv/GWe-yr for SFRs, 490 person-mSv/GWe-yr for MSRs) begins to impact the cumulative dose. This gap steadily increases over time and would continue to increase if the scenario were extended beyond 2205, with the ratio ultimately approaching the steady-state CUPu:CThU dose ratio (2.675:1) at sufficiently long times.

Compared to the magnitude of the differences between the CUPu and CThU scenarios, the differences among the various CUPu or CThU options is notably smaller. Because of CUPu-T2's smaller breeding ratio, the rate of SFR deployment is somewhat slower than in CUPu-T1 and CUPu-T3, so its associated cumulative dose is somewhat smaller by the end of the scenario in 2205 (about a 7% difference between CUPu-T1 and CUPu-T2). CUPu-T1 has a slightly faster rate of SFR deployment than CUPu-T3 due to the latter's interim allocation of plutonium to PWR MOX fuel, so it has a slightly higher cumulative dose than CUPu-T3 (a 1.8% difference in 2205). Among the two CThU scenarios, CThU-T5 has a somewhat higher cumulative dose than CThU-T4, primarily because of the larger fraction of persisting SBB-PWRs which have a higher energy-normalized reactor dose impact than MSRs.

As discussed previously in Chapter 4, the results for the dose occupational comparison are particularly uncertain, given the strong dependence on a single set of parameters (reactor dose) for which data is limited (in the case of SFRs) or unknown/speculative (in the case of MSRs). Of

the relatively small dose contribution from non-reactor facilities (between 7.59% for CUPu-T1 and 16.66% for CThU-T5), most of the remaining dose comes from a combination of natural uranium recovery (all transitions), natural thorium recovery (CThU only), and SFR fuel fabrication (CUPu only). Table 28, below, shows the breakdown of non-reactor dose contributions.

Table 28, Occupational Dose Contributions (as Percentages) from Non-Reactor Fuel Cycle Facilities

	Natural U Recovery	Natural Th Recovery	SFR Fuel Fabrication	All Other Non-Reactor	Total Non-Reactor Dose Contribution
CUPu-T1	2.81%	n/a	3.67%	1.11%	7.59%
CUPu-T2	5.02%	n/a	2.11%	1.23%	8.36%
CUPu-T3	3.35%	n/a	3.57%	1.21%	8.13%
CThU-T4	3.60%	4.35%	n/a	2.73%	10.68
CThU-T5	6.28%	7.07%	n/a	3.31%	16.66%

5.4.2. Dynamic Impacts of Waste Management (Low-Level)

As a reminder, the impact of LLW is expressed in terms of volume. Figure 70, below, shows the breakdown of LLW volumes arising from the various studied scenarios.

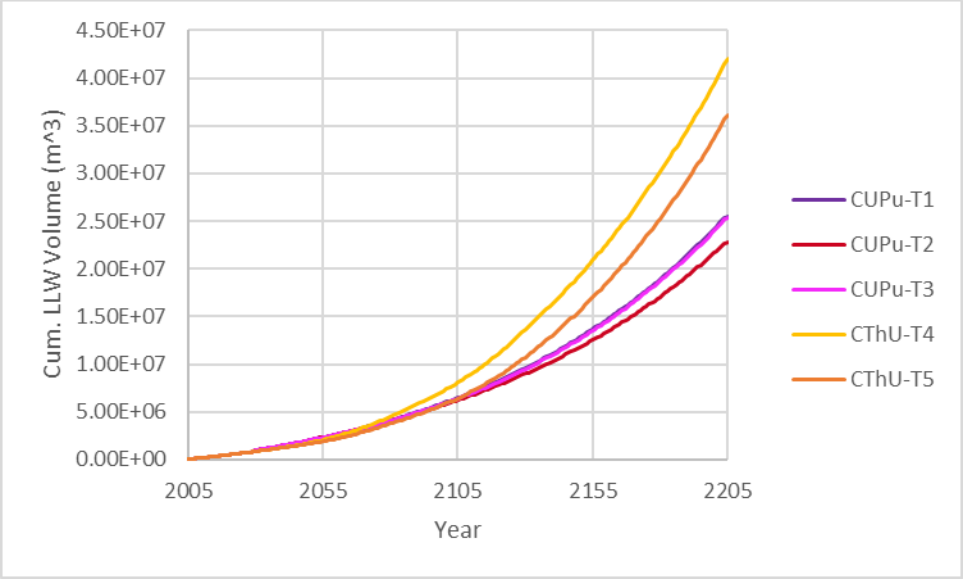

Figure 70, Comparison of Cumulative LLW Volumetric Impact for Different Transition Scenarios

Much like for occupational dose, LLW arising from reactor operations is the largest contributor for all transitions, from a minimum of 55.32% for CUPu-T1 to a maximum of 96.82% for CThU-T5. However, in comparison to dose, reprocessing plays a much more important role in contributing to overall LLW. The CUPu transitions have an average of a 36.15% LLW contribution from PWR and SFR fuel reprocessing. Furthermore, the reference MSR technology incorporates online reprocessing as part of the reactor facility, so the total CThU LLW volume is also highly influenced by the LLW arising from its fuel processing systems. As discussed in Chapter 4, the high fuel throughput of the MSR system is assumed to lead to larger volumes of LLW production compared to other reactor types; this trend also emerges during transitions, as these results show. Consequently, the CThU transitions produce considerably more LLW than the CUPu transitions.

There are also some visible distinctions among the various CUPu and CThU transition pathways. Because CThU-T4 builds MSRs at a faster rate than CThU-T5, it also produces LLW more quickly, ultimately leading to 16.3% more LLW by the end of the scenario in 2205. Among the CUPu pathways, there is virtually no distinction between CUPu-T1 and CUPu-T3, since the slightly larger contribution from SFR reprocessing in CUPu-T1 almost exactly offset the impacts of MOX fuel fabrication and slightly higher UOX fuel fabrication in CUPu-T3. The CUPu-T2 transition, however, produced 10.4% less LLW than the other CUPu transitions. This is because the rate of SFR reactor deployment, and thereby also SFR fuel reprocessing deployment, was somewhat slower in the CUPu-T2 transition scenario due to lower breeding ratios.

This section has thus far only discussed traditional LLW categories. However, in terms of volume, mining waste is by far the most abundant low-hazard waste form arising from nuclear fuel cycles. By-product thorium recovery does have some associated mill tailing volumes; however, the mining waste associated with uranium recovery dwarfs the thorium mill tailings by several orders of magnitude in all scenarios; thus, only the results for uranium mining wastes are included in the plot below. Another potentially important category of low-hazard waste is depleted uranium. Figure 71 and Figure 72, below, show the results for uranium mining waste and depleted uranium, respectively.

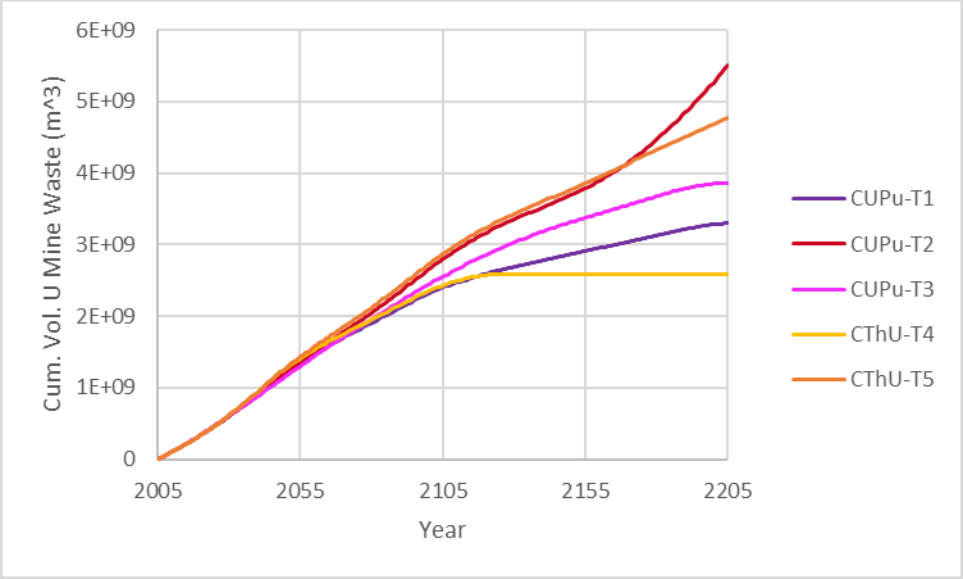

Figure 71, Comparison of Cumulative Uranium Mining Waste Volumetric Impact for Different Transition Scenarios

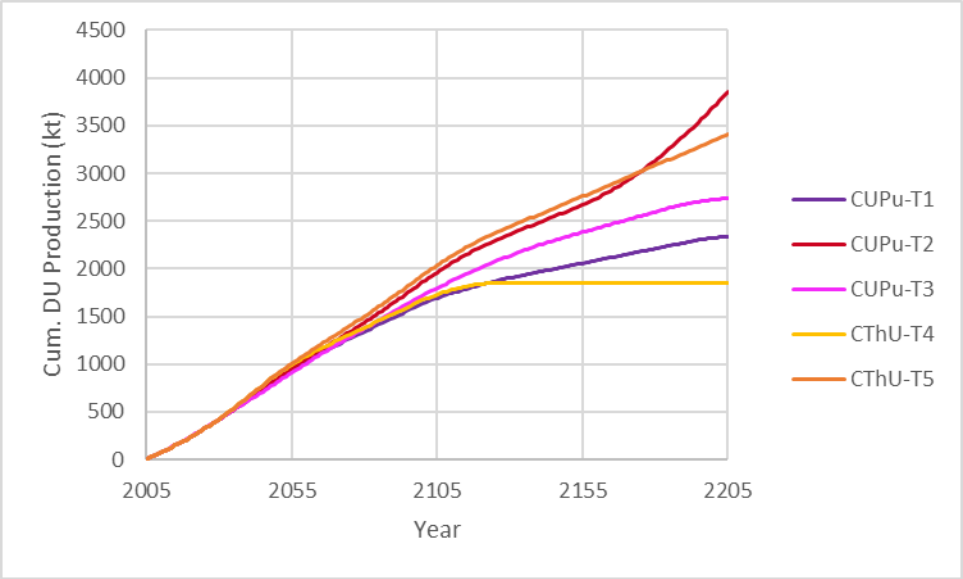

Figure 72, Comparison of Cumulative Depleted Uranium Production for Different Transition Scenarios

The estimates for uranium mining waste scale linearly (and for depleted uranium, nearly linearly) with uranium resource consumption, which is described in more detail in Section 5.4.5.

5.4.3. Dynamic Impacts of Waste Management (High-Level Waste Properties)

Recall that three different types of HLW properties are considered in this study: activity, decay heat, and radiotoxicity (the key radionuclides for repository risk will be considered separately in the next sub-section). Each of these parameters is calculated as an integral over a period of time in a repository. One potentially confusing notion regarding the cumulative dynamic impacts of HLW is deciding when to "count" the impact for an integrated parameter such as the integrated radiotoxicity from 100 years to 1,000,000 years. If the waste properties were calculated in "real time", i.e., as the radionuclides actually decay and produce heat in a repository, there would be a number of shortcomings to this method:

- The scenario would end well before the long-term impacts of the waste would become evident; fission products would overwhelm all other characteristics during these years.
- There would be no way to discriminate between fuel cycles based on meaningful waste hazard or repository results.
- It would be computationally intensive (to the point of infeasibility) to recalculate the property integrals at each time step.

Therefore, instead, the dates of the long-term waste impacts are pegged to the year corresponding to the energy production associated with that waste generation. For example, the steady-state calculations revealed that 1 GWe-yr of thorium-based MSR operations would lead to about 282 W-yr of integrated decay heat from 100 years to 1,000,000 years. In the CThU-T4 scenario, 9 GWe-yr of electricity was produced in the year 2053. In terms of integrated decay heat then, there would be 282*9=2540 W-yr of future 100-to-1,000,000 year 'full-term" integrated decay heat produced in 2053. This approach is used for the calculations for activity, decay heat, and

radiotoxicity in this section. The simplified repository risk values are simply masses of certain isotopes produced per year, so this method is not applicable to those calculations.

5.4.3.1. Activity

As was shown in Chapter 4, the trends for integrated activity (and other HLW properties) vary considerably depending on which integrated limits are applied. The results for integrated activity are first shown across a "full-term" window of time (100 to 1,000,000 years) in Figure 73, but other time intervals will be shown later.

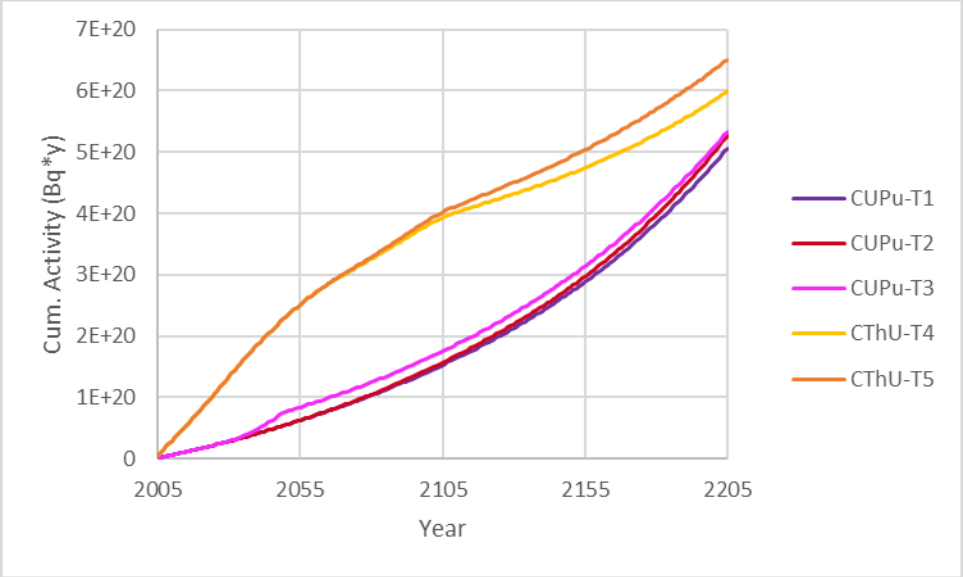

Figure 73, Comparison of Cumulative "Full-Term" (100 to 1,000,000 years) Integrated Activity for Different Transition Scenarios

In contrast to the steady-state results, where CThU had by far the lowest integrated SNF/HLW property impacts of any fuel cycle option, the CThU scenarios have a considerably *larger* full-term integrated activity impact than the CUPu scenarios. While it may not be obvious at first, the difference between the steady-state and the transition results can be attributed to the management

of uranium and plutonium, rather than thorium or uranium-233. All of the scenarios begin with a UOX-PWR-based fleet whose character influences the environmental performance of the scenario for many decades. However, in the CUPu scenarios, most or all of the uranium and plutonium in used nuclear fuel is repurposed for new fuel, regardless of whether it originated in a PWR or an SFR. The only spent fuel stream that is not reprocessed is used PWR-MOX fuel in scenario CUPu-T3, which leads to that scenario having a slightly higher integrated activity than CUPu-T1 or CUPu-T2 in earlier years.

As it turns out, the activity of spent uranium or uranium/plutonium-based fuel is dominated by several plutonium decay chains after a sufficiently long period has passed for the effects of shorter-lived fission products to have waned. In the CThU scenarios, the used UOX-PWR fuel is not reprocessed for its plutonium content, and the full inventory of uranium and plutonium is sent to disposal. Table 29, below, highlights the contributions of the uranium- and plutonium decay chains at times from 10,000 years and beyond.

Table 29, Relative Contributions to Activity for PWR-UOX UNF at Longer Timescales

	10,000 years	100,000 years	1,000,000 years
Pu-239/U-235 Series	90.65%	63.72%	17.30%
Pu-240/U-236 Series	4.82%	0.47%	0.54%
Pu-242/U-238/U-234 Series	1.99%	20.36%	77.00%
Am-241/Np-237 Series	0.03%	0.58%	1.14%
Fission Products	2.50%	14.86%	4.02%

The HLW associated with the reprocessing of UOX-PWR fuel in the CUPu scenarios still contains some uranium and plutonium due to process inefficiencies, but most of the uranium and

plutonium is re-used. In contrast, the CThU scenarios send all of these actinides to disposal in early years. The contributions of fission products (especially before 10,000 years) and actinides other than uranium and plutonium offset the difference in performance between CThU and CUPu somewhat, but nevertheless, by 2105 the cumulative integrated "full-term" activity of repository wastes from CThU-T5 is 163% larger than that of CUPu-T1 by the year 2205. Afterwards, however, the gap closes considerably since the steady-state activity from MSR HLW is quite low. By the end of the scenario in 2205, the integrated full-term activity for CThU-T5 is just 28.6% larger than that of CUPu-T1. At sufficiently long times, the integrated activity yield of CUPu would be expected to overtake that of CThU, reflecting the differences in those fuel cycles' properties at steady-state.

At a secondary level, the CThU-T5 scenario has a somewhat larger integrated full-term activity impact than CThU-T4 (8.67% higher in 2205) due to the persistence of the SBB-PWR fleet. The non-recycled plutonium content of the driver fuel of the SBB-PWR continues to accumulate even at later times, resulting in the higher activity. Among the CUPu scenarios, the performance is relatively similar, with the CUPu-T1 scenario having a slightly (4.55%) lower full-term integrated activity in 2205 than the CUPu-T2 or CUPu-T3 scenarios. This is due to the faster transition to a closed fuel cycle compared to CUPu-T2 and the avoidance of unreprocessed MOX fuel associated with CUPu-T3.

At nearer-term intervals, where the contribution from fission products becomes much more important, the trends look quite different. Figure 74, Figure 75, and Figure 76, below, show the

integrated activity for “short-term” (10 to 1000 y), “mid-term” (100 to 10,000 y), and “long-term” (10,000 to 1,000,000 y) intervals, respectively.

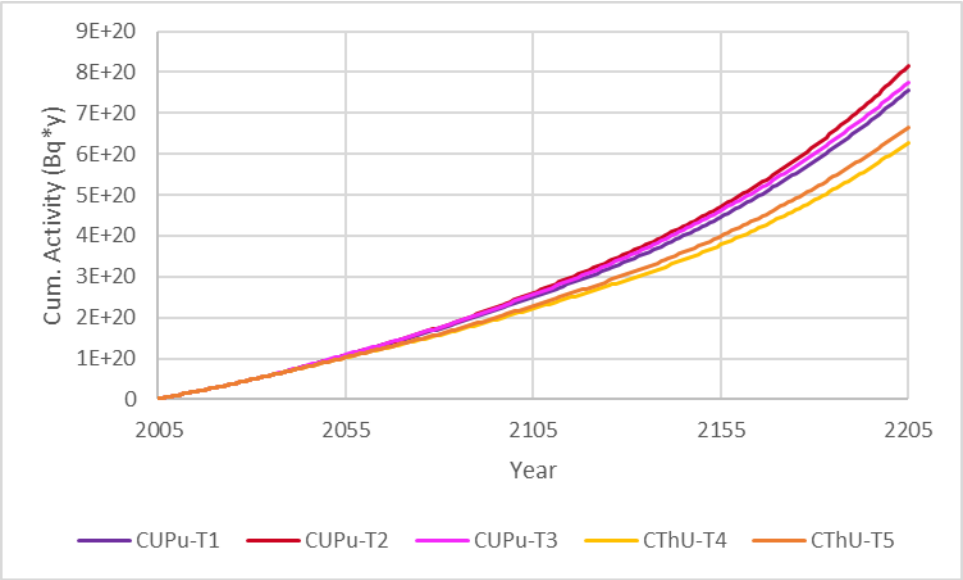

Figure 74, Comparison of Cumulative “Short-Term” (10 to 1000 years) Integrated Activity for Different Transition Scenarios

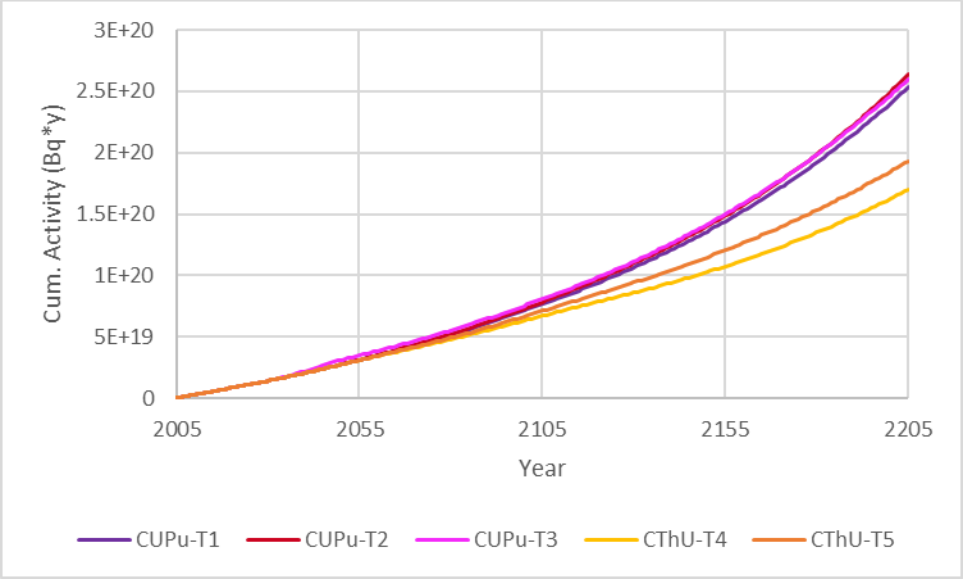

Figure 75, Comparison of Cumulative “Mid-Term” (100 to 10,000 years) Integrated Activity for Different Transition Scenarios

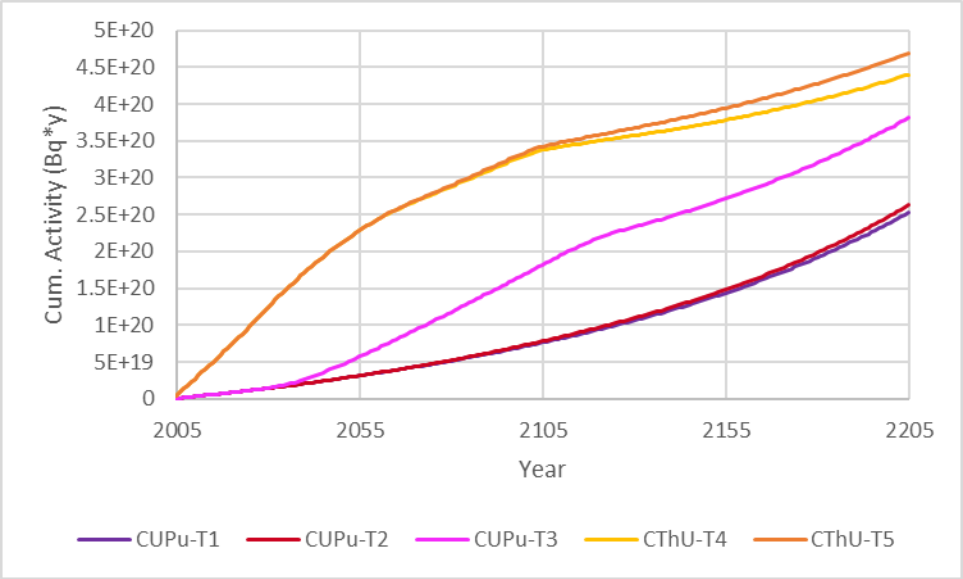

Figure 76, Comparison of Cumulative "Long-Term" (10,000 to 1,000,000 years) Integrated Activity for Different Transition Scenarios

The differences between the transitions in the short-term interval are relatively small, since each fuel cycle produces a fairly similar suite of short-lived radionuclides that dominate the short-term integral but are otherwise not regarded as critical to long-term repository risk. Examples of these fission products are Cs-137 ($t_{1/2}$=30.08 y), Sr-90 ($t_{1/2}$=28.79 y), and Sb-125 ($t_{1/2}$=2.76 y). The shape looks relatively similar for the mid-term interval except that the gap between CUPu and CThU increases somewhat. This is to be expected, since the period between 1,000 and 10,000 years favors thorium-based fuels due to the dominance of americium and plutonium decay chains during this period; thorium fuels have much lower concentrations of these elements. The long-term comparison generally mirrors the full-term trends, except that this period is where CUPu-T3 begins to separate itself from CUPu-T1 and CUPu-T2 due to the contribution from the unprocessed MOX fuel.

5.4.3.2. Decay Heat

The results for the "full-term" integrated decay heat are shown in Figure 77, below:

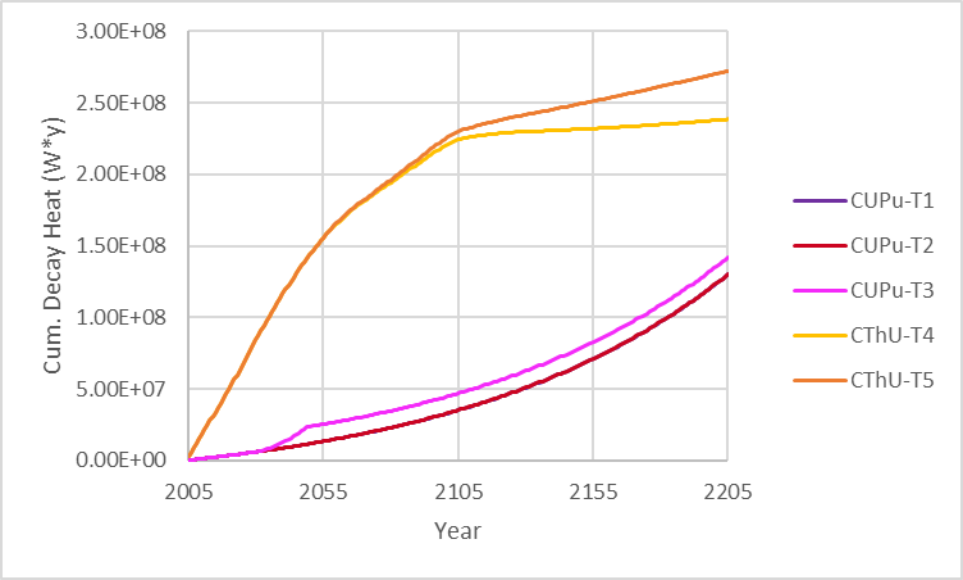

Figure 77, Comparison of Cumulative "Full-Term" (100 to 1,000,000 years) Integrated Decay Heat for Different Transition Scenarios

The integrated decay heat values are essentially a more accentuated version of the trends observed for activity; again, the transition results are opposite from the steady-state results given the contributions from non-recycled UOX UNF. The similarities to the activity results are not surprising, since decay heat is linked to the rate of radioactive decay (which is the definition of activity), and many of the same radionuclides are key contributors to both metrics (e.g., Cs-137 and Sr-90 in the short-term; Pu-239, Pu-240, and U-238 decay chains in the long term). The non-recycled UOX PWR fuel in the CThU scenarios contributes far more decay heat than all of the combined UNF streams from the CUPu scenarios at times before about 2100. After this, the decay heat from CThU-T5 is 552% higher than that from CUPu-T1. From this point on, though, the decay heat output from thorium-based fuels (especially for MSRs) is quite low, and the

CUPu scenarios slowly begin to catch up. Nonetheless, at the end of the scenario, CThU-T4's integrated decay heat is still 83.5% higher than that of CUPu-T1, while CThU-T5's integrated decay heat is 110% higher than that of CUPu-T1. If the scenario were extended beyond 2205, the CUPu scenarios would eventually overtake the CThU scenarios; however, the magnitude of the impact from the unrecycled UOX fuel takes several centuries to overcome.

Regarding the variations between specific scenarios, the trends are also essentially identical to what was observed for decay heat. By 2205, CThU-T5 has produced 14.2% more full-term integrated decay heat than CThU-T4, primarily due to the additional uranium and plutonium content of the disposed driver fuel from SBB-PWRs. Similarly, CUPu-T3 outpaces the other CUPu scenarios by 9.0% in 2205 due to the disposal of MOX fuel from PWRs.

If other time intervals are considered, the results change in the same manner that they did for the activity results. Figure 78, Figure 79, and Figure 80 below show the results for the short-term, mid-term, and long-term intervals.

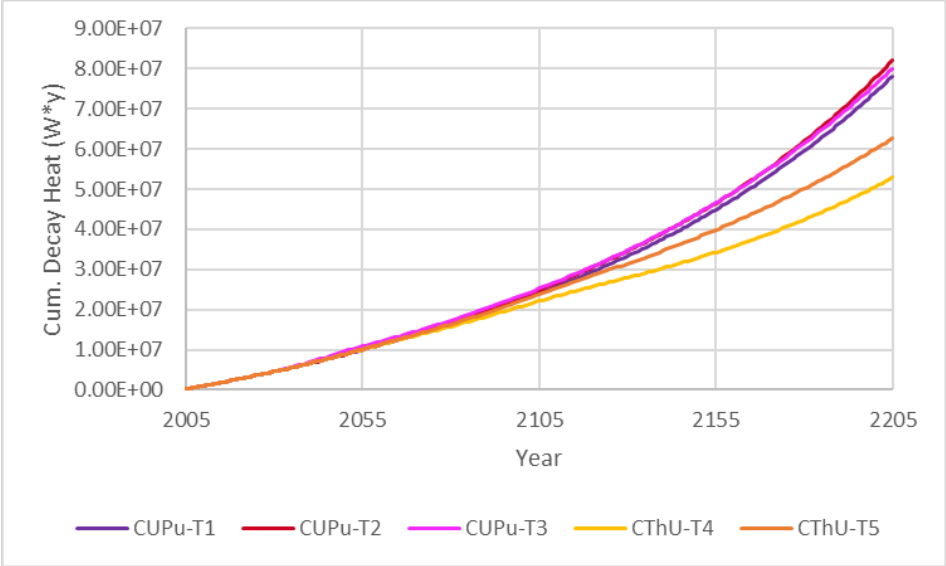

Figure 78, Comparison of Cumulative "Short-Term" (10 to 1000 years) Integrated Decay Heat for Different Transition Scenarios

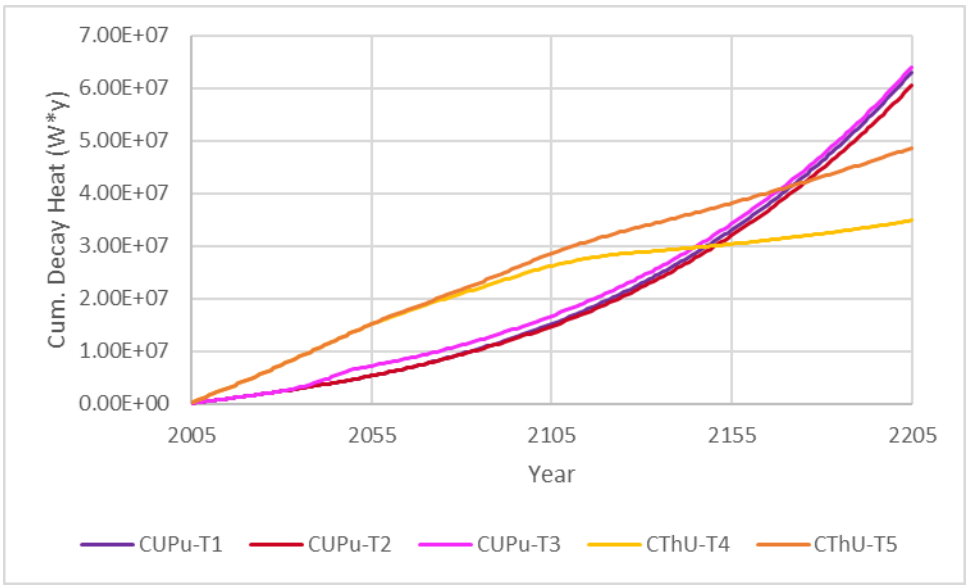

Figure 79, Comparison of Cumulative "Mid-Term" (100 to 10,000 years) Integrated Decay Heat for Different Transition Scenarios

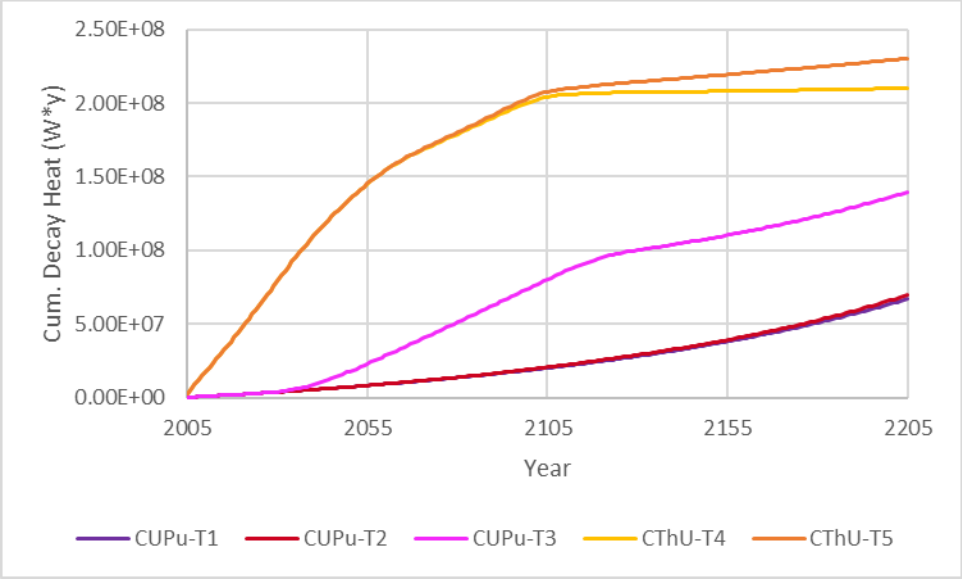

Figure 80, Comparison of Cumulative "Long-Term" (10,000 to 1,000,000 years) Integrated Decay Heat for Different Transition Scenarios

The only difference to note compared to the results for activity is that during the mid-term interval, the plutonium output from the CThU scenarios is enough to outpace the CUPu scenarios prior to 2100 or so, although the CUPu scenarios still overtake the CThU scenarios prior to the end of the simulation in 2205.

5.4.3.3. Radiotoxicity

The results for full-term integrated radiotoxicity are shown in Figure 81, below.

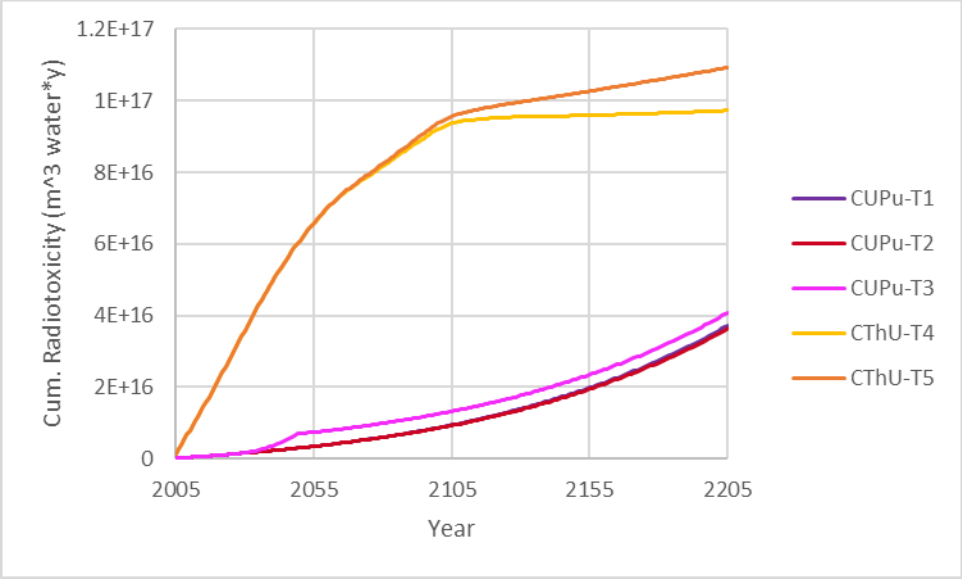

Figure 81, Comparison of Cumulative "Full-Term" (100 to 1,000,000 years) Integrated Radiotoxicity for Different Transition Scenarios

While the units for radiotoxicity are different, the ratio of the radiotoxicity impacts between scenarios is similar to those observed for decay heat and activity, but at even greater magnitudes. At the mid-point of the scenario in 2105, the CThU-T5 scenario has accumulated 922% more full-term integrated decay heat than the CUPu-T1 scenario, but this gap closes to 194% by the end of the scenario in 2205. The same radionuclides contribute to both decay heat and radiotoxicity, but actinides are weighted even more heavily for radiotoxicity. Thus, the magnitude of difference between the CThU and CUPu scenarios is attributed to the uranium and plutonium from UOX used fuel that are sent to disposal in the CThU scenarios.

The similarities to activity and decay heat extend to the other integration intervals as well, as shown in Figure 82, Figure 83, and Figure 84, below:

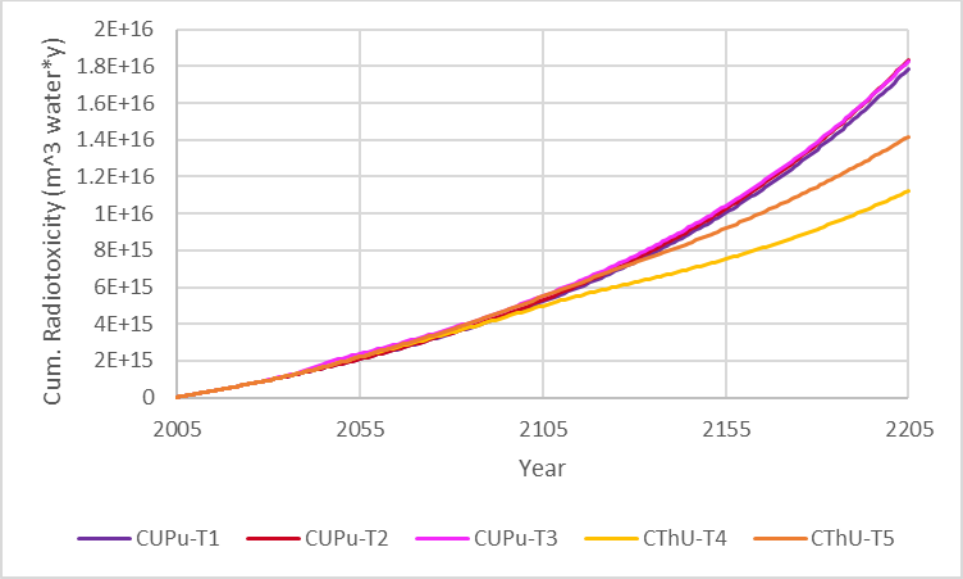

Figure 82, Comparison of Cumulative "Short-Term" (10 to 1000 years) Integrated Radiotoxicity for Different Transition Scenarios

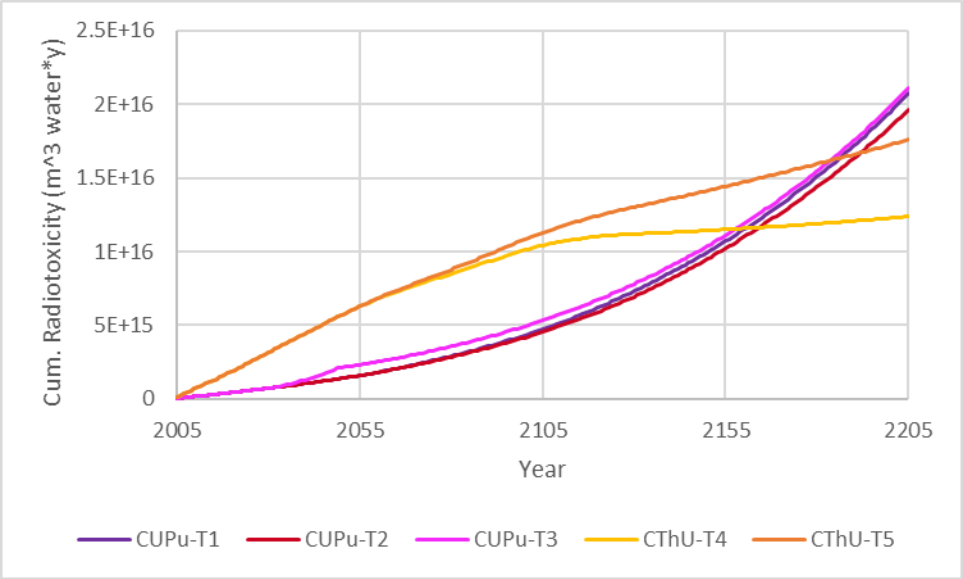

Figure 83, Comparison of Cumulative "Mid-Term" (100 to 10,000 years) Integrated Radiotoxicity for Different Transition Scenarios

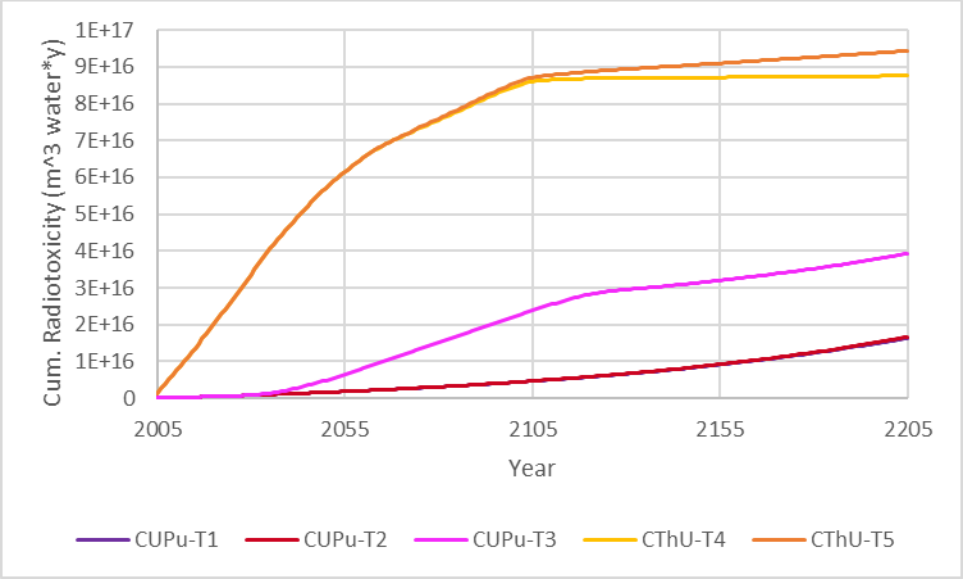

Figure 84, Comparison of Cumulative "Long-Term" (10,000 to 1,000,000 years) Integrated Radiotoxicity for Different Transition Scenarios

Much like the decay heat results, the mid-term interval features a crossing point where the CUPu scenarios' radiotoxicity trends surpass those of the CThU scenarios.

5.4.4. Dynamic Impacts of Simplified Repository Risk – Key Fission Product Accumulation

As discussed at length in Chapter 4, the "traditional" HLW properties are not accurate indicators of the actual risk posed by a repository waste; instead, repository risk is dominated by a handful of long-lived fission products and activation products. While the two key activation products (C-14 and Cl-36) were not included as there was no basis for determining their concentrations in advanced reactors, the tendency of the scenarios to produce five key fission products (I-129, Se-79, Tc-99, Sn-126, and Cs-135) is discussed in this sub-section. The results plotted in this sub-section are based on the year that these fission products were generated, rather than the year in which they were sent to disposal.

5.4.4.1. Iodine-129

I-129 is far and away the most important radionuclide in determining repository risk, regardless of the particular geology. The production of I-129 throughout the different scenarios is shown in Figure 85, below.

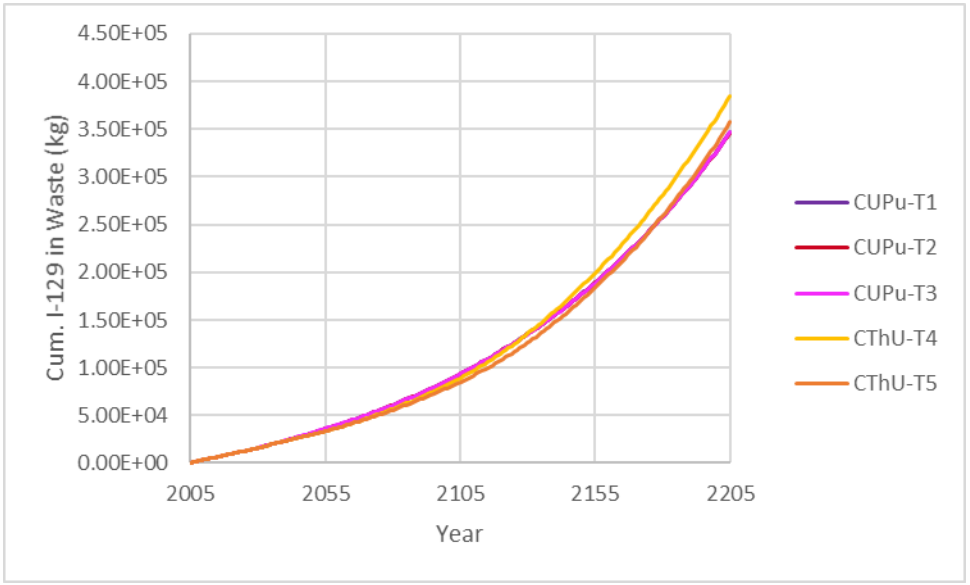

Figure 85, Comparison of Cumulative I-129 Production in Different Transition Scenarios

While I-129 is the most important contributor to repository risk, the results show relatively small differences between the various scenarios. The difference between the maximum and minimum cumulative I-129 production never exceeds 10% until the very end of the scenario, where CThU-T4 has produced about 11% more I-129 than CUPu-T2. While it is difficult to discern with the lines being close together, at early times the CUPu scenarios actually produce more I-129 than the CThU scenarios. At the peak of this difference in the year 2103, the CUPu-T2 scenario has produced 9.94% more I-129 than the CThU-T5 scenario. However, as the fraction of U-233

fissions out of total scenario fissions becomes larger in the CThU scenarios, they begin to catch up to and eventually overtake the CUPu scenarios. To understand these trends, consider the fission yields of I-129 for the primary fissioning isotopes in Table 30, below.

Table 30, Fission Yields of I-129 as % of Total Fission [JEFF 2006]

	Thermal-Induced	Fast-Induced
Th-232	n/a	0.431
U-233	1.63	1.73
U-235	0.706	1.03
U-238	n/a	0.622
Pu-239	1.407	1.31
Pu-241	1.28	1.67

In 2050, the CUPu scenarios begin to deploy SFRs in which a large fraction of the total fissions comes from Pu-239. In both the thermal and fast spectra, Pu-239 yields more I-129 per fission than U-235, which is the primary fissioning isotope for much of the lifetime of PWR-UOX fuel. The I-129 yield for Pu-239 is less than that of U-233, but the MSR fleets in the CThU scenarios have a slower initial deployment than the CUPu scenarios due to the immediately available source of fissile Pu that is available in the CUPu scenarios. However, ultimately, the fraction of total scenario fissions accounted for by U-233 becomes larger and larger for the CThU scenarios. Thus, by the end of the simulation, CThU-T4 has overtaken all other scenarios since an overwhelming portion of its fissions come from U-233, and this gap would be expected to widen if the simulation were extended beyond 2205. CThU-T5 still has a significant portion of its fissions coming from U-235 and Pu-239 due to the persistence of SBB-PWRs (and therefore, its uranium-based driver fuel) at the end of the scenario. Therefore, it overtakes the CUPu scenarios at a later time (2177, compared to 2129 for CThU-T4), and by a smaller margin.

Among the CUPu scenarios, the CUPu-T3 scenario initially slightly outpaces the other two scenarios due to its somewhat earlier deployment of Pu-laden fuel as part of its PWR-MOX fuel campaign that begins in 2030. However, the gap is small, with a peak difference of 1.73% in 2049 (the last year before the first SFR emerges). Afterwards, the CUPu-T1 and CUPu-T2 scenarios close the gap by 2074 since they deploy Pu-laden SFRs at a faster rate in the years immediately following 2050. By the end of the century, though, CUPu-T3 has largely moved towards an SFR-based fleet as well, and the three scenarios perform similarly with regards to cumulative I-129 until the end of the scenario (never more than a 0.25% difference after 2074).

5.4.4.2. Selenium-79

While I-129 is the largest contributor to repository dose, the differences in its production among different transition scenarios are relatively small, making it difficult to distinguish between different fuel cycle and/or transition options. However, this is not the case for some other key repository radionuclides, as first shown for Se-79 in Figure 86, below.

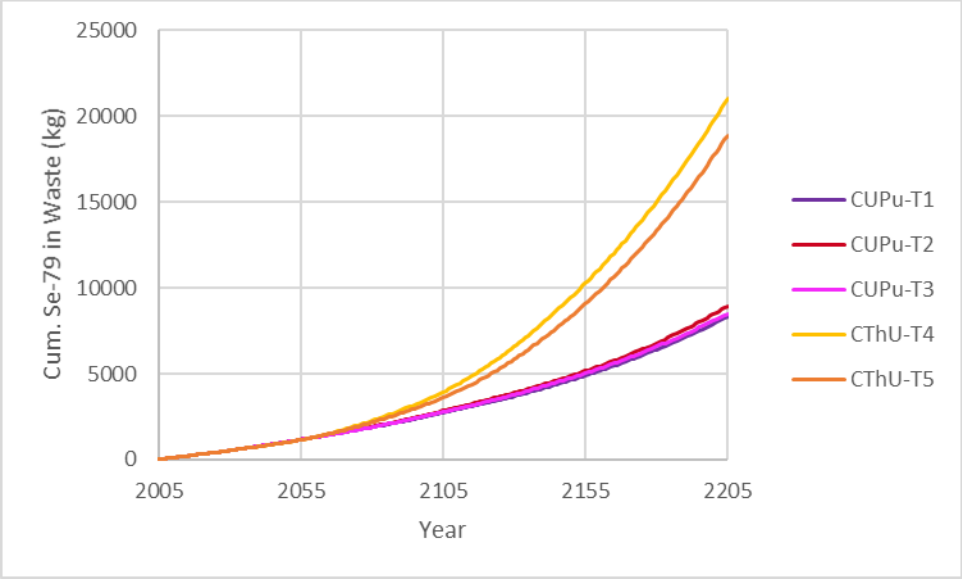

Figure 86, Comparison of Cumulative Se-79 Production in Different Transition Scenarios

Recall that in Chapter 4, it was determined that CThU and MThU produced 0.46 and 0.32 kg of Se-79 per GWe-yr, respectively, compared to 0.21 and 0.14 for MUPu and CUPu. This gap is sufficiently large that the CThU scenarios pull away from the CUPu scenarios with regards to Se-79 production almost as soon as the initial fleet of advanced reactors is deployed. By 2205, the CThU scenarios have produced an average of 132% more Se-79 than the CUPu scenarios. The CThU-T4 scenario is 11.4% above CThU-T5 in 2205 since it has more completely transitioned towards a steady-state CThU fuel cycle. Among the CUPu scenarios, the differences are relatively small, with the CUPu-T2 scenario accumulating 7.13% more Se-79 than CUPu-T1 by 2205. This is due to a somewhat larger Se-79 fission yield for U-235 compared to Pu-239; in general, since Se-79 is on the far lower end of the mass spectrum of common fission products, lighter fissile isotopes produce more Se-79.

5.4.4.3. Technetium-99

The results for the production of Tc-99 are shown in Figure 87, below.

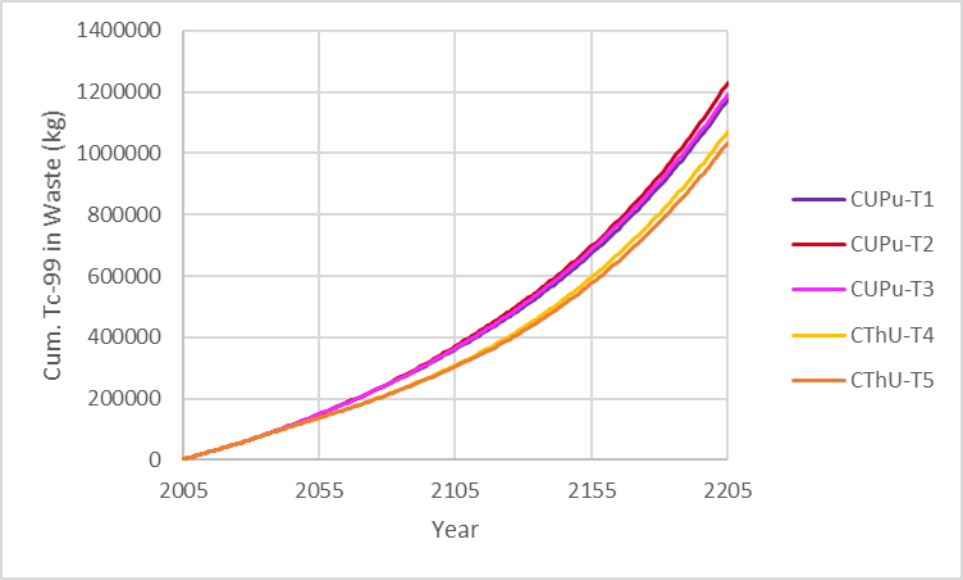

Figure 87, Comparison of Cumulative Tc-99 Production in Different Transition Scenarios

On the whole, only small differences exist between the scenarios with regards to Tc-99 production. The CUPu scenarios produce more Tc-99 than the CThU scenarios, although the difference is not large: there is an average difference of 12.7% by 2205. The difference is likely attributed to the fact that U-235 produces more Mo-99/Tc-99 than U-233: 6.132% fission yield in the thermal spectrum, compared to 5.03% for U-233 [JEFF 2006]. However, all scenarios entail a significant portion of U-235 fissions, so the cumulative Tc-99 differences between fuel cycles are small.

5.4.4.4. Tin-126

The results for the production of Sn-126 are shown in Figure 88, below.

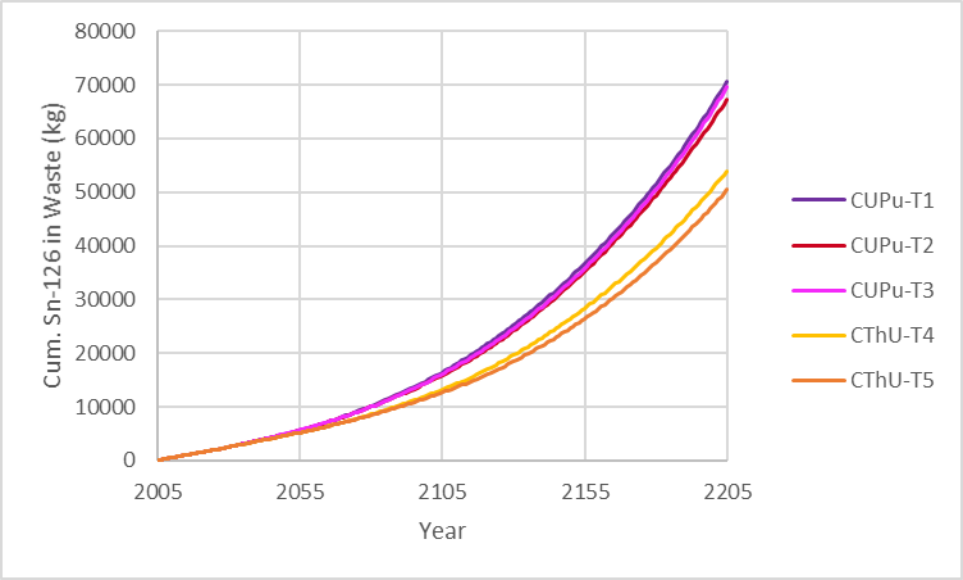

Figure 88, Comparison of Cumulative Sn-126 Production in Different Transition Scenarios

Much like the results for Tc-99, the CUPu scenarios produce somewhat, but not much, more Sn-126 than the CThU scenarios. By the end of the scenario in 2205, the CUPu scenarios have produced an average of 27.2% more Sn-126 than the CThU scenarios.

5.4.4.5. Cesium-135

The most lopsided distribution of the five key fission products belongs to Cs-135, as shown in Figure 89, below:

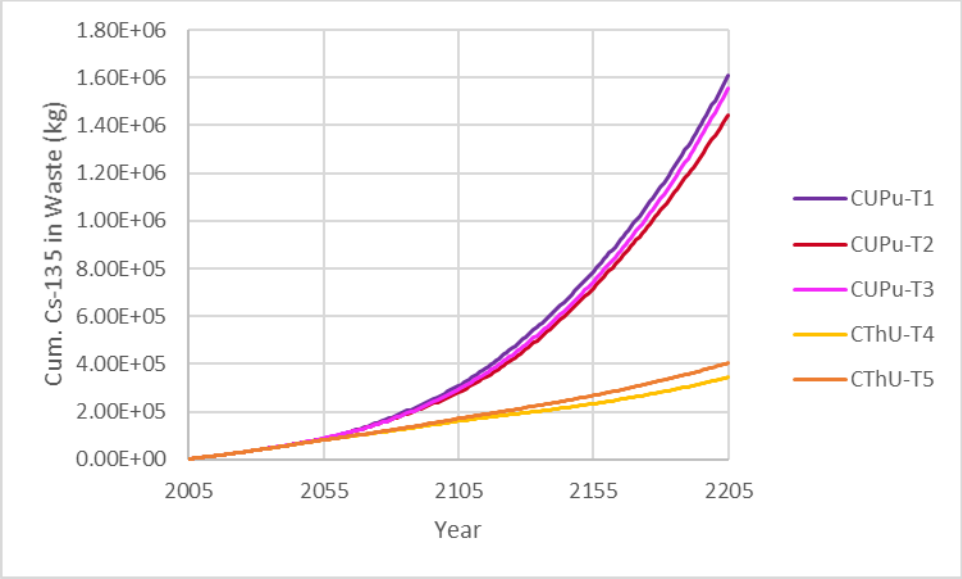

Figure 89, Comparison of Cumulative Cs-135 Production in Different Transition Scenarios

As discussed in Chapter 4, the large difference in production of Cs-135 between scenarios is due to chemical, rather than nuclear, behavior. The release of cesium from MSRs is limited by the similarity between cesium and lithium. Enriched lithium-7 is a valuable commodity in MSRs that use a lithium-based carrier salt, so reprocessing schema are designed to retain as much lithium as possible for re-use. As another alkali metal, cesium has similar properties to lithium and thus gets a "free ride" through the reprocessing system, with only a small amount going to HLW. This is an artifact of the MSR technology rather than an inherent property of the thorium fuel cycle.

The most MSR-intensive scenario, CThU-T4, therefore accumulates the least Cs-135, with CThU-T5 having the next least. Among the CUPu scenarios, the differences are relatively small. Pu-239 yields slightly more Xe-135 (Cs-135's parent isotope) than U-235, especially in the fast spectrum, so the order of the scenarios with regards to Cs-135 production is equivalent to the order of which scenarios have deployed the most SFRs: i.e., CUPu-T1, then CUPu-T3, then CUPu-T2.

5.4.5. Dynamic Impacts of Resource Stewardship

Most resource consumption, even for the CThU fuel cycles, consists of natural uranium usage. Figure 90, below, shows the trends in natural uranium consumption over time.

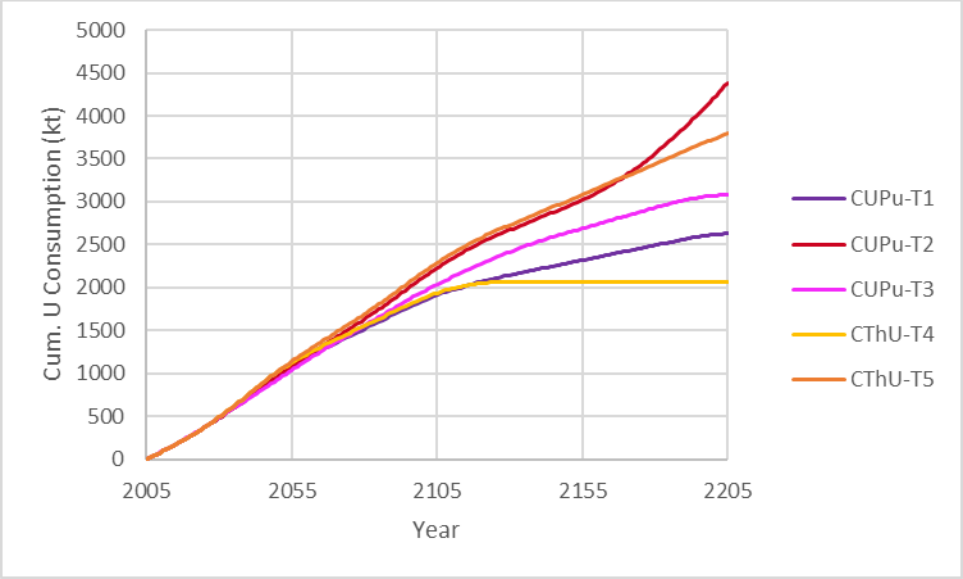

Figure 90, Comparison of Cumulative Natural Uranium Consumption in Different Transition Scenarios

In contrast to previous metrics, the results are not as simple as "CUPu vs. CThU"; the transition pathway is just as important. Interestingly, the CThU-T4 and CThU-T5 pathways placed 5th and 2nd respectively with regards to uranium consumption, with the CUPu-T3 and CUPu-T1 scenarios falling in between these two. Actually, for most of the scenario, CThU-T5 is the most resource-intensive scenario of all five, only being surpassed by CUPu-T2 in 2170.

To understand why this is the case, recall that the uranium driver fuel of the SBB-PWRs is enriched to 11.37% U-235. Even though the driver fuel of the SBB-PWR only accounts for a

relatively small portion of the total fuel in the fleet at a given time, it is quite resource-intensive. For a constant depleted uranium tails of 0.25%, 1 MT of 11.37%-enriched uranium will require 24.1 MT of naturally-enriched uranium to be consumed, compared to 8.59 MT for the reference 4.21% enrichment assumption for conventional PWR fuel. The CThU-T4 transition is able to move away from SBB-PWRs sufficiently quickly that it still consumes less uranium than the CUPu transitions. On the other hand, CThU-T5 retains a significant SBB-PWR fleet until the end of the simulation, resulting in a cumulative uranium consumption that rivals that of the slowest CUPu transition.

Only two of the scenarios use any natural thorium, in each case in much smaller than the amount of uranium usage. The results for cumulative thorium use for the two CThU scenarios are shown in Figure 91, below.

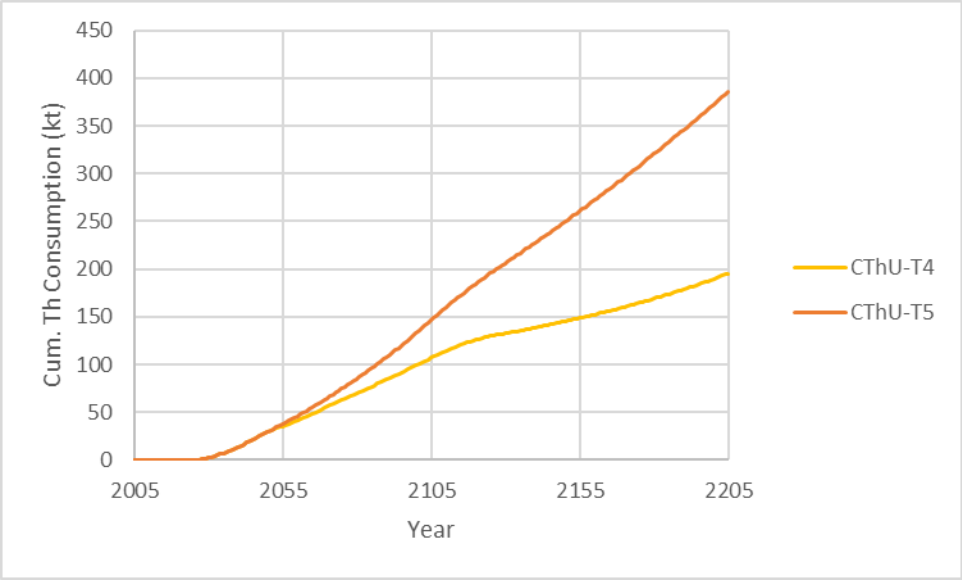

Figure 91, Comparison of Cumulative Natural Thorium Consumption in Different Transition Scenarios

While some thorium is supplied to fabricate new fuel salt for both new and existing MSRs, the majority of the thorium is consumed to fabricate blanket fuel for SBB-PWRs. Thus, it is not surprising that the transition which relies on a larger, longer-lived SBB-PWR fleet, CThU-T5, has used 97.8% more thorium than CThU-T4 by the end of the scenario. As a fraction of total natural resource usage on a mass basis, thorium accounts for 8.65% of the resource consumption in CThU-T4, compared to 9.22% in CThU-T5. Thus, even though a steady-state CThU fuel cycle does not require any natural uranium, less than 10% of the natural material used to approach steady-state consists of thorium.

5.5. Key Insights from Dynamic Comparison of Uranium/Plutonium- and Thorium-Based Options

The key insights from this chapter can be summarized along the following lines:

Transition Feasibility:

- The amount of time to reach steady-state, whether pursuing a uranium or a thorium-based option, is significant, requiring timeframes of at least 150 years (and usually longer) even under the most ideal policy circumstances.
- Each of the five transitions studied in this chapter is feasible, albeit with various types of challenges:
    - Assuming that reprocessing facilities are constructed in a timely fashion, U/Pu-fueled SFRs can be deployed in significant quantities beginning in 2050 since there is several decades' worth of used PWR fuel to draw from.

- However, the rate of SFR deployment is eventually limited by plutonium availability, so some new PWRs must continue to be constructed after 2050; the extent of this effect is inversely related to the assumed breeding ratio.
- Th/U-233-fueled MSRs initially face a fissile material availability issue, since the existing fleet of UOX-PWRs does not contribute any U-233 and new SBB-PWRs must be built at a later date.
- However, the low fissile loading requirement for MSRs offsets this issue to a large degree, and a relatively small fraction of SBB-PWRs is eventually sufficient to sustain the expansion of the MSR fleet.

Occupational Dose:

- Reactor dose dominates the contribution to the overall dose of the fuel cycle in transitions, just as it did at steady-state.
- The CThU scenarios perform more favorably than the CUPu scenarios due to the lower dose estimate for MSRs compared to SFRs.

Low-Level Waste:

- Similarly to occupational dose, reactors dominate the contributions to LLW for all of the scenarios, as was observed at steady-state.
- The CUPu scenarios perform more favorably than the CThU scenarios, given the proclivity of MSRs to produce significant quantities of LLW due to the nature of continuous processing.

- Mining waste volumes dominate the volume of low-hazard waste. CUPu-T2 and CThU-T5 produce the most mining waste since they consume the most natural uranium (see conclusions for "Resource Requirements" below).

High-Level Waste Properties:

- Any integrals of activity, decay heat, and/or radiotoxicity that include longer intervals of time (especially beyond 10,000 years) will favor CUPu scenarios over CThU scenarios, which is the opposite of the steady-state result. This is because of the large amount of unprocessed UOX fuel produced by both UOX-PWRs and the driver fuel of SBB-PWRs. This conclusion might change if the scenario were extended beyond 2205, since the steady-state contributions to the HLW properties favor CThU over CUPu, as discussed in Chapter 4.
- Shorter intervals of time marginally favor the CThU scenarios over the CUPu scenarios, although the results are close. This is primarily due to the small differences in the yields of particular medium-lived fission products such as Cs-137, Sr-90, and Sb-125.

Key Radionuclides for Repository Risk:

- The production of most important radionuclide, I-129, marginally favors CUPu over CThU, but the results are close for all scenarios; this is the same trend that was observed at steady-state.
- Tc-99 and Sn-126 production marginally favor the CThU scenarios over the CUPu scenarios, while Cs-135 production overwhelmingly favors CThU.
- Se-79 production overwhelmingly favors CUPu over CThU.

Resource Requirements:

- For all scenarios, including CThU, uranium usage dwarfs thorium usage.
- Unlike for other parameters, the selection of specific scenario had a significant impact on the natural uranium requirement. CThU-T5 used considerably more uranium than CThU-T4, and CUPu-T2 used considerably more uranium than CUPu-T3 and CUPu-T1. In fact, CUPu-T2 and CThU-T5 were the two most resource-intensive scenarios overall.

In most cases, with the notable exception of resource requirements, the differences between individual CUPu and CThU scenarios were not significant compared to the differences between CUPu and CThU as general fuel cycle options. This suggests that, at least from an environmental standpoint, selecting from among various secondary technology options (such as breeding ratios) should not have a tremendous impact on the result. However, the overall reactor technology (PWRs vs. SFRs vs. MSRs), and the overall fuel cycle (thorium vs. uranium), may be an important choice as its leads to considerably different environmental performance for certain parameters.

The conclusions regarding the HLW properties, in particular, pinpoint a promising direction for future work in this area. A major hindrance of the CThU scenarios is the failure to capitalize on existing material in the current UOX-PWR fleet; other than for electricity, the material in these reactors is not re-utilized. This is because the MSRs require uranium-233 rather than plutonium, necessitating an entirely separate fuel strategy involving the SBB-PWRs. However, an alternative approach could be to proceed directly from UOX-PWRs to the MSR technology by

initially loading the MSRs with thorium and plutonium. These would hypothetically be easier to transition with than U-235-based startups because, as a different element altogether, plutonium does not dilute the isotopic purity of the in-bred U-233. There are some studies that suggest this could be viable [Engel 1978, Merle-Lucotte 2006, Merk 2015, Green 2015], although considerably more work would be required on the reactor physics, chemistry, and isotopic evolutions of this concept before attempting to conduct fuel cycle analyses in tools such as VISION.

CHAPTER 6, CONCLUSIONS AND FUTURE WORK

This chapter is divided into two parts. The part first summarizes the key findings of the dissertation, while the second part identifies plausible future extensions of this line of research.

6.1. Summary and Conclusions

This dissertation has compared several EH&S metrics for uranium- and thorium-based fuel cycles, systematically and at a variety of levels. The representative fuel cycle options, technologies, metrics, assumptions, and approaches were selected and implemented in a way that promotes meaningful comparisons. The significance and key takeaways of the results have been reviewed and discussed in previous chapters and are summarized below.

Chapter 3 characterized a detailed comparison of the resource sustainability attribute of thorium and uranium fuel cycles, specifically by examining the environmental impacts associated with resource recovery. An integral component of this evaluation involved the elaboration of the notion of "by-product" thorium recovery. Because all prospective thorium recovery will likely be achieved as a by-product of existing mines for other commodities (especially titanium), the outlook for associated environmental impacts is fundamentally different than that for uranium recovery, which in contrast is recovered as a primary product from conventional mines. A quantitative assessment of prospective thorium by-product recovery sites indicates that by-product thorium will be sufficient to satisfy even the most optimistic world-wide demand scenarios indefinitely. Given the significant environmental and economic impact associated with opening and operating uranium mines, this represents a significant environmental advantage for thorium recovery compared to uranium recovery. Nonetheless, by-product recovery imparts

some incremental processing requirements, such as the use of strong acids and/or bases to extract thorium from its constituent minerals. The required species are commonplace, although they must be used in quantities which are larger than those required for uranium recovery.

Chapter 4 extended the comparison of uranium and thorium to the entire fuel cycle by focusing on four representative fuel cycles which encompassed a spectrum of fuel types and reprocessing strategies. These comparisons were applied at steady-state. The fuel cycle options were compared on the bases of collective occupational radiological impact, LLW volume production, HLW properties (activity, decay heat, and radiotoxicity), the production of fission products that impart repository risk, and natural resource consumption. No single fuel cycle option performed best with regards to all of these metrics. However, the closed fuel cycles tended to perform better than the modified-open fuel cycles in several aspects, especially with regards to the HLW properties and resource consumption. Because of the dominance of reactor contributions to both dose and LLW production, comparisons of those metrics were more closely tied to the reactor technology assumption rather than the general fuel cycle strategy. The radiological dose impacts appeared to favor MSRs and discourage SFRs, while for LLW production, the opposite was true. Regarding the repository-risk-inducing radionuclides, specific conclusions varied between the key radionuclides. For the most important species, I-129, the closed thorium fuel cycle produced slightly more than the other fuel cycle options.

In Chapter 5, the steady-state results were used as the basis for a comparison of transition scenarios to the closed fuel cycle options for uranium and thorium. The study focused on three plausible transition pathways for the closed uranium-based option and two for closed thorium-

based option. In all cases, the scenario took over a century to complete, and the reliance on uranium-based light water reactor technologies persisted for many decades. Each transition faced its own particular challenges, with SFRs requiring larger fissile loadings but with thermal MSRs offering slower breeding rates and relying on a currently unavailable fissile resource (U-233). For the most part, these properties seemed to balance each other out and the transitions for uranium- and thorium-based options proceeded at similar rates for similar sets of assumptions. Many of the environmental performance results mirrored those at steady-state, with a few key exceptions. First, the HLW properties for the transitions to closed thorium-based fuel cycles were less favorable than the steady-state results; this was because present uranium fuel inventories were not reprocessed during the transition analysis for thorium-based fuel cycles -- due to the focus on U-233 rather than plutonium. Also, resource consumption turns out to be more dependent on how quickly the transition takes place rather than whether the end-state is uranium- or thorium-based.

One important addendum to the conclusions above is the potential sensitivity of the results to uncertainties in certain parameters. The analyses of this dissertation were completed using a combination of, in decreasing order of fidelity: the results of irradiation and decay simulations, operational data points (often limited), and extrapolations from related processes. While the uncertainties would be difficult to quantify in most of these instances, it is nevertheless important to understand qualitatively the significance of these uncertainties and how the results might be impacted:

- Chapter 3 relied on chemical flowsheets primarily provided by limited operational experience with thorium recovery in India and mineral deposit characterization at various

sites around the world. The largest uncertainties in this chapter are probably associated with the relevant concentrations of thorium at titanium mineral deposits and the corresponding estimates for thorium by-product recovery, but the magnitude of excess thorium availability is such that the consequence of the uncertainty is of little consequence. Certain parts of the recovery flowsheets for both uranium and thorium are provided in less detail (especially the use of water and the extent of its recycle), so aside from the conclusions about the quantities of strong acids and bases, these results should probably be considered as order-of-magnitude estimates.

- Chapters 4 and 5 largely dealt with the same types of uncertainties since the same metric estimates were used in both chapters. The estimates for dose and LLW volume were the least "intrinsic" properties since they relied on a combination of limited occupational data and process extrapolations, and as such they had the largest associated uncertainties. The estimates for these parameters were generally within a factor of 2-3 of each other among the fuel cycle options (both at steady-state and in transition), so the uncertainties may be large enough that the differences might not be regarded as significant by all parties. The differences for resource requirements, HLW properties, and key-risk radionuclide concentrations are larger AND the associated uncertainties are smaller since they are the results of relatively high-fidelity simulations[36], so the conclusions associated with these parameters are more decisive than those for dose and LLW.

[36] While SCALE was used in relatively "low-fidelity" modes by the standards of reactor simulations (e.g., two-dimensional transport, simplified geometry), the associated uncertainties are thought to be much smaller than those that arise from the material flow assumptions (e.g., 99% reprocessing efficiency).

Also on the subject of the impact of assumptions on the results, Chapter 5 entailed resolute dedication to a clear policy throughout the entirety of each 200-year scenario. Even with this dedication, the fastest scenarios took over a hundred years to approach steady-state character. In reality, nuclear fuel cycles are highly impacted by changing policy trends, and experiences to-date suggest that advanced nuclear projects can be discontinued even after significant initial investment. To cite a few examples in the US alone:

- The Clinch River Breeder Reactor halted project development 13 years (1970-1983) and at least $6.9 billion after the project's initial authorization [Katz 1984];
- The Thorium-Uranium Recycle Facility was fully designed and mostly constructed in the 1960s when funding was discontinued to be allocated to other projects [Croff 2016b];
- The Mixed Oxide Fuel Fabrication facility began construction in 2007 and has not yet been cancelled, but it has continually decreased funding in the 2010s and would require another US$ 3 billion to complete [TAC 2016].

These are examples for single facilities, whereas each of the transitions entails the constructions of a series of advanced facilities of varying types. Given that society often demands immediate benefits from technology investment to warrant continued support, all of the advanced fuel cycle transitions could face considerable challenges when seeking stability between different presidential leadership, shifting national priorities, and so forth.

In combination, this sequence of related comparisons of uranium- and thorium-based options suggests that choosing between the two on an EH&S basis is complex. At a foundational level, differences between uranium-based and thorium-based fuel cycles are driven by (a) thorium

dioxide being monovalent and more refractory than uranium dioxide, (b) thorium not having a fissile isotope and thereby incurring many of the disadvantages of uranium fuel cycles, and (c) the availability of by-product thorium recovery. Neither option is unambiguously "better" than the other, and each option may offer advantages over the other depending on which metric, or set of metrics, is selected. At a minimum, this analysis should temper the enthusiasm of claims that one fuel cycle is unambiguously safer and more environmentally friendly than the other. It also suggests that unless one of the metrics included in this study eventually becomes much more important in the decision-making process than all others, other discriminators (e.g., technology maturity, capital cost, etc.) may be more important than EH&S metrics when considering a decision between uranium and thorium-based options.

6.2. Future Work

While this dissertation examined a specific set of fuel cycle options, the opportunity exists to extend the approach described in this research to comparisons of other fuel cycle options. Closed thorium- and uranium-based options represent only a handful of possible future implementations of nuclear fuel cycles. There are other closed fuel cycles that involve arrangements of multiple reactor types and/or fuel combinations, even at steady-state[37]; studies of these systems, particularly as part of transition scenarios, have hardly been studied. Potential sub-critical systems, such as accelerator-driven systems or fission-fusion hybrids[38], are another large area of fuel cycle option space that is relatively unstudied. The role of transuranic recycle could also potentially offer additional insights.

[37] E.g., a two-stage system featuring an SFR with a breeding ratio greater than 1 paired with an LWR with a breeding ratio less than 1, with both systems being fully reprocessed for their uranium and plutonium content
[38] For more background on these system, please see [Brown 2016].

There are a few extensions that are particularly worth considering for future work. One of these is the assessment of closed fuel cycles in molten salt fast reactors, potentially with either or both of uranium- and thorium-based configurations. Some of the comparisons of the reference thorium- and uranium-based fuel cycle options may have been impacted by using different reference reactor technologies as well as a different neutron energy spectrum. Conducting a similar assessment for fast-spectrum MSRs would offer a chance to gauge the extent to which results are a product of technology assumptions and which are an inherent function of the choice between thorium and uranium. One of the challenging parts of any such future line of work will be the development of material flows and inventories for a reactor system that has not been studied to the same extent as SFRs and thermal, fluoride-based MSRs.

Another intriguing option, particularly for transition analysis, would be to study the role of plutonium-based startup operational phases for transitions to MSRs. If HLW properties were deemed to be important, then the thorium-based MSR transitions were hindered by the lack of reprocessing of uranium fuel from early-fleet PWRs. Furthermore, the operation of SBB-PWRs continued to impart a significant resource consumption requirement on the fuel cycle for long time periods. The recovery of plutonium from the used PWR fuel could represent an alternative strategy for both of these problems. To conduct this line of work, additional attention would need to be placed on the long-term reactor physics implications of switching an MSR core from plutonium to uranium-233 over what would likely be several decades. The complex decline in plutonium demand over time could present a significant computational challenge for transition analysis, but the results would be interesting.

Aside from considering additional fuel cycle options, another potential line of research would be the coupling of the EH&S results to metrics for other areas, such as reactor safety (e.g., accident tolerance), economics, and proliferation resistance. Identifying and estimating meaningful metrics for these areas would also likely present a significant challenge. There are also few other metrics that may fall under the "environment" umbrella that could be applied to this group of fuel cycles in future work, including (but not limited to): CO_2 footprint, land use, and ecological impacts. Characterizing and quantifying these impacts would likely require new approaches and assumptions, but the incremental results could be of interest.

This dissertation incorporated several assumptions that simplified the fuel cycle analysis and made it easier to compare the intrinsic steady-state and transition characteristics of different options. Nonetheless, additional work could be performed to probe the impacts of some of these assumptions by considering alternative material re-use strategies. In particular, weapons-grade plutonium, the recycle of SNF stockpiles existing before the onset of the transition scenarios, depleted uranium (both pre-existing and newly-generated), and existing U-233 stockpiles could be considered as potentially available resources for jump-starting or temporarily sustaining certain portions of a transition. These could potentially accelerate the timeframe on which certain transitions occur.

Similarly, there are other input parameters that were not modified significantly between scenarios; variations of some of these parameters could be of interest to certain stakeholders. For example, the energy-growth of the scenarios was held at 1% annually, but the growth could be

allowed to fluctuate to account for potential energy market intrusions, such as the ingress from cheap coal or proliferant renewable technologies. Past analyses have at times considered upper- and lower-bounds of nuclear energy growth on a regional or global basis (e.g., 0.5%-3%) [Emsley 2014, Zhang 2012, Cao 2013], and similar approaches could be used for fuel cycle applications. Other parameters that could be varied include reactor operational lifetimes and technology deployment timeframes.

REFERENCES

[Abdou 2005] Abdou, H. "Environmental Monitoring in Radiation Field in Uranium Mines of Niger", from IAEA International Symposium on Uranium Production & Raw Materials for the Nuclear Fuel Cycle (Report IAEA-CN-128), Vienna, Austria, June 20-24, 2005

[Annesley 2010] Annesley, I. et al. "Composition and U-Th-Pb Chemical Ages of Uranium and Thorium Mineralization at Fraser Lakes, northern Saskatchewan, Canada", Geological Association of Canada – Mineral Association of Canada Joint Annual Meeting, Calgary, Canada, May 11, 2010

[APH 2006] Australia's Parliament House. "Australia's Uranium Resources, Production, and Exploration", Chapter 3 of Report "Inquiry into Developing Australia's Non-Fossil Fuel Energy Industry", 2006

[Arafat 2011] Arafat, Y. et al. "Radiotoxicity Characterization of HLW from Reprocessing of Uranium-Based and Thorium-Based Fuel", Waste Management 2011 Conference, Phoenix, USA, Feb. 27 – March 3, 2011

[Arnold 1955] Arnold, E. "Formation of U-232 and the Effects of its Decay Chain Activity on U-233, Thorium, and the THOREX Process", Oak Ridge National Laboratory Report ORNL-1869, 1955

[Ashley 2014] Ashley, S. et al. "Fuel Cycle Modelling of Open Cycle Thorium-Fuelled Nuclear Energy Systems", *Annals of Nuclear Energy,* Vol. 69, pp. 314-330, 2014

[Ault 2013] Ault, T., Wymer, R., and Krahn, S. "Thorium as a By-product: A Near-term Alternative for the Thorium Fuel Cycle", Transactions of the American Nuclear Society, Vol. 108, Atlanta, Georgia, June 16-20, 2013

[Ault 2014a] Ault, T., Krahn, S., Croff, A., and Wymer, R. "Environmental Impacts of Thorium Recovery from Titanium Mining in North America", Transactions of the American Nuclear Society, Vol. 111, Anaheim, California, November 9-13, 2014

[Ault 2014b] Ault, T., Krahn, S., Croff, A., and Wymer, R. "Supporting a Thorium-fueled Reactor Fleet in the U.S. with Domestic By-product Thorium", Transactions of the American Nuclear Society, Vol. 111, Anaheim, California, November 9-13, 2014

[Ault 2015a] Ault, T., Krahn, S., and Croff, A. "Assessment of the Potential of By-Product Recovery of Thorium to Satisfy Demands of a Future Thorium Fuel Cycle", *Nuclear Technology,* Vol. 189, 2015

[Ault 2015b] Ault, T., Krahn, S., and Croff, A. "Radiological Impacts and Regulation of Rare Earth Elements in Non-Nuclear Energy Production", Energies, Vol. 8, Issue 3, pp. 2066-2081, 2015

[Ault 2016] Ault, T., et al. “Insights and Trends from a Literature Assessment of the Thorium Fuel Cycle”, ANS Annual Meeting 2016

[Axtmann 1975] Axtmann, R. “Environmental Impact of a Geothermal Power Plant”, Science, Vol. 187, No. 4179, pp. 795-803, 1975

[Ayres 1992] Ayres, R. “Commentary: Cowboys, Cornucopians, and Long-Run Sustainability”, INSEAD Working Paper for Centre for the Management of Environmental Resources, 1992

[Bardi 2010] Bardi, U. “Extracting Minerals from Seawater: An Energy Analysis”, Sustainability, Vol. 2 980-992, 2010

[Barthel 1992] Barthel, F. and Dahlkamp, F. “Thorium Deposits and Their Availability”, Proceedings of a Technical Committee Meeting on “New Developments in Uranium Exploration, Resources, Production, and Demand”, Vienna, August 26-29, 1991

[Bell 1971] Bell, M. “Availability of Natural Resources for Molten-salt Breeder Reactors”, Oak Ridge National Laboratory Report ORNL-TM-3563, 1971

[Bergelson 2005] Bergelson, B. R., A. S. Gerasimov, and G. V. Tikhomirov. "Radiotoxicity and decay heat power of spent nuclear fuel of VVER type reactors at long-term storage." Radiation protection dosimetry 115.1-4:445-447, 2005

[Bettis 1986] Bettis Atomic Power Laboratory. “Shippingport Operations with the Light Water Breeder Reactor Core”, Bettis Atomic Power Laboratory Report WAPD-TM-1542, 1986

[Bhola 1964] Bhola, K., et al. “A Review of Uranium and Thorium Deposits in India”, OSTI Report A/CONF.28/P/752, 1964

[Bianchi 2011] F. Bianchi, et al., Regional and World Level Scenarios for Sodium Fast Reactor Deployment. Nuclear Engineering and Design, 2011. 241: p. 1145-1151

[Bishop 1968a] Bishop, W., Marsh, S., and Baroch, C. “Post Irradiation Examination of Thoria-Urania Fuel Rods – Quarterly Progress Report No. 1, March – August 1967”, Babcock & Wilcox Report BAW-3809-1, 1968

[Bishop 1968b] Bishop, W. et al. “Post Irradiation Examination of Thoria-Urania Fuel Rods – Quarterly Progress Report No. 2, September - November 1967”, Babcock & Wilcox Report BAW-3809-2, 1968

[Bishop 1968c] Bishop, W. et al. “Post Irradiation Examination of Thoria-Urania Fuel Rods – Quarterly Progress Report No. 3, December 1967 - February 1968”, Babcock & Wilcox Report BAW-3809-3, 1968

[Bishop 1968d] Bishop, W. et al. “Post Irradiation Examination of Thoria-Urania Fuel Rods – Quarterly Progress Report No. 4, March – May 1968”, Babcock & Wilcox Report BAW-3809-4, 1968

[Bishop 1968e] Bishop, W. et al. “Post Irradiation Examination of Thoria-Urania Fuel Rods – Quarterly Progress Report No. 5, June - August 1968”, Babcock & Wilcox Report BAW-3809-5, 1968

[Blaylock 1975] Blaylock, B. and Witherspoon, J. "Dose Estimation and Prediction of Radiation Effects on Aquatic Biota Resulting from Radioactive Releases from the Nuclear Fuel Cycle." Impacts of Nuclear Releases into the Aquatic Environment (1975): 377-93

[Bodenhausen 1954] Bodenhausen, J. “The Mineral Assemblage of Some Residual Monazite-and Xenotime-rich Cassiterite Deposits of Banka (Indonesia)”, Geological Institute of Amsterdam University, 1954

[Borrowman 1962] Borrowman, S. and Rosenbaum, J. “Recovery of Thorium from a Wyoming Ore”, US Department of the Interior: Bureau of Mines Report BM-RI-5917, 1962

[Boscher 2004] Boscher, T., et al. The CAFCA code for simulation of nuclear fuel cycles: Description of methodology, assumptions, and initial results. Technical Report Report No. MIT-NFC-TR-069, Massachusetts Institute of Technology, Cambridge, MA, 2004

[Bowman 2011] S. BOWMAN, "SCALE 6: Comprehensive Nuclear Safety Analysis Code System," Nuclear Technology, 174(2), 126-148, May 2011

[Brock 2014] Brock, T., Lewis, D., Hagemeyer, D, and McCormick, Y. “Occupational Radiation Exposure at Commercial Nuclear Power Reactors and Other Facilities 2012”, US Nuclear Regulatory Commission Report NUREG-0713, Vol. 34, 2014

[Brown 2016] Brown, N. et al. “Thorium Fuel Cycles with Externally Driven Systems”, Nuclear Technology, Vol. 194, No. 2, pp. 233-251, 2016

[Bucher 2009] Bucher, R. “India’s Baseline Plan for Nuclear Energy Self-Sufficiency”, Argonne National Laboratory Report ANL/NE-09/03, 2009

[Burkhardt 2013] Smith, B., K. Brown, S. Krahn, J. Clarke, A. Machiels and A. Sowder. “Modeling the Environmental Health and Safety Risks of the Present U.S. Nuclear Fuel Cycle”. International High-Level Radioactive Waste Management Conference. Albuquerque, NM American Nuclear Society (ANS), 2013

[Camper 2011] Camper, L. and Gelles, C. “Panel Session 60 – Disposal of Large Quantities of Depleted Uranium – Role of Site Specific Performance Assessment”, Waste Management 2011 (Conference Panel Report), 2011

[Cao 2013] Cao, B. et al. “Preliminary Study on Nuclear Fuel Cycle Scenarios of China Before 1950”, Energy Procedia, Vol. 39, pp. 294-299, 2013

[Carlsen 2013] Carlsen, B. et al. “Environmental Impacts, Health and Safety Impacts, and Financial Costs of the Front End of the Nuclear Fuel Cycle”, INL Report INL/EXT-14-32302

[Carlsen 2014] Carlsen, R., Gidden, M, and P. Wilson. Deployment optimization with the Cyclus fuel cycle simulator. In Proceedings of the 2014 ANS Winter Conference, volume 111, 241–244. Anaheim, CA, Nov 2014

[Carlsen 2016] Carlsen, R. “Optimizing Fuel Cycle Transitions under Uncertainty”, Technical Workshop on Fuel Cycle Simulation Paris - July 6-8, 2016

[Cave 1997] Cave, S. and Edwards, D. “Chemical Process Routes Selection Based on Assessment of Inherent Environmental Hazard”, Computers & Chemical Engineering, Vol. 21, 1997

[Chandler 1969] Chandler, J. and Bolt, S. “Preparation of Enriching Salt 7LiF-233UF4 for Refueling the Molten Salt Reactor”, Oak Ridge National Laboratory Report ORNL-4371, 1969

[Chandler 1970] Chandler, J. and Bolt, S. “Uranium-233-Bearing Salt Preparation for the Molten Salt Reactor Experiment”, Nuclear Technology, Vol. 9, No. 6, pp. 807-813

[Chandler 1971] Chandler, J. “Thorium-Uranium Recycle Facility”, Oak Ridge National Laboratory Report ORNL-TM-3422, 1971

[Chellapandi 2012] Chellapandi, P. “Overview of Indian FBR Programme”, International Workshop on ‘Prevention and Mitigation of Severe Accidents in SFR’, Tsuruga, Japan, June 11-13, 2012

[Connors 1979] Connors, D., Milani, S., Fest, J., and Atherton, R. “Design of the Shippingport Light Water Breeder Reactor”, Report WAPD-TM-1208, 1979

[Coquelet-Pascal 2013] C. Coquelet-Pascal, et al., Scenarios for Fast Reactors Deployment with Plutonium Recycling, in International Conference on Fast Reactors and Related Fuel Cycles: Safe Technologies and sustainable Scenarios (FR13). 2013: Paris, France

[Croff 2015] Croff, A. and Krahn, S. “A Simplified Improved Measure of Risk from a Geological Repository”, IHLRWM 2015, Charleston, SC, April 12-16, 2015

[Croff 2016a] Croff, A. and Krahn, S. “Comparative Assessment of Thorium Fuel Cycle Radiotoxicity”, Nuclear Technology, Vol. 194, No. 2, pp. 271-280, 2016

[Croff 2016b] Croff, A. et al. “ORNL Experience and Perspectives Related to Processing of Thorium and 233U for Nuclear Fuel”, Nuclear Technology, Vol. 194, No. 2, pp. 252-270, 2016

[Crouse 1959a] Crouse, D. and Brown, K. “Recovery of Thorium, Uranium, and Rare Earths from Monazite Sulfate Liquors by the Amine Extraction (AMEX) Process”, Oak Ridge National Laboratory Report ORNL-2720, 1959

[Crouse 1959b] Crouse, D. and Brown, K. “Solvent Extraction Recovery of Vanadium (and Uranium) from Acid Liquors with Di(2-Ethylhexyl) Phosphoric Acid”, Oak Ridge National Laboratory Report ORNL-2820, 1959

[David 2007] David, S., Huffer, E., and Nifenecker, H. “Revisiting the Thorium-Uranium Nuclear Fuel Cycle”, Europhysics News, Vol. 38, No. 2, pp. 24-27, 2007

[Davis 1977] Davis, W. “Carbon-14 Production in Nuclear Reactors”, Oak Ridge National Laboratory Report ORNL/NUREG/TM-12, 1977

[De Voto 1979] De Voto, R. and Stevens, D. “Uraniferous Phosphate Resources and Technology and Economics of Uranium Recovery from Phosphate Resources, United States and Free World”, Earth Sciences, Inc. Report GJBX-110(79) Vol. 2, 1979

[DECC 2013] Department of Energy and Climate Change (United Kingdom). “The Role of Thorium in UK Nuclear R&D: Current Trends and MSFR Modeling”, International Conference on Thorium Fuel: Thorium Energy Conference 2013, Geneva, Switzerland, October 28-31, 2013

[Del Cul 2009] Del Cul, G. et al. “Analysis of the Reuse of Uranium Recovered from the Reprocessing of Commercial LWR Spent Fuel”, Oak Ridge National Laboratory Report ORNL/TM-2007/207, 2009

[Delpech 2009] Delpech, S. et al. “Reactor Physic and Reprocessing Scheme for Innovative Molten Salt Reactor System”, Journal of Fluorine Chemistry, Vol. 130, Issue 1, 2009

[Dickey 1982] Dickey, B. and Hogg, G. “Heat Transfer in High-Level Waste Management”, Nuclear Engineering and Design, Vol. 67, Issue 3, pp. 473-487, 1982

[Dunn 1974] Dunn, F. et al. “SAS2A LMFBR Accident-Analysis Computer Code”, Argonne National Laboratory Report ANL-8138, 1974

[Els 2013] Els, F. “Largest Known Rare Earth Deposit Discovered in North Korea”, Mining.com News, December 5, 2013

[Emsley 2014] Emsley, I. “WNA 2013 Fuel Market Report”, IAEA Symposium on Uranium Raw Material for the Nuclear Fuel Cycle”, June 2014

[Engel 1975] Engel, J., Kerr, H., and Allen, E. “Nuclear Characteristics of a 1000-MW(e) Molten-Salt Breeder Reactor”, ANS Winter Meeting 1975, San Francisco, USA, November 1975

[Engel 1978] Engel, J., Grimes, W., Rhoades, W., and Dearing, J. "Molten-Salt Reactors for Efficient Nuclear Fuel Utilization without Plutonium Separation", Oak Ridge National Laboratory Report ORNL/TM-6413, 1978

[EPRI 2010a] Electric Power Research Institute, Nuclear Fuel Cycle Cost Comparison Between Once-Through and Plutonium Multi-Recycling in Fast Reactors, 2010, EPRI 1020660

[EPRI 2010b] Electric Power Research Institute, Nuclear Fuel Cycle Cost Comparison between Once-Through and Fully Closed Cycles, 2010, EPRI 1021054

[EPRI 2011] Electric Power Research Institute. "Decision Framework for Evaluating Advanced Nuclear Fuel Cycle Options", EPRI Technical Report 1022912, 2011

[EPRI 2013a] Electric Power Research Institute. "Program on Technology Innovation: A Quantitative Radiological Risk Analysis of the Once-Through Nuclear Fuel Cycle", EPRI Report 3002000807, 2013

[EPRI 2013b] Electric Power Research Institute. "Program on Technology Innovation: EPRI Framework for Assessment of Nuclear Fuel Cycle Options: Framework Description and Example Application for Evaluating Use of Reactor Grade Mixed Oxide Fuel in U.S. Light Water Reactors", EPRI Technical Report 1025208, 2013

[EPRI 2014a] Electric Power Research Institute. "Radiological Risks and Waste Management Impacts of a U.S. Transition from a Once-Through to a Modified Open Nuclear Fuel Cycle: A Quantitative Comparative Risk Analysis", EPRI Report 3002003156, 2014

[EPRI 2014b] Electric Power Research Institute. "Program on Technology Innovation: Summary of 2014 EPRI Nuclear Fuel Cycle Assessment Workshop, Day 1: Trial Implementation of EPRI Decision Framework Vanderbilt University, Nashville, Tennessee, July 22-23, 2014", EPRI Technical Report 3002002784, 2014

[EPRI 2015] Electric Power Research Institute. "Program on Technology Innovation: Technology Assessment of a Molten Salt Reactor Design – The Liquid Fluoride Thorium Reactor (LFTR)", EPRI Report 3002005460, 2015

[Ewing 2008] Ewing, R. "Nuclear Fuel Cycle: Environmental Impact", Harnessing Materials for Energy, Vol. 33, pp. 338-340, 2008

[Fisher 2009] Fisher, D. "Medical Isotope Production and Use", Pacific Northwest National Laboratory presentation PNNL-SA-65456, 2009

[Fitzgerald 1977] Fitzgerald, C., Vaughen, V., and Lamb, C. "Determination of Fission Product and Heavy Metal Inventories in FTE-4 Fuel Rods by a Grind-Burn-Leach Flowsheet", Oak Ridge National Laboratory Report ORNL/TM-5756, 1977

[Frondel 1958] Frondel, C. “Systematic Mineralogy of Uranium and Thorium”, US Department of the Interior, Geological Survey Bulletin 1064, 1958

[Furukawa 1990a] Furukawa, K., Kato, Y., Mitachi, K., and Lecocq, A. “Preliminary Safety Examination of Thorium Molten-Salt Nuclear Energy Synergetics”, Thorium Utilization: Proceedings of the Indo-Japan Seminar on Thorium Utilization, Dec. 10-13, 1990

[Furukawa 1990b] Furukawa, K., Mitachi, K., Kato, Y., and Lecocq, A. “Global Nuclear Energy System: Thorium Molten-Salt Nuclear Energy Synergetics”, Thorium Utilization: Proceedings of the Indo-Japan Seminar on Thorium Utilization, Dec. 10-13, 1990

[Furukawa 1992] Furukawa, K., Mitachi, K., and Kato, Y. “Small Molten-salt Reactors with a Rational Thorium Fuel-cycle”, Nuclear Engineering and Design, Vol. 136, pp. 157-165, 1992

[Furukawa 2007] Furukawa, K. et al. “A Road Map for the Realization of Global-Scale Thorium Breeding Fuel Cycle by Single Molten-Fluoride Flow”, 13th International Conference on Emerging Nuclear Energy Systems, Istanbul, Turkey, June 3-8, 2007

[Furukawa 2008] Furukawa, K. et al. “A Road Map for the Realization of Global-Scale Thorium Breeding Fuel Cycle by Single Molten-Fluoride Flow”, Energy Conversion and Management, Vol. 49, pp. 1832-1848, 2008

[Furukawa 2012] Furukawa, K., Erbay, L., and Aykol, A. “A Study on a Symbiotic Thorium Breeding Fuel-Cycle: THORIMS-NES through FUJI”, Energy Conversion and Management, Vol. 63, pp. 51-54, 2012

[Galperin 1999] Galperin, A., et al. “A Thorium-Based Seed-Blanket Fuel Assembly Concept to Enhance PWR Proliferation Resistance”, Proceedings of Global 1999 International Fuel Cycle Conference, 1999

[Ganda 2012] Ganda, Francesco, et al. "Self-sustaining thorium boiling water reactors." Sustainability 4.10 (2012): 2472-2497

[Gao 2012] Gao, Fanxing, and Won Il Ko. "Dynamic analysis of a pyroprocessing coupled SFR fuel recycling." Science and Technology of Nuclear Installations 2012 (2012)

[Gardiner 2015a] Gardiner, A. “Development and Testing of a Decision Framework and Decision Tool For Determining Fuel Cycle Preferences”, International High Level Radioactive Waste Management Conference 2015, Charleston, SC, USA, 2015

[Gardiner 2015b] Gardiner, A. et al. “Development of Attribute Framework and Tool to Support Evaluation of Attributes of Generation IV Nuclear Reactor Systems”, ANS Winter Meeting 2015, Washington, DC, USA, 2015

[Gidden 2012] Matthew Gidden, Paul Wilson, Kathryn Huff, and Robert Carlsen. Once-through benchmarks with Cyclus, a modular, open-source fuel cycle simulator. In Proceedings of the 2012 ANS Winter Conference. San Diego, CA, Nov 2012

[GIF 2002] Generation IV International Forum. "A Technology Roadmap for Generation IV Nuclear Energy Systems", 2002

[Gourdon 1990] Gourdon, j., Mesnage, B., Voitellier, J., and Suescun, M. "An Overview of Superphenix Commissioning Tests", Nuclear Science and Engineering, Vol. 106, No. 1, pp. 1-10, 1990

[Green 2015] Green, D. "Initial Fuel Possibilities for the Thorium Molten Salt Reactor", Missouri S&T University (Thesis), 2015

[Greenberg 1991] Greenberg, H., and Cramer, J. "Risk Assessment and Risk Management for the Chemical Process Industry", New York: John Wiley & Sons, 392 Pages, 1991

[Gregg 2014] Gregg, R. and Hesketh, K. "ORION and its Application to Fuel Cycle Assessment in the UK", National Nuclear Laboratory (NNL) Technical Conference 2014, May 2014

[Griffiths 2011] Griffiths, J. "Detection of 36Cl in Nuclear Reactor Waste", Analytical Chemistry (Research Profiles), 2011

[Gross 1965] Gross, P., and Hladek, K., "PITA-31: Fringe-Blanket Irradiation of Thorium Oxide: Supplement VI", Hanford Atomic Products Operation Report HW-84021 Sup6, 1965

[Guo 2013] Guo, Z. et al. "Simulations of Unprotected Loss of Heat Sink and Combination of Events Accidents for a Molten Salt Reactor", Annals of Nuclear Energy, Vol. 53, pp. 309-319, 2013

[Hansen 2011] Hansen, F. and Leigh, C. "Salt Disposal of Heat-Generating Nuclear Waste", Sandia National Laboratories Report SAND2011-0161, 2011

[Haridasan 2008] Haridasan, P. et al. "Occupational Radiation Exposure due to NORM in a Rare-Earths Compound Production Facility", Radiation Protection Dosimetry, Vol. 131, No. 2 (2008)

[Haridasan 2010] Haridasan, P. et al. "Operational Radiation Protection Associated with Thorium Processing in India", from Proceedings of International Symposium on Normally Occurring Radioactive Material (NORM), Marrakesh, Morocco, Mar. 22-26, IAEA STI-PUB-1497 (2010)

[Harjanto 2013] Harjanto, S., Virdhian, S., and Afrilinda, E. "Characterization of Indonesia Rare Earth Minerals and Their Potential Processing Techniques", Rare Earth Elements Conference, 2013

[Harlov 2002] Harlov, D. et al. “Apatite–Monazite Relations in the Kiirunavaara Magnetite–Apatite Ore, Northern Sweden”, Chemical Geology, Vol. 191, Issues 1-3, pp. 47-72, 2002

[Hecht 2000] Hecht, L. and Cuney, M. “Hydrothermal Alteration of Monazite in the Precambrian Crystalline Basement of the Athabasca (Saskatchewan, Canada): Implications for the Formation of Unconformity-Related Uranium Deposits”, Mineralium Deposita, Vol. 35, pp. 791-795, 2000

[Hecker 1981] Hecker, H. and Freeman, L. “Design Features of the Light Water Breeder Reactor (LWBR) Which Improve Fuel Utilization in Light Water Reactors”, Bettis Atomic Power Laboratory Report WAPD-TM-1409, 1981

[Heinonen 2010] Heinonen, O. et al. “Safeguards in Action: IAEA at Rokkasho, Japan”, June 2010

[Herring 2012] Herring, J. “Uranium and Thorium Resources”, Chapter 18 of Nuclear Energy, ed. N. Tsoulfanidis, Springer: New York, 462-490, 2012

[Hertzler 1994] Hertzler, T., Nishimoto, D., and Otis, M. “Depleted Uranium Disposal Options Evaluation”, Report EGG-MS-11297, 1994

[Hesketh 2009] Hesketh, Kevin, Robert Gregg, and Chris Phillips. "Nuclear Proliferation Risk Mitigation Approaches and Impacts in the Recycle of Used Nuclear Fuel in the USA." Wmsym. org. National Nuclear Laboratory 1 (2009)

[Hill 2010] Hill, R. “Role of Decay Heat in Advanced Fuel Cycles”, Presentation at Workshop on “Decay Spectroscopy at CARIBU”, April 14, 2010

[Himmelblau 1962] Himmelblau, D. “Basic Principles and Calculations in Chemical Engineering”, Upper Saddle River: Prentice Hall, 800 pg., 1962

[Hirakawa 1990] Hirakawa, N. and Kasma, E. “Study of Reactor Kinetics of Small Size Molten Salt Reactor”, Thorium Utilization: Proceedings of the Indo-Japan Seminar on Thorium Utilization, Dec. 10-13, 1990

[Huff 2013] Huff, K. An Integrated Used Fuel Disposition and Generic Repository Model for Fuel Cycle Analysis. Diss. Argonne National Laboratory, 2013

[Huff 2014] Huff, K, Fratoni, M. and Greenberg, H. Extensions to the cyclus ecosystem in support of market-driven transition capability. In Proceedings of the 2014 ANS Winter Conference, volume 111, 245–248. Anaheim, CA, Nov 2014

[Hughes 1980] Hughes, K. and Singh, R. “The Isolation of Thorium from Monazite by Solvent Extraction, Part I”, Hydrometallurgy, Vol. 6, 1980, pp. 25-33 (1980)

[IAEA 2001a] International Atomic Energy Agency. “Manual of Acid In Situ Leach Uranium Mining Technology”, IAEA Report IAEA-TECDOC-1239, 2001

[IAEA 2001b] International Atomic Energy Agency. “Analysis of Uranium Supply to 2050”, IAEA Report STI/PUB/1104, 2001

[IAEA 2007] International Atomic Energy Agency. “Management of Reprocessed Uranium: Current Status and Future Prospects”, IAEA Report IAEA-TECDOC-1529, 2007

[IAEA 2009] International Atomic Energy Agency. “World Distribution of Uranium Deposits (UDEPO) with Uranium Deposit Classification”, IAEA Report IAEA-TECDOC-1629, 2009

[IAEA 2011a] International Atomic Energy Agency, “Report of the Internal Review Mission on the Radiation Safety Aspects of a Proposed Rare Earths Processing Facility (The Lynas Project)”, NE/NEFW/2011, 2011

[IAEA 2011b] International Atomic Energy Agency. Radiation Protection and NORM Residue Management in the Production of Rare Earths from Thorium-Containing Minerals, Safety Reports Series No. 68, 2011

[Ismail 2001] Ismail, B. et al. “Radiological Impacts of the Amang Processing Industry on Neighboring Residents”, Applied Radiation and Isotopes, Vol. 54, pp. 393-397, 2001

[Jackson 1977] Jackson, R. and Walser, R. “PUREX Process Operation and Performance 1970 Thoria Campaign”, Atlantic Richfield Hanford Company Report ARH-2127, 1977

[Jacobson 2006] Jacobson, Jacob, et al. "VISION: Verifiable fuel cycle simulation model." TRANSACTIONS-AMERICAN NUCLEAR SOCIETY 95 (2006): 157.

[JEFF 2006] Joint Evaluated Fission and Fusion File, Incident-neutron data, http://www-nds.iaea.org/exfor/endf00.htm, 2 October 2006; see also A. Koning, R. Forrest, M. Kellett, R. Mills, H. Henriksson, Y. Rugama, The JEFF-3.1 Nuclear Data Library, JEFF Report 21, OECD/NEA, Paris, France, 2006, ISBN 92-64-02314-3

[Jenner 2013] Jenner, S. and Lamadrid, A. “Shale Gas v. Coal: Policy Implications from Environmental Impact Comparisons of Shale Gas, Conventional Gas, and Coal on Air, Water, and Land in the United States”, Energy Policy, Vol. 53, pp. 442-453, 2013

[Jeong 2006] C. Jeong and H. Choi, Estimation of the Spent Fuel and Transuranic Inventories for a Partial and Full Plutonium Recycling, in Pacific Basin Nuclear Conference. 2006: Sydney, Australia

[Jeong 2008] Jeong, Chang Joon, Chang Je Park, and Won Il Ko. "Dynamic analysis of a thorium fuel cycle in CANDU reactors." Annals of Nuclear Energy 35.10 (2008): 1842-1848.

[Jeong 2010] Jeong, Chang Joon, and Won Il Ko. "A sensitivity study on fast reactor scenarios with various conversion ratios." Annals of Nuclear Energy 37.9 (2010): 1229-1235.

[Jeong 2011] Jeong, Chang Joon, Chang Keun Jo, and Jae Man Noh. "Dynamic Analysis of Deep Burn High Temperature Reactor Scenario." Energy 38 (2011): 81.

[Jeong 2013] Jeong, Chang Joon, Chang Keun Jo, and Jae Man Noh. "A SCENARIO STUDY ON MIXING STRATEGIES OF FAST REACTOR WITH LOW AND HIGH CONVERSION RATIOS." Nuclear Engineering and Technology 45.3 (2013): 367-376

[Jiang 2004] S. JIANG, J. YU, AND J. LU. "Trace and Rare-earth Element Geochemistry in Tourmaline and Cassiterite from the Yunlong Tin Deposit, Yunnan, China: Implication for Migmatitic–hydrothermal Fluid Evolution and Ore Genesis", Chemical Geology, Vol. 209, Issue 3, pp. 193-213 (2004)

[Jones 2011] Jones, R. "Low Level Waste Disposition – Quantity and Inventory", US Department of Energy Report FCRD-USED-2010-000033, 2011

[Jones 2013] Jones, R. "Low Level Waste Disposition – Quantity and Inventory", FCRD-USED-2010-000033, Rev. 3, June 2013

[Joo 2008] Joo, H., Jang, J., Yoo, J., and Kim, Y. "SFR Breakeven Core Designs with Various Rated Powers", Transactions of the Korean Nuclear Society Spring Meeting Gyeongju, Korea, May 29-30, 2008

[Jordan 2014] Jordan, B., Eggert, R., Dixon, B., and Carlsen, B. "Thorium: Does Crustal Abundance Lead to Economic Viability?" Colorado School of Mines Working Paper 2014-07, 2014

[Kamei 2010] Kamei, T., Furukawa, K., Mitachi, K., and Kato, Y. "Mass Balance Analysis of Th-233U Based MSR (Molten-Salt Reactor) Cycle (THORIMS-NES) Transferred from Present U-Pu Based LWRs (Light Water Reactor)", Energy, Vol. 35, pp. 928-934, 2010

[Kamei 2012] Kamei, T. "Recent Research of Thorium Molten-Salt Reactor from a Sustainability Viewpoint", Sustainability, Vol. 4, pp. 2399-2418, 2012

[Kanda 1990a] Kanda, K. et al. "Reactivity Measurements and Analyses for Chemical Materials Used in a Thorium Molten Salt Reactor Fuel", Thorium Utilization: Proceedings of the Indo-Japan Seminar on Thorium Utilization, Dec. 10-13, 1990

[Kanda 1990b] Kanda, K. and Kano, I. "Effect of Uranium-235 Enrichment on Initial Reactivity of Molten Salt Reactor", Thorium Utilization: Proceedings of the Indo-Japan Seminar on Thorium Utilization, Dec. 10-13, 1990

[Kaya 2003] Kaya, M. And Bozkurt, V. "Thorium as a Nuclear Fuel", International Mining Congress and Exhibition of Turkey 2003, ISBN 975-395-605-3 (2003)

[Keegan 2008] Keegan, E. et al. “The Provenance of Australian Uranium Ore Concentrates by Elemental and Isotopic Analysis”, Applied Geochemistry, Vol. 28, pp. 765-777, 2008

[Kempe 2008] Kempe, U. et al. “U–Pb SHRIMP Geochronology of Th-poor, Hydrothermal Monazite: An Example from the Llallagua Tin-porphyry Deposit, Bolivia”, Geochimica et Cosmochimica Acta, Vol. 72, Issue 17, pp. 4352-4366, 2008

[Keni 1990] Keni, V. ‘‘Extraction and Refining of Thorium,’’ Thorium Utilization: Proc. Indo-Japan Seminar on Thorium Utilization, December 10–13, 1990

[Kessler 2011] Kessler, G. “Proliferation-Proof Uranium, Plutonium Fuel Cycles: Safeguards and Non-Proliferation”, Karlsruhe: KIT Scientific Publishing, 383 pages, 2011

[Kessler 2013] Kessler, G. “Nuclear Fission Reactors: Potential Role and Risks of Converters and Breeders”, New York: Springer, 258 pages, 2013

[Kim 2011] T. Kim, B. Feng, and T. Taiwo, Assessment of Transition Fuel Cycle Performance with and without MOC Options, ANL-FCT-328, FCRD-SYSA-2011-000336

[Ko 2012] Ko, W. and Gao, F. “Economic Analysis of Different Nuclear Fuel Cycle Options”, Science and Technology of Nuclear Installations, 2012

[Korobeinikov 2013] Korobeinikov, V. “Current Nuclear Power Issues in Russia”, Technical Meeting on the Country Nuclear Power Profiles, Vienna, Austria, March 18-21, 2013

[Krahn 2014] Krahn, S., Croff, A., Smith, B., Clarke, J., Sowder, A., and Machiels, A. “Evaluating the Collective Radiation Dose to Workers from the U.S. Once-Through Nuclear Fuel Cycle”, Nuclear Technology, Vol. 185, No. 2, pp. 192-207 (2014)

[Krishnamurthy 2004] Krishnamurthy, N. and Gupta, C. Extractive Metallurgy of Rare Earths, Boca Raton: CRC Press, 504 pages, 2004

[Kunz 2007] Kunz, T. et al. “Ecological Impacts of Wind Energy Development on Bats: Questions, Research Needs, and Hypotheses”, Frontiers in Ecology and the Environment, Vol. 5, No. 6, p. 315-324, 2007

[Kutt 2014] Kutt, M., Frieb, F., and Englert, M. “Plutonium Disposition in the BN-800 Fast Reactor: An Assessment of Plutonium Isotopics and Breeding”, Science and Global Security, Vol. 22, pp. 188-208, 2014

[Lambert 1968] Lambert, I. and Heier, K. “Estimates of the Crustal Abundance of Thorium, Potassium, and Uranium”, *Chemical Geology,* Vol. 3, Issue 4, 1968

[Latge 2012] Latge, C. et al. “Teaching Sodium Fast Reactor Technology and Operation for the Present and Future Generations of SFR Users”, Journal of Nuclear Science and Technology, Vol. 48, Issue 4, pp. 701-708, 2012

[Lindner 2014] Lindner, H. “A Cost Estimate for Uranium Recovery from Seawater Using a Chitin Nanomat Adsorbent”, University of Texas Thesis, 2014

[Lindner 2015] Lindner, H. and Schneider, E. “Review of Cost Estimates for Uranium Recovery from Seawater”, Energy Economics, Vol. 49, pp. 9-22, 2015

[Linharo 2003] Linharo, S., Pollard, P., And Born, H. “Petrology and Textural Evolution of Franites Associated with Tin and Rare-metals Mineralization at the Pitinga Mine, Amazonas, Brazil”, Lithos, Vol. 66, Issue 1, pp. 37-61, 2003

[Liu 2012] Liu, G. and Muller, D. “Addressing Sustainability in the Aluminum Industry: A Critical Review of Life Cycle Assessments”, Journal of Cleaner Production, Vol. 35, pp. 108-117, 2012

[Long 2010] Long, K. “The Principal Rare Earth Elements Deposits of the United States—A Summary of Domestic Deposits and a Global Perspective”, SIR 2010–5220, 2010

[Lottering 2008] Lottering, M. et al. “Mineralogy and Uranium Leaching Response of Low Grade South African Ores”, Minerals Engineering, Vol. 21, pp. 16-22, 2008

[Mankins 1995] Mankins, J., "Technology Readiness Levels: A White Paper". NASA, Office of Space Access and Technology, Advanced Concepts Office. April 1995

[Mathieu 2006] Mathieu, L. et al. “The Thorium Molten Salt Reactor” Moving on from the MSBR”, *Progress in Nuclear Energy*, Vol. 48, pp. 664-679, 2006

[Matthieu 2009] Matthieu, L. “Possible Configurations for the Thorium Molten Salt Reactor and Advantages of the Fast Nonmoderated Version”, Nuclear Science and Engineering, Vol. 161, pp. 78-89, 2009

[McLennan 1980] McLennan, S., Nance, W., and Taylor, S. “Rare Earth Element-Thorium Correlations in Sedimentary Rocks, and the Composition of the Continental Crust”, Geochimica et Cosmochimica Acta, Vol. 44, Issue 11, pp. 1833-1839, 1980

[McNeese 1967] McNeese, L. “Considerations of Low Pressure Distillation and its Application to Processing of Molten-Salt Breeder Reactor Fuels”, Oak Ridge National Laboratory Report ORNL-TM-1730, 1967

[Merk 2015] Merk, B. and Litskevich, D. “On the Burning of Plutonium Originating from Light Water Reactor Use in a Fast Molten Salt Reactor – A Neutron Physical Study”, Energies, Vol. 8, 2015

[Merle-Lucotte 2004] Merle-Lucotte, E. et al. “Molten Salt Reactors and Possible Scenarios for Nuclear Power Deployment”, PHYSOR 2004, Chicago, USA, April 2004

[Merle-Lucotte 2006] Merle-Lucotte, E. et al. “Fast Thorium Molten Salt Reactors Started with Plutonium”, ICAPP 2006, Reno, USA, June 2006

[Merle-Lucotte 2007a] Merle-Lucotte, E. et al. “Optimized Transition from the Reactors of Second and Third Generations to the Thorium Molten Salt Reactor”, ICAPP 2007, Nice, France, May 13-18, 2007

[Merle-Lucotte 2007b] Merle-Lucotte, E. et al. “The Thorium Fuel Molten Salt Reactor: Launching the Thorium Fuel Cycle while Closing the Current Fuel Cycle”, European Nuclear Conference (ENC 2007). European Nuclear Society, 2007

[Merle-Lucotte 2008a] Merle-Lucotte, E. et al. “Influence of the Processing and Salt Composition on the Thorium Molten Salt Reactor”, *Nuclear Technology,* Vol. 163, 2008

[Merle-Lucotte 2008b] Merle-Lucotte, E. et al. “Optimization and Simplification of the Concept of Non-moderated Thorium Molten Salt Reactor”, International Conference on the Physics of Reactors “Nuclear Power: A Sustainable Resource”, Interlaken, Switzerland, September 14-19, 2008

[Merle-Lucotte 2011] Merle-Lucotte, E. et al. “Launching the Thorium Fuel Cycle with the Molten Salt Fast Reactor”, Proceedings of ICAPP 2011, Nice, France, May 2-5, 2011

[Mernagh 2008] Mernagh, T. and Miezitis, Y. “A Review of the Geochemical Processes Controlling the Distribution of Thorium in the Earth’s Crust and Australia’s Thorium Resources”, *Geoscience Australia,* Record 2008/05, 2008

[Merritt 1971] Merritt, R. “The Extractive Metallurgy of Uranium”, Golden: Colorado School of Mines Research Institute, 576 pages, 1971

[Meyer 1982] Meyer, H., Witherspoon, J., McBride, J. and Frederick, E. “Comparison of the Radiological Impacts of Thorium and Uranium Nuclear Fuel Cycles”, Nuclear Regulatory Commission Report NUREG/CR-2184, Oak Ridge National Laboratory Report ORNL/TM-7868, 1982

[Miezitis 2013] Miezitis, Y. “Thorium”, Australian Government: Geoscience Australia, http://www.australianminesatlas.gov.au/aimr/commodity/thorium.html, Accessed October 2013, 2013

[MINDAT 2016] Mineralogy Database. http://webmineral.com/, Accessed May 2016

[Mitachi 2006] Mitachi, K., Yamamoto, T., and Yoshioka, R. “Three-region Core Design for 200-MW(electric) Molten-Salt Reactor with Thorium-Uranium Fuel”, Nuclear Technology, Vol. 158, June 2007

[Mitchell 1996] Mitchell, R. and Chakhmouradian, A. “Compositional Variation of Loparite from the Lovozero Alkaline Complex, Russia”, The Canadian Mineralogist, Vol. 34, pp. 977-990, 1996

[Mohanty 2004] Mohanty, A. et al. “Natural Radioactivity and Radiation Exposure in the High Background Area at Chhatrapur Beach Placer Deposit of Orissa, India”, Journal of Environmental Radioactivity, Vol. 75, Issue 1, pp. 15-33, 2004

[Morales 2009] Morales, J., Conejo, A., and Perez-Ruiz, J. “Economic Valuation of Reserves in Power Systems with High Penetration of Wind Power”, IEEE Transactions on Power Systems, Vol. 24, No. 2, pp. 900-910, 2009

[Mudd 2007] Mudd, G. “Global Trends in Gold Mining: Towards Quantifying Environmental and Resource Sustainability”, Resources Policy, Volume 32, Issues 1-2, pp. 42-56 2007

[Mukherjee 2003] T.K. MUKHERJEE, “Processing of Indian Monazite for the Recovery of Thorium and Uranium Values”, Chapter of C. Ganguly’s Characterisation and Quality Control of Nuclear Fuels (A collection of papers at the International Conference on Characterisation and Quality Control of Nuclear Fuels in Hyderabad, 2002), New Delhi: Allied Publishers, 2003

[Muller 2005] Muller, S. et al. “Giant Iron-ore Deposits of the Hamersley Province Related to the Breakup of Paleoproterozoic Australia: New Insights from In situ SHRIMP Dating of Baddeleyite from Mafic Intrusions”, Geology, Vol. 33, Issue 7, pp. 577-580, 2005

[Nagy 2008] Nagy, K., Kloosterman, J., Lathouwers, D., and Van Der Hagen, T. “Parametric Studies on the Fuel Salt Composition in Thermal Molten Breeder Reactors”, International Conference on the Physics of Reactors, Interlaken, Switzerland, September 2008

[Nagy 2010] Nagy, K., Kloosterman, J., Lathouwers, D., and Van Der Hagen, J. “Definition of Breeding Gain for Molten Salt Reactors”, PHYSOR 2010, Pittsburgh, USA, May 2010

[Nagy 2012] Nagy, K. “Dynamics and Fuel Cycle Analysis of a Moderated Molten Salt Reactor”, Thesis for Delft University of Technology (Netherlands), 2012

[NEA 1994] Nuclear Energy Agency (Europe). “The Economics of the Nuclear Fuel Cycle”, Technical Report, 1994

[NEA 2012] Nuclear Energy Agency (Europe). “Spent Nuclear Fuel Reprocessing Flowsheet”, Report NEA/NSC/WPFC/DOC(2012)15, 2012

[NCRP 1987] US National Council on Radiation Protection and Measurements, “Ionizing Radiation Exposure of the Population of the United States”, Book (Self-Published), 1987

[Northey 2013] Northey, S., Haque, N., and Mudd, G. “Using Sustainability Reporting to Assess the Environmental Footprint of Copper Mining”, Journal of Cleaner Production, Vol. 40, pp. 118-128, 2013

[NRC 1975] US Nuclear Regulatory Commission. “Reactor Safety Study: An Assessment of Accident Risks in U.S. Commercial Nuclear Power Plants”, Report WASH-1400 (NUREG-75/014), 1975

[NRC 1991] US Nuclear Regulatory Commission, “Subpart C--Occupational Dose Limits”, Code of Federal Regulations (CFR) 10, Part 20, Item 1201, May 21, 1991

[NRC 2010] US Nuclear Regulatory Commission, “Occupational Radiological Exposure at Commercial Nuclear Power Reactors and Other Facilities”, NUREG-0713, Volume 32, 2010

[NRC 2015] US Nuclear Regulatory Commission, “Conventional Uranium Mills”, accessed at http://www.nrc.gov/materials/uranium-recovery/extraction-methods/conventional-mills.html, updated May 2015

[NRC 2017] US Nuclear Regulatory Commission, “Appendix A to Part 40 – Criteria Relating to the Operation of Uranium Mills and the Disposition of Tailings or Wastes Produced by the Extraction or Concentration of Source Material from Ores Processed Primarily for Their Source Material Content”, NRC Regulations 10 CFR, Updated January 2017

[NWTRB 1996] US Nuclear Waste Technical Review Board. “Disposal and Storage of Spent Nuclear Fuel – Finding the Right Balance”, Report to Congress and the Secretary of Energy, 1996

[NWTRB 2010] US Nuclear Waste Technical Review Board. “Evaluation of the Technical Basis for Extended Dry Storage and Transportation of Used Nuclear Fuel”, December 2010

[OECD-NEA 2006] Nuclear Energy Agency (Organisation for Economic Co-Operation and Development). “Advanced Nuclear Fuel Cycles and Radioactive Waste Management”, NEA Report No. 5990, 2006

[OECD-NEA 2011] Organization for Economic Co-Operation and Development: Nuclear Energy Agency and the International Atomic Energy Agency. “Uranium: Resources, Production and Demand (‘Red Book’)”, 2011

[OECD-NEA 2012a] Organization for Economic Co-Operation and Development: Nuclear Energy Agency. “Benchmark Study on Nuclear Fuel Cycle Transition Scenarios Analysis Codes”, Report NEA/NSC/WPFC/DOC(2012)16

[OECD-NEA 2012b] Organization for Economic Co-Operation and Development: Nuclear Energy Agency. “Transition Towards a Sustainable Nuclear Fuel Cycle:”, NEA Report No. 7133, 2012

[OECD-NEA 2014] Organization for Economic Co-Operation and Development: Nuclear Energy Agency and the International Atomic Energy Agency. “Uranium: Resources, Production and Demand (‘Red Book’)”, 2014

[Orlov 1980] Orlov, V. et al. “Problems of Fast Reactor Physics Related to Breeding”, Atomic Energy Review, Vol. 18, No. 4, pp. 989-1077, 1980

[ORNL 2011] Oak Ridge National Laboratory. “SCALE: A Comprehensive Modeling and Simulation Suite for Nuclear Safety Analysis and Design”, Report ORNL/TM-2005/39, Version 6.1, 2011

[Oshkanov 2004] Oshkanov, N., Bakanov, M., and Potapov, O. “Experience in Operating the BN-600 Unit at the Belyi Yar Nuclear Power Plant”, Vol. 96, Issue 5, pp. 315-319, 2004

[Owen 1992] Owen, A. “Byproduct Uranium”, Resources Policy, Vol. 18, Issue 2, pp. 137-147, 1992

[Paladin 2006] Paladin (Africa) Limited and Knight Piesold Consulting. Kayelekera Uranium Project Environmental Impact Assessment Report, Report 5032/40, 2006

[Paschoa 2003] Paschoa, A. “Environmental Effects of Nuclear Power Generation”, Encyclopedia of Life Support Systems, 2003

[Pennington 2009] Pennington, C. “Comparative Population Dose Risks from Nuclear Fuel Cycle Closure and Renewal of the Commercial Nuclear Energy Alternative in the U.S.”, Progress in Nuclear Energy, Vol. 51, pp. 290-296, 2009

[Piet 2013] Piet, S. “When Is the Simple Radiotoxicity Approach Useful for Advanced Fuel Cycle System Assessments Given the Existence of Complex Performance Dose Assessments?”, Nuclear Science and Engineering, Vol. 173, No. 1, pp. 58-81, 2013

[Powers 2013] Powers, J, Harrison, T., and Gehin, J. “A New Approach for Modeling and Analysis of Molten Salt Reactors in SCALE”, International Conference on Mathematics and Computational Methods Applied to Nuclear Science & Engineering (M&C 2013), Sun Valley, Idaho, USA, May 5-9, 2013

[Rainey 1962] Rainey, R. and Moore, J. “Laboratory Development of the Acid THOREX Process for Recovery of Consolidated Edison Thorium Reactor Fuel”, Oak Ridge National Laboratory Report ORNL-3155, 1962

[Ranek 2002] Ranek, N. “Regulation of New Depleted Uranium Uses”, Argonne National Laboratory Report ANL/EAD/TM/02-5, 2002

[Rayment 2012] Rayment, F. “The Future Role of Nuclear Fuel Cycle Technology in the UK”, European Nuclear Conference 2012, Manchester, UK, Dec. 9-12, 2012

[Richardson 1987] Richardson, K. “End-of-Life Destructive Examination of Light Water Breeder Reactor Fuel Rods”, Bettis Atomic Power Laboratory Report WAPD-TM-1606, 1987

[Roelofs 2011] Roelofs, Ferry, Jaap Hart, and Aliki Van Heek. "European new build and fuel cycles in the 21st century." Nuclear Engineering and Design 241.6 (2011): 2307-2317

[Roesener 1997] Roesener, H. and Schreuder, C. "Mineral Resources of Namibia: Uranium", Geological Survey of Namibia, 1997

[Rosenthal 1969] Rosenthal, M., Kasten, P., and Briggs, R. "Molten-Salt Reactors—History, Status, and Potential", Nuclear Technology, Vol. 8, Issue 2, pp. 107-117, 1969

[Rosenthal 1972] Rosenthal, M. "The Development Status of Molten Salt Breeder Reactors", Oak Ridge National Laboratory Report ORNL-4812, 1972

[Rotty 1975] Rotty, R., Perry, A., and Reister, D. "Net Energy from Nuclear Power", Institute for Energy Analysis, Report IEA-75-3, 1975

[Ryoji 1987] Ryoji, A, Harumi, O., Yoshinori, H., and Kenji, S. "Constructional Design Principles on Radiation Protection and Methods of Radiation Control at the Large Scale Plutonium Fuel Fabrication Facility of Fully Remote Operation", IRPA 7 Sydney, April 1988

[Saling 2001] Saling, J. "Radioactive Waste Management" (Second Edition), Boca Raton: CRC Press, 2001

[Sandia 2016] SANDIA NATIONAL LABORATORIES, "Sandia Connect – Nuclear Fuel Cycle Option Catalog", available at https://connect.sandia.gov/sites/NuclearFuelCycleOption Catalog/SitePages/a/homepage.aspx, Accessed January 2016, 2016

[Sato 2007] Sato, I. et al. "Analysis of ULOF Accident in Monju Reflecting the Knowledge from CABRI In-Pile Experiments and Others", Japan Atomic Energy Report JAEA-2007-055, 2007

[Savage 1977] Savage, H. and Hightower Jr., J. "Engineering Tests of the Metal Transfer Process for Extraction of Rare-Earth Fission Products from a Molten-Salt Breeder Reactor Fuel Salt", Oak Ridge National Laboratory Report ORNL-5176, 1977

[SCDHEC 2007] South Carolina Department of Health and Environmental Control. "Commercial Low-Level Radioactive Waste Disposal in South Carolina", SCDHEC Report CR-000907, 2007

[Schmidt 2011] Schmidt, R. et al. "Sodium Fast Reactor Gaps Analysis of Computer Codes and Models for Accident Analysis and Reactor Safety", Sandia National Laboratory Report SAND2011-4145, 2011

[Schneider 2009] Schneider, M. "Fast Breeder Reactors in France", Science and Global Security, Vol. 17, pp. 36–53, 2009

[Schneider 2014] Schneider, E. and Gill, G. "Characterization and Development Studies and Cost Analysis of Seawater Uranium Recovered by a Polymeric Adsorbent System", URAM-2014, IAEA, Vienna, Austria, June 26, 2014

[Schwarz 2002] Schwarz, J., Beloff, B., and Beaver, E. “Use Sustainability Metrics to Guide Decision-Making”, Chemical Engineering Progress, Vol. 98, No. 7, pp. 58-63, 2002

[Schweitzer 2008] Schweitzer, Tyler Martin. "Improved Building Methodology and Analysis of Delay Scenarios of Advanced Nuclear Fuel Cycles with the Verifiable Fuel Cycle Simulation Model (VISION)." (2008)

[Sease 1966] Sease, J., Pratt, R., and Lotts, A., “Remote Fabrication of Thorium Fuels”, Oak Ridge National Laboratory Report ORNL-TM-1501, 1966

[Seidel 1979] Seidel, D. “Extracting Uranium from its Ores”, IAEA Bulletin, Vol. 23, No. 2, 1979

[SELA 2016] Southeastern Louisiana University. “Measurement and Uncertainty Notes: Reporting Measurements and Experimental Results”, Educational Materials, Accessed August 2016 at https://www2.southeastern.edu/Academics/Faculty/rallain/plab194/error.html

[Shaffer 1971] Shaffer, J. “Preparation and Handling of Salt Mixtures for the Molten Salt Reactor Experiment”, Oak Ridge National Laboratory Report ORNL-4616, 1971

[Shelley 2001] Shelley, A., Akie, H., Takano, H., and Sekimoto, H. “Radiotoxicity Hazard of Inert Matrix Fuels after Burning Minor Actinides in Light Water Reactors”, Progress in Nuclear Energy, Vol. 38, Issue 3, pp. 439-442, 2001

[Shiotani 2011] H. Shiotani, K. Ono, and T. Namba, Characteristic Evaluation and Scenario Study on Fast Reactor Cycle in Japan. Nuclear Power - Deployment, Operation and Sustainability, 2011

[Shire 1977] Shire, P. “SPRAY Code User’s Report [LMFBR Sodium Pipe Leaks]. Hanford Engineering Development Laboratory Report HEDL-TME-76-94, 1977

[Shropshire 2009] Shropshire, D. et al. “Advanced Fuel Cycle Cost Basis”, Idaho National Laboratory Report INL/EXT-07-12107, 2009

[Shultis 2007] Shultis, J. and Faw, R. “Fundamentals of Nuclear Science and Engineering”, 2nd Edition, Boca Raton: CRC Press, 616 pg., 2007

[Smith 2014] Smith, B. “Evaluating Environmental, Health, and Safety Impacts from Two Nuclear Fuel Cycles: A Comparative Analysis of Once-Through Uranium Use and Plutonium Recycle in Light Water Reactors”, Vanderbilt University, Dissertation, 2014

[Sovacool 2011] Sovacool, B. et al. “Evaluating Energy Security Performance from 1990 to 2010 for Eighteen Countries”, Energy, Vol. 36, No. 10, pp. 5846-5853, 2011

[Stauff 2015] Stauff, N., Kim, T., and Taiwo, T. “Variations in Nuclear Waste Management Performance of Various Fuel-Cycle Options”, Journal of Nuclear Science and Technology, Vol. 52, Issue 7-8, pp. 1058-1073, 2015

[Stosic 2008] Stosic, Z., Brettschuh, W., and Stoll, U. “Boiling Water Reactor with Innovative Safety Concept: The Generation III+ SWR-1000”, Nuclear Engineering and Design, Vol. 238, pp. 1863-1901, 2008

[Suzuki 2008] Suzuki, N. and Shimazu, Y. “Reactivitiy-Initiated-Accident Analysis Without Scram of a Molten Salt Reactor”, Journal of Nuclear Science and Technology, Vol. 45, No. 6, pp. 575-581, 2008

[Suzuki 2010] Suzuki, T. “Japan’s Plutonium Breeder Reactor and its Fuel Cycle”, Chapter 4 of “Fast Breeder Reactor Programs: History and Status”, Report by International Panel on Fissile Materials, 2010

[Szekely 2005] Szekely, F. and Knirsch, M. “Responsible Leadership and Corporate Social Responsibility: Metrics for Sustainable Performance”, European Management Journal, Vol. 23, No. 6, pp. 628-647, 2005

[TAC 2016] The August Chronicle (Staff Reports). “House Authorizes Funding Bill for MOX Project”, December 2, 2016

[Tatikonda 2007] Tatikonda, M. “Product Development Performance Measurement”, Chapter of the Handbook of New Product Development by Tatikonda, M., 2007

[Taylor 2004] Taylor, G. et al. “Review of Environmental Impacts of the Acid In-Situ Leach Uranium Mining Process”, CSIRO Land and Water Client Report, 2004

[Taylor 2008] Taylor, J'Tia, David E. Shropshire, and Jacob J. Jacobson. A VISION of Advanced nuclear system cost uncertainty. No. INL/CON-07-13312. Idaho National Laboratory (INL), 2008

[Tennery 1978] Tennery, V. et al. “Environmental Assessment of Alternate FBR Fuels: Radiological Assessment of Airborne Releases from Thorium Mining and Milling”, Oak Ridge National Laboratory Report ORNL/TM-6474, 1978

[Tennery 1980] Tennery, V. et al. “Summary of the Radiological Assessment of the Fuel Cycle for a Thorium-Uranium Carbide-Fueled Fast Breeder Reactor”, Oak Ridge National Laboratory Report ORNL/TM-6953, 1980

[Tew 1968] Tew, H., Ambrose, T., and Mathis, W., “Engineering Specifications: Thorium Oxide Target Elements”, Advanced Process Engineering Unit Report RL-REA-2177, 1965

[Thomas 1981] Thomas, K. “Management of Wastes from Uranium Mines and Mills”, IAEA Bulletin, Vol. 23, No. 2, 1981

[Thompson 1980] Thompson, T., Lyttle, T., and Pierson, J. “Genesis of the Bokan Mountain, Alaska, Uranium-Thorium Deposit”, U.S. Department of Energy, Bendix Field Engineering Report GJBX-38, 1980

[Tobita 2006] Tobita, Y., et al. “The Development of SIMMER-III, An Advanced Computer Program for LMFR Safety Analysis, and its Application to Sodium Experiments”, Nuclear Technology, Vol. 153, No. 3, pp. 245-255, 2006

[Todosow 2004] Todosow, B., and Kazimi, M. “Optimization of Heterogeneous Utilization of Thorium in PWRs to Enhance Proliferation Resistance and Reduce Waste”, Brookhaven National Laboratory Report BNL-73152-2004, 2004

[Turney 2011] Turney, D. and Fthenakis, V. “Environmental Impacts from the Installation and Operation of Large-Scale Solar Power Plants”, Renewable and Sustainable Energy Reviews, Vol. 15, pp. 3261-3270, 2011

[Ullo 1980] Ullo, J., Hardy Jr., J., and Steen, N. “Review of Thorium-U233 Cycle Thermal Reactor Benchmark Studies (AWBA Development Program)”, Bettis Atomic Power Laboratory Report WAPD-TM-1456, 1980

[UNSCEAR 1993] United Nations Scientific Committee on the Effects of Atomic Radiation (UNSCEAR), “Sources and Effects of Ionizing Radiation: UNSCEAR 1993 Report to the General Assembly, with Scientific Annexes,’’ 1993

[Usami 2001] Usami, S., Suzuoki, Z., Deshimaru, T., and Nakashima, F. “Reaction Rate Distribution Measurement and the Core Performance in the Prototype FBR Monju”, International Conference on Nuclear Engineering, Nice, France, April 2001

[USGS 2013a] US Geological Survey. Titanium Data Sheet, 2013

[USGS 2013b] US Geological Survey. Tin Data Sheet, 2013

[Van Den Durpel 2003] Van Den Durpel, Luc, et al. "Dynamic Analysis of Nuclear Energy System Strategies for Electricity and Hydrogen Production in the USA." GLOBAL 2003 Meeting. 2003

[Van Den Durpel 2006] Van Den Durpel, L., Wade, D., et al. “DANESS: A System Dynamics Code for the Holistic Assessment of Nuclear Energy System Strategies”. *The 24th International Conference of the System Dynamics Society*, Nijmegen, The Netherlands, Argonne National Laboratory (ANL), 2006

[Van Gosen 2009] Van Gosen, B., Gillerman, V., and Armbrustmacher, T. “Thorium Deposits of the United States - Energy Resources for the Future?”, USGS, Circular 1336, 2009

[Van Gosen 2014] Van Gosen, B., Krahn, S., and Ault, T. “Thorium Recovery from Rare Earth Element Deposits in the U.S.”, Transactions of the American Nuclear Society, Vol. 111, Anaheim, California, November 9-13, 2014

[Vasilyev 2010] Vasilyev, B. A., Effectiveness Evaluation for the Fast Sodium-Cooled Reactor Design Solutions and Their Evolution in New Designs. 7th International Scientific and Technical Conference "Nuclear Power Safety, Effectiveness and Economy", MNTK-2010, 2010

[Vasilyev 2013] Vasilyev, B., Shepelev, S., Ashirmetov, M., and Poplavsky, V. "BN-1200 Reactor Power Unit Design Development", International Conference on Fast Reactors and Related Fuel Cycles: Safe Technologies and Sustainable Scenarios (FR13)", Paris, France, March 2013

[Vinayagam 2014] Vinayagam, P. and Chellapandi, P. "Sustainable Energy Security from Fast Breeder Reactors", 6th Nuclear Energy Conclave, New Delhi, India, October 2014

[Vijayalakshmi 2001] Vijayalakshmi, R. et al. "Processing of Xenotime Concentrate by Sulphuric Acid Digestion and Selective Thorium Precipitation for Separation of Rare Earths", Hydrometallurgy, Vol. 61, No. 2, pp. 75-80, 2001

[USGS 2013] US Geological Survey. "Thorium Data Sheet", 2013

[Waber 1992] Waber, N. "The Supergene Thorium and Rare-Earth Deposit at Morro do Ferro, Pocos de Caldas, Minas Gerais, Brazil", Vol. 45, No. 1-3, pp. 113-157, 1992

[Wang 2013] Wang, L. et al. "Toward Greener Comprehensive Utilization of Bastnaesite: Simultaneous Recovery of Cerium, Fluorine, and Thorium from Bastnaesite Leach Liquor Using HEH (EHP)", Chemical Engineering Journal, Vol. 215, pp. 162-167, 2013

[Warner 1989] Warner, J. "Columbium-, Rare-Earth Element-, and Thorium-Bearing Veins near Salmon Bay, Southeastern Alaska", US Department of the Interior, Bureau of Mines, 1989

[Watson 2014] Watson, I., Van Straaten, P., Katz, T., and Botha, L. "Mining and Concentration: What Mining to What Costs and Benefits?" Chapter of Book *Sustainable Phosphorus Management* by Scholz, R. et al, 2014

[Westinghouse 2009] Westinghouse Electric Company LLC. "AP1000 Pre-Construction Safety Report", UKP-GW-GL-732, 2009

[Wigeland 2014] Wigeland, R. et al. "Nuclear Fuel Cycle Evaluation and Screening – Final Report", Report No. INL/EXT-14-31465, 2014

[Wilson 1994] Wilson, M. et al. "Total-System Performance Assessment for Yucca Mountain – SNL Second Iteration (TSPA-1993): Executive Summary", Sandia National Laboratory Report SAND93-2675, 1994

[Wilson 2014] Wilson, P. and Scopatz, A. "Cyclus: The Next Generation Fuel Cycle Simulator", FCO Quarterly Meeting 2014 Q4. Dec. 16th, 2014

[Wittenberg 2006] Wittenberg, A. et al. “μ-EDXRF Tracing of Uranium Redistribution in Volcanic Rocks”, Geochimica et Cosmochimica Acta, Vol. 70, Issue 18, 2006

[WNA 2009] World Nuclear Association. “In Situ Leach (ISL) Mining of Uranium”, http://www.world-nuclear.org/info/inf27.html, Updated 2009

[WNA 2013] World Nuclear Association. “World Nuclear Power Reactors and Uranium Requirements”, http://world-nuclear.org/info/reactors.html, 2012, Accessed Oct. 2013, 2013

[WNA 2015a] World Nuclear Association. “The Nuclear Fuel Report: Global Scenarios for Demand and Supply Availability 2015-2035”, 2015

[Worrall 2007] Worrall, Andrew, and Robert Gregg. "Scenario Analyses of Future UK Fuel Cycle Options." Journal of nuclear science and technology 44.3 (2007): 249-256

[Wu 2010] Wu Q. “The Use and Management of NORM Residues in Processing Bayan Obo Ores in China”, Presented at 6th International Symposium on Naturally Occurring Radioactive Material, 2010

[Wymer 2012] Wymer, R., Krahn, S., and Ault, T. “The Thorium Fuel Cycle: Challenges and Opportunities”, Presentation for the Thorium Experts Meeting, Colorado School of Mines, December 12, 2012

[Yacout 2004] Yacout, A. M., et al. "Dynamic analysis of the AFCI scenarios." PHYSOR 2004 (2004): 25-29.

[Yacout 2006] Yacout, A. M., et al. "VISION–verifiable fuel cycle simulation of nuclear fuel cycle dynamics." Waste Management (2006)

[Zhang 2009] Zhang, D., Qiu, S., and Su, G. “Development of a Safety Analysis Code for Molten Salt Reactors”, Nuclear Engineering and Design, Vol. 239, No. 12, pp. 2778-2785, 2009

[Zhang 2012] Zhang, Q., Ishihara, R., McClellan, B., and Tezuka, T. “Scenario Analysis on Future Electricity Supply and Demand in Japan”, Energy, Vol. 38, pp. 376-385, 2012

APPENDIX A, BACKGROUND ON EXPERIENCE, DESIGN, AND OPERATION OF THORIUM-BASED MOLTEN SALT REACTORS

The MSR concept with the most extensive amount of experience of study is the liquid-fueled, fluoride-salt-cooled configuration. There are variations within this concept, at the highest level distinguishing between those that use a "one-fluid" design (all fertile and fissile material are contained in a single stream) and a "two-fluid" design (fertile material is not allowed to physically contact fissile material, although heat transfer and neutron transfer occurs between the two streams).

The work by ORNL and collaborating organizations prior to the end of the Molten Salt Breeder Reactor (MSBR) project accounts for somewhere around two-thirds of the total thorium-fuel-cycle-related MSR reports and publications collected to-date. The earliest phases of the project primarily focused on systems which fission uranium-235, with studies on U-233 being limited to "a few calculations" [MacPherson 1958a]. More detailed studies in the earliest years were limited by a poor understanding of thorium cross-sections data and the corrosive properties of salts with high thorium concentrations [MacPherson 1958a]. Studies in this phase were limited to two-fluid designs. The emphasis on thorium increased when improved calculations determined that uranium-233 had the potential to reduce the total fissile requirement by about a factor of 2 [MacPherson 1958b]. Chemical experiments with thorium in unirradiated salt test-loops also expanded at this time, examining different species and concentrations of lithium, beryllium, sodium, potassium, and zirconium fluorides with thorium and uranium [MacPherson 1958b]. Ultimately, ORNL's improvements in ORNL's computational abilities enabled a detailed comparison of U-233 and U-235 two-fluid systems with thorium fluoride concentrations ranging

from 0 to 1 mole percent [MacPherson 1958c], as well as between the MSR concept on the whole against solid-fueled breeders [Alexander 1959]. The comparisons did not conclude an absolute "favorite" but at least confirmed that thorium-based MSRs were worth extended study. Subsequent efforts aimed to optimize core sizes and thorium fluoride concentrations [MacPherson 1959a]. The findings of the first year or so of the project were tabulated to focus future efforts [MacPherson 1958d].

As the optimized high-level design parameters were determined, more detailed work was carried out regarding reactor safety and component testing. By this time, the reference two-fluid design used 1 mole % thorium fluoride in the blanket salt and 13 mole % thorium fluoride in the fuel (core) salt [MacPherson 1959b]. In parallel, work was initiated on the feasibility of a one-fluid system with thorium fluoride mole percentages ranging from 7 to 13. Ultimately, the single-fluid design was selected for development of a 30-Mw experimental reactor (the power rating would later be scaled back) [MacPherson 1959c]. The selection was primarily due to the shorter timescales on which a single-fluid design could be assembled; the two-fluid design continued to be the subject of extensive characterization, as illustrated in Figure A-1. Around 1960, the MSR project changed hands within ORNL leadership. A summary report of the work-to-date at this time identified a preferred design: a two-fluid system with 15% of the core volume being fuel salt and 5% being blanket salt, with a net breeding ratio of about 1.06 [MacPherson 1960d]. Many of these early perspectives were catalogued at a summary-level in a review of various reactor concepts by Argonne National Laboratory (ANL). This summary included a succinct qualitative comparison of the pros-and-cons of the one-fluid vs. the two-fluid design: the one-fluid design is cheaper to assemble and may be suitable for small burners, while the two-fluid

design was viewed as having a better neutron economy (and by extension, superior breeding capabilities) and thus lower fuel-cycle costs [Teeter 1965].

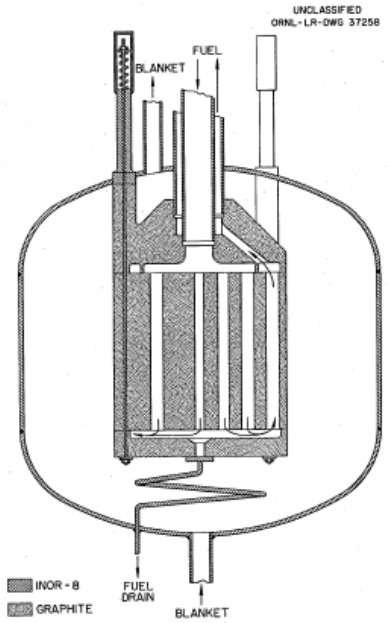

Figure A-1, Graphite-Moderated Two-Region Molten-Salt Thorium Breeder [MacPherson 1959d]

As designs continued to become more detailed, the challenges associated with water and oxygen exclusion were recognized as being more important than previously thought. The magnitude of undesirable oxide or oxyfluoride formation was characterized in focused studies on molten-salt phase equilibria [Weaver 1960]. The phase behavior of this system continued to challenge researchers throughout the 1960s (e.g., [Smith 1969, Thoma 1969]), and while "no fundamental chemical difficulty with design and operation" of MSRs was observed, plate-out and subsequent purge gas release of noble metals and noble gas permeation of graphite moderators remained notable problems [Grimes 1969]. Studies on the degradation of the moderator, primarily due to xenon, were estimated to limit the lifetime of the moderator to about four years before requiring

full replacement [Scott 1970]. With frequent (every two years) replacement of the graphite, xenon poisoning could be mitigated by using pyrolytic carbon as a pore impregnant. With these modifications, development of a moderator for a scaled-up MSBR was deemed to be feasible [Kasten 1969].

ORNL initially continued to lead two-fluid MSR efforts in the 1960s. The two-fluid design was determined to be capable of fuel yields of 7%/year, although the fuel cycle cost increased with increasing fuel yields [Carter 1961]. The two-fluid study also included a sensitivity analysis of reactor performance with respect to key nuclear parameters; a 10% variation in the neutron yield (η) of U-233 and a 33% variation in the resonance integral of Pa-233 resulted in fuel yield impacts of 2.5-3% and 0.25%, respectively [Carter 1961]. While developments on the two-fluid system were de-emphasized as MSRE-related (one-fluid) work gained traction, a design study was performed for a 1000-MWe two-fluid design called the Molten Salt Breeder Reactor[39] [Kasten 1966a, Kasten 1966b]. Some of the key parameters of this design are described in Table 1. One report proposed that this design called for the construction of a two-region "Molten-Salt Breeder Experiment" (MSBE) to follow operation of the one-fluid Molten Salt Reactor Experiment [Briggs 1967b], but the MSBE test reactor was not realized. This campaign was the last major effort to ORNL to explore true two-fluid MSR systems. While some progress was made in overcoming some of the challenges associated with two-fluid systems, such as adapting the graphite moderator to utilize a liquid-liquid seal which would allow tubes to expand or contract freely during temperature variations [Alexander 1965], the cost barriers were still viewed as prohibitively high. In 1968, the concept of a one-fluid, two-region gained traction as

[39] The label "MSBR" is used by ORNL (rather confusingly) to describe either one-fluid or two-fluid systems at various points during the project's lifetime.

having much of the breeding benefits of a true two-fluid system without the additional challenges, and the two-fluid design was specifically de-emphasized [Rosenthal 1968]. Select design parameters are shown in Table A-1 below.

Table A-1, Design Parameters for the Early Two-Fluid 1000 MWe-MSBR [Kasten 1966a]

Fuel Salt	$LiF\text{-}BeF_2\text{-}^{233}UF_4$
Blanket Salt	$LiF\text{-}BeF_2\text{-}ThF_4$
Fuel Salt Flow Rate	44,000 gallons per minute
Fuel Salt Temperatures	1000 ^oF inlet, 1300 ^oF outlet
Blanket Salt Temperatures	1150 ^oF inlet, 1250 ^oF outlet
Reactor Vessel Size	14 ft. diameter, 19 ft. high
Core Size	10 ft. diameter, 12.5 ft. high
Core Composition (by volume)	75% graphite, 18% fuel salt, 7% blanket salt

The efforts for one-fluid designs in the 1960s centered on the Molten Salt Reactor Experiment (MSRE) and subsequent plans for scale-up. Much of the MSRE work in the first few years of the 1960s was not especially focused on thorium as ORNL prepared for the first fissile loading with uranium-235 salts. However, this period continued to make progress on topics such as materials durability and component design which were useful for all future iterations of MSRs [Briggs 1961a, Briggs 1961b, Briggs 1962a, Briggs 1962b, Briggs 1963a, Briggs 1963b, Briggs 1964a, Briggs 1964b, Briggs 1965a, Briggs 1965b, Briggs 1966]. Eventually, ORNL began to prepare for futures in which the MSRE might incorporate small amounts (1%) of thorium [Briggs 1962b, Robertson 1965]. A fuel with 1% thorium and 93% highly-enriched uranium was reviewed as one of three candidate fuels (the other two being thorium-free) in a preliminary nuclear analysis leading up to MSRE operation [Haubenreich 1964]. However, effective breeding of fissile material in a thorium-based system was viewed as somewhat of a challenge. The exact optimal balance of fissile and fertile material in the reactor continuously changed as the quality of the

physics data regarding thorium, protactinium, and uranium-233 improved, so it was difficult to make conclusive arguments about the viability of thorium-breeding in MSREs. In general, a U-233 phase of operation for the MSRE, following that of U-235 operation, was highly recommended [Briggs 1964b, Guymon 1966].

While the MSRE was initially driven by U-235, it was eventually fueled with LiF-UF_4 with uranium that was 91.4% U-233. The preferred preparation methodology was a two-step process in which uranium oxide was reduced to UO_2 with hydrogen gas and then converted to UF4 by hydrofluorination [Chandler 1969]. Sixty-three kilograms of U-233 was made into fuel that was prepared in a shielded-cell environmental at ORNL's Thorium-Uranium Recycle Facility [Chandler 1970]. In actuality, the critical loading of the core required about 40 kg of U-233, compared to about 70 kg of U-235 that was used in the earlier loadings of the core [Rosenthal 1967b]. Prior to loading, the fabricated LiF-UF_4 salt was tested for fluid properties such as solubility [Rosenthal 1969a]. In late 1968, the MSRE became the world's first reactor to operate with loaded uranium-233 (not counting reactors which had produced their own U-233 from thorium) [Haubenreich 1970a]. One interesting observation, even before reaching criticality, was that the presence of uranium-233 (as well as U-232 and U-234 impurities) in lithium-bearing salts created a non-trivial neutron source due to intense alpha irradiation leading to alpha-neutron reactions in the lithium [Steffy 1969b].

The earliest portions of the uranium-233 operation phase entailed zero-power tests, including criticality, control rod calibration, temperature coefficient of reactivity tests, and concentration coefficient of reactivity tests [Rosenthal 1969b, Engel 1972]. As the power was allowed increase

up to about 7-8 MW, long-term isotopic changes and reactivity effects were monitored [Rosenthal 1969b, Steffy 1970]. Fuel quality during dynamic operation was also monitored [Steffy 1969a]. Physics data was also collected, most importantly the ratio of the neutron capture cross section to the absorption cross section of U-233 at a high-fidelity [Rosenthal 1970a]. Operating a reactor with such a high concentration of U-233 enabled collection of reactivity-to-power response measurements for U-233 for a number of operational points and test procedures [Kerlin 1971]. At the culmination of the MSRE's operation, the program was viewed as a moderate success and described the potential advantages of a scaled-up system as high thermal efficiency, low primary system pressure, and potentially favorable economic, fuel utilization, and safety characteristics [Rosenthal 1970c].

A review of the uranium-233 phase of operation determined that U-233 did not compromise the MSRE's reliability, and loading procedures did not pose an excessive challenge [Guymon 1973]. On the whole, observed fission product during the U-233 operational period was similar to what was observed for U-235, in spite of slight variations in the abundances of particular fission product species [Houtzeel 1972, Compere 1975]. One possible exception was the behavior of xenon; the U-233 phase of operation observed a void fraction about ten times larger than that of the U-235 phase of operation [Engel 1971]. This may have been due in part to the different physical properties of the salt used in this phase, but the fission-product-yield differences probably played at least some role. In any case, the overall impact on reactor operation as a result was minimal [Engel 1971]. Noble metal behavior was slightly different than the U-233 run than the U-235 run, but this was later determined to be due to factors other than the difference in fissile material [Kedl 1972, McCoy 1972].

After the MSREs operation, ORNL and associated contractors developed a scaled-up one-fluid design called the Molten Salt Breeder Reactor (MSBR)[40], which was intended to operate at 1000 MWe with an estimated fuel yield of 3.3% per year [Bettis 1970, Ebasco 1972, AEC 1972]. Extended neutronic analyses confirmed a breeding ratio of about 1.06[41], a specific fissile inventory of 1.5 kg/MWe, a fuel doubling time of about 20 years, and relatively competitive fuel cycle costs, with start-up schemes envisioned for either enriched uranium or plutonium [Perry 1969]. The MSBR project eventually called for a demonstration-scale 150 MWt reactor with a primary salt containing both thorium and U-233 [McWherter 1970, Bettis 1972], as visualized in Figures A-2 and A-3.

[40] The label "MSBR" is used by ORNL (rather confusingly) to describe either one-fluid or two-fluid systems at various points during the project's lifetime.

[41] Uncertainties in physics data at this time suggested a breeding ratio uncertainty of about +/- 0.026 [Perry1967]. It should be noted that specific estimates of the MSBR's breeding ratio were revised from 1.054 to 1.062 during this period [Carlsmith 1967].

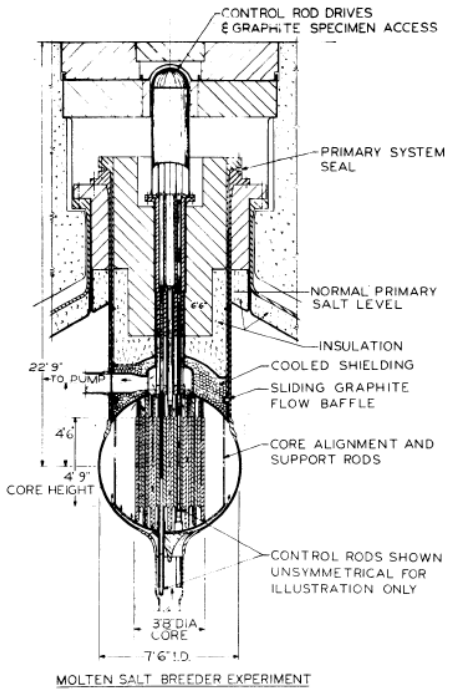

Figure A-2, Molten Salt Breeder Reactor Experiment (150 MWt) Reactor Core Assay [McWherter 1970]

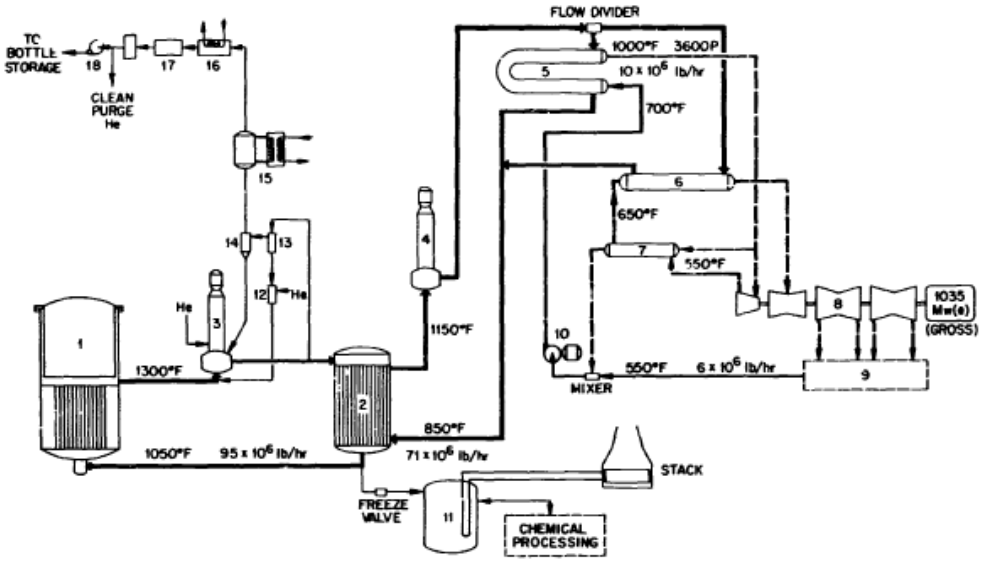

Figure A-3, Simplified Flow Diagram of MSBR System [Robertson 1971]

As the MSBR design evolved, it was fixed with an optimal equilibrium composition of 71.7% LiF, 16.0% BeF_2, 12.0% ThF_4, and 0.3 % UF_4 (molar), an salt inlet temperature of 839 K, and an

outlet temperature of 978 K [Robertson 1971]. A NaBF4-NaF eutectic mixture would be used as the secondary coolant salt [Kelmers 1976]. In the early part of the 1970s, the MSBR campaign continued to refine its understanding of reactor physics optimization, components development, instrumentation, reactor chemistry, and heat/mass transfer [Rosenthal 1971a, Rosenthal 1971b, Rosenthal 1972a, Rosenthal 1972b, Rosenthal 1972c, Rosenthal 1973, McNeese 1974, McNeese 1975a, McNeese 1975b, McNeese 1976a, McNeese 1976b]. Refinement of physics calculations for the MSBR was facilitated by the development of a fuel-cycle analysis code called Reactor Optimum Design (ROD), which was specifically designed for circulating-fuel reactors [Bauman 1971].

Certain reactor safety characteristics are influenced by the concentration of thorium, uranium-233, or the balance of the two. In an analysis of filling-induced criticality accidents, it was determined that using larger amounts of thorium greatly reduces the severity of filing accidents due to poisoning effects [Engel 1966]. The same conclusion was also true about uranium-238, but in general, molten-salt configurations with a significant fertile concentration were more resistant to filling criticality incidents [Beall 1964]. Eventually, a detailed eight-year safety program for MSBRs was outlined in 1967 which would consider all reactor components and safety aspects [Kasten 1967]. An early component of this effort specifically examined the hazards posed by uranium-233. Uranium-233 was not expected to change the structural or monitoring requirements relative to U-235, but due to uranium-233's relatively small critical mass, special precautions were addressed during handling and loading [Haubenreich 1968]. Chemical safety aspects were also noted. After operation, fluoride salts were found to produce

diatomic fluorine gas as a result of radiolysis if allowed to cool below about 80°C. Keeping the canisters heated largely eliminated these effects [Haubenreich 1970b].

The completion of the irradiation of uranium-233 fuel salt in the MSRE enabled experience with the processing of the fuel and flush salts for fuel recovery. The reprocessing of such fuel was comparatively straightforward since no thorium or protactinium was present. Processing losses were less than 0.1% [Lindauer 1969]. The MSRE salt also enabled ORNL to conduct an assay to assess impurity accumulation and effects [Thoma 1971].

The MSBR campaign of the 1970s entailed a specific reactor processing component, the efforts of which were catalogued in a series of programmatic update reports [McNeese 1971a, McNeese 1971b, McNeese 1971c, McNeese 1971d, McNeese 1971e, McNeese 1972a, McNeese 1972b, McNeese 1972c, Hightower 1975b, Hightower 1975c, Hightower 1976a, Hightower 1976b]. During this period, many of the processing concepts and techniques initiated in the 1960s were advanced and refined, leading to the creation of a new comprehensive flowsheet for the single-fluid MSBR. The overall processing system relied on fluorination and bismuth-lithium extraction. This flowsheet is visualized in Figure A-4. The overall cost of such a processing facility was deemed to be manageable, although there were admittedly many uncertainties in the estimates [Carter 1972].

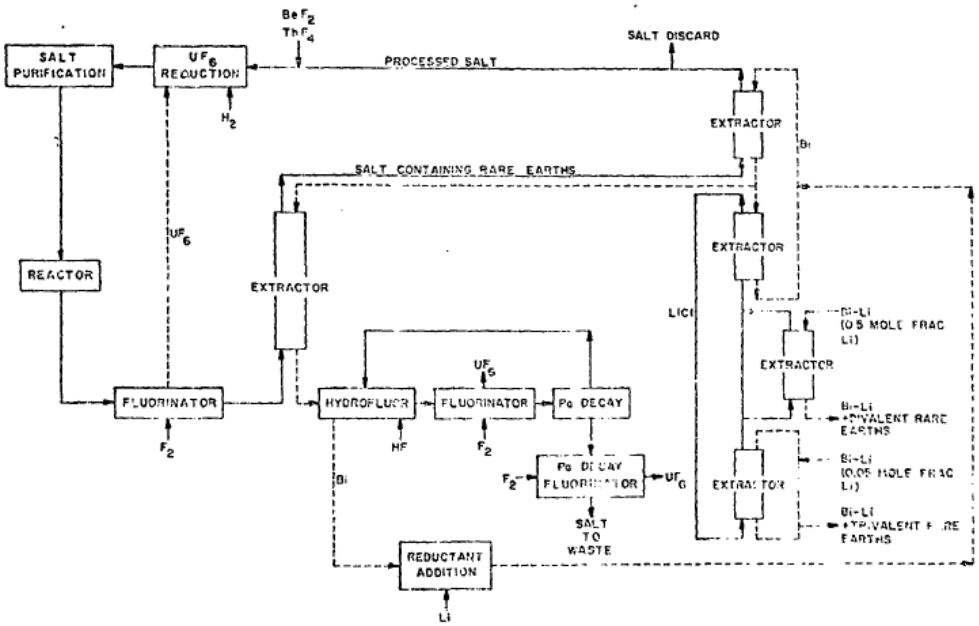

Figure A-4, Flowsheet for Processing Single-Fluid MSBR by Fluorination-Reductive Extraction and the Metal-Transfer Process [Hightower 1975a]

While demonstrated to be chemically effective, some of these approaches were later criticized for their proliferation risks (e.g., relatively pure U-233 streams). Near the end of the MSBR era, some effort was taken to adapt these approaches to be more proliferation-resistant [Bauman 1977]. However, these measures were only examined at the precursory-study level. It was also argued that the use of a thorium/uranium-233 fuel cycle in an MSR was inherently a non-proliferation choice since it circumvented the production separation of plutonium [Engel 1978, Engel 1979]. Implementing MSRs without reprocessing further reduced the risk of proliferation, although admittedly at the expense of other capabilities of the fuel cycle [Engel 1980].

Some systems studies have referred to data collected in the MSBR period in the hopes of applying the technology to new problems. For instance, MSRs were proposed as an effective way of utilizing the fissile material from dismantled weapons [Gat 1991]. Other possible

missions for MSRs include actinide burning and/or fissile fuel production, which can be accomplished in both the thermal and the fast spectrum (see following section for details on fast-spectrum MSRs) [Forsberg 2007b]. A design for the specific purpose of TRU elimination that can incorporate either uranium or thorium fuel cycles has been developed in Russia [Ignatiev 2011]. The process heat available from high-temperature operation of MSRs may also be appealing (see discussion under "Solid-Fueled, Salt-Cooled Reactors"). A number of studies have re-iterated the attributes and potential benefits and challenges associated with implemented of liquid-fueled MSRs with thorium on the whole [Moir 2002, Nuttin 2004, Moir 2005, Mathieu 2006, Juhasz 2009, Hargraves 2010, Kamei 2012, Sajo-Bohus 2012, Durham 2013, Madden 2013, Turner 2013, Uhlir 2013]. Furthermore, individual MSR designs have received some updated examinations and physics analyses in the US as part of the Fuel Cycle Option Evaluation & Screening effort. These studies identified full and partial recycle MSRs to be viable in both the thermal and fast spectra, while once-through systems required an external neutron source [Powers 2013, Gehin 2014].

List of MSR References

[AEC 1972] US Atomic Energy Commission Division of Reactor Development and Technology. "An Evaluation of the Molten Salt Breeder Reactor", Report WASH-1222, 1972
[Alexander 1959] Alexander, L., Carrison, D., MacPherson, H., and Roberts, J. "Nuclear Characteristics of Spherical Homogeneous, Two-Region, Molten-Fluoride-Salt Reactors", Oak Ridge National Laboratory Report ORNL-2751, 1959
[Alexander 1963] Alexander, L. "Molten-Salt Fast Reactors", Proc. Conf. Breeding, Economics and Safety in Large Fast Power Reactors, October 7-10, 1963, Argonne National Laboratory Report ANL-6792, 1963
[Alexander 1965] Alexander, L. et al. "Molten-Salt Converter Reactor: Design Study and Power Cost Estimates for a 1000-MWe Station", Oak Ridge National Laboratory Report ORNL-TM-1060, 1965
[Barton 1966] Barton, C. and Stone, H. "Removal of Protactinium from Molten Fluoride Breeder Blanket Mixtures", Oak Ridge National Laboratory Report ORNL-TM-1543, 1966

[Barton 1967] Barton, C. and Stone, H. “Reduction of Iron Dissolved in Molten LiF-ThF4”, Oak Ridge National Laboratory Report ORNL-TM-2036, 1967
[Bauman 1971] Bauman, H. et al. “ROD: A Nuclear and Fuel-Cycle Analysis Code for Circulating-Fuel Reactors”, Oak Ridge National Laboratory Report ORNL-TM-3359, 1971
[Bauman 1977] Bauman, H. et al. “Molten-Salt Reactor Concepts with Reduced Potential for Proliferation of Special Nuclear Materials”, Oak Ridge National Laboratory Report ORNL-IEA-77-13, 1977
[Beall 1964] Beall, S., Haubenreich, P., Lindauer, B., and Tallackson, J. “MSRE Design and Operations Report Part V, Reactor Safety Analysis Report”, Oak Ridge National Laboratory Report ORNL-TM-732, 1964
[Bell 1970] Bell, M. “Calculated Radioactivity of MSRE Fuel Salt”, Oak Ridge National Laboratory Report ORNL-TM-2970, 1970
[Bettis 1970] Bettis, E. and Robertson, R. “The Design and Performance Features of a Single-Fluid Molten-Salt Breeder Reactor”, *Nuclear Applications & Technology*, Vol. 8, 1970
[Bettis 1972] Bettis, E., Alexander, L., and Watts, H. “Design Studies of a Molten-Salt Reactor Demonstration Facility”, Oak Ridge National Laboratory Report ORNL-TM-3832, 1972
[Briggs 1961a] Briggs, R. “Molten-Salt Reactor Program Progress Report for Period from August 1, 1960 to February 28, 1961”, Oak Ridge National Laboratory Report ORNL-3122, 1961
[Briggs 1961b] Briggs, R. “Molten-Salt Reactor Program Progress Report for Period from March 1, 1961 to August 31, 1961”, Oak Ridge National Laboratory Report ORNL-3215, 1961
[Briggs 1962a] Briggs, R. “Molten-Salt Reactor Program Semiannual Progress Report for Period Ending February 28, 1962”, Oak Ridge National Laboratory Report ORNL-3282, 1962
[Briggs 1962b] Briggs, R. “Molten-Salt Reactor Program Semiannual Progress Report for Period Ending August 31, 1962”, Oak Ridge National Laboratory Report ORNL-3369, 1962
[Briggs 1963a] Briggs, R. “Molten-Salt Reactor Program Semiannual Progress Report for Period Ending January 31, 1963”, Oak Ridge National Laboratory Report ORNL-3419, 1963
[Briggs 1963b] Briggs, R. “Molten-Salt Reactor Program Semiannual Progress Report for Period Ending July 31, 1963”, Oak Ridge National Laboratory Report ORNL-3529, 1963
[Briggs 1964a] Briggs, R. “Molten-Salt Reactor Program Semiannual Progress Report for Period Ending January 31, 1964”, Oak Ridge National Laboratory Report ORNL-3626, 1964
[Briggs 1964b] Briggs, R. “Molten-Salt Reactor Program Semiannual Progress Report for Period Ending July 31, 1964”, Oak Ridge National Laboratory Report ORNL-3708, 1964
[Briggs 1965a] Briggs, R. “Molten-Salt Reactor Program Semiannual Progress Report for Period Ending February 28, 1965”, Oak Ridge National Laboratory Report ORNL-3812, 1965
[Briggs 1965b] Briggs, R. “Molten-Salt Reactor Program Semiannual Progress Report for Period Ending August 31, 1965”, Oak Ridge National Laboratory Report ORNL-3872, 1965
[Briggs 1966] Briggs, R. “Molten-Salt Reactor Program Semiannual Progress Report for Period Ending February 28, 1966”, Oak Ridge National Laboratory Report ORNL-3936, 1966
[Briggs 1967a] Briggs, R. “Molten-Salt Reactor Program Semiannual Progress Report for Period Ending August 31, 1966”, Oak Ridge National Laboratory Report ORNL-4037, 1967
[Briggs 1967b] Briggs, R. “Summary of the Objectives, the Design, and a Program of Development of Molten-Salt Breeder Reactors”, Oak Ridge National Laboratory Report ORNL-TM-1851, 1967
[Campbell 1959] Campbell, D. and Cathers, G. “Processing of Molten Salt Power Reactor Fuel”, Oak Ridge National Laboratory Report CF-59-2-61

[Cardwell 1971] Cardwell, D. and Haubenreich, P. “Indexed Abstracts of Selected References of Molten-Salt Reactor Technology”, Oak Ridge National Laboratory Report ORNL-TM-3595, 1971
[Carlsmith 1967] Carlsmith, R. et al. “Review of Molten Salt Reactor Physics Calculations”, Oak Ridge National Laboratory Report ORNL-TM-1946, 1967
[Carter 1961] Carter, W. and Alexander, L. “Thorium Breeder Reactor Evaluation. Part I: Fuel Yields ad Fuel Cycle Costs of a Two-Region, Molten-Salt Breeder Reactor”, Oak Ridge National Laboratory Report CF-61-8-86, 1961
[Carter 1962] Carter, W., Milford, R., and Stockdale, W. “Design Studies and Cost Estimates of Two Fluoride Volatility Plants”, Oak Ridge National Laboratory Report ORNL-TM-522, 1962
[Carter 1967] Carter, W. and Whatley, M. “Fuel and Blanket Processing Development for Molten Salt Breeder Reactors”, Oak Ridge National Laboratory Report ORNL-TM-1852, 1967
[Carter 1972] Carter, W. and Nicholson, E. “Design and Cost Study of a Fluorination-Reductive Extraction-Metal Transfer Processing Plant for the MSBR”, Oak Ridge National Laboratory Report ORNL-TM-3579, 1972
[Chandler 1969] Chandler, J. and Bolt, S. “Preparation of Enriching Salt 7LiF-233UF4 for Refueling the Molten Salt Reactor”, Oak Ridge National Laboratory Report ORNL-4371, 1969
[Chandler 1970] Chandler, J. and Bolt, S. “Uranium-233-Bearing Salt Preparation for the Molten Salt Reactor Experiment”, *Nuclear Applications & Technology*, Vol. 9, 1970
[Compere 1975] Compere, E. et al. “Fission Product Behavior in the Molten Salt Reactor Experiment”, Oak Ridge National Laboratory Report ORNL-4865
[Delpech 2008] Delpech, S. et al. “Reactor Physic and Reprocessing Scheme for Innovative Molten Salt Reactor System”, *Journal of Fluorine Chemistry*, 2008
[DeVan 1969] DeVan, J. “Effect of Alloying Additions on Corrosion Behavior of Nickel-Molybdenum Alloys in Fused Fluoride Mixtures (Thesis)”, Oak Ridge National Laboratory Report ORNL-TM-2021, Vol. 1, 1969
[DiStefano 1972] DiStefano, J. et al. “Development and Construction of a Molybdenum Test Stand”, Oak Ridge National Laboratory Report ORNL-4874, 1972
[Durham 2013] Durham, J. “The Road to Enablement for Thorium-fueled Molten Salt Reactors", International Conference on Thorium Fuel: Thorium Energy Conference 2013, Geneva, Switzerland, October 28-31, 2013
[Ebasco 1972] Ebasco Services, Inc. “1000 MW€ Molten Salt Breeder Reactor Conceptual Design Study: Final Report – Task I”, Report TID-26156, 1972
[Engel 1966] Engel, J., Haubenreich, P., and Ball, S. “Analysis of Filling Accidents in MSRE”, Oak Ridge National Laboratory Report ORNL-TM-497, 1966
[Engel 1971] Engel, J. and Steffy, R. “Xenon Behavior in the Molten Salt Reactor Experiment”, Oak Ridge National Laboratory Report ORNL-TM-3464, 1971
[Engel 1972] Engel, J. and Prince, B. “Zero-Power Experiments with 233U in the MSRE”, Oak Ridge National Laboratory Report ORNL-TM-3963, 1972
[Engel 1978] Engel, J. et al. “Molten-Salt Reactors for Efficient Nuclear Fuel Utilization without Plutonium Separation”, Oak Ridge National Laboratory Report ORNL-TM-6413, 1978
[Engel 1979] Engel, J. et al. “Development Status and Potential Program for Development of Proliferation-Resistant Molten-Salt Reactors”, Oak Ridge National Laboratory Report ORNL-TM-6415, 1979

[Engel 1980] Engel, J. et al. “Conceptual Design Characteristics of a Denatured Molten-Salt Reactor with Once-Through Fueling”, Oak Ridge National Laboratory Report ORNL-TM-7207, 1980
[Ferris 1969] Ferris, L. “Some Aspects of the Thermodynamics of the Extraction of Uranium, Thorium, and Rare Earths from Molten LiF-BeF2 into Liquid Li-Bi Solutions”, Oak Ridge National Laboratory Report ORNL-TM-2486, 1969
[Ferris 1972] Ferris, L. “Estimated Behavior of Titanium in MSBR Chemical Processing Systems”, Oak Ridge National Laboratory Report ORNL-TM-3763, 1972
[Fiorina 2013] Fiorina, C. “The Molten Salt Fast Reactor as a Fast-Spectrum Candidate for Thorium Implementation”, Politecnico di Milano Doctoral Dissertation, 2013
[Forsberg 2004] Forsberg, C. “Reactors with Molten Salts: Options and Missions”, 2004 Frederic Joliot and Otto Hahn Summer School, Cadarache, France, August 25-September 3, 2004
[Forsberg 2007a] Forsberg, C. et al. “Liquid Salt Applications and Molten Salt Reactors”, Proceedings of ICAPP 2007, Nice, France, May 13-18, 2007
[Forsberg 2007b] Forsberg, C. “Thermal- and Fast-Spectrum Molten Salt Reactors for Actinide Burning and Fuel Production”, Global 2007: Advanced Nuclear Fuel Cycles and System, Boise, ID, USA, September 9-13, 2007
[Forsberg 2015a] Forsberg, C., Peterson, P., Hu, L., and Sridharan, K. “Baseload Nuclear with Variable Electricity to the Grid”, *Nuclear News*, March 2015 Issue, pp. 77-81, 2015
[Forsberg 2015b] Forsberg, C. “Achieving Salt-Cooled Reactor Goals: Economics, Variable Electricity, No Major Fuel Failures”, ICAPP 2015, Nice, France, May 3-6, 2015
[Forsberg 2015c] Forsberg, C. “Fluoride Salt-Cooled High-Temperature Reactors (FHR): Competing with Stand-Alone Natural Gas and Enabling Zero-Carbon Electricity Grid”, Massachusetts Institute of Technology, 2015
[Fredricksen 1969] Fredricksen, J., Gilpatrick, L., and Barton, C. “Solubility of Cerium Trifluoride in Molten Mixtures of LiF, BeF2, and ThF4”, Oak Ridge National Laboratory Report ORNL-TM-2335, 1969
[Furukawa 1990a] Furukawa, K., Kato, Y., Mitachi, K., and Lecocq, A. “Preliminary Safety Examination of Thorium Molten-Salt Nuclear Energy Synergetics”, Thorium Utilization: Proceedings of the Indo-Japan Seminar on Thorium Utilization, Dec. 10-13, 1990
[Furukawa 1990b] Furukawa, K., Mitachi, K., Kato, Y., and Lecocq, A. “Global Nuclear Energy System: Thorium Molten-Salt Nuclear Energy Synergetics”, Thorium Utilization: Proceedings of the Indo-Japan Seminar on Thorium Utilization, Dec. 10-13, 1990
[Furukawa 1992] Furukawa, K., Mitachi, K., and Kato, Y. “Small Molten-salt Reactors with a Rational Thorium Fuel-cycle”, Nuclear Engineering and Design, Vol. 136, pp. 157-165, 1992
[Furukawa 2007] Furukawa, K. et al. “A Road Map for the Realization of Global-Scale Thorium Breeding Fuel Cycle by Single Molten-Fluoride Flow”, 13th International Conference on Emerging Nuclear Energy Systems, Istanbul, Turkey, June 3-8, 2007
[Furukawa 2008] Furukawa, K. et al. “A Road Map for the Realization of Global-Scale Thorium Breeding Fuel Cycle by Single Molten-Fluoride Flow”, *Energy Conversion and Management*, Vol . 49, pp. 1832-1848, 2008
[Furukawa 2012] Furukawa, K., Erbay, L., and Aykol, A. “A Study on a Symbiotic Thorium Breeding Fuel-Cycle: THORIMS-NES through FUJI”, *Energy Conversion and Management*, Vol. 63, pp. 51-54, 2012

[Gat 1991] Gat, U. and Engel, J. “The Molten Salt Reactor Operation for Beneficial Use of Fissile Material from Dismantled Weapons”, Oak Ridge National Laboratory (No Report Number), 1991
[Gehin 2014] Gehin, J. and Powers, J. “Liquid Fuel Molten Salt Reactors for Thorium Utilization”, Transactions of the American Nuclear Society, Vol. 111, Anaheim, California, November 9–13, 2014
[Grimes 1967] Grimes, W. “Chemical Research and Development for Molten-Salt Breeder Reactors”, Oak Ridge National Laboratory Report ORNL-TM-1853, 1967
[Grimes 1970] Grimes, W. “Molten-Salt Reactor Chemistry”, *Nuclear Applications & Technology*, Vol. 8, 1970
[Grimes 1978] Grimes, W. “Molten Fluoride Mixtures as Possible Fission Reactor Fuels”, Electrochemical Society Meeting, Seattle, Washington, May 21-25, 1978
[Guymon 1966] Guymon, R., Haubenreich, P., and Engel, J. “MSRE Design and Operations Report Part XI: Test Program”, Oak Ridge National Laboratory Report ORNL-TM-911, 1966
[Guymon 1973] Guymon, R. “MSRE Systems and Components Performance”, Oak Ridge National Laboratory Report ORNL-TM-3039, 1973
[Hargraves 2010] Hargraves, R. and Moir, R. “Liquid Fluoride Thorium Reactors: An Old Idea Gets Reexamined”, American Scientist, Vol. 98, 2010
[Haubenreich 1964] Haubenreich, P., Engel, J., Prince, B., and Claiborne, H. “MSRE Design and Operations Report Part III, Nuclear Analysis”, Oak Ridge National Laboratory Report ORNL-TM-730, 1964
[Haubenreich 1968] Haubenreich, P. et al. “MSRE Design and Operations Report Part V-A, Safety Analysis of Operation with 233U”, Oak Ridge National Laboratory Report ORNL-TM-2111, 1968
[Haubenreich 1970a] Haubenreich, P. and Engel, J. “Experience with the Molten-Salt Reactor Experiment”, *Nuclear Applications & Technology*, Vol. 8, 1970
[Haubenreich 1970b] Haubenreich, P. “Fluoride Production and Recombination in Frozen MSR Salts after Reactor Operation”, Oak Ridge National Laboratory Report ORNL-TM-3144, 1970
[Heuer 2014] Heuer, D. et al. “Towards the Thorium Fuel Cycle with Molten Salt Fast Reactors”, Annals of Nuclear Energy, Vol. 64, pp. 421-429, 2014
[Hightower 1975a] Hightower Jr., J. “Process Technology for the Molten-Salt Reactor 233U-Th Cycle”, ANS 1975 Winter Meeting, San Francisco, CA, USA, November 16-21, 1975
[Hightower 1975b] Hightower Jr., J. “Engineering Development Studies for Molten-Salt Breeder Reactor Processing No. 18”, Oak Ridge National Laboratory Report ORNL-TM-4698, 1975
[Hightower 1975c] Hightower Jr., J. “Engineering Development Studies for Molten-Salt Breeder Reactor Processing No. 19”, Oak Ridge National Laboratory Report ORNL-TM-4863, 1975
[Hightower 1976a] Hightower Jr., J. “Engineering Development Studies for Molten-Salt Breeder Reactor Processing No. 20”, Oak Ridge National Laboratory Report ORNL-TM-4870, 1976
[Hightower 1976b] Hightower Jr., J. “Engineering Development Studies for Molten-Salt Breeder Reactor Processing No. 21”, Oak Ridge National Laboratory Report ORNL-TM-4894, 1976
[Hirakawa 1990] Hirakawa, N. and Kasma, E. “Study of Reactor Kinetics of Small Size Molten Salt Reactor”, Thorium Utilization: Proceedings of the Indo-Japan Seminar on Thorium Utilization, Dec. 10-13, 1990
[Holcomb 2009] Holcomb, D. et al. “An Analysis of Testing Requirements for Fluoride Salt-cooled High Temperature Reactor Components”, Oak Ridge National Laboratory Report ORNL/TM-2009/297, 2009

[Holcomb 2011] Holcomb, D. et al. “Fast Spectrum Molten Salt Reactor Options”, Oak Ridge National Laboratory Report ORNL/TM-2011/105, 2011
[Holcomb 2013] Holcomb, D. et al. “Fluoride Salt-Cooled High-Temperature Reactor Technology Development and Demonstration Roadmap”, ORNL/TM-2013/401, 2013
[Houtzeel 1972] Houtzeel, A. and Dyer, F. “A Study of Fission Products in the Molten-Salt Reactor Experiment by Gamma Spectrometry”, Oak Ridge National Laboratory Report ORNL-TM-3151, 1972
[Hu 2013] Hu, L. and Forsberg, C. “Goals and Licensing Strategy for a Fluorine Salt-Cooled High Temperature Test Reactor (FHTR)”, ANS Winter Meeting 2013, Washington DC, Nov. 10-14, 2013
[Ignatiev 2011] Ignatiev, V. and Feynberg, O. “Molten Salt Reactor for TRU Transmutation without and with Th-U Support”, Transactions of the American Nuclear Society, Vol. 104, Hollywood, FL, USA, June 26-30, 2011
[Juhasz 2009] Juhasz, A., Rarick, R., and Rangarajan, R. “High Efficiency Nuclear Power Plants Using Liquid Fluoride Thorium Reactor Technology”, National Aeronautics and Space Administration Report NASA-TM-2009-215829, 2009
[Kamei 2010] Kamei, T., Furukawa, K., Mitachi, K., and Kato, Y. “Mass Balance Analysis of Th-233U Based MSR (Molten-Salt Reactor) Cycle (THORIMS-NES) Transferred from Present U-Pu Based LWRs (Light Water Reactor)”, *Energy*, Vol. 35, pp. 928-934, 2010
[Kamei 2012] Kamei, T. “Recent Research of Thorium Molten-Salt Reactor from a Sustainability Viewpoint”, *Sustainability*, Vol. 4, pp. 2399-2418, 2012
[Kanda 1990a] Kanda, K. et al. “Reactivity Measurements and Analyses for Chemical Materials Used in a Thorium Molten Salt Reactor Fuel”, Thorium Utilization: Proceedings of the Indo-Japan Seminar on Thorium Utilization, Dec. 10-13, 1990
[Kanda 1990b] Kanda, K. and Kano, I. “Effect of Uranium-235 Enrichment on Initial Reactivity of Molten Salt Reactor”, Thorium Utilization: Proceedings of the Indo-Japan Seminar on Thorium Utilization, Dec. 10-13, 1990
[Kasten 1966a] Kasten, P., Bettis, E., and Robertson, R. “Design Studies of 1000-MWe Molten Salt Breeder Reactors”, Oak Ridge National Laboratory Report ORNL-3996
[Kasten 1966b] Kasten, P. et al. “Summary of Molten-Salt Breeder Reactor Design Studies”, Oak Ridge National Laboratory Report ORNL-TM-1467, 1966
[Kasten 1967] Kasten, P. “Safety Program for Molten-Salt Breeder Reactors”, Oak Ridge National Laboratory Report ORNL-TM-1858, 1967
[Kasten 1969] Kasten, P. et al. “Graphite Behavior and its Effects on MSBR Performance”, Oak Ridge National Laboratory Report ORNL-TM-2136, 1969
[Kedl 1972] Kedl, R. “The Migration of a Class of Fission Products (Noble Metals) in the Molten-Salt Reactor Experiment, Oak Ridge National Laboratory Report ORNL-TM-3884, 1972
[Kelmers`1976] Kelmers, A et al. “Evaluation of Alternative Secondary (and Tertiary) Coolants for the Molten-Salt Breeder Reactor”, Oak Ridge National Laboratory Report ORNL-TM-5325, 1976
[Kennedy 1950] Kennedy, J. “Lithium Isotope Separation by Electrolysis”, Los Alamos National Laboratory Report LA-1156, 1950
[Kerlin 1971] Kerlin, T., Ball, S., Steffy, C., and Buckner, M. “Experiences with Dynamic Testing Methods at the Molten-Salt Reactor Experiment”, *Nuclear Technology*, Vol. 10, 1971
[Koger 1972] Koger, J. “Alloy Compatibility with LiF-BeF2 Salts Containing ThF4 and UF4”, Oak Ridge National Laboratory Report ORNL-TM-4286, 1972

[Li 2015] Li, X. et al. “Analysis of Thorium and Uranium Based Nuclear Fuel Options in Fluoride Salt-Cooled High-Temperature Reactor”, *Progress in Nuclear Energy*, Vol. 78, pp. 285-290, 2015
[Lindauer 1969] Lindauer, R. “Processing of the MSRE Flush and Fuel Salts”, Oak Ridge National Laboratory Report ORNL-TM-2578, 1969
[MacPherson 1957] MacPherson, H. “Molten Salts for Civilian Power”, Oak Ridge National Laboratory Report CF-57-10-41, 1957
[MacPherson 1958a] MacPherson, H. “Molten-Salt Reactor Program Quarterly Progress Report for Period Ending October 31, 1957”, Oak Ridge National Laboratory Report ORNL-2431, 1958
[MacPherson 1958b] MacPherson, H. “Molten-Salt Reactor Program Quarterly Progress Report for Period Ending January 31, 1958”, Oak Ridge National Laboratory Report ORNL-2474, 1958
[MacPherson 1958c] MacPherson, H. “Molten-Salt Reactor Program Quarterly Progress Report for Period Ending June 30, 1958”, Oak Ridge National Laboratory Report ORNL-2551, 1958
[MacPherson 1958d] MacPherson, H. “Molten-Salt Reactor Program Status Report”, Oak Ridge National Laboratory Report ORNL-2634, 1958
[MacPherson 1959a] MacPherson, H. “Molten-Salt Reactor Program Quarterly Progress Report for Period Ending October 31, 1958”, Oak Ridge National Laboratory Report ORNL-2626, 1959
[MacPherson 1959b] MacPherson, H. “Molten-Salt Reactor Program Quarterly Progress Report for Period Ending January 31, 1959”, Oak Ridge National Laboratory Report ORNL-2684, 1959
[MacPherson 1959c] MacPherson, H. “Molten-Salt Reactor Program Quarterly Progress Report for Period Ending April 30, 1959”, Oak Ridge National Laboratory Report ORNL-2723, 1959
[MacPherson 1959d] MacPherson, H. “Molten-Salt Reactor Program Quarterly Progress Report for Period Ending July 31, 1959”, Oak Ridge National Laboratory Report ORNL-2799, 1959
[MacPherson 1960a] MacPherson, H. “Molten-Salt Reactor Program Quarterly Progress Report for Period Ending October 31, 1959”, Oak Ridge National Laboratory Report ORNL-2890, 1960
[MacPherson 1960b] MacPherson, H. “Molten-Salt Reactor Program Quarterly Progress Report for Periods Ending January 31 and April 30, 1960”, Oak Ridge National Laboratory Report ORNL-2973, 1960
[MacPherson 1960c] MacPherson, H. “Molten-Salt Reactor Program Quarterly Progress Report for Period Ending July 31, 1960”, Oak Ridge National Laboratory Report ORNL-3014, 1960
[MacPherson 1960d] MacPherson, H. “Molten-Salt Breeder Reactors”, Oak Ridge National Laboratory Report CF-59-12-64, 1960
[MacPherson 1985] MacPherson, H. “The Molten Salt Reactor Adventure”, *Nuclear Science and Engineering*, Vol. 90, pp. 374-380, 1985
[Madden 2013] Madden, P., Salanne, M., and Levesque, M. “Thorium Molten Salts, Theory and Practice”, International Conference on Thorium Fuel: Thorium Energy Conference 2013, Geneva, Switzerland, October 28-31, 2013
[Mathieu 2006] Mathieu, L. et al. “The Thorium Molten Salt Reactor” Moving on from the MSBR”, *Progress in Nuclear Energy*, Vol. 48, pp. 664-679, 2006
[Mathieu 2009] Mathieu, L. et al. “Possible Configurations for the Thorium Molten Salt Reactor and Advantages of the Fast Nonmoderated Version”, *Nuclear Science and Engineering*, Vol. 161, pp. 78-89, 2009
[McCoy 1967] McCoy, H., and Weir Jr, J. “Materials Development for Molten-Salt Breeder Reactor”, Oak Ridge National Laboratory Report ORNL-TM-1854, 1967
[McCoy 1972] McCoy, H. and McNabb, B. “Postirradiation Examination of Materials from the MSRE”, Oak Ridge National Laboratory Report ORNL-TM-4174, 1972

[McNeese 1967] McNeese, L. “Considerations of Low Pressure Distillation and its Application to Processing of Molten-Salt Breeder Reactor Fuels”, Oak Ridge National Laboratory Report ORNL-TM-1730, 1967
[McNeese 1971a] McNeese, L. “Engineering Development Studies for Molten-Salt Breeder Reactor Processing No. 2”, Oak Ridge National Laboratory Report ORNL-TM-3137, 1971
[McNeese 1971b] McNeese, L. “Engineering Development Studies for Molten-Salt Breeder Reactor Processing No. 3”, Oak Ridge National Laboratory Report ORNL-TM-3138, 1971
[McNeese 1971c] McNeese, L. “Engineering Development Studies for Molten-Salt Breeder Reactor Processing No. 4”, Oak Ridge National Laboratory Report ORNL-TM-3139, 1971
[McNeese 1971d] McNeese, L. “Engineering Development Studies for Molten-Salt Breeder Reactor Processing No. 5”, Oak Ridge National Laboratory Report ORNL-TM-3140, 1971
[McNeese 1971e] McNeese, L. “Engineering Development Studies for Molten-Salt Breeder Reactor Processing No. 6”, Oak Ridge National Laboratory Report ORNL-TM-3141, 1971
[McNeese 1972a] McNeese, L. “Engineering Development Studies for Molten-Salt Breeder Reactor Processing No. 7”, Oak Ridge National Laboratory Report ORNL-TM-3257, 1972
[McNeese 1972b] McNeese, L. “Engineering Development Studies for Molten-Salt Breeder Reactor Processing No. 8”, Oak Ridge National Laboratory Report ORNL-TM-3258, 1972
[McNeese 1972c] McNeese, L. “Engineering Development Studies for Molten-Salt Breeder Reactor Processing No. 10”, Oak Ridge National Laboratory Report ORNL-TM-3352, 1972
[McNeese 1974] McNeese, L. “Program Plan for Development of Molten-Salt Breeder Reactors”, Oak Ridge National Laboratory Report ORNL-5018, 1974
[McNeese 1975a] McNeese, L. “Molten-Salt Reactor Program Semiannual Progress Report for Period Ending August 31, 1974”, Oak Ridge National Laboratory Report ORNL-5011, 1975
[McNeese 1975b] McNeese, L. “Molten-Salt Reactor Program Semiannual Progress Report for Period Ending February 28, 1975”, Oak Ridge National Laboratory Report ORNL-5047, 1975
[McNeese 1976a] McNeese, L. “Molten-Salt Reactor Program Semiannual Progress Report for Period Ending August 31, 1975”, Oak Ridge National Laboratory Report ORNL-5078, 1976
[McNeese 1976b] McNeese, L. “Molten-Salt Reactor Program Semiannual Progress Report for Period Ending February 29, 1976”, Oak Ridge National Laboratory Report ORNL-5132, 1976
[McWherter 1970] McWherter, J. “Molten Salt Breeder Experiment Design Bases”, Oak Ridge National Laboratory Report ORNL-TM-3177, 1970
[Merle-Lucotte 2006] Merle-Lucotte, E. et al. “Fast Thorium Molten Salt Reactors Started with Plutonium”, Proceedings of ICAPP 2006, Reno, NV, USA, June 4-8, 2006
[Merle-Lucotte 2007a] Merle-Lucotte, E. et al. “Optimized Transition from the Reactors of Second and Third Generations to the Thorium Molten Salt Reactor”, ICAPP 2007, Nice, France, May 13-18, 2007
[Merle-Lucotte 2007b] Merle-Lucotte, E. et al. “The Thorium Fuel Molten Salt Reactor: Launching the Thorium Fuel Cycle while Closing the Current Fuel Cycle”, European Nuclear Conference (ENC 2007). European Nuclear Society, 2007
[Merle-Lucotte 2008a] Merle-Lucotte, E. et al. “Influence of the Processing and Salt Composition on the Thorium Molten Salt Reactor”, *Nuclear Technology*, Vol. 163, 2008
[Merle-Lucotte 2008b] Merle-Lucotte, E. et al. “Optimization and Simplification of the Concept of Non-moderated Thorium Molten Salt Reactor”, International Conference on the Physics of Reactors “Nuclear Power: A Sustainable Resource”, Interlaken, Switzerland, September 14-19, 2008

[Merle-Lucotte 2011] Merle-Lucotte, E. et al. “Launching the Thorium Fuel Cycle with the Molten Salt Fast Reactor”, Proceedings of ICAPP 2011, Nice, France, May 2-5, 2011
[Mitachi 2006] Mitachi, K., Yamamoto, T., and Yoshioka, R. “Three-region Core Design for 200-MW(electric) Molten-Salt Reactor with Thorium-Uranium Fuel”, Nuclear Technology, Vol. 158, June 2007
[Moir 2002] Moir, R. et al. “Deep-Burn Molten-Salt Reactors”, Application Under Solicitation No. LAB NE 2002-1, 2002
[Moir 2005] Moir, R., and Teller, E. “Thorium-Fueled Underground Power Plant Based on Molten Salt Technology”, *Nuclear Technology*, Vol. 151, 2005
[Novikov 1995] Novikov, V. “The Results of the Investigations of Russian Research Center – “Kurchatov Institute” on Molten Salt Applications to Programs of Nuclear Energy Systems”, American Institute of Physics Conference Proceedings, Vol. 346, No. 138, 1995
[Numakura 2011] Numakura, M. et al. “Structural Investigations of Thorium in Molten Lithium-Calcium Fluoride Mixtures for Salt Treatment Process in Molten Salt Reactor”, Progress in Nuclear Energy, Vol. 53, pp. 994-998, 2011
[Nuttin 2004] Nuttin, A. et al. “Potential of Thorium Molten Salt Reactors: Detailed Calculations and Concept Evolutions in View of a Large Nuclear Energy Production”, HYSOR-2004-The Physics of Fuel Cycles and Advanced Nuclear Systems: Global Developments. American Nuclear Society, 2004
[Ottewitte 1982] Ottewitte, E. “Configuration of a Molten Chloride Fast Reactor on a Thorium Fuel Cycle to Current Nuclear Fuel Cycle Concerns”, University of California, Los Angeles Thesis, 1982
[Ottewitte 1992] Ottewitte, E. “Cursory First Look at the Molten Chloride Fast Reactor as an Alternative to the Conventional BATR Concept”, Idaho National Laboratory (No Report Number), 1992
[Perry 1967] Perry, A. “Physics Program for Molten-Salt Breeder Reactors”, Oak Ridge National Laboratory Report ORNL-TM-1857, 1967
[Perry 1970] Perry, A., and Bauman, F. “Reactor Physics and Fuel-Cycle Analyses”, *Nuclear Applications & Technology*, Vol. 8, 1970
[Powers 2013] Powers, J. et al. “Reactor Physics Analysis of Thorium Fuel Cycles Using Molten Salt Reactors”, ANS Winter Meeting 2013, Washington DC, Nov. 10-14, 2013
[Robertson 1965] Robertson, R. “MSRE Design and Operations Report Part I: Description of Reactor Design”, Oak Ridge National Laboratory Report ORNL-TM-728, 1965
[Robertson 1970] Robertson, R., Briggs, R., Smith, O., and Bettis, E. “Two-Fluid Molten-Salt Breeder Reactor Design Study (Status as of January 1, 1968)”, Oak Ridge National Laboratory Report ORNL-4528, 1970
[Robertson 1971] Robertson, R. et al. “Molten-Salt Reactor Program: Conceptual Design Study of a Single-Fluid Molten-Salt Breeder Reactor”, Oak Ridge National Laboratory Report ORNL-4541, 1971
[Rosenthal 1967a] Rosenthal, M., Briggs, R, and Kasten, P. “Molten-Salt Reactor Program Semiannual Progress Report for Period Ending February 28, 1967”, Oak Ridge National Laboratory Report ORNL-4119, 1967
[Rosenthal 1967b] Rosenthal, M., Briggs, R, and Kasten, P. “Molten-Salt Reactor Program Semiannual Progress Report for Period Ending August 31, 1967”, Oak Ridge National Laboratory Report ORNL-4191, 1967

[Rosenthal 1968] Rosenthal, M., Briggs, R, and Kasten, P. "Molten-Salt Reactor Program Semiannual Progress Report for Period Ending February 29, 1968", Oak Ridge National Laboratory Report ORNL-4254, 1968
[Rosenthal 1969a] Rosenthal, M., Briggs, R, and Kasten, P. "Molten-Salt Reactor Program Semiannual Progress Report for Period Ending August 31, 1968", Oak Ridge National Laboratory Report ORNL-4344, 1969
[Rosenthal 1969b] Rosenthal, M., Briggs, R, and Kasten, P. "Molten-Salt Reactor Program Semiannual Progress Report for Period Ending February 28, 1969", Oak Ridge National Laboratory Report ORNL-4396, 1969
[Rosenthal 1970a] Rosenthal, M., Briggs, R, and Kasten, P. "Molten-Salt Reactor Program Semiannual Progress Report for Period Ending August 31, 1969", Oak Ridge National Laboratory Report ORNL-4449, 1970
[Rosenthal 1970b] Rosenthal, M., Briggs, R, and Kasten, P. "Molten-Salt Reactor Program Semiannual Progress Report for Period Ending February 28, 1970", Oak Ridge National Laboratory Report ORNL-4548, 1970
[Rosenthal 1970c] Rosenthal, M., Kasten, P., and Briggs, R. "Molten-Salt Reactors – History, Status, and Potential", *Nuclear Applications & Technology*, Vol. 8, 1970
[Rosenthal 1971a] Rosenthal, M., Briggs, R., and Haubenreich, P. "Molten-Salt Reactor Program Semiannual Progress Report for Period Ending August 31, 1970", Oak Ridge National Laboratory Report ORNL-4622, 1971
[Rosenthal 1971b] Rosenthal, M., Briggs, R., and Haubenreich, P. "Molten-Salt Reactor Program Semiannual Progress Report for Period Ending February 28, 1971", Oak Ridge National Laboratory Report ORNL-4676, 1971
[Rosenthal 1972a] Rosenthal, M., Briggs, R., and Haubenreich, P. "Molten-Salt Reactor Program Semiannual Progress Report for Period Ending August 31, 1971", Oak Ridge National Laboratory Report ORNL-4728, 1972
[Rosenthal 1972b] Rosenthal, M., Briggs, R., and Haubenreich, P. "Molten-Salt Reactor Program Semiannual Progress Report for Period Ending February 29, 1972", Oak Ridge National Laboratory Report ORNL-4782, 1972
[Rosenthal 1972c] Rosenthal, M., Haubenreich, P., and Briggs, R. "The Development Status of Molten-Salt Breeder Reactors", Oak Ridge National Laboratory Report ORNL-4812, 1972
[Rosenthal 1973] Rosenthal, M., Briggs, R., and Haubenreich, P. "Molten-Salt Reactor Program Semiannual Progress Report for Period Ending August 31, 1972", Oak Ridge National Laboratory Report ORNL-4832, 1973
[Sajo-Bohus 2012] Sajo-Bohus, L. et al. "An Alternative Source for Venezuelan Nuclear Energy Production: The Thorium Molten Salt Reactor", 13th International Conference on Nuclear Reaction Mechanisms, Villa Monastero, Varenna, Italy, 11 - 15 Jun 2012
[Sargent & Lundy 1962] Sargent & Lundy Engineers Chicago. "Capital Cost Evaluation 1000 MWe Molten Salt Converter Reactor Power Plants", Report SL-1954, 1962
[Savage 1977] Savage, H. and Hightower Jr., J. "Engineering Tests of the Metal Transfer Process for Extraction of Rare-Earth Fission Products from a Molten-Salt Breeder Reactor Fuel Salt", Oak Ridge National Laboratory Report ORNL-5176, 1977
[Scott 1966] Scott, C. and Carter, W. "Preliminary Design Study of a Continuous Fluorination-Vacuum-Distillation System for Regenerating Fuel and Fertile Streams in a Molten Salt Breeder Reactor", Oak Ridge National Laboratory Report ORNL-3791, 1966

[Scott 1970] Scott, D. and Eatherly, W. “Graphite and Xenon Behavior and Their Influence on Molten-Salt Reactor Design”, *Nuclear Applications & Technology,* Vol. 8, 1970
[Shapiro 1970] Shapiro, M. and Reed, C. “Removal of Tritium from the Molten Salt Breeder Reactor Fuel”, Oak Ridge National Laboratory Report ORNL-MIT-117, 1970
[Smith 1969] Smith, F., Ferris, L., and Thompson, C. “Liquid-Vapor Equilibria in LiF-BeF2 and LiF-BeF2-ThF4 Systems”, Oak Ridge National Laboratory Report ORNL-4415, 1969
[Steffy 1969a] Steffy Jr., R. and Wood, P. “Theoretical Dynamic Analysis of the MSRE with 233U Fuel”, Oak Ridge National Laboratory Report ORNL-TM-2571, 1969
[Steffy 1969b] Steffy Jr., R. “Inherent Neutron Source in MSRE with Clean 233U Fuel”, Oak Ridge National Laboratory Report ORNL-TM-2685, 1969
[Steffy 1970] Steffy Jr., R. “Experimental Dynamic Analysis of the MSRE with 233U Fuel”, Oak Ridge National Laboratory Report ORNL-TM-2997, 1970
[Teeter 1965] Teeter, C., Lecky, J., and Martens, J. “Catalog of Nuclear Reactor Concepts: Part I, Homogeneous and Quasi-homogeneous Reactors, Section III, Reactors Fueled with Molten-salt Solutions”, Argonne National Laboratory Report ANL-7092, 1965
[Thoma 1968] Thoma, R. “Chemical Feasibility of Fueling Molten Salt Reactors with PuF3”, Oak Ridge National Laboratory Report ORNL-TM-2256, 1968
[Thoma 1969] Thoma, R., and Ricci, J. “Fractional Crystallization Reactions in the System LiF-BeF2-ThF4”, Oak Ridge National Laboratory Report ORNL-TM-2596, 1969
[Thoma 1971] Thoma, R. “Chemical Aspects of MSRE Operations”, 1971
[Turner 2013] Turner, J. “Opportunities and Challenges for Thorium in Commercial MSRs”, International Conference on Thorium Fuel: Thorium Energy Conference 2013, Geneva, Switzerland, October 28-31, 2013
[Uhlir 2013] Uhlir, J. and Juricek, V. “Current Czech R&D in Thorium MSR Technology and Future Directions”, International Conference on Thorium Fuel: Thorium Energy Conference 2013, Geneva, Switzerland, October 28-31, 2013
[Weaver 1960] Weaver, C., Thoma, R., Insley, H., and Friedman, H. “Phase Equilibria in Molten Salt Breeder Reactor Fuels: I, The System LiF-BeF2-UF4-ThF4”, Oak Ridge National Laboratory Report ORNL-2896, 1960
[Wheatley 1970] Wheatley, M. et al. “Engineering Development of the Thorium Fuel Cycle”, *Nuclear Applications & Technology*, Vol. 8, 1970
[Yoder 2014] Yoder Jr., G. et al. “Liquid Fluoride Salt Experiment Using a Small Natural Circulation Cell”, Oak Ridge National Laboratory Report ORNL/TM-2014/56
[Zhu 2013] Zhu, X., He, Z., Peng, C., and Chen, K. “The Analysis of Tritium Generation in the Solid Fuel Thorium Molten Salt Reactor”, ANS Winter Meeting 2013, Washington DC, Nov. 10-14, 2013

APPENDIX B, CALCULATION NOTES FOR FUEL CYCLE MATERIAL FLOW DEVELOPMENT SAMPLE

Fuel Cycle Overview

This document summarizes the development of burnup analysis and mass flows for a two-stage fuel cycle. The first stage is a pressurized water reactor (PWR) with two distinct fuel types, a seed fuel and a blanket fuel. The driver fuel contains low-enriched uranium and is intended to provide high-flux regions of the core to breed U-233 in the blanket fuel, which is mostly thorium with some low-enriched uranium homogenously mixed in. After irradiation, the driver fuel is directed to interim storage and then disposal, while the blanket fuel is reprocessed for its thorium and uranium content. Much of the thorium is recycled back to the first stage, while the remainder of the thorium and all of the uranium in the blanket fuel are sent to stage 2 (minor actinides, plutonium, and fission products in the blanket fuel are sent for storage/disposal). Stage 2 uses the recycled thorium and uranium in a "deep-burn" high-temperature gas reactor (HTGR).

The following sections will describe how this fuel cycle was computationally analyzed in order to document the methodology and to enable reproducibility of the results.

Modeling Tool – SCALE

To carry out the necessary depletion calculations, various modules of SCALE were used. SCALE "is a comprehensive modeling and simulation suite for nuclear safety analysis and design developed and maintained by Oak Ridge National Laboratory under contract with the U.S. Nuclear Regulatory Commission, U.S. Department of Energy, and the National Nuclear Security Administration to perform reactor physics, criticality safety, radiation shielding, and

spent fuel characterization for nuclear facilities and transportation/storage package designs"[42]. The primary capabilities of SCALE relevant to FCDP development are two- and three-dimensional radiation transport and depletion analysis.

Pressurized Water Reactor: Parameters and Modeling Approach

As a reference design for Stage 1, the seed-blanket fuel assembly concept developed by Brookhaven National Laboratory in collaboration with other organizations [1] and further elaborated upon in later studies [2,3] was used. In this design, each fuel assembly consists of an inner low-enriched uranium-oxide seed fuel region to supply a sufficient neutron flux to enable uranium-233 breeding in an outer, primarily-thorium blanket fuel region. The blanket fuel also has some low-enriched uranium homogenously mixed with the thorium to sustain neutron fluxes in the blanket region.

This design was selected as a reference for the following reasons:

- Analysis has demonstrated this design to be viable from neutronic, thermal, and other important perspectives.
- The documentation of this design is sufficient to enable reproducible modeling results.
- The design is readily compatible with the modeling capabilities of SCALE.
- For consistency with other FCDPs, this design has been used as part of fuel cycles which are already part of the Nuclear Fuel Cycle Option (NFCO) Catalog.

[42] http://scale.ornl.gov, Accessed November 2014

The enrichments, compositions, configurations, and dimensions of the blanket fuel and the seed fuel (henceforth referred to as “driver fuel” to be more consistent with previously used language of the NFCO Catalog) are well-documented. A number of specific fuel characteristics were discussed in the BNL reports. Table B-1 summarizes the characteristics adopted for the two fuel types for this FCDP.

.

Table B-1, Fuel Characteristics of Driver-Blanket PWR [1, 3]

	Driver Fuel	Blanket Fuel
Average Fuel Temperature (°C)	469	532
Fuel Density (g/cm^3)	10.302	9.403
Fuel Composition	100% uranium oxide	85.9% thorium oxide; 14.1% uranium oxide (by vol.)
Uranium Enrichment (% of U that is U-235)	19.9	12.2
Residence Time (years)	4	8
Cell (Pin) Pitch (cm)	1.26	1.26
Central Hole Radius (cm)	0.22	n/a
Fuel Radius (cm)	0.385	0.4646
Gas (Outer) Gap (cm)	0.0082	0.0082
Cladding Thickness (cm)	0.0572	0.0572
Cladding Material	Zircaloy-4	Zircaloy-4
Cladding Temperature (°C)	349	349

Table B-2 summarizes other key core characteristics that were assumed (these generally reflect default settings in SCALE which were not observed to have a significant impact on the results with small perturbations):

Table B-2, Key Parameters for PWR Core

Average Coolant Temperature (°C)	307
Boron Concentration in Coolant (ppm)	630
Guide Tube Material	Zircaloy-4
Guide Tube Temperature (°C)	307

For simplicity, the core was modeled as a quarter-assembly of a 17x17 fuel pin assembly, with a fuel arrangement adopted from the BNL design [1]. A reflective boundary condition was assumed at the inner boundaries (where the rest of the assembly would be). Figure B-1 illustrates this arrangement:

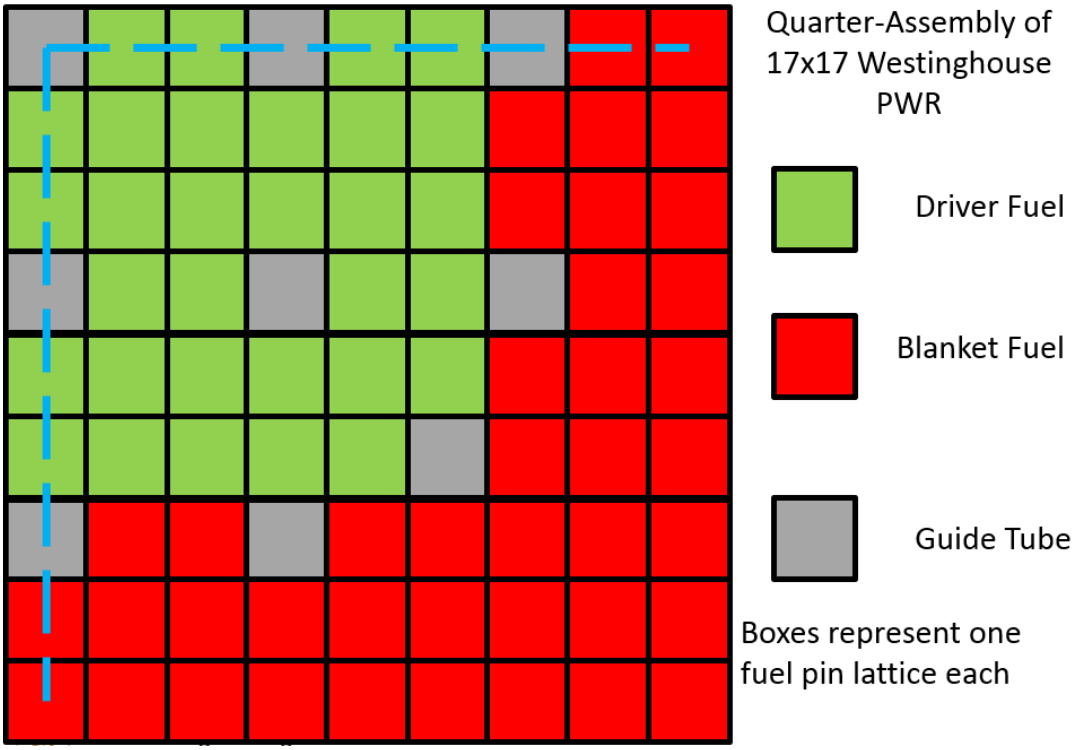

Figure B-1, Configuration of Quarter of 17x17 Fuel Array for Driver-Blanket Fuel in PWR

In spite of the geometrical simplicity of this configuration, three complications were acknowledged:

- The need to simultaneously deplete two different fuel materials
- The need to address the different residence times of the two fuels (driver fuel at four years, blanket fuel at eight years)
- The need to address the different ages of driver fuel introduced at different refueling cycles).

To address these challenges, the depletion period was subdivided between each refueling period. In other words, refueling of one-third of the driver fuel inventory was assumed to occur three times during the driver fuel lifetime (every 1.33 years) which was approximated as 486 days. To improve the granularity of the analysis, each 486-day irradiation period was divided into nine 54-day timesteps. The blanket lifetime extended over six of these irradiation periods, or 2916 days (approximately 8 years).

In actuality, a fuel assembly in the reactor at any given time would have one of three driver fuel ages (see Figure B-2), but it was not desired to manage the complications of simultaneously modeling different arrays or to optimize a fuel reloading scheme. Instead, while holding the blanket at constant (initial) composition, the driver fuel was aged, with compositions taken at 0, 486, and 972 days. These three compositions were then averaged, and this average driver composition was then held constant as the blanket fuel was depleted. This resolution is illustrated in Figure B-3.

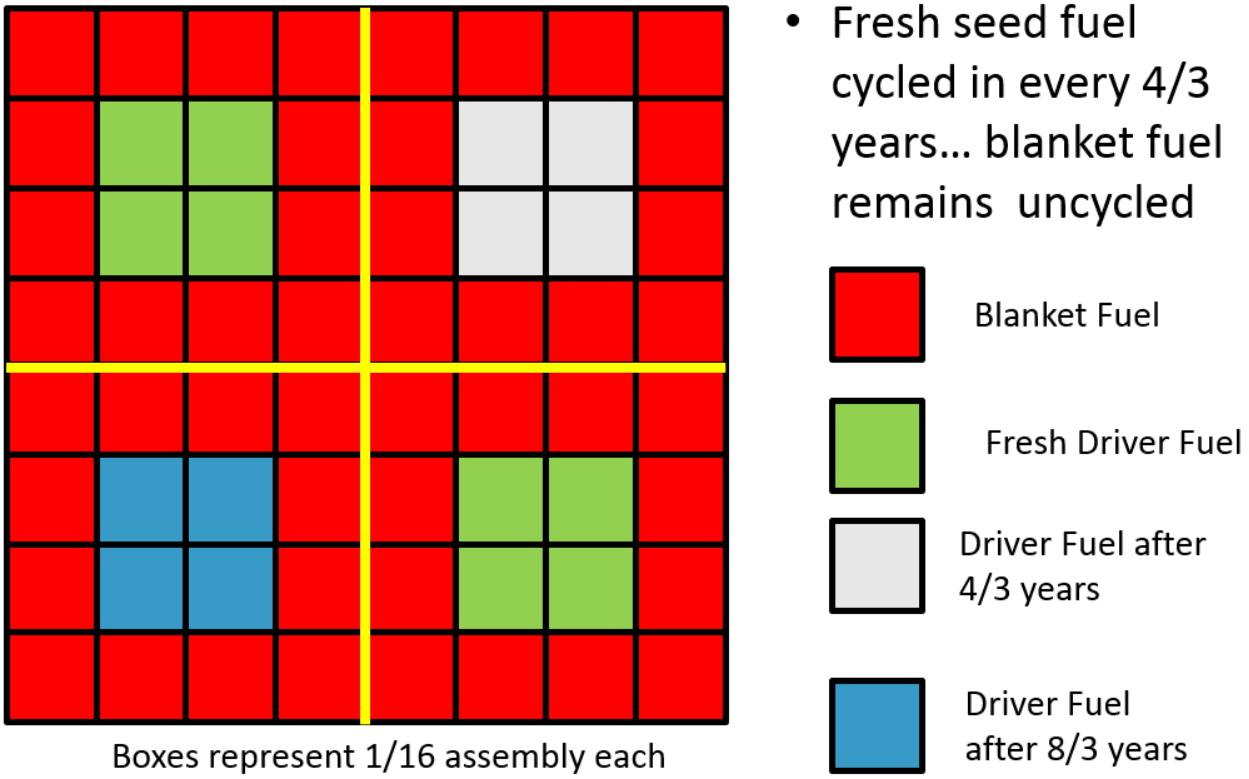

Figure B-2, Cross Section of Several Fuel Arrays to Illustrate Challenge of Different Driver Fuel Ages

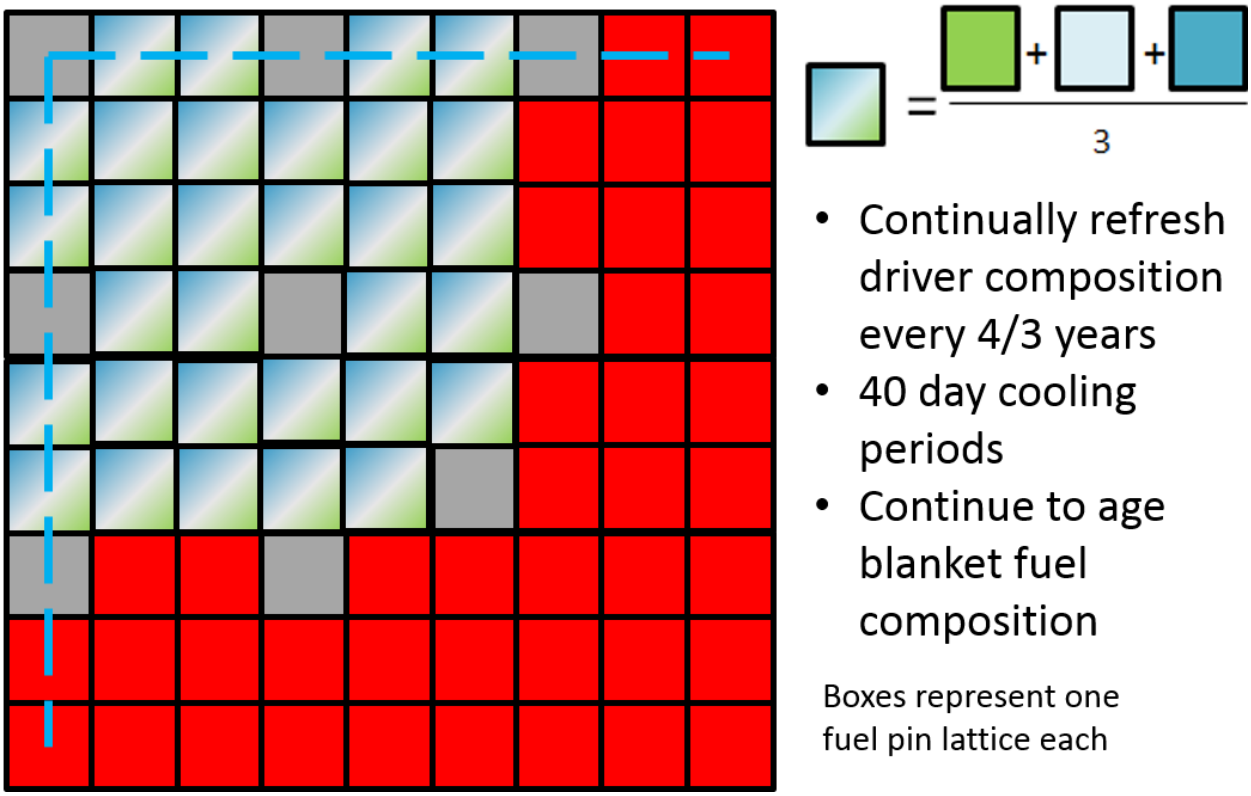

Figure B-3: Resolution to Problem in Figure A-2, using a Constant Driver Fuel Composition which is the Average of the Three Possible Driver Fuel Ages

The PWR quarterly-assembly was modeled using SCALE's "T-DEPL" module using the most up-to-date and extensive ("v7-238") of the available built-in cross section libraries. Masses were obtaining by saving an "f71" mass file at the end of each 486-day irradiation period. After each irradiation period, the fuel was aged for 40 days without irradiation to represent the refueling period; this aging was performed on the "f71" file using SCALE's ORIGEN-S module and correspondingly listed using SCALE's OPUS module. In order to convert the format of the mass output of OPUS for the nth irradiation period into the required input format for T-DEPL for the (n+1)th irradiation period, inter-processing capabilities were developed in Visual Basic using Microsoft Excel as a platform. This re-formatting also included the removal of certain radionuclides which were not recognized in SCALE as acceptable for T-DEPL input files.

However, it was determined that these nuclides represented only a small portion (<0.001%) of the total mass of the fuel.

High Temperature Gas Reactor: Parameters and Modeling Approach

The reference HTGR design is based on Japan's High Temperature Engineering Test Reactor (HTTR), which uses hexagonal-graphite (prismatic) fuel blocks. This design was ideal for a number of reasons, foremost that:

- This system has been extensively examined by DOE national laboratories and correspondingly has sufficient documentation in English.
- ORNL had developed a SCALE input file based on the HTTR which could be obtained and readily adapted by the FCDP development team.

Detailed design parameters are available in a 2009 Idaho National Laboratory report [4]. The geometric parameters associated with this design are advanced and extensive, and the INL report should be consulted for detailed fuel parameters (the associated SCALE input file is also available upon request). However, the active portion of the HTGR fuel rods (the center of silicon-carbide- and pyrocarbon-coated microspheres) contains 20% of the thorium and all of the uranium from the blanket fuel from Stage 1 (subtracting reprocessing and fabrication losses).

The HTGR depletion was modeled in SCALE's "T6-DEPL" module to capture the double-heterogeneity of the prismatic fuel blocks with embedded thorium-uranium carbide microspheres. The irradiation period was fixed at a constant power density of 100 MWth/MTIHM over a period of 1000 days (subdivided into 20 50-day timesteps for improved

granularity), resulting in a total burnup of 100 MWd/MTIHM. As with the PWR, an "f71" mass file was saved to indicate the mass inventory of the spent fuel after irradiation, with processing in ORIGEN-S and OPUS.

Fuel Cycle Parameter Calculation and Associated Formulae

The aforementioned procedures resulted in mass inventories for each stage of the combined fuel cycle at a number of time-steps. Combined with this information and a number of additional assumptions about the fuel cycle, it was possible to determine overall mass flow requirements of the system to populate the FCDP. The variables which are used in the following equation-oriented narrative are listed in the following Table B-3.

Table B-3, Table of Variable Definitions

Variable	Definition Description	Assumed Value (if applicable)
a_b	Enrichment of U-235 in blanket fuel uranium	0.122
a_{nat}	Natural Enrichment of U-235 in uranium	0.007
a_d	Enrichment of U-235 in driver fuel uranium	0.199
a_{tail}	Enrichment of U-235 in enrichment tails uranium	0.0025
B	Total mass of blanket fuel used in Stage 1, normalized by E_{basis}	Calculated
c	Capacity Factor (assumed same for both PWR & HTGR)	0.9
D	Total mass of driver fuel used in Stage 1, normalized by E_{basis}	Calculated
d_y	Days in a year	365.242 days
DF_{s1}	Discharged Fuel from Stage 1, normalized by E_{basis}	Calculated
DF_{s2}	Discharged Fuel from Stage 2, normalized by E_{basis}	Calculated
DF_{tot}	Total Discharged Fuel, normalized by E_{basis}	Calculated

DU_b	Depleted uranium yield arising from blanket fuel production, normalized by E_{basis}	Calculated
DU_d	Depleted uranium yield arising from driver fuel production, normalized by E_{basis}	Calculated
DU_{tot}	Total depleted uranium yield of fuel cycle, normalized by E_{basis}	Calculated
e_e	Thermal-to-Electric Efficiency (assumed same for both PWR & HTGR)	0.333333
e_f	Fuel Fabrication Efficiency; fraction of entering material which is not lost to tails	0.999
e_r	Reprocessing Efficiency; fraction of entering material which is not lost to tails (assumed to be 1 for TRU and FPs)	0.999
E_{basis}	Reference fuel cycle energy production for mass flow analysis	100 GWe-yr
$\dot{E}_{basis}$	Reference fuel cycle annual energy production for mass flow analysis	Not actually used, but has been used in past FCDP templates
E_{FC}	Electrical Energy Produced by fuel cycle based on initial M_{PWR}	Calculated
$\dot{E}_{FC}$	Annual Electrical Energy Produced by fuel cycle based on initial M_{PWR}	Calculated
E_{HTGR}	Electrical Energy Produced by a HTGR normalized to mass M_{HTGR}	Calculated
E_{mHTGR}	Electrical Energy Produced by a HTGR which accounts for PWR's rate of used fuel production	Calculated
E_{PWR}	Electrical Energy Produced by a PWR normalized to mass M_{PWR}	Calculated
$\dot{E}_{mHTGR}$	Annual Electrical Energy Produced by a HTGR which accounts for PWR's rate of used fuel production	Calculated

$\dot{E}_{PWR}$	Annual Electrical Energy Produced by a PWR normalized to mass M_{PWR}	Calculated
$f_{Th,S1}$	Fraction of RTh which is re-used in Stage 1 Fuel	0.8
FPs	Amount of recycled fission products available from reprocessing, normalized by E_{basis}	Calculated
$L_{f,s1}$	Fuel Fabrication Losses, Stage 1, normalized by E_{basis}	Calculated
$L_{f,s2}$	Fuel Fabrication Losses, Stage 2, normalized by E_{basis}	Calculated
L_r	Reprocessing Losses, normalized by E_{basis}	Calculated
L_{tot}	Total fuel cycle losses, normalized by E_{basis}	Calculated
M_{HTGR}	Initial Mass Heavy Metal in HTGR	Determined from burnup calculations (SCALE) based on M_{PWR} amount of initial heavy metal in PWR
M_{PWR}	Mass Basis – Initial Mass Heavy Metal in PWR	1 MTIHM
$m_{x,z}$	Mass of some isotope or element "x" in stream "z"	Determined from burnup calculations (SCALE)
$n_{R,s1}$	Number of Refueling Periods per PWR Blanket Lifetime	6
$n_{R,s2}$	Number of Refueling Periods per HTGR Lifetime	1
NTh	Natural thorium requirement of fuel cycle, normalized by E_{basis}	Calculated
NU_b	Natural uranium requirement arising from blanket fuel, normalized by E_{basis}	Calculated
NU_d	Natural uranium requirement arising from driver fuel, normalized by E_{basis}	Calculated
NU_{tot}	Total natural uranium requirement of fuel cycle, normalized by E_{basis}	Calculated
p_{HTGR}	Instantaneous Power Density of HTGR	100 MWth/MTIHM
p_{PWR}	Instantaneous Power Density of PWR	49 MWth/MTIHM

$R_{s2/s1}$	Ratio of T_{s2} over T_{s1} (Useful for calculations)	Calculated
$R_{td/tb}$	Ratio of driver fuel lifetime over blanket fuel lifetime	0.5
$R_{U/B}$	Ratio of uranium fuel in blanket to total mass of blanket fuel	Calculated
RTh_{s1r}	Portion of RTh_{tot} allocated to Stage 1 Re-Use, normalized by E_{basis}	Calculated
RTh_{s2f}	Amount of RTh in Stage 2 Fuel, normalized by E_{basis}	Calculated
RTh_{s2r}	Portion of RTh_{tot} allocated to Stage 2 Re-Use, normalized by E_{basis}	Calculated
RTh_{tot}	Total amount of recycled thorium available from reprocessing, normalized by E_{basis}	Calculated
RU_{tot}	Total amount of recycled uranium available from reprocessing, normalized by E_{basis}	Calculated
RU_{s2f}	Amount of RU in Stage 2 Fuel, normalized by E_{basis}	Calculated
T_{HTGR}	Total HTGR in-reactor cycle time	1000 days
T_{PWR}	Total PWR in-reactor cycle time (one blanket lifetime)	2916 days
T_{rf}	Length of refueling period (assumed same for both PWR & HTGR)	40 days
T_{s1}	Combined in-reactor and refueling cycle time for lifetime of blanket fuel in Stage 1	Calculated
T_{s2}	Combined in-reactor and refueling cycle time for lifetime of fuel in Stage 2	Calculated
TRU	Amount of transuranics (plus protactinium) available from reprocessing, normalized by E_{basis}	Calculated
Y	Normalization Factor Used to Scale-up Mass Flows to basis of E_{basis}	Calculated

SCALE automatically normalizes its input mass flows to one metric ton of heavy metal. Thus, in order to obtain electrical-energy-normalized mass flows, one needs make assumptions regarding capacity factors and electricity conversion efficiencies. Since the power density is held constant and the fuel is irradiated for a fixed period of time for both stages, it is fairly straightforward to compute the amount of electricity generated by one metric ton of initial heavy metal.

Electrical Energy Produced by Modeled PWR over Blanket Fuel Lifetime:

$$E_{PWR} = \frac{p_{PWR} * M_{PWR} * T_{PWR} * e_e * c}{\left(1000 \frac{GW}{MW}\right) * d_y}$$

Even though SCALE will automatically re-normalize to 1 t initial heavy metal, in order to develop a consistent normalization unit for the combination of Stages 1 & 2 Combined, one should renormalize to the amount of Stage 2 fuel that results from 1 t of Stage 1 fuel.

Electrical Energy Produced by Modeled HTGR over Fuel Lifetime:

$$E_{HTGR} = \frac{p_{HTGR} * M_{HTGR} * T_{HTGR} * e_e * c}{\left(1000 \frac{GW}{MW}\right) * d_y}$$

These two values are then combined:

Combined Electrical Energy Produced on M_{PWR} Basis:

$$E_{FC} = E_{PWR} + E_{HTGR}$$

Once this mass-basis value is known, a normalization factor can be developed to convert between the mass files that leave SCALE and mass values on some energy-normalized basis (for FCDPs, this has been 100 GWe-yr).

Electrical Energy Normalization Factor:

$$Y = \frac{E_{basis}}{E_{FC}}$$

The fraction of electricity produced by each stage is then straightforward to determine:

Fractions of Electrical Energy Produced from Stages 1 & 2:

$$f_{E,s1} = \frac{E_{PWR}}{E_{FC}}$$

$$f_{E,s2} = \frac{E_{HTGR}}{E_{FC}}$$

If one wanted to normalize on a basis of annual electrical energy production, instead of a fixed amount of electrical energy, an alternative approach is available. This requires determining the rate at which each system produces electrical energy, which involves accounting for refueling/maintenance periods as well as operation:

Full PWR Blanket Fuel Lifetime (Stage 1):

$$T_{s1} = T_{PWR} + n_{R,s1} * T_{rf}$$

HTGR Fuel Lifetime:

$$T_{s2} = T_{HTGR} + n_{R,s2} * T_{rf}$$

Determining the electrical generation for Stage 1 is straightforward at this point:

Annual Energy Production of PWR:

$$\dot{E_{PWR}} = \frac{E_{PWR} * d_y}{T_{s1}}$$

However, the previously calculated electrical energy for the HTGR cannot be used as-is because its fueling cycle is considerably shorter than that of the PWR; if an HTGR immediately used all the Stage 1 fuel provided by a single PWR, it would use its fuel and then wait around non-operational while Stage 1 produced more fuel. However, a smaller (henceforth called "mini") HTGR could divide the Stage 1 fuel into multiple fuel batches and use one batch at a time until more PWR fuel was available. To account for this issue, we introduce a correctional factor:

Stage Cycle-Time Ratio:

$$R_{s2/s1} = \frac{T_{s2}}{T_{s1}}$$

Electrical Energy Produced by "Mini" HTGR over Fuel Lifetime:

$$E_{mHTGR} = E_{HTGR} * R_{s2/s1}$$

This can then be converted into an electrical energy generation rate.

Annual Energy Production of "Mini" HTGR:

$$\dot{E}_{mHTGR} = \frac{E_{mHTGR} * d_y}{T_{s2}}$$

The remaining steps parallel what was done for the electrical-energy (not-rate) basis:

Combined Electrical Energy Produced on M_{PWR} Basis:

$$\dot{E_{FC}} = \dot{E_{PWR}} + \dot{E_{mHTGR}}$$

Fractions of Electrical Energy Produced from Stages 1 & 2:

$$f_{E,s1} = \frac{\dot{E_{PWR}}}{\dot{E_{FC}}}$$

$$f_{E,s2} = \frac{\dot{E_{mHTGR}}}{\dot{E_{FC}}}$$

With the electrical energy normalization factor, it is possible to determine a number of energy-normalized mass flows quite readily. For Stage 1, the energy-normalized amount of driver fuel and blanket fuel entering the PWR can be determined by adding the mass of each isotope as output by SCALE at time zero (since the driver fuel is replaced more frequently than the blanket fuel, a correctional factor is added accordingly).

Reactor Mass Inventories:

$$D = \frac{(m_{U-235,driver} + m_{U-238,driver})}{R_{td/tb}} * Y$$

$$B = \left(m_{U-235,blanket} + m_{U-238,blanket} + m_{Th,blanket}\right) * Y$$

Since the driver fuel is sent to storage and disposal, only the used blanket fuel composition from Stage 1 is of interest from the perspective of fuel cycle mass flow. After including a factor accounting for reprocessing efficiency (which is also used to determine losses from reprocessing), a number of parameters can be readily determined. Note that protactinium is listed here among the "TRU" elements as it will require comparable management to neptunium, plutonium, americium, and curium if thorium-based fuel cycles are implemented. The amount of fission products could be determined by adding the masses of each fission product, but given the quantity of fission product species it is easier to "calculate by exclusion".

Reprocessing:

$$RU_{tot} = (\sum m_{U-isotopes,blanket}) * e_r * Y$$

$$RTh_{tot} = (\sum m_{Th,b}) * e_r * Y$$

$$TRU = (\sum m_{Pa,b} + \sum m_{Pu,b} + \sum m_{Np,b} + \sum m_{Am,b} + \sum m_{Cm,b}) * Y$$

$$FP = B - TRU - \frac{RU_{tot} + RTh_{tot}}{e_r}$$

$$L_r = (RU_{tot} + RTh_{tot}) * \frac{1 - e_r}{e_r}$$

Note that if all the thorium from Stage 1 is passed to Stage 2, then Stage 2 is so thorium-laden that is not neutronically viable for sustained vision. Instead, most of the thorium must be re-used in Stage 1 (as this FCDP assumes) or otherwise stored and disposed. A number of thorium

recycle fractions were examined; an 80% recycle rate yielded a Stage 2 fuel content with approximately equal parts (by mass) thorium and uranium, with about 10% of the uranium being fissile, which was enough to yield sustained fission over the lifetime of the fuel.

$$RTh_{s1r} = RTh_{tot} * f_{Th,S1}$$

$$RTh_{s2r} = RTh_{tot} * (1 - f_{Th,S1})$$

There are some small losses during fuel fabrication; the following parameters account for this efficiency factor.

Fuel Fabrication:

$$L_{f,s1} = \frac{(D + B) * (1 - e_f)}{e_f}$$

$$RU_{s2f} = RU_{tot} * e_f$$

$$RTh_{s2f} = RTh_{tot} * e_f$$

$$L_{f,s2} = \left(RU_{s2f} + RTh_{s2f}\right) * (1 - e_f)$$

While all of the fuel from Stage 1 is briefly "discharged fuel", the blanket fuel is reprocessed in its entirety. So, the only fuel from Stage 1 that requires management as discharged fuel is the driver fuel (although the reprocessing of blanket fuel will produce high-level waste). The entirety of the output from Stage 2 must be managed as discharged fuel.

Discharged Fuel:

$$DF_{s1} = (D + B) - B = D$$

$$DF_{s2} = RU_{s2f} + RTh_{s2f}$$

$$DF_{tot} = DF_{s2} + DF_{s1}$$

Since Stage 2 is entirely fed by reprocessed material, only Stage 1 contributes to the demand of natural resources. The natural thorium demand is fairly straightforward, requiring the normalized amount of thorium in the blanket subtracted by the amount that is recycled back to Stage 1 (also accounting for fabrication losses). Natural uranium is used in both the driver and the blanket fuel; these demands can be determined separately (the equations are derived by performing mass balances on both total uranium and uranium-235). An assumption is required regarding enrichment of the tails. For the blanket fuel calculation, the fraction of fresh fuel that is comprised of uranium must be known.

Natural Resource Requirements

$$R_{U/B} = \frac{\left(m_{U-235,blanket} + m_{U-238,blanket}\right) * Y}{B}$$

$$NU_d = \frac{D * (a_d - a_{tail})}{e_f * (a_{nat} - a_{tail})}$$

$$NU_b = \frac{B * R_{U/B} * (a_b - a_{tail})}{e_f * (a_{nat} - a_{tail})}$$

$$NU_{tot} = NU_s + NU_b$$

$$NTh = \frac{B * (1 - R_{U/B}) - RTh_{s1r}}{e_f}$$

Once the natural uranium demand is known, the amount of depleted uranium which is generated during enrichment can be calculated by subtracting the amount of uranium in fuel from the total demand (while accounting for fabrication losses).

Other Important Parameters

$$DU_d = NU_d - \frac{D}{e_f}$$

$$DU_b = NU_b - \frac{B * R_{U/B}}{e_f}$$

$$DU_{tot} = DU_s + DU_b$$

Total losses are determined by summing the three sources of losses (reprocessing, fabrication of Stage 1 fuel, fabrication of Stage 2 fuel).

$$L_{tot} = L_r + L_{f,s1} + L_{f,s2}$$

Appendix B References

1. A. Galperin, M. Todosow, A. Morozov, N. Ponomarev-Stepnoi, M. Kazimi, A. Radkowsky, S. Grae. "A Thorium-Based Seed-Blanket Fuel Assembly Concept to Enhance PWR Proliferation Resistance", Proceedings of the International Conference on Future Nuclear Systems – Global '99, August 29 – September 3, Jackson Hole, Wyoming, 1999
2. M. Todosow, M. Kazimi. "Optimization of Heterogeneous Utilization of Thorium in PWRs to Enhance Proliferation Resistance and Reduce Waste", Report BNL-73152-2004, 2004
3. G. Raitses, M. Todosow, A. Galperin, "Non-Proliferative, Thorium-Based, Core and Fuel Cycle for Pressurized Water Reactors", Proceeding of the 17th International Conference on Nuclear Engineering, Upton, NY, 2009, Revision, April 2012
4. J. Bess, N. Fujimoto. "Evaluation of the Start-up Core Physics Tests at Japan's High Temperature Engineering Test Reactor (Fully-Loaded Core), INL/EXT-08-14767, Revision 0, March 2009

APPENDIX C, SOME PERSPECTIVES ON FISSILE MATERIAL BALANCES FOR DYNAMIC TRANSITIONS

The underlying principle of a material balance is that the net accumulation or depletion of a substance is equal to the rate of its production and/or entry minus the rate of its consumption and/or loss. For a material balance on a non-natural fissile isotope such as Pu-239, Pu-241, or U-233 (generically called F), in the event that the total electricity demand is unchanging, this material balance is relatively straightforward when all outgoing streams are reprocessed and recovered:

$$\frac{dF}{dt} = \sum \frac{M_i x_{Fi,out} e_{net,i}}{\tau_i} - \sum \frac{M_i x_{Fi,in}}{\tau_i}$$

The lower case "i" refers to individual stage numbers, "M_i" is the total heavy metal mass of fuel for that stage on some normalization basis (usually energy output), "τ_i" is the fuel residence time for that stage, "x_{Fi}" is the mass fraction of heavy metal that is comprised of the isotope, and "$e_{net,i}$" is a net efficiency term that encompasses the fraction of recovered material that is NOT lost to reprocessing and re-fabrication losses. At steady-state, all differential terms are equal to zero (i.e., there is no net accumulation or depletion), and the left summation term is precisely equal to the right summation term. For the steady-state calculations conducted in Chapter 4, this equivalence greatly simplified the material balance. By extension, it implies that for single-stage systems, such as the CUPu and CThU fuel cycles, at steady-state, $x_{Fi,in}$ must be equal to $x_{Fi,out} e_{net,i}$. Since $e_{net,i}$ is very nearly equal to one[43], $x_{Fi,out}$ needs to be only slightly larger

[43] For solid-fueled systems (e.g., CUPu), a 99% reprocessing efficiency times a 99.8% fuel fabrication efficiency yields a 98.802% combined efficiency (approximated as 98.8% in VISION due to input restrictions). For fluid-fueled

than $x_{Fi,in}$ to sustain a steady-state, single-stage system with reprocessing. If F is the only important fissile isotope (true for U-233 and also true if we consider "*F*" to be the combination of the two fissile plutonium isotopes), then the breeding ratio requirement of the system is just:

$$R_{breed} = \frac{x_{Fi,out}}{x_{Fi,in}} = \frac{1}{e_{net,i}}$$

For solid-fueled systems (e.g., CUPu), a 99% reprocessing efficiency times a 99.8% fuel fabrication efficiency yields a 98.802% combined efficiency (approximated as 98.8%), implying a steady-state breeding ratio requirement of 1.012. For fluid-fueled systems (e.g., CThU), reprocessing losses are negligible in the continuous reprocessing system (consistent with assumptions applied in Chapter 4), so only the 99.8% fuel fabrication efficiency is applied. This implies a breeding ratio requirement of 1.002. Both of these should be readily achievable with the SFR and MSR technologies, and are more correctly identified as "breakeven" core configurations rather than "breeders".

For dynamic transitions, this relationship changes. If new reactors are being constructed at some fixed rate for perpetuity, then there is another "consumption term" in the material balance that corresponds to the startup fissile material required for new reactors:

$$\frac{dF}{dt} = (\frac{Mx_{F,out}e_{net}}{\tau} - \frac{Mx_{F,in}}{\tau})n_{reactor} - \frac{dn_{reactor}}{dt}Mx_{F,in}$$

systems (e.g., CThU), reprocessing losses are negligible in the continuous reprocessing system (consistent with assumptions applied in Chapter 4), so only the 99.8% fuel fabrication efficiency is applied.

The new variables are $n_{reactor}$ for the number of reactors that are already operating, and $\frac{dn_{reactor}}{dt}$ for the rate at which new reactors are being brought online. If the number of reactors always immediately scales up to match some steady exponential increase in power demand so that the ratio of $\frac{dn_{reactor}}{dt}$ and $n_{reactor}$ is a constant called p_{growth} (with units of inverse time), then the minimum breeding requirement to precisely sustain this growth for perpetuity would be:

$$R_{breed} = \frac{1 + p_{growth}\tau}{e_{net}}$$

While p_{growth} is not an intuitive parameter, it is directly related to the concept of an annual exponential increase in power demand through a logarithmic relationship. Figure XX, below, shows the relationship between the breeding ratio requirement and the annual percent increase in electricity demand, assuming a constant rate of increase. The plot also incorporates representative values for the residence time of these systems. A residence time of 5.44 years is adopted for the SFR based on data from the FCO-ESS [Sandia 2016], while an "effective" residence time is determined for the MSR based on the ratio of material inventory to material flow rates from FCO-ESS work; the result of this calculation is 8.8 years (explained further in Section 5.3.4).

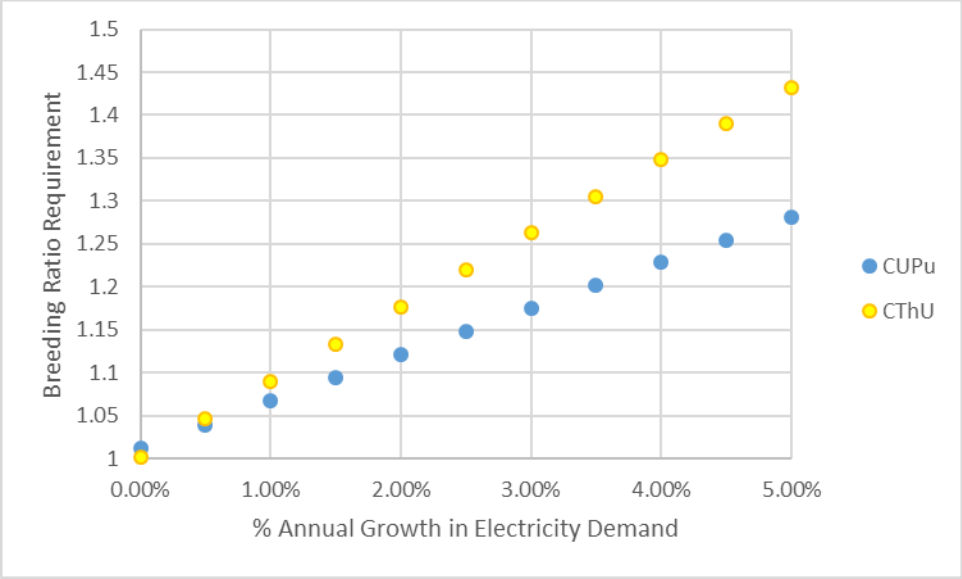

Figure C-1, Breeding Ratio Required to Support Continued Closed Fuel Cycle Growth for Various Exponential Energy Demand Increases

The difference in the magnitude of the CUPu and CThU relationships is due to the longer fuel residence time assumption of the MSR technology versus the SFR technology. The relationship between electricity demand and breeding ratio is not truly linear, but it does appear approximately linear in this range of limited, albeit realistic, electricity demand values. For both CUPu and CThU, an increasingly greater burden is placed on the need to generate more fissile material as the extent of annual electricity demand increases.

APPENDIX D, REVIEW OF SELECTED FUEL CYCLE SIMULATION TOOLS

A number of pre-developed tools exist to model the deployment of nuclear technologies. Each of these tools is multi-faceted and capable of accommodating a range of problems; however, each also comes with its own strengths and weaknesses. While a number of tools exist at widely varying levels of refinement, this literature search will focus on four tools which are known to have diverse capabilities and whose uses in prior work have been well-documented: DANESS, VISION, ORION, and CYCLUS. There are other fuel cycle analysis tools which have developed and used at other times, but these seem to either have been outmoded (e.g., DYMOND being succeeded by VISION) or withdrawn from active recent development (e.g., CAFCA [Boscher 2004]). Thus, this appendix will just focus on DANESS, VISION, ORION, and CYCLUS.

Modeling with ORION

ORION is a fuel cycle modeling computer code that was originally developed by British Nuclear Fuels Limited (BNFL), who desired a code which was easy to use, employed robust physics, and was designed generally to model virtually any fuel cycle, at either steady-state or in transition. ORION's graphical user interface was an integral part of its development from the onset. The software is object-oriented, and six types of objects exist [Gregg 2014]:

- Buffer
- Fabrication Plant
- Reactor
- Active Process Plant (e.g., reprocessing plant)
- Passive Process Plant (e.g., cooling pond)
- External Feed

Time steps can be varied, and the code is capable of performing decay and transmutation calculations; over 2500 nuclides are tracked [Gregg 2014]. Furthermore, ORION can be readily integrated with other computer codes to enable such capabilities as fuel cycle cost and proliferation risks. Although originally designed to meet the needs of agencies in the United Kingdom, ORION has begun to expand its user base elsewhere, particularly in the United States [Rayment 2012].

ORION has already been applied to studies involving thorium-based fuel cycle options. The United Kingdom's Universe of Cambridge applied ORION to a comparison of the uranium- and thorium-based variants of an open nuclear fuel cycle in European Pressurized Reactors (EPRs). Three varieties of the thorium-based core were examined, and only of these three designs exhibited a modest improvement in uranium ore requirements; none offered notable waste or proliferation resistance advantages [Ashley 2014]. The UK's Department of Energy & Climate Change worked with the National Nuclear Laboratory (NNL) to examine transition scenarios to closed fuel cycles and their impact on radiotoxicity, decay heat, and waste volume. One of these scenarios involved a molten salt fast reactor using previously-developed neutronics data from France's Thorium Molten Salt Reactor (TMSR) efforts (see [Mathieu 2009] and [Merle-Lucotte 2006-2011] for details about the TMSR design). From a waste perspective, a fast MSR started up on U-233 initially produces fewer long-lived radionuclides, although eventually heavy metal inventories from the two options converge [DECC 2013].

Other applications have not been focused on thorium-based options but may still afford valuable insights regarding ORION's capabilities. BNFL used ORION to compare different transition scenarios to various fuel cycle options for the UK. By coupling ORION to the physics codes CASMO and ERANOS, the study was able to determine which options were available ovr short, medium, and long timescales [Worrall 2007]. The UK's NNL collaborated with EnergySolutions in the US to evaluate proliferation risk mitigation approaches for recycle strategies of used nuclear fuel in the US. The study made use of ORION's capabilities to accommodate many different nodes and grouped them by functionality into several categories such as historical used fuel, first-generation new build reactor fleet, used nuclear fuel recycle, fuel fabrication, etc. ORION was found to be capable of realistic and complex time evolutions without making premature assumptions about equilibrium reactor fleet compositions [Hesketh 2009].

Modeling with VISION

The Verifiable Fuel Cycle Simulation Model (VISION) is a computer software modeling tool, developed at INL, which enables dynamic fuel cycle simulations to determine material flows and potentially other parameters of interest. It was originally developed based on a preceding tool, DYMOND, but added additional functionalities such as economics and isotopic decay. VISION was intended to be general tool, without limitations to particular reactor or fuel cycle technologies. It is rooted in the system dynamics software tool, PowerSim [Yacout 2006]. The VISION model consists of three key functionalities: tracing the flow of material through the entire fuel cycle, tracking the life cycle of essential strategic fuel cycle facilities, and calculation of a variety of fuel cycle metrics. 81 isotopes or isotope groups are tracked by the tool [Jacobson 2006].

There is no published work on the application of VISION to thorium fuel cycles (although the tool has been demonstrated to be viable for this purpose). VISION's predecessor, DYMOND, has been applied to dynamic analyses of thorium fuels in heavy water reactors by the Korea Atomic Energy Research Institute (KAERI); there is a good chance that the methodology described in this study could be applied to studies in VISION, although this would need to be verified. However, insights from the application of VISION to non-thorium systems may still be valuable. INL has used the tool internally for a variety of purposes. Among these, VISION was used to simulate the impacts of system uncertainties on partial and total fuel cycle costs. This approach was extended to both light water reactors and fast-spectrum reactors with recycle. The simulations showed significant variations in costs in response to changes in burnup, capacity factor, and reactor power [Taylor 2008]. North Carolina State University has used to VISION to support build schedules for constituent facilities of advanced nuclear fuel cycles. VISION was selected for its commercial availability (VISION is freely available, although PowerSim requires a license), its modeling of facilities that are commonly found in the US nuclear fuel cycle as well as those anticipated for advanced fuel cycles, and for its fluid performance compared to other options available at the time of the study. The model successfully provided information regarding ideal facility sizes, lead times, and building schedules under a variety of constraints [Schweitzer 2008].

Modeling with CYCLUS

CYCLUS is a dynamic fuel cycle simulation tool, developed at the University of Wisconsin, which applies an agent-based approach where facility agents behave with regard to physics

modeling constraints and social interaction models. The behavior and interactions of the agents are influenced by regional and institutional preferences. The tool is still under development, and more recently efforts have focused on the tool's user interface and visualization. A central feature of CYCLUS is its use of open-source dependencies and platforms, along with a public and transparent user community [Wilson 2014]. Many of the publications pertaining to CYCLUS to-date have involved improving or adding capabilities to the tool, such as deployment optimization capabilities [Carlsen 2014] and extensions based on market-driven transition factors [Huff 2014]. A model for used fuel disposition and repositories was the subject of a dissertation at the University of Wisconsin; this model takes into account disposal environments (e.g., hydrology, geochemistry, thermal behavior), waste form release models, waste package failure models, and other detailed factors [Huff 2013]. These efforts highlight the modular nature of CYCLUS; individuals can continue to develop and add their own integrateable modules for eventual use by the rest of the fuel cycle community. The software has also undergone benchmarking exercises for the once-through fuel cycle, which indicated successful replication of results [Gidden 2012].

Because CYCLUS is actively under development, publications which have applied CYCLUS to specific nuclear fuel cycle scenarios are not presently available. However, this may change on fairly rapid timescales (before the end of this dissertation work) as the user interface approaches completion.

Modeling with DANESS

Originally developed at Argonne National Laboratory, the Dynamic Analysis of Nuclear Energy System Strategies (DANESS) modeling tool integrates material flow accounting, economic, socio-political, and related functionalities to capture the extensive details associated with a fuel cycle deployment scenario. Advanced capabilities of the code include the ability to modeling time-varying compositions of reactors and fuels and the ability to model other sub-models to calculate parameters related to waste management or economics [Van Den Durpel 2006].

While no results with DANESS pertaining to thorium have been published, insights from studies on non-thorium systems provide insights about the effectiveness of the tool. At ANL, DANESS was used to assess the capability of reactors in the US to produce either electricity or hydrogen. Reactor "parks" using only LWRs were evaluated for the potential to generate electricity, while combined fleets of LWRs and HTGRs were considered to support combined missions of electricity and hydrogen production; incorporating fast reactors along with LWRs and HTGRs mitigated waste disposal requirements [Van Den Durpel 2003]. ANL also supported the Advanced Fuel Cycle Initiative (AFCI) by using DANESS to simulate transitions from the once-through fuel cycle in the US with PWRs and boiling water reactors (BWRs) to a variety of scenarios, including single MOX recycle and single-tier or double-tier transmutation involving the recycle of transuranic elements in fast reactors [Yacout 2004]. In the Netherlands, the Nuclear Research and Consultance Group (NRG) has used DANESS to simulate material flows for various European new reactor build scenarios, including various rates and compositions of mixed LWR-SFR fleets. DANESS was appealing for the study for its capability to simulate facilities over their entire lifetime while simultaneously calculating natural resource and waste

disposal requirements [Roelofs 2011]. KAERI has used DANESS to consider future nuclear fuel cycles where electrochemical processing is integrated with the use of SFRs. DANESS enabled the study to consider factors such as resource utilization, waste management, and cost [Gao 2012]. KAERI has also used DANESS to conduct sensitivity studies on the impact of fast reactor conversion ratios on deployment scenarios [Jeong 2010] as well as for scenarios involving the deployment of high-temperature, deep-burn gas reactors [Jeong 2011].

It should be noted that the studies described above exclusively used the fourth or fifth version of DANESS. Studies based on the more recent versions of DANESS (6 or 7) have not been identified.